

ADSORPTION OF Pb(II) AND Cu(II) ON  $\alpha$ -QUARTZ  
FROM AQUEOUS SOLUTIONS: INFLUENCE OF pH,  
IONIC STRENGTH, AND COMPLEXING LIGANDS

Thesis by

Jasenska Vuceta

In Partial Fulfillment of the Requirements  
for the Degree of  
Doctor of Philosophy

California Institute of Technology  
Pasadena, California

1976

(Submitted January 29, 1976)

## ACKNOWLEDGMENTS

I am especially grateful to my research advisor, Professor James J. Morgan, whose advice, extensive discussions, encouragement, patience, and understanding have been invaluable for completion of this research. I am also thankful to Professor Clair C. Patterson who provided helpful suggestions on the clean-room techniques. I wish also to thank many other members of the faculty who have aided my work both professionally and personally.

The discussions, suggestions, and encouragements of all the students and associates in our department are greatly appreciated, especially George Jackson, William Faisst, Tom Sibley, Francois Morel, Daniel Chang, and Dennis Kasper. I thank Jim Pankow, William Faisst, and Tom Holm for their critical reading of this manuscript and invaluable help which led to numerous editorial improvements.

The contributions of the following are also greatly appreciated: Miss Sylvia Garcia for her aid in performing some experiments; Messrs. Elton Daly, Joe Fontana, and Larry McClellan for technical assistance, and Messrs. David Byrum and Robert Schultz for the preparation of the drawings.

Helen Fabel is thanked for her excellent typing of this manuscript.

The financial support of the National Institute of Environmental Health Sciences is greatly appreciated.

Finally, this work is dedicated to my parents, Marija and Ivan Vuceta, and my grandparents, Katarina and Melhior Braun, whose love and constant encouragement helped me through difficult times.

## ABSTRACT

Adsorption of aqueous Pb(II) and Cu(II) on  $\alpha$ -quartz was studied as a function of time, system surface area, and chemical speciation. Experimental systems contained sodium as a major cation, hydroxide, carbonate, and chloride as major anions, and covered the pH range 4 to 8. In some cases citrate and EDTA were added as representative organic complexing agents. The adsorption equilibria were reached quickly, regardless of the system surface area. The positions of the adsorption equilibria were found to be strongly dependent on pH, ionic strength and concentration of citrate and EDTA. The addition of these non-adsorbing ligands resulted in a competition between chelation and adsorption. The experimental work also included the examination of the adsorption behavior of the doubly charged major cations Ca(II) and Mg(II) as a function of pH.

The theoretical description of the experimental systems was obtained by means of chemical equilibrium-plus-adsorption computations using two adsorption models: one mainly electrostatic (the James-Healy Model), and the other mainly chemical (the Ion Exchange-Surface Complex Formation Model). Comparisons were made between these two models.

The main difficulty in the theoretical predictions of the adsorption behavior of Cu(II) was the lack of the reliable data for the

second hydrolysis constant ( $*\beta_2$ ). The choice of the constant was made on the basis of potentiometric titrations of  $\text{Cu}^{2+}$ .

The experimental data obtained and the resulting theoretical observations were applied in models of the chemical behavior of trace metals in fresh oxic waters, with emphasis on Pb(II) and Cu(II).

## TABLE OF CONTENTS

Chapter	Title	Page
1	INTRODUCTION	1
	1.1 Introduction	1
	1.2 Limnological Studies on the Distributions of Pb(II) and Cu(II)	3
	1.3 Objectives of the Present Work and Organization of this Thesis	5
2	THEORETICAL CONSIDERATIONS IN METAL ADSORPTION AT OXIDE SURFACES	8
	2.1 James-Healy Model	8
	2.1.1 Coulombic Energy	8
	2.1.2 Secondary Solvation Energy	10
	2.1.3 Chemical Interactions	16
	2.2 Ion Exchange-Surface Complex Formation Model	16
	2.2.1 Electrostatic Influence	22
	2.3 Influence of Ligands on the Adsorption of Metal Ions	25
	2.3.1 Introduction	25
	2.3.2 Literature Review	25
	2.3.3 Model Predictions	32
3	EXPERIMENTAL METHODS AND MATERIALS	35
	3.1 Chemicals	35
	3.2 $\alpha$ -Quartz	36
	3.3 Cleaning Techniques	37
	3.4 Reaction Vessel	39
	3.5 pH Control	39

Chapter	Title	Page
	3.6 Sample Processing and Analysis	40
	3.7 Adsorption Measurements with C <sup>14</sup> -Citric Acid	43
	3.8 Adsorption Measurements with C <sup>14</sup> -NaHCO <sub>3</sub>	45
4	HYDROLYSIS OF Pb(II) AND Cu(II)	49
	4.1 Introduction	49
	4.2 Hydrolysis of Pb(II)	49
	4.2.1 Introduction	49
	4.2.2 Mononuclear Pb(II)-Hydrolysis Products	51
	4.2.3 Polynuclear Pb(II)-Hydrolysis Products	52
	4.2.4 Summary	54
	4.3 Hydrolysis of Cu(II)	56
	4.3.1 Introduction	56
	4.3.2 Mononuclear Cu(II)-Hydrolysis Products	56
	4.3.3 Cu <sub>2</sub> (OH) <sub>2</sub> <sup>2+</sup>	60
	4.3.4 Summary	60
	4.4 Second Hydrolysis Constant for Cu(II)	61
	4.4.1 Equilibrium Computations with Different Values for *β <sub>2</sub>	61
	4.4.2 Potentiometric Titrations of Cu <sup>2+</sup> as a Function of pH	67
5	ADSORPTION OF Cu(II), Pb(II), Mg(II), AND Ca(II) ON α-QUARTZ IN A CARBONATE-FREE SYSTEM	75
	5.1 Adsorption of Cu(II) and Pb(II) on α-Quartz as a Function of Time, Metal Ion Concentration, and System Surface Area	75
	5.1.1 Adsorption of Cu(II) and Pb(II) on α-Quartz as a Function of Time	75
	5.1.2 Adsorption of Cu(II) and Pb(II) on α-Quartz as a Function of Metal Concentration and System Surface Area	79

Chapter	Title	Page
5.2	Adsorption of Cu(II), Pb(II), Mg(II), and Ca(II) on $\alpha$ -Quartz as a Function of pH and Ionic Strength	79
5.2.1	Equilibrium Modeling	79
5.2.2	Adsorption of Cu(II) on $\alpha$ -Quartz as a Function of pH and Ionic Strength	87
5.2.3	Adsorption of Pb(II) on $\alpha$ -Quartz as a Function of pH	91
5.2.4	Adsorption of both Cu(II) and Pb(II) on $\alpha$ -Quartz from Equimolar Solutions as a Function of pH	93
5.2.5	Adsorption of Mg(II) and Ca(II) on $\alpha$ -Quartz as a Function of pH	95
5.3	Influence of Citrate and EDTA on the Adsorption of Cu(II) and Pb(II) on $\alpha$ -Quartz	102
5.3.1	Modeling Considerations	102
5.3.2	Adsorption of Cu(II) on $\alpha$ -Quartz in the Presence of Citrate	102
5.3.3	Adsorption of Pb(II) on $\alpha$ -Quartz in the Presence of Citrate	111
5.3.4	Adsorption of Cu(II) and Pb(II) on $\alpha$ -Quartz in the Presence of EDTA	117
5.4	Conclusions	123
6	ADSORPTION OF Pb(II) AND Cu(II) ON $\alpha$ -QUARTZ IN A CARBONATE SYSTEM	130
6.1	Introduction	130
6.2	Adsorption of Pb(II) on $\alpha$ -Quartz in the Presence and Absence of Citrate	132
6.3	Adsorption of Cu(II) on $\alpha$ -Quartz in the Presence and Absence of Citrate	138
6.4	Conclusions	153

Chapter	Title	Page
7	SUMMARY OF CHAPTERS 2-6	156
8	CHEMICAL MODELS OF FRESH WATERS UNDER OXIDIZING CONDITIONS	160
	8.1 Introduction	160
	8.2 Inorganic Models	161
	8.2.1 General Considerations	161
	8.2.2 Distributions of Metals as a Function of pH	163
	8.2.3 Distributions of Metals at a Constant pH as a Function of Different Adsorbing Surfaces	167
	8.2.4 Adsorption of Metals as a Function of Surface Area	174
	8.3 Organic Models	176
	8.3.1 General Considerations	176
	8.3.2 EDTA	177
	8.3.3 Citrate	177
	8.3.4 Histidine	179
	8.3.5 Aspartic Acid	182
	8.3.6 Cysteine	182
	8.3.7 Distribution of Metals in the Presence of Organic Ligands as a Function of Surface Area	185
	8.3.8 Adsorption of Metals at Constant pH as a Function of Surface Area and Citrate Concentration	187
	8.4 Conclusions	191
Appendix	Title	
1	TABLE OF NOTATIONS	194
	REFERENCES	198

## LIST OF TABLES

Table	Title	Page
3.1	Spectrographic Analysis of $\alpha$ -Quartz	38
3.2	Tests for the Adsorption of $C^{14}$ -CIT on Min-U-Sil in the Absence of Copper	46
3.3	Tests for the Adsorption of $C^{14}$ -CIT on Min-U-Sil in the Presence of Copper	46
3.4	Tests for the Adsorption of $C^{14}$ - $NaHCO_3$ on Min-U-Sil	47
4.1	Summary of the Hydrolysis of Pb(II)	50
4.2	Hydrolysis Constants for Pb(II) Used in Equilibrium Computations	55
4.3	Stability Constants for Pb-Cl Complexes	57
4.4	Reported Equilibrium Constants for the Hydrolysis of Cu(II)	58
4.5	Stability Constants for Hydrolysis Products of Cu(II)	62
4.6	Stability Constants for Cu-Cl Complexes	63
5.1	Specific Adsorption Potentials for $\alpha$ -Quartz Used for the Modeling of the Experimental Systems with the James-Healy Model	86
5.2	Parameters Used for the Modeling of Cu(II) and Pb(II) Adsorption on $\alpha$ -Quartz with the Ion Exchange-Surface Complex Formation Model	88
5.3	Chemical Free Energies Used for Modeling the Adsorption of Mg(II) on $SiO_2(s)$ with the James-Healy Model	103
5.4	Chemical Free Energies Used for Modeling the Adsorption of Ca(II) on $SiO_2(s)$ with the James-Healy Model	104

Table	Title	Page
5.5	Equilibrium Constants for Cu(II)-Citrate Complexes	106
5.6	Equilibrium Constants for Pb(II)-Citrate Complexes	114
5.7	Stability Constants for the Cu(II)-EDTA and Pb(II)-EDTA Complexes	120
6.1	Aqueous Carbonate Solution Opened to the Atmosphere with Constant $p_{\text{CO}_2}$	131
6.2	Equilibrium Constants for the Pb(II)-CO <sub>2</sub> -HCO <sub>3</sub> <sup>-</sup> -CO <sub>3</sub> <sup>2-</sup> System	133
6.3	Equilibrium Constants for the Cu-CO <sub>2</sub> -HCO <sub>3</sub> <sup>-</sup> -CO <sub>3</sub> <sup>2-</sup> System	140
8.1	Inputs of Metals and Ligands Used for Modeling Oxidic Fresh Waters ( $p_{\text{e}}=12$ , $p_{\text{CO}_2}=10^{-3.5}$ atm)	162
8.2	Equilibrium Speciation in an Oxidic River Water of pH 7 in the Presence of 1.55 m <sup>2</sup> /l SiO <sub>2</sub> (s)	169
8.3	Equilibrium Speciation of Metals in an Oxidizing Fresh Water in the Presence of 1.55 m <sup>2</sup> /l, SiO <sub>2</sub> (s), Fe(OH) <sub>3</sub> (s), and 0.08 m <sup>2</sup> /l MnO <sub>2</sub> (s)	172
8.4	Compilation from Tables 8.2 and 8.3	173

## LIST OF FIGURES

Figure	Title	Page
2.1	Locations of a metal ion in the double layer of the Oxide-Water Interface according to the James-Healy Model	13
2.2	Free energies of adsorption of charged and uncharged Me(II)-species on $\text{Fe}(\text{OH})_3(\text{s})$ , $\text{SiO}_2(\text{s})$ , $\text{TiO}_2(\text{s})$ , and $\text{MnO}_2(\text{s})$ .	15
4.1a	Speciation of Cu(II) in the carbonate-free system: $\text{Cu}_T = 1.5 \times 10^{-8} \text{M}$ , $I = 10^{-3}$ , $\log^* \beta_2 \text{Cu}(\text{OH})_2(\text{aq}) = -13.7$	64
4.1b	Speciation of Cu(II) in the carbonate-free system: $\text{Cu}_T = 1.5 \times 10^{-8} \text{M}$ , $I = 10^{-3}$ , $\log^* \beta_2 \text{Cu}(\text{OH})_2(\text{aq}) = -17.3$	64
4.2a	Speciation of Cu(II) in the carbonate-free system: $\text{Cu}_T = 5 \times 10^{-8} \text{M}$ , $I = 10^{-3}$ , $\log^* \beta_2 \text{Cu}(\text{OH})_2(\text{aq}) = -13.7$ .	65
4.2b	Speciation of Cu(II) in the carbonate-free system: $\text{Cu}_T = 5 \times 10^{-8} \text{M}$ , $I = 10^{-3}$ , $\log^* \beta_2 \text{Cu}(\text{OH})_2(\text{aq}) = -17.3$ .	65
4.3a	Speciation of Cu(II) in the carbonate-free system: $\text{Cu}_T = 10^{-7} \text{M}$ , $I = 10^{-3}$ , $\log^* \beta_2 \text{Cu}(\text{OH})_2(\text{aq}) = -13.7$ .	66
4.3b	Speciation of Cu(II) in the carbonate-free system: $\text{Cu}_T = 10^{-7} \text{M}$ , $I = 10^{-3}$ , $\log^* \beta_2 \text{Cu}(\text{OH})_2(\text{aq}) = -17.3$ .	66
4.4	Measurements with the copper ion-selective electrode as a function of pH ( $I = 10^{-3}$ ).	69
4.5	Potentiometric titration of $\text{Cu}^{2+}$ ( $\text{Cu}_T = 1.5 \times 10^{-8} \text{M}$ , $I = 10^{-3}$ ) with copper ion-selective electrode.	71
4.6	Potentiometric titration of $\text{Cu}^{2+}$ ( $\text{Cu}_T = 5 \times 10^{-8} \text{M}$ , $I = 10^{-3}$ ) with copper ion-selective electrode.	73
4.7	Potentiometric titration of $\text{Cu}^{2+}$ ( $\text{Cu}_T = 10^{-7} \text{M}$ , $I = 10^{-3}$ ) with copper ion-selective electrode.	74
5.1	Adsorption of Cu on Min-U-Sil at different surface areas as a function of time.	77

Figure	Title	Page
5.2	Adsorption of Pb on Min-U-Sil at different surface areas as a function of time.	78
5.3	Adsorption isotherm of Cu(II) on $\alpha$ -quartz at pH 7 and $I=10^{-3}$ .	80
5.4	Adsorption isotherm of Pb(II) on $\alpha$ -quartz at pH 7 and $I=10^{-3}$ .	81
5.5a	Equilibrium speciation of Cu as a function of pH in the solution: $Cu_T=10^{-6}M$ , $I=10^{-3}$ , carbonate-free.	90
5.5b	Equilibrium distribution of Cu as a function of pH in the system: $Cu_T=10^{-6}M$ , $S=50m^2/l$ Min-U-Sil, $I=10^{-3}$ , carbonate-free. (James-Healy Model)	90
5.6	Adsorption of Cu(II) from solutions of different ionic strengths. (James-Healy Model)	92
5.7a	Normalized equilibrium speciation of Pb vs. pH in solution: $Pb_T=5 \times 10^{-7}M$ , $I=10^{-3}$ , carbonate-free.	94
5.7b	Normalized equilibrium speciation of Pb vs. pH in aqueous phase of the system: $Pb_T(aq)=Pb_T-Pb_{ads}$ , $Pb_T=5 \times 10^{-7}M$ , $S=75m^2/l$ Min-U-Sil, $I=10^{-3}$ , carbonate-free.	94
5.7c	Equilibrium distribution of Pb vs. pH in the system: $Pb_T=5 \times 10^{-7}M$ , $S=75m^2/l$ Min-U-Sil, $I=10^{-3}$ , carbonate-free. (James-Healy Model)	94
5.8	Equilibrium speciation of Cu and Pb vs. pH in the solution: $Cu_T=Pb_T=5 \times 10^{-7}M$ , $I=10^{-3}$ , carbonate-free.	96
5.9	Equilibrium distribution of Cu and Pb vs. pH in the system: $Cu_T=Pb_T=5 \times 10^{-7}M$ , $S=50m^2/l$ Min-U-Sil, $I=10^{-3}$ , carbonate-free. (James-Healy Model)	97
5.10	Theoretical artifact of the James-Healy Model in modeling the adsorption of Ca(II) and Mg(II) on $\alpha$ -quartz at low ionic strengths.	99

Figure	Title	Page
5.11	Adsorption of Mg as a function of pH; $Mg_T = 3 \times 10^{-5} M$ , $S = 75 m^2/\ell$ , $I = 10^{-3}$ , carbonate-free system. (James-Healy)	100
5.12	Adsorption of Ca on $\alpha$ -quartz as a function of pH; $Ca_T = 10^{-4} M$ , $I = 10^{-3}$ , carbonate-free. (James-Healy Model)	101
5.13a	Equilibrium speciation of Cu vs. pH in the solution: $Cu_T = 10^{-6} M$ , $CIT_T = 0.5 Cu_T$ , $I = 10^{-3}$ , carbonate-free.	107
5.13b	Equilibrium distribution of Cu vs. pH in the system: $Cu_T = 10^{-6} M$ , $CIT_T = 0.5 Cu_T$ , $S = 50 m^2/\ell$ Min-U-Sil, $I = 10^{-3}$ , carbonate-free. (James-Healy Model)	107
5.14a	Equilibrium speciation of Cu vs. pH in the solution: $Cu_T = 10^{-6} M$ , $CIT_T = 10 Cu_T$ , $I = 10^{-3}$ , carbonate-free.	108
5.14b	Equilibrium distribution of Cu vs. pH in the system: $Cu_T = 10^{-6} M$ , $CIT_T = 10 Cu_T$ , $S = 50 m^2/\ell$ Min-U-Sil, $I = 10^{-3}$ , carbonate-free. (James-Healy Model)	108
5.15	Adsorption of Cu vs. pH in the presence and absence of citrate. $Cu(OH)_2(aq)$ not included in computations.	109
5.16	Adsorption of Cu vs. pH in the presence and absence of citrate. $\log^* \beta_2 Cu(OH)_2(aq) = -13.7$ . (James-Healy)	110
5.17	Adsorption of Cu vs. pH in the presence and absence of citrate. $\log^* \beta_2 Cu(OH)_2(aq) = -17.3$ . (IE-SC Model)	112
5.18	Adsorption of Cu vs. pH in the presence and absence of citrate. $Cu_T = 10^{-6} M$ , $S = 2.4 \times 10^{-4} M$ , $I = 10^{-3}$ , carbonate-free. (Ion Exchange-Surface Complex Model)	113
5.19a	Equilibrium speciation of Pb as a function of pH in solution: $Pb_T = 5 \times 10^{-7} M$ , $CIT_T = 10 Pb_T$ , $I = 10^{-3}$ , carbonate-free.	115
5.19b	Equilibrium distribution of Pb as a function of pH in the system: $Pb_T = 5 \times 10^{-7} M$ , $CIT_T = 10 Pb_T$ , $S = 75 m^2/\ell$ Min-U-Sil, $I = 10^{-3}$ , carbonate-free. (James-Healy)	115

Figure	Title	Page
5.20a	Equilibrium speciation of Pb vs. pH in the solution: $Pb_T = 5 \times 10^{-7} M$ , $CIT_T = 100Pb_T$ , $I = 10^{-3}$ , carbonate-free	116
5.20b	Equilibrium speciation of Pb vs. pH in the system: $Pb_T = 5 \times 10^{-7} M$ , $CIT_T = 100Pb_T$ , $S = 75 m^2/l$ Min-U-Sil, $I = 10^{-3}$ , carbonate-free. (James-Healy Model)	116
5.21	Adsorption of Pb on Min-U-Sil vs. pH in the presence and absence of citrate in the system: $Pb_T = 5 \times 10^{-7} M$ , $S = 75 m^2/l$ , $I = 10^{-3}$ , carbonate-free. (James-Healy Model)	118
5.22	Adsorption of Pb on Min-U-Sil vs. pH in the presence and absence of citrate in the system: $Pb_T = 5 \times 10^{-7} M$ , $S = 75 m^2/l$ , $I = 10^{-3}$ , carbonate-free. (Ion Exchange- Surface Complex Formation Model).	119
5.23	Equilibrium speciation of Cu and Pb vs. pH in the solution: $Cu_T = Pb_T = 5 \times 10^{-7} M$ , $EDTA_T = 0.5Cu_T = 0.5Pb_T$ , $I = 10^{-3}$ , carbonate-free.	121
5.24	Equilibrium distribution of Cu and Pb vs. pH in the system: $Cu_T = Pb_T = 5 \times 10^{-7} M$ , $EDTA_T = 0.5Cu_T = 0.5Pb_T$ , $S = 50 m^2/l$ Min-U-Sil, $I = 10^{-3}$ , carbonate-free. (J-H Model)	122
5.25	Equilibrium speciation of Cu and Pb vs. pH in the solution: $Cu_T = Pb_T = 5 \times 10^{-7} M$ , $EDTA_T = Cu_T = Pb_T$ , $I = 10^{-3}$ , carbonate- free.	124
5.26	Equilibrium distribution of Cu and Pb vs. pH in the system: $Cu_T = Pb_T = 5 \times 10^{-7} M$ , $EDTA_T = Cu_T = Pb_T$ , $S = 50 m^2/l$ , Min- U-Sil, $I = 10^{-3}$ , carbonate-free. (James-Healy Model)	125
5.27	Adsorption of Pb on Min-U-Sil vs. pH in the presence and absence of EDTA in the system: $Pb_T = Cu_T = 5 \times 10^{-7} M$ , $S = 50 m^2/l$ , $I = 10^{-3}$ , carbonate-free. (James-Healy Model)	126
5.28	Adsorption of Cu on Min-U-Sil vs. pH in the presence and absence of EDTA in the system: $Cu_T = Pb_T = 5 \times 10^{-7} M$ , $S = 50 m^2/l$ , $I = 10^{-3}$ , carbonate-free. (James-Healy Model)	127

Figure	Title	Page
6.1a	Equilibrium speciation of Pb vs. pH in the solution: $Pb_T = 5 \times 10^{-7} M$ , $I = 10^{-3}$ , $pCO_2 = 10^{-3.5}$ atm.	134
6.1b	Equilibrium distribution of Pb vs. pH in the system: $Pb_T = 5 \times 10^{-7} M$ , $S = 50 m^2/l$ , $I = 10^{-3}$ , $pCO_2 = 10^{-3.5}$ atm.	134
6.2a	Equilibrium speciation of Pb vs. pH in the solution: $Pb_T = 5 \times 10^{-7} M$ , $CIT_T = 10 Pb_T$ , $I = 10^{-3}$ , $pCO_2 = 10^{-3.5}$ atm.	135
6.2b	Equilibrium distribution of Pb vs. pH in the system: $Pb_T = 5 \times 10^{-7} M$ , $CIT_T = 10 Pb_T$ , $S = 50 m^2/l$ Min-U-Sil, $I = 10^{-3}$ , $pCO_2 = 10^{-3.5}$ atm. (James-Healy Model)	135
6.3a	Equilibrium speciation of Pb vs. pH in the solution: $Pb_T = 5 \times 10^{-7} M$ , $CIT_T = 100 Pb_T$ , $I = 10^{-3}$ , $pCO_2 = 10^{-3.5}$ atm.	136
6.3b	Equilibrium distribution of Pb vs. pH in the system: $Pb_T = 5 \times 10^{-7} M$ , $CIT_T = 100 Pb_T$ , $S = 50 m^2/l$ Min-U-Sil, $I = 10^{-3}$ , $pCO_2 = 10^{-3.5}$ atm. (James-Healy Model)	136
6.4	Adsorption of Pb on Min-U-Sil vs. pH in the presence and absence of citrate in the system: $Pb_T = 5 \times 10^{-7} M$ , $S = 50 m^2/l$ , $I = 10^{-3}$ , $pCO_2 = 10^{-3.5}$ atm. (James-Healy)	137
6.5	Adsorption of Pb on Min-U-Sil vs. pH in the presence and absence of citrate in the system: $Pb_T = 5 \times 10^{-7} M$ , $S = 2.4 \times 10^{-4} M$ ( $50 m^2/l$ ), $I = 10^{-3}$ , $pCO_2 = 10^{-3.5}$ atm.	139
6.6a	Equilibrium speciation of Cu vs. pH in the solution: $Cu_T = 10^{-7} M$ , $I = 10^{-3}$ , $pCO_2 = 10^{-3.5}$ atm.	141
6.6b	Equilibrium distribution of Cu vs. pH in the system: $Cu_T = 10^{-7} M$ , $S = 50 m^2/l$ Min-U-Sil, $I = 10^{-3}$ , $pCO_2 = 10^{-3.5}$ atm. (James-Healy Model)	141
6.7a	Equilibrium speciation of Cu vs. pH in the solution: $Cu_T = 10^{-7} M$ , $CIT_T = 0.5 Cu_T$ , $I = 10^{-3}$ , $pCO_2 = 10^{-3.5}$ atm.	143
6.7b	Equilibrium distribution of Cu vs. pH in the system: $Cu_T = 10^{-7} M$ , $CIT_T = 0.5 Cu_T$ , $S = 50 m^2/l$ Min-U-Sil, $I = 10^{-3}$ , $pCO_2 = 10^{-3.5}$ atm. (James-Healy Model)	143

Figure	Title	Page
6. 8a	Speciation of Cu vs. pH in the solution: $Cu_T=10^{-7} M$ , $CIT_T=Cu_T$ , $I=10^{-3}$ , $pCO_2=10^{-3.5}$ atm.	144
6. 8b	Distribution of Cu vs. pH in the system: $Cu_T=10^{-7} M$ , $CIT_T=Cu_T$ , $S=50m^2/l$ Min-U-Sil, $I=10^{-3}$ , $pCO_2=10^{-3.5}$ atm. (James-Healy Model)	144
6. 9a	Equilibrium speciation of Cu vs. pH in the solution: $Cu_T=10^{-7} M$ , $CIT_T=10Cu_T$ , $I=10^{-3}$ , $pCO_2=10^{-3.5}$ atm.	145
6. 9b	Equilibrium distribution of Cu vs. pH in the system: $Cu_T=10^{-7} M$ , $CIT_T=10Cu_T$ , $S=50m^2/l$ Min-U-Sil, $I=10^{-3}$ , $pCO_2=10^{-3.5}$ atm. (James-Healy Model)	145
6. 10	Adsorption of Cu on $\alpha$ -quartz vs. pH in the presence and absence of citrate in the system: $Cu_T=10^{-7} M$ , $S=2.4 \times 10^{-4} M$ , $I=10^{-3}$ , $pCO_2=10^{-3.5}$ atm. $Log^* \beta_2 Cu(OH)_2(aq) = -17.3$ . (Ion Exchange-Surface Complex)	146
6. 11	Adsorption of Cu vs. pH in the presence and absence of citrate in the system: $Cu_T=10^{-7} M$ , $S=2.4 \times 10^{-4} M$ , $I=10^{-3}$ , $pCO_2=10^{-3.5}$ atm. $Log^* \beta_2 Cu(OH)_2(aq) = -13.7$ .	148
6. 12	Adsorption of Cu on Min-U-Sil vs. pH in the presence and absence of citrate in the system: $Cu_T=10^{-7} M$ , $S=50m^2/l$ , $I=10^{-3}$ , $pCO_2=10^{-3.5}$ atm. $Cu(OH)_2(s)$ not included in computations. (James-Healy Model)	150
6. 13	Adsorption of Cu on Min-U-Sil vs. pH in the presence and absence of citrate in the system: $Cu_T=10^{-7} M$ , $S=50m^2/l$ , $I=10^{-3}$ , $pCO_2=10^{-3.5}$ atm. $Log^* \beta_2 Cu(OH)_2(aq) = -17.3$ . (James-Healy Model)	151
6. 14	Adsorption of Cu on Min-U-Sil vs. pH in the presence and absence of citrate in the system: $Cu_T=10^{-7} M$ , $S=50m^2/l$ , $I=10^{-3}$ , $pCO_2=10^{-3.5}$ atm. $Log^* \beta_2 Cu(OH)_2(aq) = -13.7$ . (James-Healy Model)	152
7. 1	Flow chart summary of the present research.	158
8. 1	Speciation of Pb(II) in natural fresh waters as a function of pH in the presence of $1.55 m^2/l$ $SiO_2(s)$ .	165

Figure	Title	Page
8.2	Speciation of Cu(II) in natural fresh waters as a function of pH ( $\log^*\beta_2 \text{Cu(OH)}_2(\text{aq}) = -13.7$ ) in the presence of $1.55 \text{ m}^2/\ell \text{ SiO}_2(\text{s})$ .	166
8.3	Distribution of Cu(II) in natural fresh waters as a function of pH ( $\log^*\beta_2 \text{Cu(OH)}_2(\text{aq}) = -17.3$ ) in the presence of $1.55 \text{ m}^2/\ell \text{ SiO}_2(\text{s})$ .	166
8.4	Speciation of Co(II) in natural fresh waters as a function of pH in the presence of $1.55 \text{ m}^2/\ell \text{ SiO}_2(\text{s})$ .	168
8.5	Speciation of Ni(II) in natural fresh waters as a function of pH in the presence of $1.55 \text{ m}^2/\ell \text{ SiO}_2(\text{s})$ .	168
8.6	Speciation of Zn(II) in natural fresh waters as a function of pH in the presence of $1.55 \text{ m}^2/\ell \text{ SiO}_2(\text{s})$ .	168
8.7	Distribution of Cd(II) in natural fresh waters as a function of pH in the presence of $1.55 \text{ m}^2/\ell \text{ SiO}_2(\text{s})$ .	168
8.8	Speciation of Hg(II) in natural fresh waters as a function of pH in the presence of $1.55 \text{ m}^2/\ell \text{ SiO}_2(\text{s})$ .	168
8.9	Adsorption of trace metals in oxidizing fresh waters as a function of surface area of $\text{SiO}_2(\text{s})$ in $\text{ha}/\ell$ .	175
8.10	Distribution of metals in natural waters at pH 7 as a function of pEDTA.	178
8.11	Distribution of metals in natural fresh waters at pH 7 as a function of pCIT.	180
8.12	Distribution of metals in natural fresh waters in the presence of different amounts of histidine.	181
8.13	Distribution of metals in natural fresh waters in the presence of different amounts of aspartic acid.	183
8.14	Distribution of metals in fresh waters in the presence of different amounts of cysteine.	184

Figure	Title	Page
8.15	Speciation of trace metals in natural fresh waters in the presence of organic ligands as a function of surface area of $\text{SiO}_2(\text{s})$ in $\text{ha}/\ell$ .	186
8.16	Adsorption of Cu on $\text{SiO}_2(\text{s})$ in oxidizing fresh waters of pH 7 as a function of surface area ( $\text{ha}/\ell$ ) and concentration of citrate.	189
8.17	Adsorption of Pb on $\text{SiO}_2(\text{s})$ in oxidizing fresh waters of pH 7 as a function of surface area ( $\text{ha}/\ell$ ) in the presence and absence of citrate.	189
8.18	Adsorption of Ni on $\text{SiO}_2(\text{s})$ in oxidizing fresh waters of pH 7 as a function of surface area ( $\text{ha}/\ell$ ) in the presence and absence of citrate.	189
8.19	Speciation of Cd in oxidizing fresh waters of pH 7 as a function of surface area ( $\text{ha}/\ell$ ) in the absence and presence of citrate.	190
8.20	Speciation of Fe in oxidizing fresh waters of pH 7 as a function of surface area ( $\text{ha}/\ell$ ) in the absence and presence of citrate.	190

## Chapter 1

## INTRODUCTION

1.1 Introduction

Previous investigations into the factors that control the species distributions of trace metals in natural waters indicate that in the case of adsorption of trace metals on solid surfaces, the most important environmental parameters are (a) the type of trace metal and its concentration, (b) the type of the adsorbent and the available surface area, (c) pH, (d) temperature, and (e) types and concentrations of organic and inorganic ligands present. Our present knowledge concerning the influence of organic and inorganic ligands, however, is lacking detailed and systematic analyses. There is, therefore, a need to investigate the effect of complexation on the chemical speciation and adsorption of trace metals on solid surfaces.

This research is concerned with the adsorption of Pb(II) and Cu(II) on  $\alpha$ -quartz as a function of the composition of the aquatic environment. Pb(II) and Cu(II) were selected for the following reasons:

- 1) The biological availability of these metals is expected to depend upon the concentrations of their free metal ions.

Adsorption, the formation of precipitates and complexation with inorganic and organic ligands (of bio-as well as

anthropogenic origin), all serve to determine the equilibrium concentrations of free metal ions.

- 2) No comprehensive investigation into the correlation between the adsorption of Pb(II) and Cu(II) and the composition of aqueous solution has yet been carried out, insofar as a literature search has determined.
- 3) The experimental data obtained will not only improve our knowledge about the chemical behavior of Pb(II) and Cu(II) in natural waters, but will also aid our understanding of the factors that control the distributions of all trace metals in natural waters.
- 4) The information obtained about the interactions between adsorption and complexation, when coupled with some intelligent estimates and the results of other investigators, can be used in models of chemical behavior of trace metals in natural aquatic systems.

Prior to a more detailed description of the purpose and organization of this thesis, some observations concerning the distributions of Pb(II) and Cu(II) in fresh waters will be made. Special attention will be given to the role of organic matter in determining the species distributions.

## 1.2 Limnological Studies on the Distributions of Pb(II) and Cu(II)

Kopp and Kroner (1968) attempted to measure the distributions of some trace metals between the dissolved and suspended fractions in the major rivers of the United States. Their results show that elements such as copper, lead, and zinc were found in both the suspended and the dissolved fractions. Aluminum, manganese, and iron were found to be predominantly associated with the suspended matter. The average dissolved barium concentration was two to three times that of the suspended barium concentration. Strontium was rarely observed to be in the suspended fraction, but was found in solution in almost all of the samples.

Perhac (1972) collected samples from two streams in Tennessee. He extracted three classes of solids from these samples by continuous flow ultracentrifugation: coarse particulates ( $>1500 \text{ \AA}$ ), colloidal particulates ( $<1500 \text{ \AA}$ ,  $>100 \text{ \AA}$ ), and dissolved solids. The dissolved solids in the remaining effluent were recovered by evaporation. The three solid fractions were dissolved by treatment in  $\text{HNO}_3$ ,  $\text{HF}$ ,  $\text{HClO}_4$ , and  $\text{HCl}$ , and analyzed for Pb, Cu, Cd, Co, Ni, Zn, Mn, and Fe. The highest concentrations of metals (ppm metal in solid) were found in the colloidal, and the lowest ones in the dissolved solids fraction. In particular, 62 to 2820 ppm Pb and 1575 to 4750 ppm Cu were found in colloidal particulates, 124 to 653 ppm Pb and 85 to 647 ppm Cu in coarse particulates, and only 75 to 96 ppm Pb and 72 to 170 ppm Cu

in dissolved solids.

Gibbs (1973) studied the distributions of trace metals in the Amazon and Yukon Rivers and suggested that Cu and Cr are found mainly in crystalline solids, that Mn is present mostly as particle coatings, and that Fe, Ni, and Co are approximately equally distributed between precipitated particle coatings and crystalline solids.

Organic matter is an important factor controlling the distribution and speciation of trace metals in natural waters. Barsdate and Matson (1967) measured the concentrations of metals in some Alaskan lakes using anodic stripping voltammetry. In the lakes with high organic contents, they found that copper, lead, and zinc are present as free metal ions or as weak complexes at low concentrations (less than  $0.1 \mu\text{g}/\text{l}$ ). The oxidation of the organic substances in the samples with persulfate resulted in significant release of each metal from what were, apparently, strong complexes. In lakes with low organic matter contents, the concentrations of metal-organic complexes (if present) were small compared to the concentrations of the free metal ions.

Allen et al. (1970) also analyzed a number of lake and river water samples (the Rouge and Detroit Rivers and Lake Erie) for their free and complexed (acid-exchangeable) metal content by anodic stripping voltammetry. Concentrations of free metal ions of Pb and Cu ranged from  $0.07$  to  $2.2 \mu\text{g}/\text{l}$  and from  $0.5$  to  $18 \mu\text{g}/\text{l}$ , respectively.

Concentrations of the acid-exchangeable Pb and Cu (obtained after acidification of samples) were much higher, ranging from 0.6 to 37  $\mu\text{g}/\text{l}$  for Pb and 0.4 to 108  $\mu\text{g}/\text{l}$  for Cu. The addition of 0.13  $\mu\text{g}/\text{l}$  of  $\text{Cu}^{2+}$  to a 10-ml sample of the Rouge River water resulted in a decrease of the peak current with time. This decrease was ascribed to the complexation of copper with naturally occurring ligands in the water.

### 1.3 Objectives of the Present Work and Organization of this Thesis

It was the purpose of this research to investigate the conditions under which the trace metals are retained by a  $\text{SiO}_2$  surface, ( $\alpha$ -quartz), and to determine the variations of this adsorption behavior as a function of pH and the concentration of organic and inorganic ligands. In particular, laboratory experiments were designed to provide adsorption data for Pb(II) and Cu(II) on  $\alpha$ -quartz as a function of time, surface area, pH, ionic strength, and organic ligand concentrations. Particular attention was given to the adsorption behavior of these metals in carbonate-containing solutions. Citrate and EDTA (ethylenediaminetetraacetate) were included as representative complexing agents. The experimental work also included the examination of the adsorption behavior of doubly charged major cations, Ca(II) and Mg(II), as a function of pH. Concentrations of metals were followed by atomic absorption spectrophotometry (Chapter 3 contains descriptions of the experimental and analytical techniques employed). The chemical

speciation in solution and the positions of the adsorption equilibria were demonstrated to be strongly affected by pH, ionic strength, and the concentrations of organic ligands (Chapters 5 and 6).

The experimental results were interpreted in terms of chemical equilibrium-plus-adsorption computations using two different adsorption models: one that is mainly an electrostatic model, i. e. , the James-Healy Model for the adsorption of hydrolyzable metal ions (James and Healy (1972c)), and one that is mainly chemical, i. e. , the Ion Exchange-Surface Complex Formation Model (Dugger et al. (1964)); Schindler and Gamsjäger (1972); Stumm et al. (1970); Schindler et al. (1975)). Detailed descriptions and analyses of both models together with theoretical considerations concerning the influence of organic and inorganic ligands on the adsorption of metals are given in Chapter 2.

The equilibrium computations were obtained using the REDEQL2 program (McDuff and Morel (1973)). REDEQL2 is a chemical equilibrium program that includes acid-base, precipitation-dissolution, redox, and adsorption processes. The subroutines INADS and ADSORP are used together with the rest of the program to compute adsorption equilibria for an oxide surface according to the James-Healy Model. In addition to INADS, the IONADS subroutine is employed in place of the ADSORP subroutine in order to compute the adsorption equilibria according to the Ion Exchange-Surface Complex Formation Model. More

detailed information about the REDEQL2 program is offered in Chapter 5.

The main difficulty with the theoretical predictions was the lack of the reliable data for the second hydrolysis constant for Cu(II). Chapter 4 examines the hydrolysis behavior of Pb(II) and Cu(II) and discusses the choice of the second hydrolysis constant of Cu(II), based on potentiometric titrations of  $\text{Cu}^{2+}$ .

Chapter 7 gives a brief summary of Chapters 2-6. In Chapter 8 the experimental data and the conclusions drawn from this work are applied in models of the chemical behavior of trace metals in oxic fresh waters. Special emphasis is given to Pb(II) and Cu(II). Several conclusions are reached concerning the chemical behavior of trace metals in fresh oxic aquatic environments.

## Chapter 2

THEORETICAL CONSIDERATIONS IN METAL  
ADSORPTION AT OXIDE SURFACES2.1 James-Healy Model

James and Healy (1972a, 1972b, 1972c) developed a model for the adsorption of hydrolyzable metal ions at the oxide-water interface. The model is based on simple electrostatic ion-solid and ion-solvent interactions. The energy of adsorption of metal ions at the solid oxide-water interface is treated in terms of the combination of energy changes; the change of the standard free energy of adsorption ( $\Delta G_{ads,i}^{\circ}$ ) of each species "i" is the sum of the change in the coulombic energy ( $\Delta G_{coul,i}^{\circ}$ ), the solvation energy ( $\Delta G_{solv,i}^{\circ}$ ), and the specific (chemical) energy ( $\Delta G_{chem,i}^{\circ}$ ):

$$\Delta G_{ads,i}^{\circ} = \Delta G_{coul,i}^{\circ} + \Delta G_{solv,i}^{\circ} + \Delta G_{chem,i}^{\circ} \quad (2.1)$$

2.1.1 Coulombic Energy

The electrostatic work required to bring an ion from the bulk solution to the interface is, as in the classical models of Gouy-Chapman, Stern and Stern-Grahame, given by:

$$\Delta G_{coul,i}^{\circ} = z_i F \Delta \Psi_x \quad (2.2)$$

where  $z_i$  is the charge of the adsorbing species and  $F$  is the Faraday constant. The change in the potential across the distance  $x$  from the surface,  $\Delta\Psi_x$ , is given by

$$\Delta\Psi_x = \frac{2RT}{zF} \ln \frac{\left( \frac{zF\Psi_o}{2RT} + 1 \right) + \left( \frac{zF\Psi_o}{2RT} - 1 \right) e^{-\kappa x}}{\left( \frac{zF\Psi_o}{2RT} + 1 \right) - \left( \frac{zF\Psi_o}{2RT} - 1 \right) e^{-\kappa x}} \quad (2.3)$$

where  $\Psi_o$  = potential of the surface

$R$  = gas constant

$\kappa$  = double layer parameter

The surface potential,  $\Psi_o$ , is determined by the solution pH and the  $\text{pH}_{\text{PZC}}$  by the Nernst equation

$$\Psi_o = \frac{2.3RT}{zF} (\text{pH}_{\text{PZC}} - \text{pH}) \quad (2.4)$$

For water at 20°C the double layer parameter  $\kappa$  is

$$\kappa = 0.328 \times 10^{10} (I^{1/2}) \quad (2.5)$$

The ionic strength,  $I$ , together with the surface potential, controls the electrical double layer around the particle. If the ionic strength is increased at a constant pH the electrical double layer will be compressed (the double layer thickness  $1/\kappa$  becomes smaller) and  $\Delta G_{\text{coul},i}^o$  becomes smaller. If the pH is increased at a constant ionic strength, the surface potential becomes more negative, resulting in

stronger coulombic interactions between the surface and the metal ions in solution.

### 2.1.2 Secondary Solvation Energy

Ion-solvent interactions oppose adsorption and, therefore, present a barrier which must be overcome in order to accomplish the adsorption of metals on the surfaces. The free energy required to establish a field in a continuous dielectric medium about a spherically symmetric ion is given by Andersen and Bockris (1964) as

$$G^{\circ} = \frac{1}{8\pi} \iiint_{\text{volume}} \bar{X}Ddv \quad (2.6)$$

where  $D$  is the dielectric displacement and  $\bar{X}$  is the electric field vector ( $\bar{X}=D/\epsilon$ ).

In polar coordinates,  $(\theta, \phi, R)$ , originating at the center of the ion of charge  $z$ , and in a medium characterized by its dielectric constant  $\epsilon$ ,  $G$  is always positive since the zero of energy is the uncharged ion (Andersen and Bockris (1964)):

$$G^{\circ} = \frac{z^2 e^2}{4\pi} \int_{\phi=0}^{2\pi} \int_{\zeta=0}^{\pi} \int_{\rho=r_i}^{\infty} \frac{\sin\zeta d\zeta d\phi d\rho}{\epsilon\rho^2} \quad (2.7)$$

where  $e$  = elementary charge.

When an ion moves from one environment to another of different dielectric constant, the corresponding free-energy change

$$\Delta G^{\circ} = \frac{z^2 e^2}{4\pi} \int_{\phi=0}^{2\pi} \int_{\zeta=0}^{\pi} \int_{\rho=r_i}^{\infty} \frac{\sin \zeta d\zeta d\phi d\rho}{\rho^2} \left( \frac{1}{\epsilon_b} - \frac{1}{\epsilon_a} \right) \quad (2.8)$$

shows that moving an ion from a particular medium (a) to one of higher dielectric constant (b) decreases the free energy. Hence, the change in the free energy in moving an ion from a vacuum to a real (uncharged) medium ( $\epsilon > 1$ ) is always negative.

In order to solve Equation 2.8 it is necessary to evaluate the change in the dielectric constant of interfacial water as a function of increasing field strength and set the limits for integration. James and Healy (1972c) evaluated the dielectric constant of interfacial water from the following expression:

$$\epsilon_{\text{int}} = \frac{\epsilon_{\text{bulk}}^{-A}}{1 + B \left( \frac{d\Psi}{dx} \right)_x} + A \quad (2.9)$$

where  $A (=6)$  is the dielectric constant of the oriented water molecules (owing to electronic and nuclear polarization), and  $\epsilon_{\text{bulk}} (=78.5)$  is the dielectric constant of water in bulk solution where the field strength is zero.  $B$  is an experimentally determined parameter with the value of  $1.2 \times 10^{-17} \text{ m}^2 \text{ V}^{-2}$ . The electric field strength  $\left( \frac{d\Psi}{dx} \right)_x$  can be estimated from the Gouy-Chapman Model

$$\frac{d\Psi}{dx} = -2\kappa \frac{RT}{zF} \sinh \left( \frac{zF\Delta\Psi x}{2RT} \right) \quad (2.10)$$

The metal ion can be found at two locations: in the diffuse layer or in the compact part of the double layer (Figure 2.1). For adsorption into the compact double layer the distance between the ion and the interface is, according to James and Healy (1972c), fixed by the hydrated ionic radius, ( $r_{\text{ion}} + 2r_{\text{w}} = x$ ). This sets the limits for integration of Equation 2.8. The resulting expression for the change in secondary solvation free energy of an ion moving from the bulk solution to the IHP (inner Helmholtz plane) is

$$\Delta G_{\text{solv},i}^{\circ} = \left( \frac{z_i^2 e^2}{16\pi\epsilon_o} \right) \left( \frac{1}{r_{\text{ion}} + 2r_{\text{w}}} - \frac{r_{\text{ion}}}{2(r_{\text{ion}} + 2r_{\text{w}})^2} \right) \left( \frac{1}{\epsilon_{\text{int}}} - \frac{1}{\epsilon_{\text{bulk}}} \right) + \left( \frac{z_i^2 e^2 N}{32\pi\epsilon_o} \right) \left( \frac{1}{r_{\text{ion}} + 2r_{\text{w}}} \right) \left( \frac{1}{\epsilon_{\text{solid}}} - \frac{1}{\epsilon_{\text{int}}} \right) \quad (2.11)$$

where  $\epsilon_o = 8.85 \times 10^{-12}$  Farad meter<sup>-1</sup>

$N$  = Avogadro's number

$r_{\text{ion}}$  = radius of the ion

$r_{\text{w}}$  = radius of water

$\epsilon_{\text{solid}}$  = dielectric constant of the solid

Owing to the quadratic dependence of the solvation energy on the charge of the ion, reduction in the charge by hydrolysis will result in an abrupt decrease in  $\Delta G_{\text{solv}}^{\circ}$ . Once the solvation energy barrier is overcome, coulombic and other short-range interactions may be

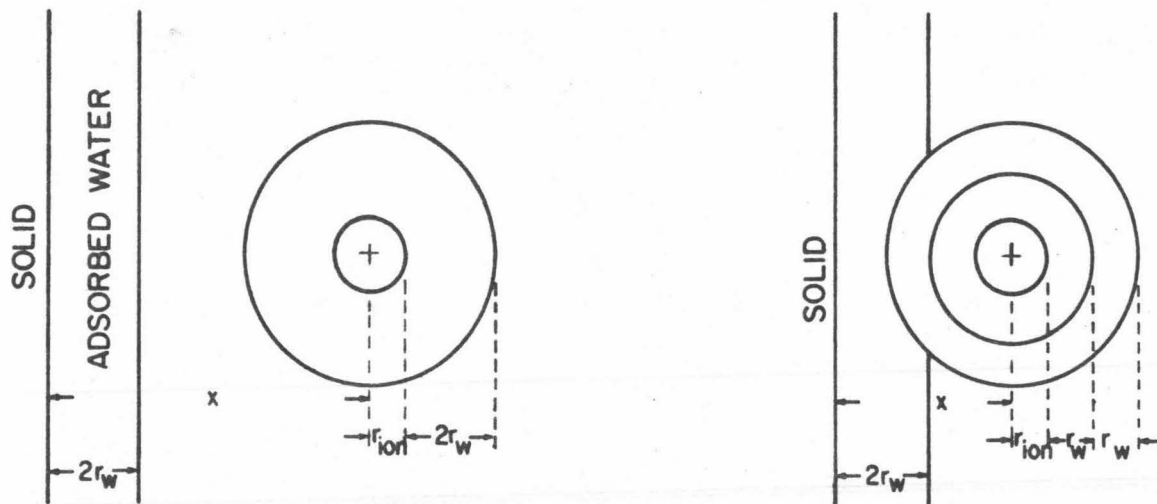


Figure 2.1 Locations of a metal ion in the double layer of the Oxide-Water Interface according to the James-Healy Model.

sufficiently large to prevail, resulting in increased adsorption.

The dielectric constant of the solid ( $\epsilon_{\text{solid}}$ ) is an important property in determining the changes in  $\Delta G_{\text{solv}}^{\circ}$ . For insulating oxides, i. e., for oxides with a low dielectric constant (such as  $\text{SiO}_2$  with  $\epsilon_{\text{solid}}=4.3$ ) work must be done to remove the secondary hydration sheath. This work results in a large positive solvation energy (Figure 2.2b). For high dielectric solids, such as  $\text{TiO}_2$  ( $\epsilon_{\text{solid}}=78.5$ ) the change in the solvation energy is small compared with the change in the solvation energy for  $\text{SiO}_2$  (Figure 2.2c). The coulombic and chemical interactions will dominate the free energy of adsorption. Since  $\delta\text{-MnO}_2$  and  $\text{SiO}_2$  have similar  $\text{pH}_{\text{PZC}}$  the same basic adsorption characteristics would be expected for both. However, since they differ markedly in their dielectric constants,  $\delta\text{-MnO}_2$  has adsorption characteristics similar to  $\text{TiO}_2$ , rather than  $\text{SiO}_2$  (Figure 2.2d).  $\text{Fe(OH)}_3$  has a dielectric constant of 14.2 and, therefore, the change in the solvation energy is expected to be less positive than in the case of  $\text{SiO}_2$ , but more than for  $\delta\text{-MnO}_2$ . However, because of the high  $\text{pH}_{\text{PZC}}$ ,  $\text{Fe(OH)}_3$  has adsorption characteristics similar to  $\text{SiO}_2$  rather than  $\delta\text{-MnO}_2$  (Figure 2.2a). Hence, the difference between the metal ion adsorption on different oxides resides in both substrate properties: the dielectric constant of the solid and the  $\text{pH}_{\text{PZC}}$ .

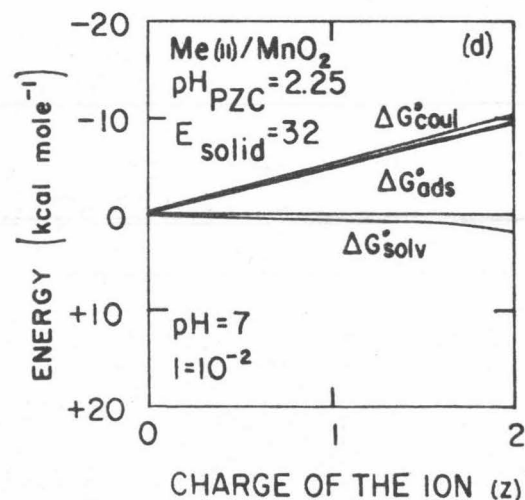
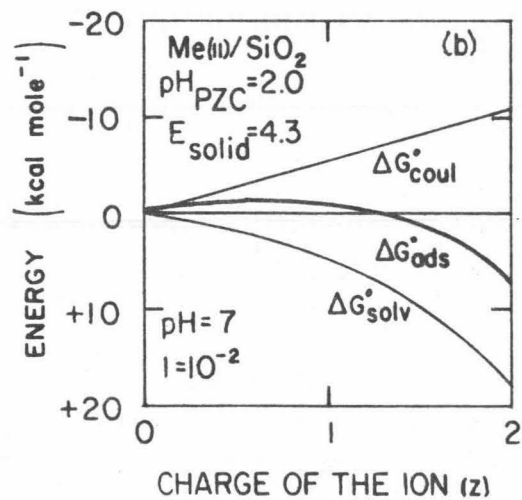
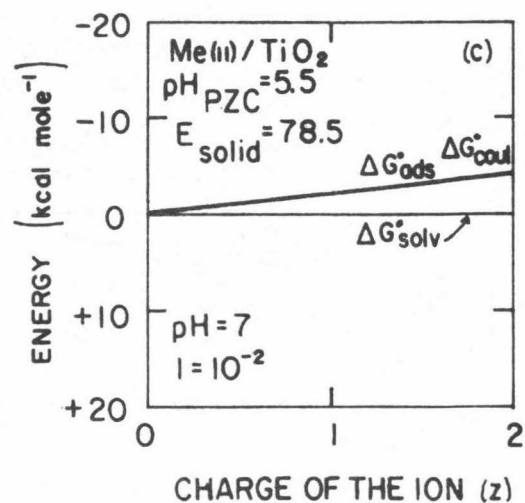
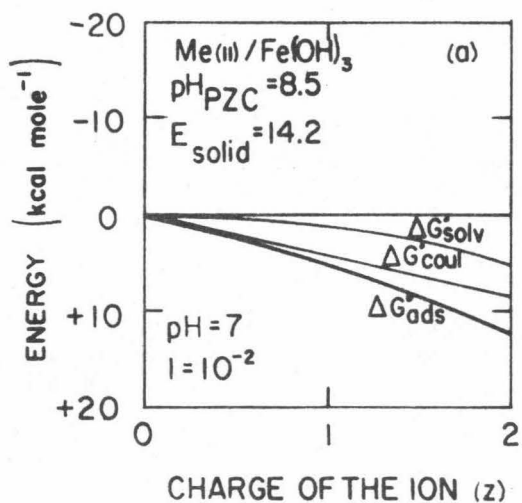


Figure 2.2 Free energies of adsorption of charged and uncharged Me(II)-species on Fe(OH)<sub>3</sub>(s), SiO<sub>2</sub>(s), TiO<sub>2</sub>(s) and MnO<sub>2</sub>(s). The  $\Delta G_{\text{chem}}^{\circ}$  is not shown because it only shifts the  $\Delta G_{\text{ads}}^{\circ}$ -curve, without changing the shape.

### 2.1.3 Chemical Interactions

$\Delta G_{\text{chem}}^{\circ}$  is a term which takes into account all the metal species-solid surface interactions, other than the coulombic and solvation energy: attractive image and dispersion forces suggested by Bockris et al. (1963) and Andersen and Bockris (1964), van der Waals forces and hydrogen bonding through hydroxyl groups in the coordination sphere of the hydrolysis products of the ion.  $\Delta G_{\text{chem},i}^{\circ}$  can be evaluated experimentally only in the case of metal oxide surfaces with sufficiently high  $\text{pH}_{\text{PZC}}$  (e.g.,  $\text{TiO}_2$  which has a  $\text{pH}_{\text{PZC}}$  of 5.5) by obtaining adsorption data. But for surfaces with low  $\text{pH}_{\text{PZC}}$  (such as  $\text{SiO}_2$  with the  $\text{pH}_{\text{PZC}}$  of 2.0)  $\Delta G_{\text{chem},i}^{\circ}$  can be obtained only as a best fit between experimental results and theoretical predictions. In that case  $\Delta G_{\text{chem},i}^{\circ}$  can be also called a "fitting parameter". Consequently, one can say that the James-Healy Model is an electrostatic model which uses chemical interactions primarily as a correction factor.

### 2.2 Ion Exchange-Surface Complex Formation Model

Greenberg (1956), Ahrlund et al. (1960), and Dugger et al. (1964) introduced a completely chemical model based on the idea that the metal oxide surface acts as an ion exchanger. Namely, the surface hydroxyl groups of hydrous metal oxides can be treated as weak acids capable of exchanging their protons for aqueous metal ions. This exchange of protons is not to be confused with the "ion exchange"-term used in the double-

-layer theory, which refers to the electrostatic exchange of counter ions in the diffuse layer or the outer Helmholtz plane for other ions of the same sign in the bulk solution. One can describe a chemical ion-exchange system with a set of two equations:



where  $(-\text{SOH})$  and  $(-\text{SO}^-)$  are surface hydroxyl groups

$n$  = number of protons released per  $\text{Me}^{z+}$

$z$  = valence of the metal ion  $\text{Me}$

The stability constant,  $*K^S$ , for reaction 2.13 is

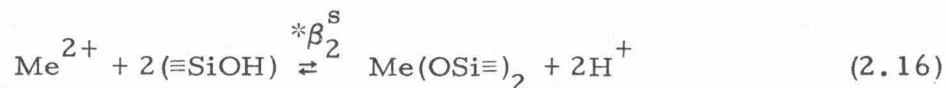
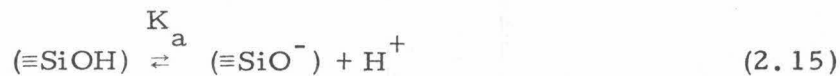
$$*K^S = \frac{[(-\text{SO})_n \text{Me}^{(z-n)}][\text{H}^+]^n}{[-\text{SOH}]^n [\text{Me}^{z+}]} \quad (2.14)$$

where  $[ ]$  means concentrations in moles per liter of solution.

In the experiments performed with silica gel by Maatman and coworkers (Dugger et al. (1964)) measurements were made at low pH ( $\text{pH} \ll \text{pK}_{a, \text{silanol groups}}$ ) so that all the surface groups could be assumed to be in silanol form ( $\equiv\text{SiOH}$ ). Similarly (because of low pH), hydrolysis of the metal ions was assumed to be unimportant. In view of the large range of pH values found in natural waters (4-10), however,

the results of such work are of limited applicability in natural systems. It is necessary, therefore, to develop analytical expressions suitable for the study of metal ion adsorption phenomena on silica over a much larger pH range as well as in the presence of ligands besides  $\text{OH}^-$ .

In the case of two silanol groups reacting with one doubly charged metal ion (i. e.,  $n=m=2$  in equations 2.12 and 2.13), the equilibrium can be given by



where  $\text{K}_a$  is the acidity constant of the surface OH groups, and the equilibrium constant is

$$*\beta_2^s = \frac{[\text{Me}(\text{OSi}\equiv)_2][\text{H}^+]^2}{[\equiv\text{SiOH}]^2[\text{Me}^{2+}]} \quad (2.17)$$

If one assumes that the surface species  $(\equiv\text{SiOH})$  and  $\text{Me}(\text{SiO}\equiv)_2$  constitute a very dilute surface solution, the activities of the surface species can be taken to be proportional to their mole fractions.

The total number of silanol sites is expressed as

$$S = [\equiv\text{SiO}^-] + [\equiv\text{SiOH}] + 2[\text{Me}(\text{OSi}\equiv)_2] \quad (2.18)$$

Let  $\theta$  be the fraction of the protonated silanol sites,  $\eta$  the fraction of the unprotonated ones and  $\xi$  the silanol sites bound to the metal, i. e.,

$$\theta = \frac{[\equiv\text{SiOH}]}{S} \quad \eta = \frac{[\equiv\text{SiO}^-]}{S} \quad \xi = \frac{2[\text{Me}(\text{OSi}\equiv)_2]}{S} \quad (2.19)$$

$$\theta + \eta + \xi = 1 \quad (2.20)$$

According to Equation 2.15  $\eta$  can be written as

$$\eta = \frac{K_a}{[\text{H}^+]} \frac{[\equiv\text{SiOH}]}{S} = \frac{K_a}{[\text{H}^+]} \theta \quad (2.21)$$

Equation 2.20 can be rewritten as

$$\left(1 + \frac{K_a}{[\text{H}^+]}\right) \theta + \xi = \alpha_o^{-1} \theta + \xi = 1 \quad (2.22)$$

From Equation 2.19 one obtains

$$[\equiv\text{SiOH}] = \theta S \quad (2.23)$$

and from Equations 2.18, 2.21 and 2.23

$$[\text{Me}(\text{OSi}\equiv)_2] = \frac{S}{2} (1 - \alpha_o^{-1} \theta) \quad (2.24)$$

The mole fractions of these surface species  $\left(\frac{\text{surface species}}{\sum \text{surface species}}\right)$

are, then, given by

$$X_{(\equiv\text{SiOH})} = \frac{\theta}{\alpha_o^{-1} \theta + \frac{1 - \alpha_o^{-1}}{2}} = \frac{2\theta}{1 + \alpha_o^{-1} \theta} \quad (2.25)$$

$$X_{\text{Me(OSi}\equiv)_2} = \frac{(1-\alpha_o^{-1}\theta)/2}{\alpha_o^{-1}\theta + (1-\alpha_o^{-1}\theta)/2} = \frac{1-\alpha_o^{-1}\theta}{1+\alpha_o^{-1}\theta} \quad (2.26)$$

By substituting Equations 2.25 and 2.26 into Equation 2.17 one can obtain the following equation for the ion-exchange stability constant of the reaction between the free metal ion and the surface silanol groups, assuming 1:2 stoichiometry:

$$*\beta_2^s = \frac{1}{4\theta^2} [1 - (\alpha_o^{-1}\theta)^2] \frac{[\text{H}^+]^2}{[\text{Me}^{2+}]} \quad (2.27)$$

Assuming 1:1 stoichiometry between the adsorbing metal ion and the surface, i. e., the reaction

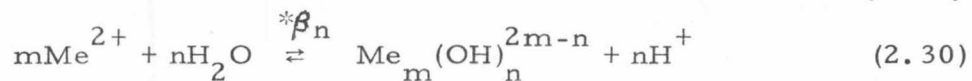


one can derive the corresponding expression for the stability constant

$$*\text{K}_1^s = \frac{1-\alpha_o^{-1}\phi}{\phi} \frac{[\text{H}^+]}{[\text{Me}^{2+}]} \quad (2.29)$$

where  $\phi$  is the fraction of the silanol sites present in their protonated form.

If the solution conditions are such that the metal ion is hydrolyzed



where  $*\beta_n$  = overall hydrolysis constant

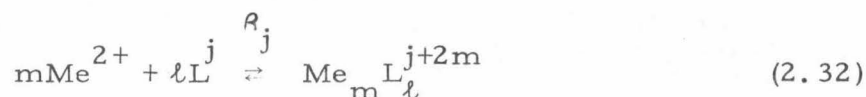
$m, n$  = stoichiometric coefficients of the (+2) charged metal and OH groups, respectively

it is necessary to determine the concentration of the free metal ion by

$$[Me^{2+}] = Me_{TOT(aq)} \sum_n \left( \frac{[H^+]^n}{*\beta_n} \right)^{\frac{1}{m}} \quad (2.31)$$

where  $Me_{TOT(aq)}$  = total concentration of metal in solution

In the most general case one must take into account all complexing ligands present in the system. Letting L denote all ligands except hydroxide, the following reaction describes the influence of complexation of the free metal ion:



where  $\beta_j$  = stability constant

$\ell$  = stoichiometric coefficient of ligand L having a charge j

In this case Equation 2.31 can be expanded into

$$[Me^{2+}] = Me_{TOT(aq)} \left[ \sum_n \frac{[H^+]^n}{*\beta_n} + \sum_\ell \frac{1}{\beta_\ell L^\ell} \right]^{\frac{1}{m}} \quad (2.33)$$

Substituting this expression for  $[Me^{2+}]$  into Equations 2.27 and 2.29 results in two general equations describing the equilibria for the reactions between a surface that contains silanol groups and an aqueous

solution containing a divalent metal ion and different (non-adsorbing) organic and inorganic ligands:

$$*\beta_2 = \frac{1}{4\theta^2} [1 - (\alpha_o^{-1}\theta)^2] \frac{[H^+]^2}{Me_{TOT(aq)} \left[ \sum_n \frac{[H^+]^n}{*\beta_n} + \sum_\ell \frac{1}{\beta_\ell L^\ell} \right]^{\frac{1}{m}}} \quad (2.34)$$

$$*K_1^s = \frac{1 - \alpha_o^{-1}\theta}{\theta} \frac{[H^+]}{Me_{TOT(aq)} \left[ \sum_n \frac{[H^+]^n}{*\beta_n} + \sum_\ell \frac{1}{\beta_\ell L^\ell} \right]^{\frac{1}{m}}} \quad (2.35)$$

where  $\alpha_o^{-1} = 1 + \frac{K_a}{[H^+]}$

### 2.2.1 Electrostatic Influence

Onoda and De Bruyn (1966) have pointed out that when ferric oxide is placed in contact with an aqueous solution its surface becomes hydrated to some depth. By a process of adsorption (or desorption) a distribution of protons between the surface of the hydrated region and the solution phase takes place and leads to the charging of the electrical double layer at the interface. Protons diffusing into or out of this region create a proton-excess or a proton-deficit in the lattice and build up a proton-excess or proton-deficit space charge, thereby extending the double layer into the solid.

Schindler and Kamber (1968), Stumm, Huang and Jenkins (1970) and Block and DeBruyn (1970a, 1970b) also observed the electrostatic influence of the charge groups on the leaving protons. Lohman (1972) found that, if one looks at the adsorption of the ions at the oxide/electrolyte interface in terms of the stability of the complexes which are formed in the solution by corresponding ions, one finds a strong parallel between the ion adsorbability and the complex stability. But, he points out, generalization of this model is not possible without additional assumptions about the influence of the oxide lattice structure and the hydroxylation of the oxide interface.

Protolysis of the surface OH groups, according to Schindler and Gamsjäger (1972), results in a change in surface charge; transferring the proton against this field of charged groups to the bulk solution involves electrical work. The acidity constant of the surface OH groups must be corrected for the presence of the electric field. Schindler and Gamsjäger (1972) gave the following expression for the acidity constant of the surface OH groups:

$$K_a = K_{int} \exp(F\Psi_o/RT) \quad (2.36)$$

where  $K_{int}$  (intrinsic acidity constant) denotes the acidity constant in the absence of an electric field, and  $\Psi_o$  the difference in potentials between the site of dissociation and the bulk solution.  $\Psi_o$  is given by

Nernst equation (Equation 2.4).

The intrinsic acidity constant for silanol groups was reported by Schindler and Kamber (1968) as  $\log K_{int} = -6.8$ .

Investigations of Weber and Stumm (1964) and Olson and O'Melia (1973) have shown that partially deprotonated orthosilicic acid can act as a monodentate and bidentate ligand for metal ions. Schindler et al. (1975) and Hohl and Stumm (1975) stated that hydrous oxide surface groups can be treated in a similar fashion as species capable of forming bonds with metal ions. Hence, one can state that Greenberg (1956), Ahrland et al. (1960) and Dugger et al. (1964) using the term "ion exchange", and Schindler et al. (1975) and Hohl and Stumm (1975), using the term "surface complex formation", are referring to the same chemical reactions between the surface OH groups and metal ions.

The overall distribution of a given metal ion, according to this Ion Exchange-Surface Complex Formation Model, can be, therefore, computed by the use of Equations 2.34 and 2.35, and of the value for the acidity constant of the surface OH groups, corrected for the presence of the electric field (Equation 2.36). Thus, the Ion Exchange-Surface Complex Formation Model, which uses the physical (i. e., electrostatic) phenomena only as a correction factor, is an antithesis of the James-Healy Model.

## 2.3 Influence of Ligands on the Adsorption of Metal Ions

### 2.3.1 Introduction

The addition of a ligand may have the following effects on the adsorption of a given metal:

1. It may reduce the adsorption because of a) high concentration, b) strong complex formation with metal ions, and c) lack of affinity for the surface, or d) by competition for the surface area because of high affinity for the surface and weak complexing tendency.
2. It may not influence the adsorption because of a) low concentration, b) low stability constants for complexation with metal ions, and c) lack of affinity for the surface.
3. It may enhance the adsorption because of the affinity for the surface coupled with strong complex formation with metal ions.

### 2.3.2 Literature Review

It has been inferred from numerous studies that the adsorption of metal ions is not only due to the adsorption of free metal ion, but also to the adsorption of metal-hydroxo or other complexes. If the amount of the adsorption of a hydrolyzable metal ion is plotted as a function of pH, one observes a very sharp increase in the adsorption at a particular pH. Furthermore, hydrolyzable metal ions have been

shown to reverse the charge of their adsorbates and cause destabilization of colloidal systems.

Healy and Jellet (1967) have postulated that polymeric, soluble, uncharged  $Zn(OH)_2$ -polymer is capable of being catalytically nucleated at  $ZnO-H_2O$  interface, resulting in the coagulation of colloidal  $ZnO$ . Healy et al. (1968) proposed that the free aquo  $Co(II)$  ion is not specifically adsorbed without the participation of surface hydroxyls. At pH and concentration conditions just below saturation, they speculated that the adsorbed species is probably a polymeric form of  $Co(II)$  hydroxyde. Hahn and Stumm (1968), similarly, attribute the destabilization of silica dispersions by  $Al(III)$  to the partial or complete neutralization of the negative surface charge by the adsorption of the positively charged multinuclear aluminum-hydroxo complexes.

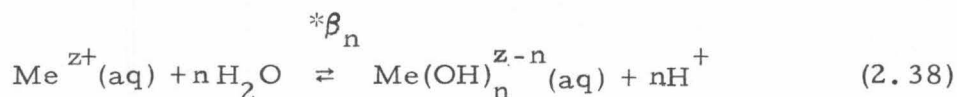
Matijević and coworkers (1960, 1961) studied the influence of various metals on the coagulation and charge reversal of lyophobic colloids (e.g., silver halides). They concluded that the hydrolyzed species of the coagulating electrolyte are responsible for charge reversals and proposed methods for determining the charges of these hydrolyzed species. The methods are based upon the determination of the critical coagulation concentration. The direct relationship between the presence of the mononuclear and polynuclear hydrolyzed species of metal ions ( $ThOH^{3+}$ ,  $Th(OH)_2^{2+}$ ,  $Th(OH)_4$ ,  $Zn(OH)_2$ , and  $Al_8(OH)_{20}^{4+}$ )

and the charge reversal of lyophobic colloids has been discussed by Matijević (1967) in a more elaborate survey presented at the 4th Rudolfs Conference: "... Apparently there is little doubt that reversal of charge by metal ions is accomplished by the adsorption of their hydrolyzed species. It is interesting that most of the compounds active in charge reversal... contain hydroxyl groups... It appears, therefore, that the hydroxyl group is responsible for the adsorption of these ions on colloidal particles leading to charge reversal..." Since the hydrolyzed ions are bonded strongly in various colloidal systems (i. e., they behave in the same manner regardless of the type of the surface), Matijević (1967) concluded that specific chemical interactions are not likely to have a predominant effect on the adsorption of hydrolyzed species. "... Hydrogen bonding, however, may play the decisive role..." The formation of hydrogen bonds between the  $\text{MeOH}^+$  and the surface has been also stressed by McKenzie and O'Brien (1969) and Clark and Cooke (1968).

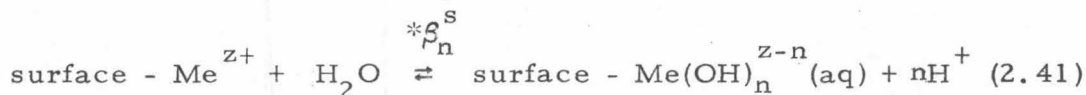
Stumm and O'Melia (1968) offered the following explanation for the observed relationship between adsorption and hydrolysis of metal ions: "... First, hydrolyzed species are larger and less hydrated than nonhydrolyzed species. Second, the enhancement of adsorption is due apparently to the presence of a coordinated hydroxyde group. Simple hydroxide ions are bound strongly at many surfaces and are frequently

potential determining ions; hydroxo-metal complexes may similarly or to an even larger extent be adsorbed to the solid surface. Alternatively, the replacement of an aquo group by a hydroxo-group in the coordination sheath of a metal atom may render the complex more hydrophobic by reducing the interaction between the central metal and the remaining aquo groups...'' As a result, this reduction of solvent-metal ion interactions will enhance the formation of covalent bonds between the colloidal particles and the metal ions. This effect becomes even more pronounced in the case of the formation of polyhydroxopolymetal species, since more than one OH group per "molecule" can be attached to the solid surface (Stumm and O'Melia (1968)).

According to MacNaughton and James (1974), hydrolysis followed by adsorption



is thermodynamically indistinguishable from adsorption of metal ions followed by hydrolysis at the surface



since the combination of reaction 2.38 and 2.39 results in reaction 2.40 plus reaction 2.41. Hence, the stability constant for both sets of equations is  $*\beta_n K_{ads}$ .

MacNaughton (1973) demonstrated the drastic influence of chloride ions on the adsorption of Hg(II) by freshly precipitated ferric hydroxide. Addition of 0.56M  $Cl^-$  resulted in almost completely suppressed adsorption. Addition of  $Cl^-$  to Hg(II)- $SiO_2$  system resulted in the displacement of the adsorption edge. The addition of silicate, sulfate, bicarbonate, and phosphate to a Hg(II)-montmorillonite system did not cause any appreciable changes in the adsorption density (MacNaughton (1973)).

When a complexing agent is introduced into an aqueous system containing metal ions it reacts with cations to form metal-ligand complexes. These complexes have the ability to keep metals in a soluble form under many conditions in which they otherwise would be removed from the solution by precipitation or adsorption.

Soil chemists showed an interest in chelates as trace metal carriers much earlier than water chemists. Investigations included aminopolyacetate chelating agents (Wallace et al. (1955); Wallace and Lunt (1956); Hill-Cottingham and Lloyd-Jones (1957, 1958a, 1958b); Hodgson et al. (1966); Lindsay et al. (1966); Lindsay and Norvell (1969); Norvell and Lindsay (1969, 1970)) and organic acids

(Schnitzer (1969)). A comprehensive review on this subject was done by Norvell (1972), who selected existing information from the fields of chelate chemistry and soil chemistry and combined them to provide a better quantitative understanding of the equilibria of metal chelates in soil solutions.

Stumm (1967) treated the competing effects of  $H^+$  at low pH values and of  $OH^-$ , at high pH values, Fe(III) in solution, organic ligands and precipitation of  $Fe(OH)_3(s)$ , as well as the effect of  $Ca^{2+}$  on complex formation. He showed, for example, that an excess of EDTA at a concentration of  $10^{-3} M$  can keep  $10^{-5} M$  Fe(III) in solution at pH values up to 8. At low pH,  $Ca^{2+}$  does not appreciably interfere with Fe(III) complex formation by  $10^{-3} M$  EDTA. At higher pH values the concentration of soluble Fe(III) falls drastically, as  $Ca^{2+}$  concentration is increased. In this case even higher concentrations of complexing ligand ( $10^{-2} M$  EDTA) are not able to keep  $10^{-3} M$  Fe(III) in solution.

In 1968 Duursma proposed that competition between chelation and sorption determines the amount of metal sorbed by sediment. He found that relatively high amounts of leucine ( $10^{-3} M$  to  $10^{-2} M$ ) must be added if any change in the sorption of Co and Zn by sediments, either under sea water or fresh water conditions, is to be detected (Duursma (1970)). Assuming that the concentration of leucine in sea

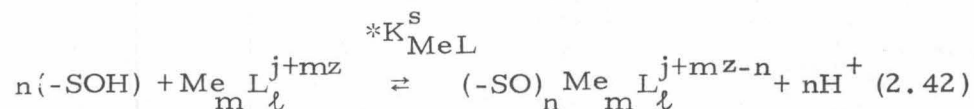
water is 0.9 to 3.8  $\mu\text{g}/\text{l}$  implies that the influence of leucine is measurable only at levels at least  $10^4$  times the natural concentration, because of complexation of leucine by  $\text{Ca}^{2+}$ ,  $\text{Mg}^{2+}$ , and  $\text{H}^+$ .

Siegel (1966) studied the uptake of Zn on ion-exchange resins and clays in the presence of glycine. The addition of glycine reduced the uptake of Zn on the anion-exchange resin in a manner predicted by the use of the stability constants of the zinc-glycine system, indicating no uptake of the zinc-glycine complex by the resin. The cationic-exchange resins, on the other hand, had higher uptakes of zinc in the presence of glycine than predicted by the stability constants. Siegel explained this observation in terms of the adsorption of zinc-(glycine)<sub>1</sub><sup>+</sup> complexes.

MacNaughton (1973) investigated the adsorption of Hg(II) by amorphous iron hydroxide and montmorillonite in the presence of humic acid, glycine, cysteine, quinaldic acid and leucine. The experimental results suggested that the adsorption on amorphous iron hydroxide was not influenced by the addition of cysteine, but was reduced in the presence of humic acid, glycine, quinaldic acid, and leucine. The adsorption of Hg(II) by montmorillonite was not affected by leucine. Humic acid, however, reduced the adsorption of Hg(II) very much.

### 2.3.3 Model Predictions

Predictions made with the Ion Exchange-Surface Complex Formation Model are based entirely on the competition between the reactions of free metal ions with the surface hydroxo groups and all other chemical reactions necessary to characterize a given system. Consequently, the addition of any ligand reduces the adsorption by reducing the concentration of the free metal ion. This model is thus capable of quantitatively interpreting the decreased adsorption of metals brought about by complexation. However, in order to explain the phenomenon of the increased adsorption of metals in presence of certain ligands it would be necessary to include the following reaction:



where L stands for any ligand, including OH, and m, n, l are stoichiometric coefficients of metal Me of charge z, surface hydroxo-groups (-SOH) and ligand L of charge j.

James and Healy (1972c) did not explicitly account for either a decrease or an increase in adsorption brought about by complexation, apart from hydroxo complexes. In that case an increased adsorption was attributed to a reduction in desolvation energy. They let the chemical free energy ( $\Delta G_{\text{chem}}^{\circ}$ ) be a correction parameter for any additional adsorption of free metal ions and the metal-hydroxo complexes, outside

the coulombic and secondary solvation term. This parameter was given the same value (negative and, therefore, favorable for the adsorption) for all species in order to prevent a preferential adsorption of any one hydrolysis product over another. But,  $\Delta G_{\text{chem},i}^{\circ}$  can also be thought of as a parameter accounting for interactions between the adsorbate and any metal species present in the system. Hence, more than one chemical free energy is needed in order to distinguish among the following cases:

1. adsorption of free metal ions
2. adsorption of metal-hydroxo complexes
3. adsorption of metal-ligand complexes (ligand other than OH).

In the general case there should be as many chemical free energies as there are species present in a given system, i.e.,

$$\Delta G_{\text{chem}, (M_i)_{\alpha} (L_j)_{\beta} (H)_{\gamma}}^{\circ}$$

$$\alpha = 1, 2, \dots$$

$$\beta = 0, 1, 2, \dots$$

$$\gamma = 0, \pm 1, \pm 2, \dots$$

where  $i$  is an index specifying the metal  $M$  whose stoichiometric coefficient is  $\alpha$ ,  $j$  is an index specifying the ligand  $L$  whose stoichiometric coefficient is  $\beta$ , and  $\gamma$  is the stoichiometric coefficient of  $H^+$  or  $OH^-$  (for  $H^+ \gamma > 0$ ; for  $OH^- \gamma < 0$ ). When a given species does not have any affinity for the surface, the corresponding chemical energy should be made unfavorable for adsorption by assigning a sufficiently positive

value so that  $\Delta G_{\text{ads}}^{\circ}$  is sufficiently unfavorable for the adsorption; if a given species has a high affinity for the surface, the corresponding chemical free energy should be made more favorable for adsorption by assigning a more negative value. With these additional provisions, the James-Healy Model can be made to account for decreased or increased adsorption of metals brought about by complexation.

## Chapter 3

## EXPERIMENTAL METHODS AND MATERIALS

3.1 Chemicals

All the chemical reagents used in this research were Analytical Reagent Grade. All solutions were made with quartz-distilled water (Q-water) (obtained through the courtesy of Dr. Clair Patterson). Q-water is, essentially, equivalent to quadruply distilled water.\* Ionic strength was varied with NaCl. In some experiments with Pb(II), NaClO<sub>4</sub> was used to investigate the influence of Cl<sup>-</sup> on the adsorption of Pb(II).

All trace metal stock solutions were prepared from the chloride salts. Solutions of citrate were prepared from its tri-sodium salt, and those of EDTA from the di-sodium salt. All the solutions were stored in polyethylene or teflon containers. NaHCO<sub>3</sub> solutions were prepared freshly for each experiment.

---

\* Deionized water is fed into a double-stage still. The distillate is passed through an ion-exchange resin and SiO<sub>2</sub> beds (the latter for removal of organics) into a polyethylene reservoir, and from there into a quartz still. From this point on every part of the apparatus is made from either quartz or teflon, except the collecting reservoir, which is polyethylene.

An analysis of Q-water with a Dohrmann Envirotech Total Carbon Analyzer (Model DC-50) showed that organic carbon concentration was less than the 1 mg/l detection limit of the instrument. Additional verification by infrared spectrophotometry indicated no absorption owing to the presence of organics.

### 3.2 $\alpha$ -Quartz

Adsorption studies were performed with finely divided crystalline silica, commercially available under the trade name "Min-U-Sil 5" (Pennsylvania Glass Sand Corp.). X-ray diffraction analysis\* confirms its structure to be that of  $\alpha$ -quartz. BET analysis shows the specific surface area to be  $4.23 \text{ m}^2/\text{gr}$ ,<sup>+</sup> a value which is in agreement with that obtained by MacNaughton and James (1974). However, the manufacturers report that the specific surface area is only  $2.06 \text{ m}^2/\text{gr}$ . This discrepancy is a result of the manufacturer's use of an air permeability method for specific surface area determinations.

Chemical composition of Min-U-Sil 5, as reported by the manufacturers, shows 99.9%  $\text{SiO}_2$  with traces of iron, aluminum, titanium, calcium, and magnesium. Spectrographic analysis<sup>#</sup> confirms the presence of these as well as some other impurities (Table 3.1). Organic impurities were removed by heating at  $500^\circ\text{C}$  for 24 hours (MacNaughton and James (1974)). The inorganic impurities were removed to a large extent by refluxing stirred particles in 4 N redistilled

---

\* X-ray diffraction analyses were performed by Dr. Pol Duwez's group in the Department of Material Sciences, Caltech.

+ BET analyses were conducted by Mr. William Cannon at the Jet Propulsion Laboratory, Pasadena.

# Spectrographic analyses were performed by Ms. Elizabeth Bingham in the Department of Geological and Planetary Sciences, Caltech.

GFS  $\text{HNO}_3$  (G. Frederick Smith Chemical Co.). The suspension was subsequently washed with Q-water until the pH of the supernatant was approximately 6. Particles were then shaken in 4 N  $\text{NH}_4\text{OH}$  and again carefully washed with Q-water until the pH of the supernatant was again 6. A subsequent spectrographic analysis of these cleaned particles showed a remarkable decrease in the level of inorganic impurities (Table 3.1).

### 3.3 Cleaning Techniques

In order to avoid contamination, all the equipment which came in contact with the solutions and suspensions was cleaned according to the following procedure. All of the glass and teflon objects were passed through a series of four soaks, remaining in each of them for 24 hours (marks on glassware were removed with HF). The first soak was in cold conc.  $\text{HNO}_3$  (Baker Analyzed Reagent Grade). The second and third soaks consisted of hot, redistilled conc.  $\text{HNO}_3$  (GFS) and the fourth soak was carried out in double-distilled water ( $\text{D}^2$ -water). When being transferred from one soak to another, the objects were very carefully rinsed with  $\text{D}^2$ -water. All the pipets and burettes were cleaned the same way. Polyethylene bottles were also passed through another set of four soaks, each lasting 24 hours, but in this case the second and the third soaks were not heated. All the teflon tubes and

Table 3.1  
Spectrographic Analysis of  $\alpha$ -Quartz

	Concentration (mg/kg)						
	Ba	Fe <sub>2</sub> O <sub>3</sub>	Ti	Zr	Mg	Al <sub>2</sub> O <sub>3</sub>	Ca
Min-U-Sil 5 prior to cleaning	3.5	400	200	16	30	800	3
Min-U-Sil 5 after cleaning	1	30	110	9	<10	70	<3

tips used in experiments and analyses were boiled in conc. redistilled  $\text{HNO}_3$  (GFS), and then boiled in  $\text{D}^2$ -water.

### 3.4 Reaction Vessel

Adsorption experiments were carried out in a 400 ml teflon beaker. This beaker was placed in a double jacketed constant temperature bath. The temperature was maintained at  $25 \pm 0.5^\circ\text{C}$ . The beaker was covered with a cover, also of teflon. The reaction suspension was mixed with a motor-driven polyethylene stirrer. Plugs and electrode holders were also constructed from teflon. Gases were introduced to the reaction vessel through teflon tubing. Prior to entering the reaction vessel these gases were scrubbed with Q-water.

### 3.5 pH Control

Experiments were carried out under two different sets of experimental conditions:

1. This system was carbonate free and the reaction suspension was purged with high purity  $\text{N}_2$ (g). pH was established and maintained through the addition of HCl and NaOH by an automatic titrator (Titrator 11 and Autoburette ABU 11, Radiometer, Copenhagen). The tubing and all the fittings on the titrator were made from teflon.
2. This system contained carbonate, and the pH was established and maintained by a certain amount of  $\text{NaHCO}_3$  and purging

with an appropriate partial pressure of  $\text{CO}_2$ .

In both cases pH measurements were obtained using a Radiometer Copenhagen pH Meter (Model 27) with a glass and reference electrode also manufactured by Radiometer Copenhagen.

### 3.6 Sample Processing and Analysis

All Min-U-Sil suspensions were purged with either  $\text{N}_2$ (g) or the appropriate  $\text{N}_2$ - $\text{CO}_2$  gas mixture for 24 hours prior to the addition of metals. After obtaining the desired pH, the organic ligand (if used) was added, followed by the appropriate quantity of metal. In those cases when Cu(II) and Pb(II) were simultaneously present, they were added to the reaction vessel as an equimolar mixture. After addition of the metal, the time allowed for equilibration was 1 hour. The reaction suspensions were separated from the sediment by centrifugation for 30 minutes at 3100 RPM in the IEC International Centrifuge Universal (Model UV) in polyethylene centrifuging bottles. The supernatant was decanted, acidified, and stored in teflon bottles.

The concentrations of the metals were measured using a Varian Techtron Atomic Absorption Spectrophotometer (Model AA-5). Samples containing Ca and Mg were analyzed using the flame-technique, and Cu and Pb by the flameless method using a Varian Techtron Carbon Rod Atomizer (Model 63). Pb-containing samples were analyzed directly with the carbon rod atomizer, as were the Cu-containing samples in

experiments with  $Cu_T = 5 \times 10^{-7} M$  and  $Cu_T = 10^{-6} M$ . For  $Cu_T = 10^{-7} M$ , it was necessary to preconcentrate the sample in order to get a better signal. The method applied was a solvent extraction technique using 0.1% dithiozone (Dz) in chloroform. Cu can be extracted with Dz at low and high pH values (Morrison and Freiser (1957), Sandell (1959)). It was found that the Dz-extracts obtained at low pH values were very unstable. However, if the extraction was performed at pH 9 in the presence of citrate, the extracts were stable, especially if they were wrapped in aluminum foil (to prevent photochemical reactions) and stored at low temperature, but not allowed to freeze.

Extractions were performed in glass separatory funnels with teflon stopcocks. Ten ml of acidified sample were pipetted into the funnel. 5 ml of 20% ammonium citrate were added, the solution pH was brought up to 9, and the desired amount of Dz-chloroform was added. The funnel was shaken for five minutes and then shaken again. After separation of the two phases, the lower, Cu-containing layer was stored in a teflon bottle. The yield obtained using this technique was 99%. Standards were prepared by extracting copper from solutions of  $CuCl_2$  obtained by diluting a  $10^{-4} M$   $CuCl_2$  stock solution.

The analyses of samples of high ionic strength were carried out according to a method described by Ediger et al. (1974). Such samples may present problems in non-flame atomic absorption analysis

because of two possible interferences. Firstly, the volatilization of the matrix components into the light path during atomization introduces a great deal of background absorption, and secondly, volatilization of the matrix can introduce a variety of chemical interferences. Both of these matrix effects lead to a reduction of the overall sensitivity of the method.

These problems can be overcome by use of solvent extraction. Ediger et al. (1974) designed a very simple and elegant technique for modifying the sample matrix by volatilizing the matrix components during the ashing cycle so as to remove them before atomization. This removal can be accomplished through the addition of a large excess of ammonium nitrate to the sample. The result is a conversion of undesired sodium chloride to the more volatile salts, sodium nitrate and ammonium chloride. Since ammonium nitrate itself is volatile, all three compounds volatilize out of the carbon rod during the ashing cycle. This minimizes the interference and any remaining background absorption can be corrected for through the use of the hydrogen lamp. In this research, therefore, samples were mixed 1:1 with 25% ammonium nitrate solution prior to analysis. Three  $\mu$ l of the mixed solution was then injected into the carbon rod. These measurements, as well as other measurements with carbon rod atomizer, were done with  $N_2$  as the purging gas.

The analyses of the stock solutions of organic ligands were carried out using two different methods. The first method was a complexometric titration of a solution of Cu(II) (prepared by diluting a commercially obtained Cu-standard with Q-water) with a solution of the ligand. A Cu ion-selective electrode (Orion Model 94-29) was used to follow the Cu concentrations. A commercial silver-silver chloride electrode was used (Orion Model 90-01) as the reference electrode. Measurements were obtained with the Orion Research pH Meter (Model 801).

The second method utilized the Dohrmann Envirotech Total Carbon Analyzer (Model DC-50) to determine the concentration of organic carbon present. Since it was possible for some inorganic carbon also to be present in the solution, measurements were carried out in the total carbon mode. Thus, the measured value consisted of  $C_{\text{inorg}} + C_{\text{org}}$ . After subtracting the value of  $C_{\text{inorg}}$ , the molar concentration of the organic ligand solution was determined.

### 3.7 Adsorption Measurements with $C^{14}$ -Citric Acid

In order to understand the experimental results, it was necessary to investigate possible adsorption of citrate on  $\alpha$ -quartz. The tests were made with  $C^{14}$ -labeled citric acid (International Chemical and Nuclear Corporation).

Activities of the labeled solutions were determined by liquid scintillation spectrometry using a Beckman LS-100 Liquid Scintillation System. Samples were counted in linear-polyethylene vials. Counting of the aqueous phase was done by adding 1 ml of the filtered sample to 10 ml Aquasol (a pre-mixed xylene-based scintillation cocktail obtained from New England Nuclear Pilot Chemical Division). The physical characteristics of Aquasol change upon dilution with water (New England Nuclear (1974)). If the water content is below ca. 12% the mixture will remain a clear solution. If the water content is above ca. 18% the mixture will become a stiff gel. The transition region is characterized by a non-homogeneous, two-phase system. In order to carry out the counting of suspensions in a reproducible manner, it was necessary to prevent the sedimentation of the particles. This prevention was accomplished by allowing Aquasol to form a gel with water. Therefore, 2 ml of D<sup>2</sup>-water and 1 ml of sample were added to 10 ml of Aquasol.

Counting times of samples were determined either by total number of counts (which corresponds to a standard error of 0.5%) or by the counting period of one minute -- whichever occurred first. The specific activity of C<sup>14</sup>-labeled citric acid was 8.01 mCi/mole.

Adsorption of citrate on  $\alpha$ -quartz was investigated in the carbonate-containing system at pH 7. CIT<sub>T</sub> at  $6.25 \times 10^{-8}$  (CIT<sub>carrier</sub> =  $5 \times 10^{-8}$  M and C<sup>14</sup>-CIT =  $1.25 \times 10^{-8}$  M) was added to the equilibrated

Min-U-Sil. After one hour of equilibration, two samples were taken out; one was counted directly, and the other one after filtering through a  $0.45 \mu$  Millipore filter. Cu was added to the remaining solution so that  $Cu_T = 10^{-7} M$ , and equilibrated for one hour. Again, counts were taken for both  $CIT_T$  and  $CIT_{(aq)}$ . The resulting measurements showed no evidence of adsorption of CIT or Cu-CIT complexes on  $SiO_2(s)$  (Tables 3.2 and 3.3).

### 3.8 Adsorption Measurements with $C^{14}$ - $NaHCO_3$

$C^{14}$ - $NaHCO_3$  was obtained from International Nuclear and Chemical Corp. (the specific activity was 56.5 mCi/mmole).

After equilibration of  $50 m^2/1$  Min-U-Sil with  $10^{-3} M$  NaCl,  $10^{-4} M$   $NaHCO_3$  carrier, and gas with  $pCO_2$  of  $10^{-3.5}$  atm, bubbling of  $CO_2$  was stopped and  $2 \times 10^{-6} M$   $C^{14}$ - $NaHCO_3$  was added to the suspension. Samples were taken after 14 and 15 min. Analyses of these samples are shown on Table 3.4. Change in the total number of counts at the beginning and the number of counts in the solution after 15 min. of equilibration was ascribed to adsorption on Min-U-Sil and to loss as  $CO_2$ -evaporation and adsorption on the filter paper or the glass. The amount of  $C^{14}$  lost in these ways was experimentally determined by carrying out the same experiments in the absence of Min-U-Sil ("Blank" on Table 3.4). Based on these measurements, it was possible to calculate the amount of carbon which adsorbed on  $\alpha$ -quartz. In the

Table 3.2

Tests for the Adsorption of  $C^{14}$ -CIT on  
Min-U-Sil in the Absence of Copper

Time mixing (min)	Filtered	CPM
0	no	2116
59	no	2046
60	yes	2034

Table 3.3

Tests for the Adsorption of  $C^{14}$ -CIT on  
Min-U-Sil in the Presence of Copper

Time mixing (min)	Filtered	CPM
0	no	2040
55	no	2046
60	yes	2086

Table 3.4

Tests for the Adsorption of  $C^{14}$ - $NaHCO_3$  on Min-U-Sil

Type of Experiment	Sample No.	Time mixing (min)	Filtered	CPM	$\frac{A-C}{A} \times 100$	% $C_T$ adsorbed on Min-U-Sil
Blank	A	0	No	191800	35.3%	-
	B	14	No	157720		
	C	15	Yes	124080		
In the Absence of Cu(II)	A	0	No	123340	45.2%	9.9
	B	14	No	91148		
	C	15	Yes	67588		
In the Presence of Cu(II)	A	0	No	129899	45.4%	10.1
	B	14	No	97619		
	C	15	Yes	70815		
In the Presence of Cu(II) and CIT	A	0	No	67343	47.9%	12.6
	B	14	No	48467		
	C	15	Yes	35036		

absence of Cu it was found that 9.9%  $C_T$  adsorbed. In the presence of  $10^{-7}$  M  $Cu_T$  essentially the same amount adsorbed (ca. 10.1%). This was also the case in the experiments carried out in the presence of  $10^{-7}$  M  $Cu_T$  and  $10^{-6}$  M  $CIT_T$  (ca. 12.6% apparently adsorbed).

## Chapter 4

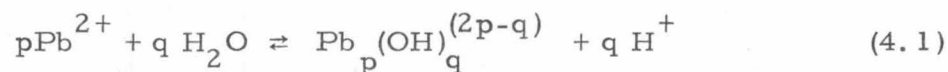
## HYDROLYSIS OF Pb(II) AND Cu(II)

4.1 Introduction

The hydrolysis of metal ions is a function of both metal ion concentration and pH. Hydrolysis increases with dilution and pH, while the fraction of polynuclear hydroxo complexes decreases with dilution. The hydrolysis products formed regulate the concentration of metals in solution through precipitation, adsorption, and coagulation. Information about the identity and the stability of metal-hydroxo complexes is thus necessary to understand and predict the chemical behavior of metals in natural aquatic environments.

4.2 Hydrolysis of Pb(II)4.2.1 Introduction

The hydrolysis of Pb(II), that is, the reaction



has been the subject of many studies, resulting in the identification of seven hydroxo species ( $\text{PbOH}^+$ ,  $\text{Pb}(\text{OH})_2(\text{aq})$ ,  $\text{Pb}(\text{OH})_3^-$ ,  $\text{Pb}_2\text{OH}^{3+}$ ,  $\text{Pb}_3(\text{OH})_4^{2+}$ ,  $\text{Pb}_4(\text{OH})_4^{4+}$ ,  $\text{Pb}_6(\text{OH})_8^{4+}$ ) and the determination of their stability constants (Table 4.1).

Table 4.1  
Summary of the Hydrolysis of Pb(II)

Electrolyte	log Equilibrium Constant (References are shown in parenthesis)						
	PbOH <sup>+</sup> (aq)	Pb(OH) <sub>2</sub> (aq)	Pb(OH) <sub>3</sub> <sup>-</sup> (aq)	Pb <sub>2</sub> OH <sup>+</sup> (aq)	Pb <sub>3</sub> (OH) <sub>4</sub> <sup>2+</sup> (aq)	Pb <sub>4</sub> (OH) <sub>4</sub> <sup>4+</sup> (aq)	Pb <sub>6</sub> (OH) <sub>8</sub> <sup>4+</sup> (aq)
→ 0 Ba(NO <sub>3</sub> ) <sub>2</sub>	-7.8 (7)			-7.2 (1)		-20.9 (1)	
0.06M Ba(ClO <sub>4</sub> ) <sub>2</sub>						-18.05 (2)	
0.3M NaCl					-23.35 (4)		-42.66 (4)
0.3M NaClO <sub>4</sub>	-7.9 (3)	-17.2 (5)	-27.99 (5)				
0.5M Mg(ClO <sub>4</sub> ) <sub>2</sub>				-6.49 (6)		-18.949 (6)	
0.5M Ba(ClO <sub>4</sub> ) <sub>2</sub>				-6.3 (6)		-19.12 (6)	
0.6M Ba(ClO <sub>4</sub> ) <sub>2</sub>	-8.7 (2)					-18.75 (3)	
1M Mg(ClO <sub>4</sub> ) <sub>2</sub>				-6.57 (6)		-18.978 (6)	
1M Ba(ClO <sub>4</sub> ) <sub>2</sub>				-6.39 (6)		-19.11 (6)	
1.45 M Mg(ClO <sub>4</sub> ) <sub>2</sub>						-19.045 (6)	
1.45M Ba(ClO <sub>4</sub> ) <sub>2</sub>						-19.12 (6)	
1.5M Mg(ClO <sub>4</sub> ) <sub>2</sub>				-6.45 (6)			
1.5M Ba(ClO <sub>4</sub> ) <sub>2</sub>				-6.24 (6)			
2M NaClO <sub>4</sub>	-7.9 (7)					-19.35 (8)	
2M NaNO <sub>3</sub>	-8.8 (8)			-7.1 (7)		-21.72 (7)	
3M NaClO <sub>4</sub>	-7.9 (3)	-17.5 (5)	-29 (5)	-6.45 (3)		-19.25 (3)	
3M NaCl		-20.3 (9)	-32.3 (9)		-22.87 (4)		-42.14 (4)

(1) Pedersen (1945); (2) Faucherre(1954); (3) Olin (1960a); (4) Olin (1960b); (5) Carell and Olin (1960);  
(6) Pajdowski and Olin (1962); (7) Hugel (1964); (8) Hugel (1965); (9) Schorsch and Ingri (1967)

#### 4.2.2 Mononuclear Pb(II)-Hydrolysis Products

The stability of  $\text{PbOH}^+$  has been determined by several investigators. Olin (1960b) obtained the value of  $\log^*\beta_1 = -7.9$  (3M  $\text{NaClO}_4$ ) and  $\log^*\beta_1 = -7.8$  (0.3M  $\text{NaClO}_4$ ) by potentiometric titrations. The same value was obtained by Hugel (1964) in 2M  $\text{NaClO}_4$  and Pedersen (1945) in  $\text{Ba}(\text{NO}_3)_2$ . The lowest values ( $\log^*\beta_1 = -8.8$  in 2M  $\text{NaNO}_3$  and  $\log^*\beta_1 = -8.7$  in 0.6M  $\text{Ba}(\text{ClO}_4)_2$ ) were obtained by Hugel (1965) and Faucherre (1954), respectively.

$\text{Pb}(\text{OH})_2(\text{aq})$  and  $\text{Pb}(\text{OH})_3^-$  were identified only by two investigators. The reported stability constants for each of the species differ by approximately three orders of magnitude. Carell and Olin (1960) studied the complex formation between  $\text{Pb}^{2+}$  and  $\text{OH}^-$  in alkaline solutions of 3M  $\text{NaClO}_4$  and 0.3M  $\text{NaClO}_4$ . The constants obtained for the formation of  $\text{Pb}(\text{OH})_2(\text{aq})$  were

3M $\text{NaClO}_4$	$\log^*\beta_2 = -17.5$	$\log^*\beta_3 = -29$
0.3M $\text{NaClO}_4$	$\log^*\beta_2 = -17.2$	$\log^*\beta_3 = -27.99$

Schorsch and Ingri (1967), studied the complex formation in alkaline 3M  $\text{NaCl}$  using a lead amalgam electrode. They obtained the values of  $\log^*\beta_2 = -20.3$  and  $\log^*\beta_3 = -32.3$ . They attributed the discrepancy between their results and the results obtained by Carell and Olin (1960)

to stronger complex formation between  $\text{Pb}^{2+}$  and  $\text{Cl}^-$ , than between  $\text{Pb}^{2+}$  and  $\text{ClO}_4^-$ .

#### 4.2.3 Polynuclear Pb(II)-Hydrolysis Products

The stability constants for the polynuclear species,  $\text{Pb}_2\text{OH}^{3+}$  and  $\text{Pb}_4(\text{OH})_4^{4+}$ , were determined by Pedersen (1945), Olin (1960b), Pajdowski and Olin (1962), and Hugel (1964, 1965) by electromotive-force measurements. Pajdowski and Olin (1962) obtained the following values for the stability constants for  $\text{Pb}_2\text{OH}^{3+}$ , and  $\text{Pb}_4(\text{OH})_4^{4+}$ :

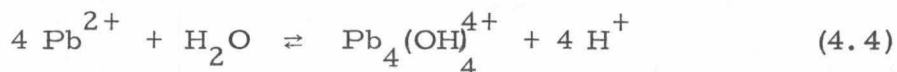
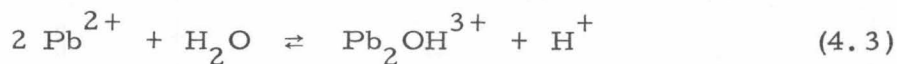
0.5M	$\text{Mg}(\text{ClO}_4)_2$	$\log^*\beta_{21} = -6.49$	$\log^*\beta_{44} = -18.949$
	$\text{Ba}(\text{ClO}_4)_2$	$\log^*\beta_{21} = -6.3$	$\log^*\beta_{44} = -19.12$
1M	$\text{Mg}(\text{ClO}_4)_2$	$\log^*\beta_{21} = -6.57$	$\log^*\beta_{44} = -18.978$
	$\text{Ba}(\text{ClO}_4)_2$	$\log^*\beta_{21} = -6.39$	$\log^*\beta_{44} = -19.11$
1.5M	$\text{Mg}(\text{ClO}_4)_2$	$\log^*\beta_{21} = -6.45$	$\log^*\beta_{44} = -19.045$
	$\text{Ba}(\text{ClO}_4)_2$	$\log^*\beta_{21} = -6.24$	$\log^*\beta_{44} = -19.12$

Olin (1960b) determined the stability constants for  $\text{Pb}_2\text{OH}^{3+}$  and  $\text{Pb}_4(\text{OH})_4^{4+}$  in 3M  $\text{NaClO}_4$  to be  $\log^*\beta_{21} = -6.45$  and  $\log^*\beta_{44} = -19.25$ , respectively.

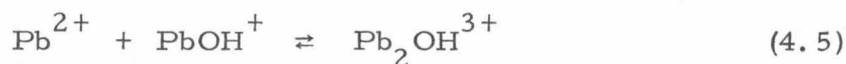
The stability constants for the formation of  $\text{Pb}_2\text{OH}^{3+}$  ( $\log^*\beta_{21} = -7.11$ ) and  $\text{Pb}_4(\text{OH})_4^{4+}$  ( $\log^*\beta_{44} = -21.72$ ) reported by Hugel (1964) are slightly different from the values obtained by Olin (1960) and

Pajdowski and Olin (1962). Hugel (1965) made another set of measurements in 2M NaClO<sub>4</sub>. He obtained the value of  $\log^*\beta_{44} = -19.35$ , which is similar to the value reported by Olin (1960b) for the same supporting electrolyte.

Pedersen (1945) carried out potentiometric titrations of Pb(NO<sub>3</sub>)<sub>2</sub> solutions by the addition of NaOH, and explained his experimental data in terms of the formation of Pb<sub>2</sub>OH<sup>3+</sup>, PbOH<sup>+</sup>, and Pb<sub>4</sub>(OH)<sub>4</sub><sup>4+</sup>



or



Extrapolating to I=0 resulted in the values of  $\log^*\beta_{21} = -7.2$  and  $\log^*\beta_{44} = -20.9$ .

The solubility of the basic lead nitrates is so low, that only one percent of the Pb(II) in Pedersen's experiments was hydrolyzed before precipitation started. For that reason Fauchere (1954) decided to study Pb(II) perchlorate solutions. Potentiometric titrations of these solutions showed that if less than one OH<sup>-</sup> per Pb(II) had been added, the complex Pb<sub>4</sub>(OH)<sub>4</sub><sup>4+</sup> was formed, as indicated by spectro-

photometric and cryoscopic measurements. His reported values for the stability constants of these complexes are  $\log^*\beta_{44} = -18.75$  and  $\log^*\beta_{44} = -18.05$  in  $0.6\text{M Ba}(\text{ClO}_4)_2$  and  $0.06\text{M Ba}(\text{ClO}_4)_2$ , respectively. At the hydroxide-to-lead ratio of 4:3 the precipitation of  $\text{Pb}(\text{ClO}_4)_2 \cdot 5\text{Pb}(\text{OH})_2(\text{s})$  started; therefore, this ratio was the limit of the titration.

The same limit of the titration was found by Olin (1960a) who suggested that a trimer,  $\text{Pb}_3(\text{OH})_4^{2+}$ , and a hexamer,  $\text{Pb}_6(\text{OH})_8^{4+}$ , are formed for hydroxyl numbers greater than one. Their respective hydrolysis constants are

3M NaCl	$\log^*\beta_{34} = -22.87$	$\log^*\beta_{68} = -42.14$
0.3M NaCl	$\log^*\beta_{34} = -23.35$	$\log^*\beta_{68} = -42.66$

#### 4.2.4 Summary

The preceding information is best summarized by Mesmer and Baes (1974). They state that hydrolysis of Pb(II) ion is "... a model case in which the species identification from most of the information... obtained by a large number of physical chemical techniques... is quite consistent".

Table 4.2 gives the hydrolysis constants of Pb(II) used for the computations in this research. The higher polynuclear hydrolytic species of Pb(II), because of their importance only at higher total concentration of Pb ( $\text{Pb}_T^*$ ) and at higher pH, did not prove to be

---

\* The subscript T in the notation in this thesis means the total concentration of a given constituent.

Table 4.2  
 Hydrolysis Constants for Pb(II)  
 Used in Equilibrium Computations

Species	log Equilibrium Constant ( $I=10^{-3}$ ) <sup>*</sup>	
$\text{PbOH}^+(\text{aq})$	$*K_1$	-7.13
$\text{Pb}(\text{OH})_2(\text{aq})$	$*\beta_2$	-16.54
$\text{Pb}(\text{OH})_3^-(\text{aq})$	$*\beta_3$	-27.42
$\text{Pb}_2\text{OH}^{3+}(\text{aq})$	$*\beta_{21}$	-6.27
$\text{Pb}(\text{OH})_2(\text{s})$	$*K_{\text{so}}$	-12.94 <sup>#</sup>

\* All equilibrium constants at  $I=10^{-3}$  were obtained from the output of the REDEQL2 program (McDuff and Morel (1973)). The thermodynamic data for this program are compiled for infinite dilution, i. e.,  $I=0$ . Special subroutines correct the activities for the appropriate ionic strength using the Davies equation, and compute the corresponding stability constants.

# from Sillén and Martell (1971)

important in this research. Hence, their stability constants were not included in computations.

Since the supporting electrolyte used throughout this research (NaCl) affects the equilibrium distribution of Pb by forming different chloro complexes, it was necessary to include the stability constants for those complexes. Table 4.3 shows the complexes selected and their equilibrium constants.

### 4.3 Hydrolysis of Cu(II)

#### 4.3.1 Introduction

Hydrolysis of Cu(II) ion results in the formation of a number of mononuclear ( $\text{CuOH}^+$ ,  $\text{Cu}(\text{OH})_2(\text{aq})$ ,  $\text{Cu}(\text{OH})_3^-$ ,  $\text{Cu}(\text{OH})_4^{2-}$ ) and polynuclear species ( $\text{Cu}_2(\text{OH})_2^{2+}$ ,  $\text{Cu}_3(\text{OH})_4^{2+}$ , ...,  $\text{Cu}_{n+1}(\text{OH})_{2n}^{2+}$ ). It has been studied by many investigators. The identified species and their respective stability constants are listed in Table 4.4.

#### 4.3.2 Mononuclear Cu(II)-Hydrolysis Products

Pedersen (1943) made an extensive investigation of the hydrolysis of Cu(II), measuring the pH of  $\text{Cu}(\text{NO}_3)_2$  solutions of varying ionic strengths. He explained his results assuming the following equilibria:

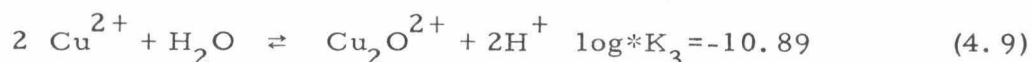
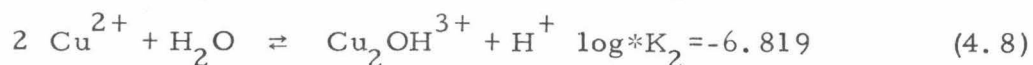


Table 4.3  
Stability Constants for Pb-Cl Complexes

Species	log Equilibrium Constant (I=10 <sup>-3</sup> )	
PbCl <sup>+</sup> (aq)	K <sub>1</sub>	1.63
PbCl <sub>2</sub> (aq)	β <sub>2</sub>	2.50
PbCl <sub>3</sub> <sup>-</sup> (aq)	β <sub>3</sub>	3.80
PbClOH(aq)	K <sub>1OH</sub>	-6.60

Table 4.4

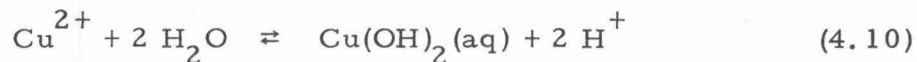
## Reported Equilibrium Constants for the Hydrolysis of Cu(II)

Medium	log Equilibrium Constant (References are in parenthesis)				
	$\text{CuOH}^2$	$\text{Cu(OH)}_2(\text{aq})$	$\text{Cu(OH)}_3^-$	$\text{Cu(OH)}_4^{2-}$	$\text{Cu}_2(\text{OH})_2^{2+}$
dil $\text{Cu(NO}_3)_2$	-7.97 (3)				-10.89 (3)
dil $\text{Cu(NO}_3)_2$	-8.0 (4)				-10.95 (4)
3M $\text{NaClO}_4$					-10.6 (4)
→ 0	<-8 (5)				$\frac{3833}{T} + 2.497$ (5)
0.04M to 8M KOH			<-27.8 (1)	<-39.6 (1)	
Cu-benzenesulphonate		-13.7 (2)			
wide range of LiCl concentration		-13.2 (6)			
1M		<-17.3 (7)			

(1) McDowell and Johnston (1936); (2) Quintin (1937); (3) Pedersen (1943); (4) Berecki-Biedermann (1955); (5) Perrin (1960); (6) Spivakovskii and Makovskaya (1968); (7) Mesmer and Baes (1974)

Berecki-Biedermann (1955) recalculated the same constants obtaining the value of  $\log^*K_1 = -8.0$ , and Perrin (1960) stated that  $\log^*K_1 < -8$ .

The stability constant for  $\text{Cu}(\text{OH})_2(\text{aq})$  was determined experimentally by Quintin (1937) and Spivakovskii and Makovskaya (1968). Quintin (1937) followed the change in  $\text{Cu}^{2+}$  as a function of pH by potentiometry. She attributed this change to the reaction:

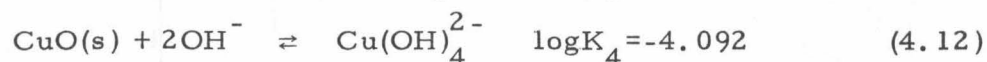


for which  $\log^*R_2 = -13.7$ .

Spivakovskii and Makovskaya (1968) studied the behavior of Cu(II) as a function of pH during the precipitation with alkali from chloride solutions over varying concentrations of Cu(II) and chloride. The experimental results were interpreted in terms of the formation of hydroxo, chloro, and hydroxo-chloro complexes. Their reported value of the stability constant for  $\text{Cu}(\text{OH})_2(\text{aq})$  is  $\log^*R_2 = -13.2$ .

Mesmer and Baes (1974) estimated the second hydrolysis constant for Cu(II) to be  $\log^*\beta_2 < -17.3$ , which is almost four orders of magnitude lower than the previous ones. This estimate was based on the assumption that the stepwise constants ( $^*\beta_{1,y+1} / ^*\beta_{1,y}$ ) for copper decrease in a manner typical for other metals.

McDowell and Johnston (1936) observed the solubility of CuO(s) in KOH and interpreted their results with the following equilibrium relationships:



Combining these equations with the solubility product of CuO(s) they obtained:



#### 4.3.3 $\text{Cu}_2(\text{OH})_2^{2+}$

$\text{Cu}_2(\text{OH})_2^{2+}$  has been determined to be the principal polynuclear hydrolytic species of Cu(II). Pedersen (1943) reported  $\log^* \beta_{22} = -10.89$  and Berecki-Biedermann (1955),  $\log^* \beta_{22} = -10.6$ . From Pedersen's experimental results Berecki-Biedermann (1955) recalculated his constants and obtained  $\log^* \beta_{22} = -10.95$ .

Perrin (1960) found the relation between the stability constant  $^* \beta_{22}$  and temperature to be

$$\log^* \beta_{22} = \frac{3833}{T} - 2.497 \quad (4.15)$$

#### 4.3.4 Summary

The studies on the hydrolysis of Cu(II) resulted in the identification of five hydrolysis products ( $\text{CuOH}^+(\text{aq})$ ,  $\text{Cu(OH)}_2(\text{aq})$ ,  $\text{Cu(OH)}_3^-(\text{aq})$ ,

$\text{Cu}(\text{OH})_4^{2-}(\text{aq})$ , and  $\text{Cu}_2(\text{OH})_2^{2+}(\text{aq})$ ), and determination of their respective stability constants. Mesmer and Baes (1974) state that the first hydrolysis constant,  $*K_1$ , is probably less than  $10^{-8}$ , despite several estimates of the stability of  $\text{CuOH}^+(\text{aq})$ ; nor is the estimate for  $\text{Cu}(\text{OH})_3^-(\text{aq})$  very reliable. The most uncertain stability constant for the hydrolysis of Cu(II) is  $*\beta_2$ ; the reported values for  $*\beta_2$  differ by almost four orders of magnitude. Hence, there is a definite need for more accurate measurements of the hydrolysis behavior of Cu(II).

#### 4.4 Second Hydrolysis Constant for Cu(II)

##### 4.4.1 Equilibrium Computations with Different Values for $*\beta_2$

The choice of  $*\beta_2$  will have a great influence on the calculated equilibrium composition of a solution containing Cu(II). Figures 4.1a, b, 4.2a, b, and 4.3a, b show the distribution of Cu(II) as a function of pH in a carbonate-free system for two different values of  $*\beta_2$ . The computations were based on the stability constants listed in Tables 4.5 and 4.6.

In all three cases (i. e.,  $\text{Cu}_T = 1.5 \times 10^{-8}$  M (Figures 4.1a, b),  $\text{Cu}_T = 5 \times 10^{-8}$  M (Figures 4.2a, b), and  $\text{Cu}_T = 10^{-7}$  M (Figures 4.3a, b)) the concentrations of free copper ions vary over two orders of magnitude over a pH range of 6-8 if  $\log *R_2 = -13.7$ . Computations with  $\log *R_2 = -17.3$  result in very small changes in the concentrations of  $\text{Cu}^{2+}$  (ca. one-quarter of an order of magnitude).

Table 4.5

## Stability Constants for Hydrolysis Products of Cu(II)

Species	log Equilibrium Constant (I=10 <sup>-3</sup> )	
CuOH <sup>+</sup> (aq)	*K <sub>1</sub>	-7.9
Cu(OH) <sub>2</sub> (aq)	*β <sub>2</sub>	-13.7 <sup>#</sup>
Cu(OH) <sub>3</sub> <sup>-</sup> (aq)	*β <sub>3</sub>	-26.8
Cu(OH) <sub>4</sub> <sup>2-</sup> (aq)	*β <sub>4</sub>	-39.9
Cu <sub>2</sub> (OH) <sub>2</sub> <sup>2+</sup> (aq)	*β <sub>22</sub>	-10.3
Cu(OH) <sub>2</sub> (s)	*K <sub>so</sub>	-8.4

<sup>#</sup> A recent lower estimate for log\*β<sub>2</sub> is -17.3.

Table 4.6

## Stability Constants for Cu-Cl Complexes

Species	log Equilibrium Constant ( $I=10^{-3}$ )	
$\text{CuCl}^+(\text{aq})$	$K_1$	0.5
$\text{CuCl}_2(\text{aq})$	$\beta_2$	0.3

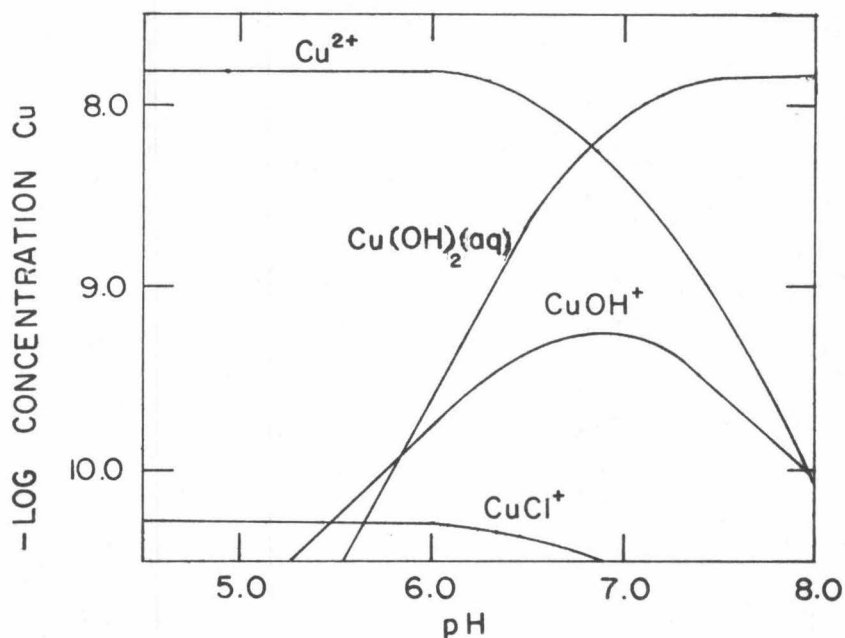


Figure 4.1a Speciation of Cu(II) in the carbonate-free system;  
 $\text{Cu}_T = 1.5 \times 10^{-8} \text{ M}$ ,  $I = 10^{-3}$ ,  $\log * \beta_2 \text{Cu}(\text{OH})_2(\text{aq}) = -13.7$ .

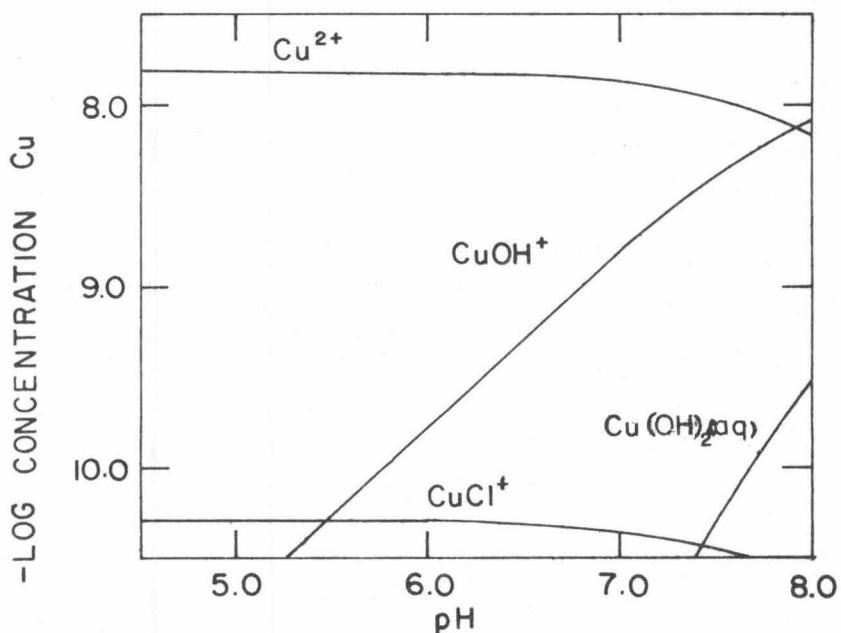


Figure 4.1b Speciation of Cu(II) in the carbonate-free system;  
 $\text{Cu}_T = 1.5 \times 10^{-8} \text{ M}$ ,  $I = 10^{-3}$ ,  $\log * \beta_2 \text{Cu}(\text{OH})_2(\text{aq}) = -17.3$ .

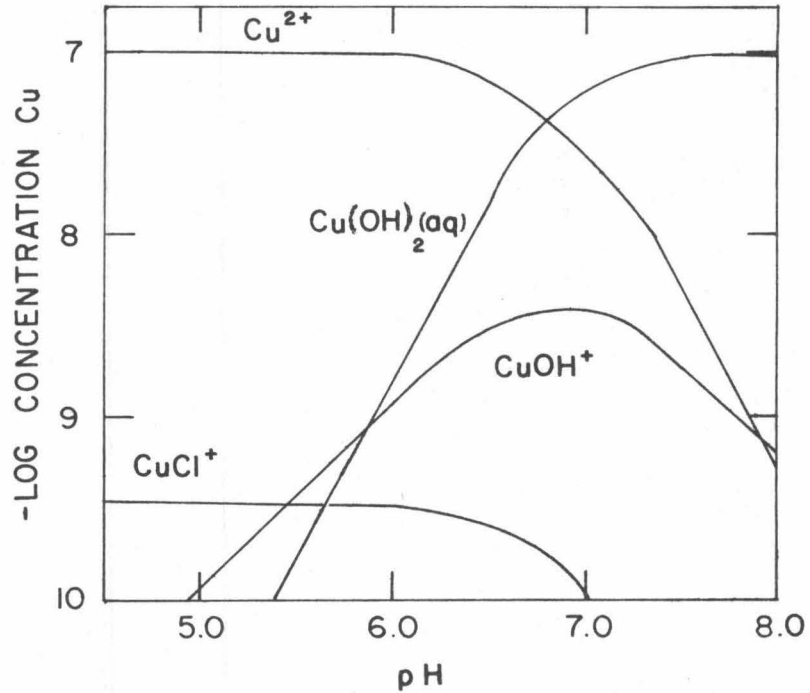


Figure 4.3a Speciation of Cu (II) in the carbonate-free system;  
 $\text{Cu}_T = 10^{-7} \text{ M}$ ,  $I = 10^{-3}$ ,  $\log * \beta_2 \text{Cu}(\text{OH})_2(\text{aq}) = -13.7$ .

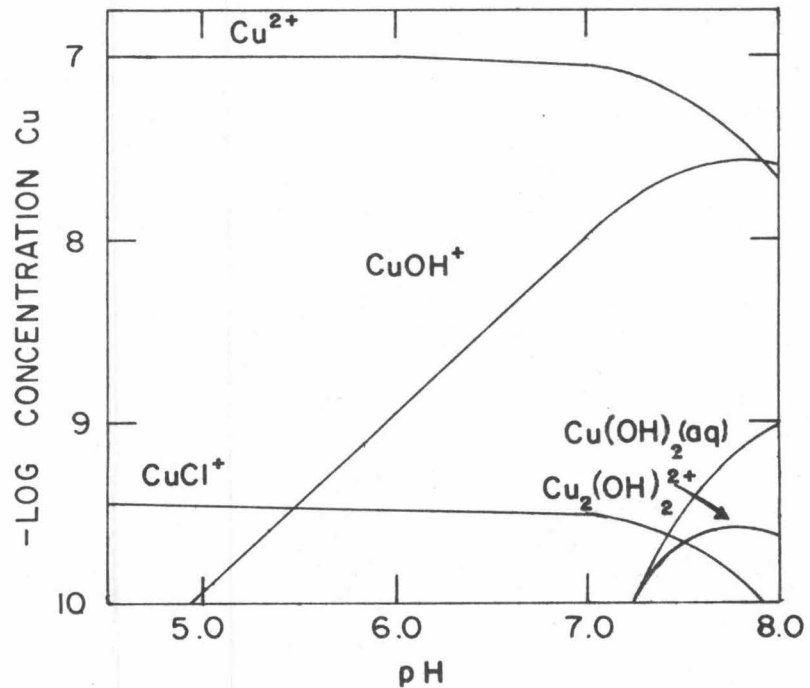


Figure 4.3b Speciation of Cu (II) in the carbonate-free system;  
 $\text{Cu}_T = 10^{-7} \text{ M}$ ,  $I = 10^{-3}$ ,  $\log * \beta_2 \text{Cu}(\text{OH})_2(\text{aq}) = -17.3$ .

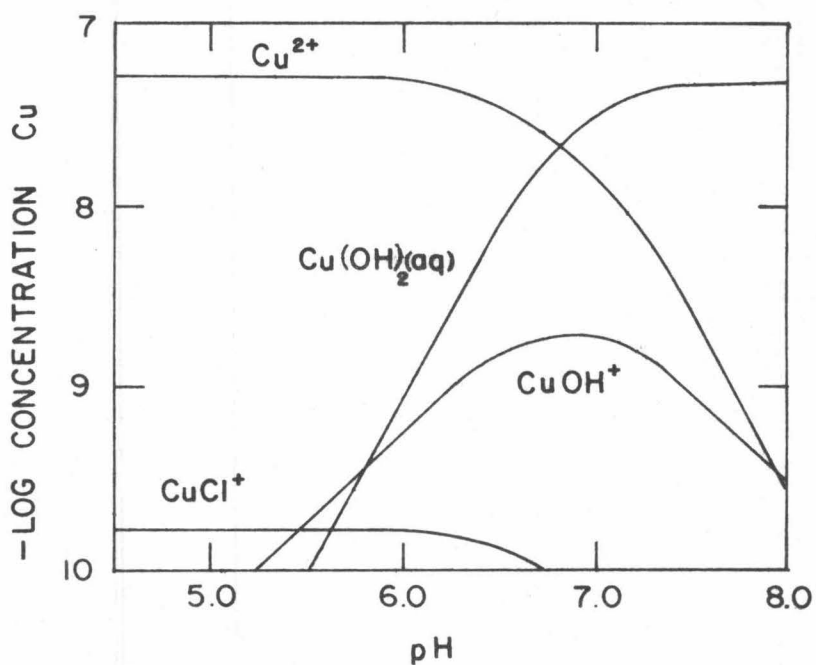


Figure 4.2a Speciation of Cu(II) in the carbonate-free system;  
 $\text{Cu}_T = 5 \times 10^{-8} \text{ M}$ ,  $I = 10^{-3}$ ,  $\log * \beta_2 \text{Cu(OH)}_2(\text{aq}) = -13.7$ .

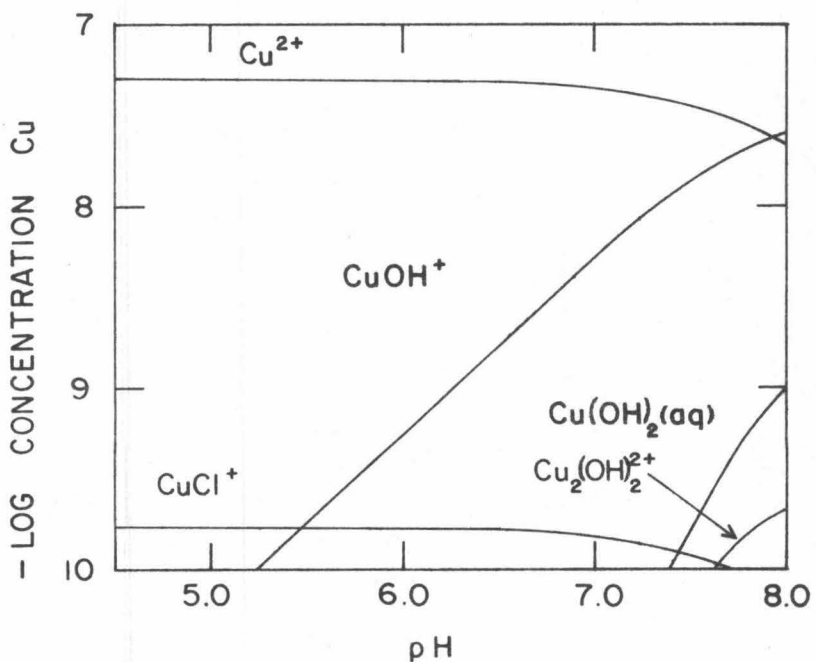


Figure 4.2b Speciation of Cu(II) in the carbonate-free system;  
 $\text{Cu}_T = 5 \times 10^{-8} \text{ M}$ ,  $I = 10^{-3}$ ,  $\log * \beta_2 \text{Cu(OH)}_2(\text{aq}) = -17.3$ .

The system containing  $1.5 \times 10^{-8}$  M  $\text{Cu}_T$  is below the point of precipitation of  $\text{Cu}(\text{OH})_2(\text{s})$  for this pH range, regardless of the choice of the second hydrolysis constant for  $\text{Cu}(\text{II})$ . If the concentration of  $\text{Cu}_T$  is increased to  $\text{Cu}_T = 5 \times 10^{-8}$  M there is no precipitation if  $\log^* \beta_2 = -13.7$  (Figure 4.2a) but approximately 2% precipitates at pH 8 if  $\log^* \beta_2 = -17.3$  (Figure 4.2b). When  $\text{Cu}_T$  is increased to  $10^{-7}$  M (Figure 4.3a, b) there is no precipitation if  $\log^* \beta_2 = -13.7$ , but approximately 50% of the total copper is precipitated at pH 8 if  $\log^* \beta_2 = -17.3$ .

For all three choices of total copper the main hydroxo complex depends on the stability constant for the second hydrolysis product. If  $\log^* \beta_2 = -13.7$  the dominant hydroxo complex is  $\text{Cu}(\text{OH})_2(\text{aq})$ , and if  $\log^* \beta_2 = -17.3$ , it is  $\text{Cu}(\text{OH})^+$ .

#### 4.4.2 Potentiometric Titrations of $\text{Cu}^{2+}$ as a Function of pH

$\text{Cu}(\text{OH})_2(\text{aq})$  is a very important species as predicted by the James-Healy Model. Since its charge is zero, its  $\Delta G_{\text{solv}}^{\circ}$  and  $\Delta G_{\text{coul}}^{\circ}$  are also zero and the species is very easily adsorbed on the surface. Obviously the choice of  $\log^* \beta_2$  will be very important in modeling experimental systems.

As was shown above, the change in activities of  $\text{Cu}^{2+}$  ( $\{\text{Cu}^{2+}\}$ ) between pH 6 and 8 is drastic when  $\log^* \beta_2 = -13.7$  and very small when  $\log^* \beta_2 = -17.3$ . Therefore, hydrolysis of  $\text{Cu}(\text{II})$  can be followed by

measuring  $\{\text{Cu}^{2+}\}$  using a copper ion-selective electrode, and the results used to choose between  $\log^*\beta_2 = -13.7$  and  $\log^*\beta_2 = -17.3$ .

The limit of detection of cupric ion activity in non-complexing solutions using a  $\text{CuS-Ag}_2\text{S}$ -electrode (solid state Cu-electrode) was reported to be  $10^{-8}$  M (Orion Research, Inc. (1968); Ion Selective Electrodes (1969); Jasinski et al. (1974)). Blaedel and Dinwiddie (1974) reported a lower value of  $10^{-9}$  M. In solutions containing a complexing agent measurements were obtained with very low concentrations of  $\text{Cu}^{2+}$  (as low as  $10^{-20}$  M) (Orion Research, Inc. (1968)).

Electrode interferences occur with silver and mercuric ions, as well as ferric ions (Orion Research, Inc. (1968); Ion Selective Electrodes (1969)). Interferences of silver and mercuric ions can be very easily overcome by holding their concentrations below one-tenth of the concentration of cupric ion, and those of ferric ion by adjusting the pH of the sample above 4 .

The measurements done with a Cu-electrode-reference electrode system showed a definite pH effect (Figure 4.4). Tests were done with four different concentrations of  $\text{Cu}_T$ . In each case the highest reading was obtained at pH 5.6-5.7. Above that pH the decrease in the reading was due to the decrease in  $\{\text{Cu}^{2+}\}$  resulting from hydrolysis, and below that pH the decrease in the reading can be explained in terms of the increased solubility of metal sulfides in acidic solutions

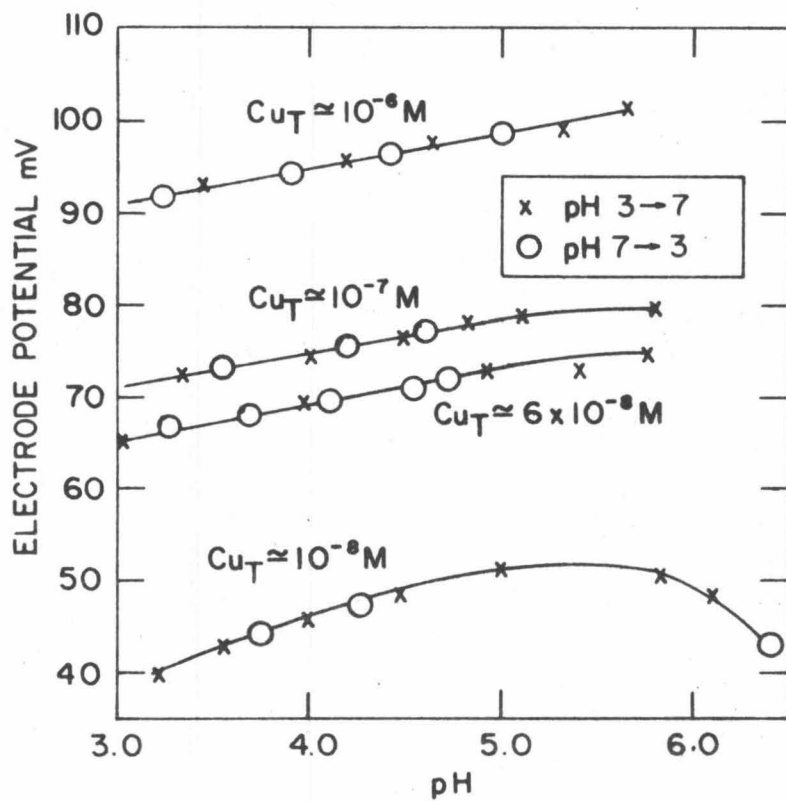


Figure 4.4 Measurements with the copper ion-selective electrode as a function of pH ( $I = 10^{-3}$ ).

(i. e., formation of  $\text{HS}^-$  and  $\text{H}_2\text{S}$ ) (Ion-Selective Electrodes (1969)).

Preparatory cleaning of the Cu-electrode is very important since it effects the rate of approach to steady state (Johansson and Edström (1972); Blaedel and Dinwiddie (1974)). The effect is attributed to the removal of a thin porous surface layer of  $\text{Ag}_2\text{S}$  left after leaching out of  $\text{CuS}$  through heavy use of the electrode (Blaedel and Dinwiddie (1974)).

The surface of the Cu-electrode was cleaned by polishing with polyethylene paper (Orion Research, Inc. (1972)), followed by soaking in stirred Q-water outside of the reaction vessel.

In the reaction vessel, the electrodes were equilibrated with  $\text{N}_2(\text{g})$ -purged  $10^{-3}$  M  $\text{NaCl}$  before the addition of  $\text{Cu}$ . The response time of the  $\text{Cu}^{2+}$ -electrode was observed to be two minutes. Calibration curves were obtained by the addition of  $\text{Cu}$  to the same solution. Nernstian behavior (at pH 5.6-5.7) was observed for all solutions containing  $\text{Cu}_T \geq 10^{-8}$  M.

To study hydrolysis of  $\text{Cu}(\text{II})$ , the electrodes were brought to a low reading outside the reaction vessel following the procedure described above. After equilibration with  $\text{N}_2(\text{g})$ -purged  $10^{-3}$  M  $\text{NaCl}$  at pH 8,  $\text{Cu}(\text{II})$  was added so that  $\text{Cu}_T = 1.5 \times 10^{-8}$  M (Figure 4.5). The pH was decreased by adding  $\text{HCl}$ . The lowest four points were obtained after a 15-minute equilibration, and all other points by a two-minute

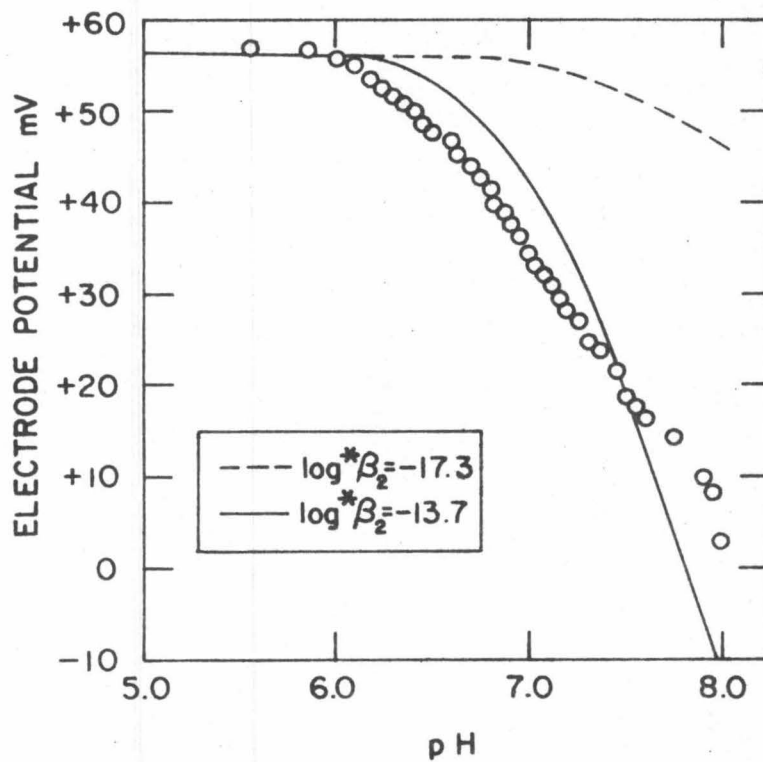


Figure 4.5 Potentiometric titration of  $\text{Cu}^{2+}$  ( $\text{Cu}_T = 1.5 \times 10^{-8} \text{ M}$ ,  $I = 10^{-3}$ ) with copper ion-selective electrode. Solid and broken line correspond to theoretical computations based on the equilibrium constants listed in Tables 4.5 and 4.6.

equilibration. If the system was back-titrated, the measured points were observed to agree very closely with the ones obtained by the addition of HCl.

The solid line in Figure 4.5 is a theoretical line based on  $\log^*\beta_2 = -13.7$  and assuming Nernstian behavior of the electrodes at the indicated pH values and concentrations of  $\text{Cu}^{2+}$ . The dotted line is based on  $\log^*\beta_2 = -17.3$  and the same assumptions as for the solid line. The points are the experimental results.

After the lowest pH was reached the pH was brought up to 8 by addition of NaOH. Then more Cu(II) was added to the system so that  $\text{Cu}_T = 5 \times 10^{-8} \text{ M}$  (Figure 4.6). Again, the first four points were taken after a 15 minute equilibration and the others after a two minute equilibration. When pH 5.5 was reached, the pH was again brought up to 8 and the concentration of Cu was increased to  $10^{-7} \text{ M}$  (Figure 4.7).  $\{\text{Cu}^{2+}\}$  was measured as before.

Based on the assumption that all hydrolysis constants except for  $^*\beta_2$  are well established, the results obtained with the  $\text{Cu}^{2+}$ -selective electrode strongly indicate that the hydrolysis constant for the formation of  $\text{Cu}(\text{OH})_2(\text{aq})$  is closer to  $\log^*\beta_2 = -13.7$  than to  $\log^*\beta_2 = -17.3$ . Nevertheless, in some of the following analyses of the adsorption systems both values for  $\log^*\beta_2$  will be used in order to illustrate their influence on the modeling of the experimental systems.

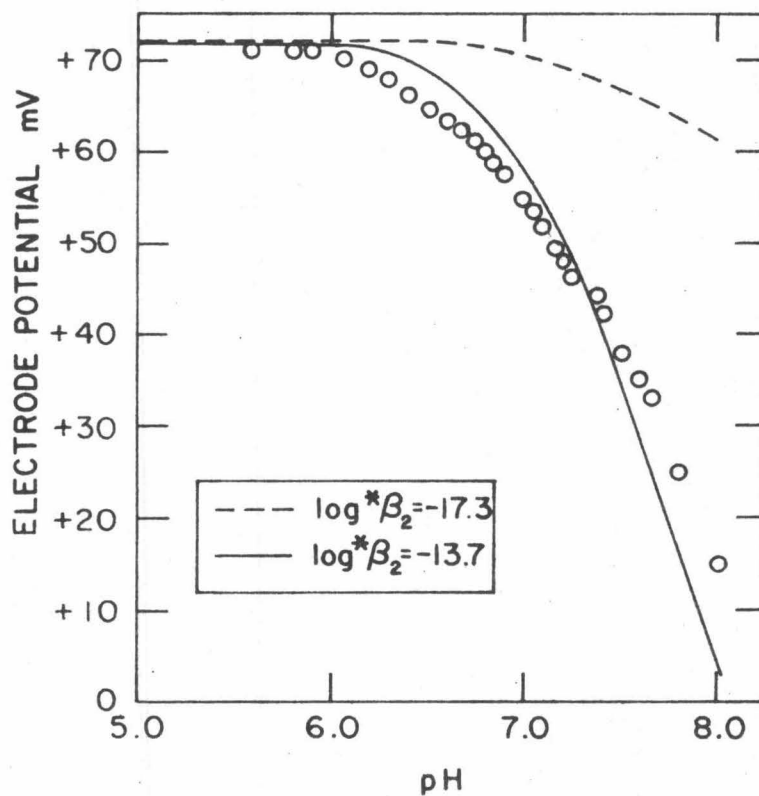


Figure 4.6 Potentiometric titration of  $\text{Cu}^{2+}$  ( $\text{Cu}_T = 5 \times 10^{-8} \text{ M}$ ,  $I = 10^{-3}$ ) with copper ion-selective electrode. Solid and broken lines correspond to theoretical computations based on the equilibrium constants listed in Tables 4.5 and 4.6.

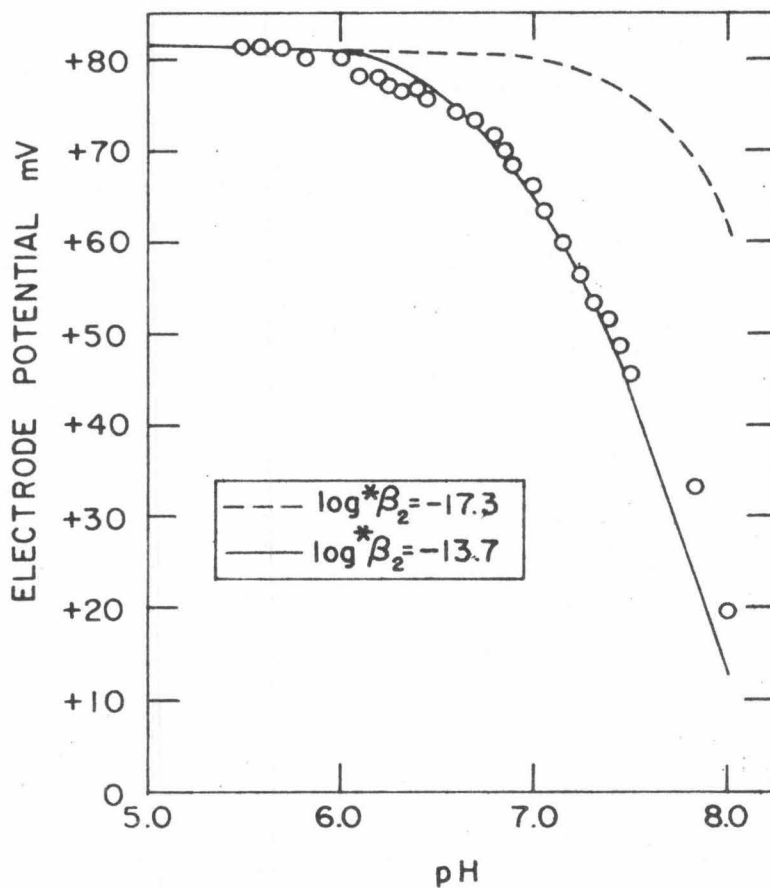


Figure 4.7 Potentiometric titration of  $\text{Cu}^{2+}$  ( $\text{Cu}_T = 10^{-7} \text{ M}$ ,  $I = 10^{-3}$ ) with copper ion-selective electrode. Solid and broken lines correspond to theoretical computations based on the equilibrium constants listed in Tables 4.5 and 4.6.

## Chapter 5

ADSORPTION OF Cu(II), Pb(II), Mg(II) AND Ca(II)  
ON  $\alpha$ -QUARTZ IN A CARBONATE-FREE SYSTEM

- 5.1 Adsorption of Cu(II) and Pb(II) on  $\alpha$ -Quartz as a Function of Time, Metal Ion Concentration and System Surface Area
- 5.1.1 Adsorption of Cu(II) and Pb(II) on  $\alpha$ -Quartz as a Function of Time

The rate of adsorption of metal ions is a function of both the surface (its chemical characteristics and physical structure) and the metal ion in question. The times reported necessary to obtain equilibration of metal ions with the hydrous iron oxides range from 3 hours for Pb(II), Zn(II), Cd(II), and Tl(I) (Gadde and Laitinen (1974)) and up to 20 hours for Co(II) (Kurbatov and Wood (1952)).

Morgan and Stumm (1964) and Posselt et al. (1968) observed a very rapid adsorption of the alkaline earth and the transition metal ions on  $\delta$ -MnO<sub>2</sub> (<5 min. and 5-10 min., respectively). Gadde and Laitinen (1974) reported a 3-hour equilibration time between hydrous manganese oxide and Pb(II), Cd(II), Zn(II), and Tl(I). Similarly, Murray et al. (1968) found that the final attainment of equilibrium between manganese (II) manganite and Ni(II), Cu(II), and Co(II) was reached after several hours, whereas Loganathan (1971) reported

an equilibration time of 2 days for  $\delta$ - $\text{MnO}_2$  and  $\text{Co(II)}$ ,  $\text{Zn(II)}$ , and  $\text{Ca(II)}$ .

Greenberg (1956) found that equilibrium between silica and calcium hydroxide was reached in 15 sec. Ahrlund et al. (1960) showed that ions such as  $\text{Na}^+$ ,  $\text{Ca}^{2+}$ ,  $\text{Gd}^{3+}$  and  $\text{UO}_2^{2+}$  are sorbed by silica very rapidly (in general, more than 95% of the final amount was sorbed within 5 min), whereas ions formed by  $\text{Zr(IV)}$ ,  $\text{U(IV)}$ , and  $\text{Pu(IV)}$  were taken up more slowly (75-150 hours). Kozawa (1961) reported that the adsorption of  $\text{Zn(II)}$  on silica reaches equilibrium in 2 hours and that of  $\text{Cu(II)}$  requires about 6 hours. Equilibration times of  $\text{Fe}^{3+}$ ,  $\text{Cu}^{2+}$ ,  $\text{Cd}^{2+}$ , and  $\text{Pb}^{2+}$  with Silikagel H and Aerosil 200, as observed by Schindler et al. (1975), were short, never exceeding 30 min.

Starik and Kositsyn found that in the period of 1 hour no less than 80-90% of ruthenium (1957a) and thorium (1957b) was adsorbed on glass. According to MacNaughton (1973) the reaction between  $\text{Zn(II)}$  and  $\alpha$ -quartz is completed almost instantaneously.  $\text{Hg(II)}$ , on the contrary, has a very long equilibration time with  $\alpha$ -quartz. The time necessary for establishing the equilibrium between  $\text{Co(II)}$  and  $\alpha$ -quartz is 3 hours (Healy et al. (1968)).

In the present study the equilibration time between  $\text{Cu(II)}$  and  $\text{Pb(II)}$  and  $\alpha$ -quartz was found to be very fast. Regardless of the system surface area involved, it was found that 90-100% of  $\text{Cu}_{\text{ads}}$  and  $\text{Pb}_{\text{ads}}$  was adsorbed during the first five minutes (Figure 5.1 and 5.2 respectively).

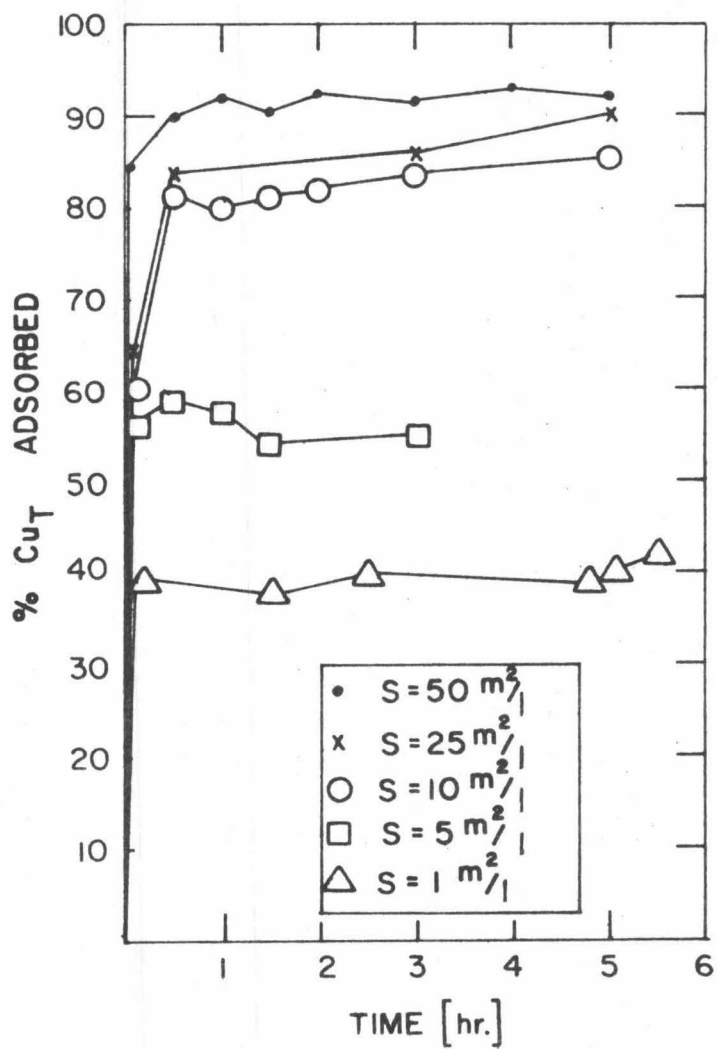


Figure 5.1 Adsorption of Cu on Min-U-Sil at different surface areas as a function of time.  $Cu_T = 10^{-6}$  M,  $I = 10^{-3}$ , pH = 7, carbonate-free system.

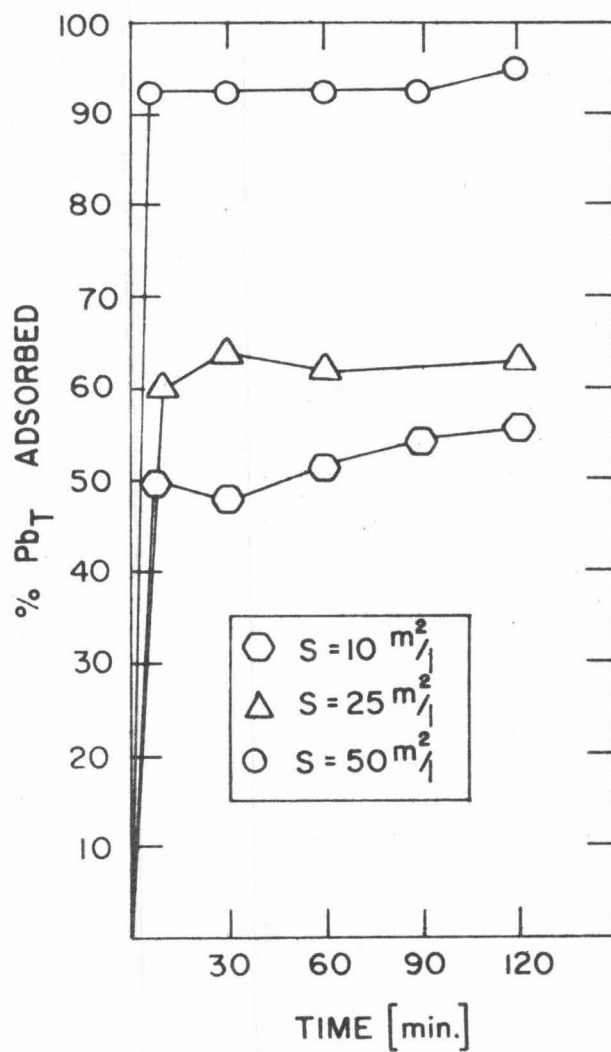


Figure 5.2 Adsorption of Pb on Min-U-Sil at different surface areas as a function of time.  $Pb_T = 10^{-6} \text{ M}$ ,  $i = 10^{-3}$ ,  $\text{pH} = 7$ , carbonate-free system.

### 5.1.2 Adsorption of Cu(II) and Pb(II) on $\alpha$ -Quartz as a Function of Metal Concentration and System Surface Area

At equilibrium the amount of the adsorbed metal ion, with a fixed pH and ionic strength, is a function of the total concentration of the metal and the available surface area. Figures 5.3 and 5.4 show the adsorption density measurements of Cu(II) and Pb(II) on  $\alpha$ -quartz, which were obtained by varying the  $Me_T$  and the surface area.

The maximum coverage,  $\Gamma_{\max}$ , assuming a monolayer of hydrated ions, is given by James and Healy (1972a, 1972b, 1972c) as

$$\Gamma_{\max} = \frac{1}{\pi(r_{\text{ion}} + 2r_w)^2} \quad (5.1)$$

For Cu(II) ( $r_{\text{ion}} = 0.78\text{\AA}$ ) the calculated  $\Gamma_{\max} = 4.2 \times 10^{-6}$  moles/m<sup>2</sup> and for Pb(II) ( $r_{\text{ion}} = 1.20\text{\AA}$ )  $\Gamma_{\max} = 3.37 \times 10^{-6}$  moles/m<sup>2</sup>. The results in Figures 5.3 and 5.4 show that the experimentally found adsorption densities have not reached their maximum theoretical values.

## 5.2 Adsorption of Cu(II), Pb(II), Mg(II), and Ca(II) on $\alpha$ -Quartz as a Function of pH and Ionic Strength

### 5.2.1 Equilibrium Modeling

The equilibrium computations were obtained using the REDEQL2 numerical method (McDuff and Morel (1973)). REDEQL2 is a general purpose computer program especially adapted to study acid-base,

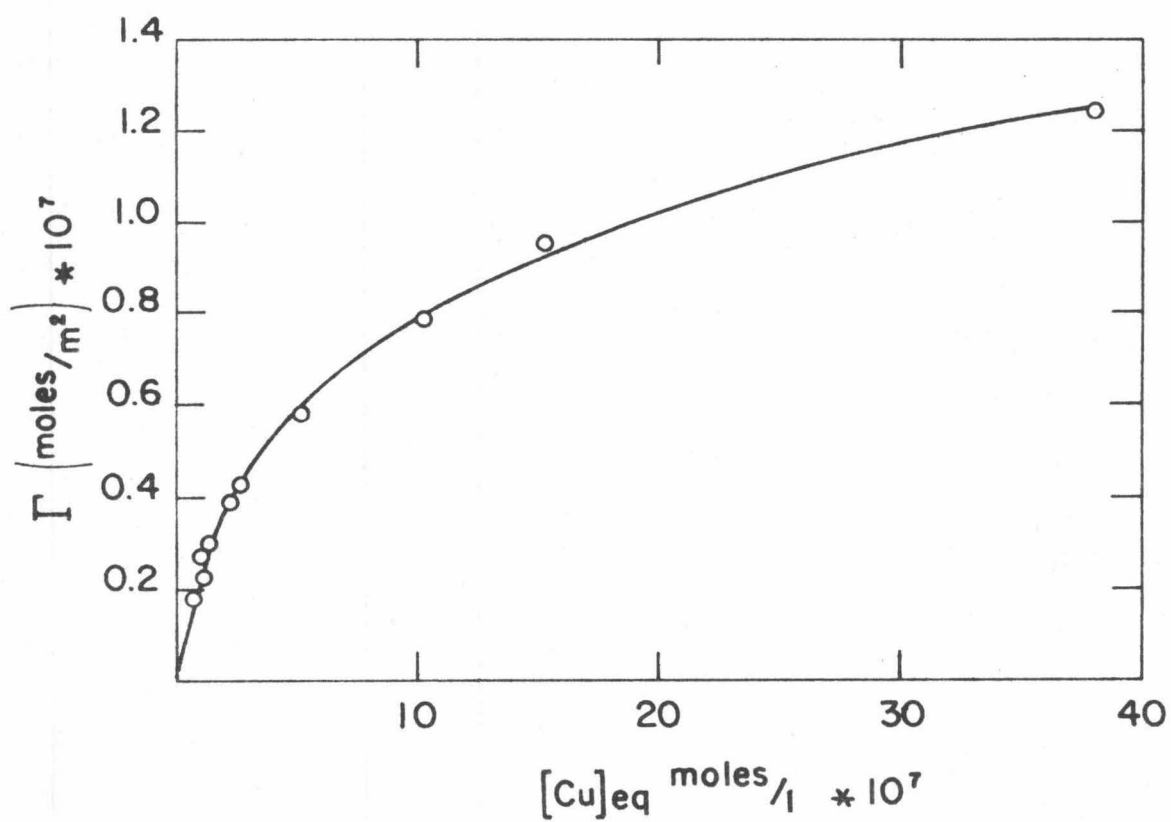


Figure 5.3 Adsorption isotherm of Cu(II) on  $\alpha$ -quartz at pH 7 and  $I = 10^{-3}$ .

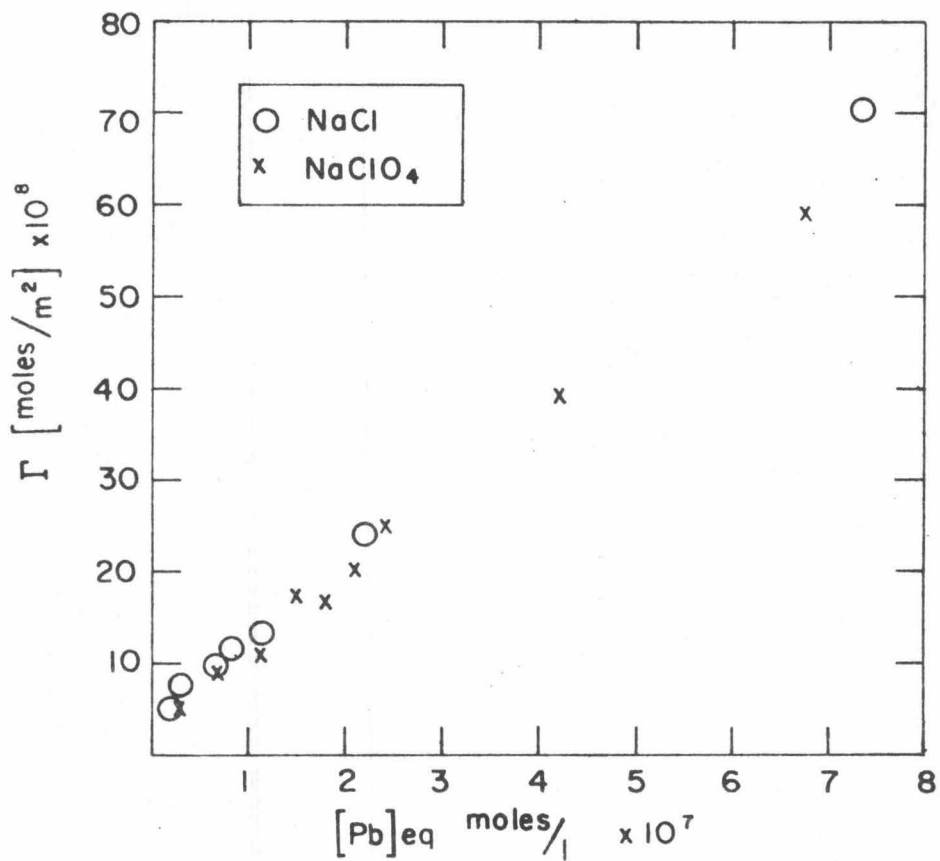


Figure 5.4 Adsorption isotherm of Pb(II) on  $\alpha$ -quartz at pH 7 and  $I = 10^{-3}$ .

precipitation-dissolution, redox, and adsorption processes. The program uses the stability constant approach and the Newton-Raphson method for digital computations of equilibria. It can determine the composition of the aqueous phase and the corresponding set of solids in equilibrium at a given pH,  $p_{\text{e}}$ , temperature, pressure and gas-phase component partial pressure by simultaneously solving the various characteristic equations. Special subroutines correct the activities for the appropriate ionic strength using the Davies equation (i. e. ,  $\log \gamma = AZ^2 \left( \frac{\sqrt{I}}{\sqrt{I+1}} - 0.2I \right)$ ) and compute the corresponding corrected stability constants. The subroutines INADS, ADSORP, and IONADS are used together with the rest of the program to compute adsorption equilibria. The INADS subroutine reads the thermodynamic, stoichiometric and analytical data for adsorption.

The ADSORP subroutine computes the constants for adsorption for each pH and ionic strength considered, using the James-Healy Model. Equilibrium computations including these constants are achieved by considering the adsorbing surface as another constituent of the system as explained below.

Adsorption of a metal ion can be described by the following expression:

unoccupied surface + Me = adsorbed metal (or occupied surface)

This is treated as a chemical reaction because it depends on bulk concentration of metal ion and adsorbent. Hence,

$$[\text{Me}_{\text{ads}}] = k[\text{Me}][\text{u}] \quad (5.2)$$

where  $[\text{u}]$  is unoccupied surface in  $\text{cm}^2/\text{l}$ ,  $[\text{Me}]$  is the concentration of metal ion in moles/l and  $k$  is a constant. Then

$$\text{Me}_T = [\text{Me}_{\text{ads}}] + [\text{Me}] \quad (5.3)$$

and

$$[\text{S}] = [\text{u}] + [\text{o}] \quad (5.4)$$

where  $[\text{S}]$  is the total surface and  $[\text{o}]$  is the occupied surface, both in  $\text{cm}^2/\text{l}$ . Then by definition

$$[\text{o}] = \gamma [\text{Me}_{\text{ads}}] \quad (5.5)$$

where  $\gamma$  is the area in  $\text{cm}^2$  covered by each mole of adsorbed metal species. Thus,

$$[\text{S}] = [\text{u}] + \gamma [\text{Me}_{\text{ads}}] \quad (5.6)$$

Substituting Equation 5.6 into 5.2 results in

$$[\text{Me}_{\text{ads}}] = k[\text{Me}]([\text{S}] - \gamma [\text{Me}_{\text{ads}}]) \quad (5.7)$$

or

$$\frac{[\text{Me}_{\text{ads}}]}{[\text{S}]} = \frac{k[\text{Me}]}{1+k\gamma[\text{Me}]} = \frac{\frac{1}{\gamma}[\text{Me}]}{\frac{1}{k\gamma} + [\text{Me}]} \quad (5.8)$$

Since

$$\frac{[\text{Me}_{\text{ads}}]}{[\text{S}]} = \Gamma_{\text{Me}} = \begin{array}{l} \text{the adsorption density in moles/cm}^2 \\ \text{of species Me} \end{array} \quad (5.9)$$

$$\frac{1}{\gamma} = \Gamma_{\text{Me}}^{\text{max}} = \text{the saturation value of } \Gamma_{\text{Me}} \quad (5.10)$$

$$\frac{1}{k\gamma} = K_{\text{ads, Me}} = \text{the constant for adsorption of species Me} \quad (5.11)$$

Equation 5.8 can be rewritten as

$$\Gamma_{\text{Me}} = \frac{\Gamma_{\text{Me}}^{\text{max}} [\text{Me}]}{K_{\text{ads, Me}} + [\text{Me}]} \quad (5.12)$$

which is the classical Langmuir adsorption isotherm. Hence, equilibrium computations including adsorption on surfaces can be achieved by considering the surface as a ligand and adsorption reactions as complex formation between the metal and the surface. To treat adsorption equilibria one thus needs, in addition to the usual thermodynamic, stoichiometric, and analytical equilibrium data, the following:

1. system surface area(s) of adsorbent(s)
2. list of adsorbing species

3. maximum adsorption densities of adsorbing species
4. equilibrium constants of adsorption

In the James-Healy Model the maximum adsorption densities are computed from Equation 5.1. The constants of adsorption are related to the energy of adsorption  $\Delta G_{\text{ads}}^{\circ}$  by

$$K_{\text{ads},i} = \exp(+\Delta G_{\text{ads},i}^{\circ}/RT) \quad (5.13)$$

$\Delta G_{\text{ads},i}^{\circ}$  can be generated from the James-Healy Model according to Equation 2.1 by specifying  $\Delta G_{\text{chem},i}^{\circ}$ . The chemical free-energy term for adsorption on  $\text{SiO}_2$  is an adjustable parameter selected to obtain adequate fit between the experimental and the theoretical increase in adsorption as a function of pH. For the  $\text{Cu(II)-SiO}_2$  system, the specific adsorption potential was found to be -8.0 kcal/mole, and for  $\text{Pb(II)-SiO}_2$  system -6.5 kcal/mole. The specific adsorption potential for  $\text{Na-SiO}_2$  system (-3.0 kcal/mole) was estimated indirectly, by examining the adsorption behavior of  $\text{Cu(II)}$  under conditions of changing ionic strength (Table 5.1).

The IONADS subroutine is employed in place of the ADSORP subroutine in order to compute adsorption equilibria according to the Ion Exchange-Surface Complex Formation Model. These computations are obtained by specifying the total number of sites/l, the intrinsic acidity constant of the surface OH groups, and the constants for the

Table 5.1  
Specific Adsorption Potentials for  $\alpha$ -Quartz Used for  
the Modeling of the Experimental Systems  
with the James-Healy Model

---

$$\Delta G_{\text{chem,Na}}^{\circ} = -3.0 \text{ kcal mole}^{-1}$$

$$\Delta G_{\text{chem,Cu}}^{\circ} = -8.0 \text{ kcal mole}^{-1}$$

$$\Delta G_{\text{chem,Pb}}^{\circ} = -6.5 \text{ kcal mole}^{-1}$$

---

adsorption of a metal ion on a given oxide surface (see Chapter 2). The adsorption constants for the Ion Exchange-Surface Complex Formation Model were obtained by fitting the experimental results, analogous to the procedure used for  $\Delta G_{\text{chem}}^{\circ}$  in the James-Healy Model. Namely, the adsorption constants  $*K_1^s$  and  $*\beta_2^s$  were adjusted so that a close fit was obtained between the experimental pH-dependent adsorption isotherms for Cu(II) and Pb(II) on  $\text{SiO}_2$ , and the model computations for the same system. Parameters used for the computations using the Ion Exchange-Surface Complex Formation Model are listed in Table 5.2.

At the present time the program handles only the adsorption of metal ions on oxides, the surface potential of which is determined by pH. Provisions were made to handle the adsorption of ligands on the same kind of oxide surfaces. No provisions have been made for handling surfaces with fixed surface charge.

### 5.2.2 Adsorption of Cu (II) on $\alpha$ -Quartz as a Function of pH and Ionic Strength

For an aqueous solution containing  $10^{-6}$  M  $\text{Cu}_T$ , the equilibrium speciation shows that the hydrolysis of Cu(II) starts at pH 5.5 (Figure 5.5a). It is characterized by a steep curve; at about pH 6.9 the concentration of copper free ions is equal to the concentration of the Cu(II)-hydroxo complexes, shown as Cu-OH. According to Table 4.5 these complexes include  $\text{CuOH}^+(\text{aq})$ ,  $\text{Cu}(\text{OH})_2(\text{aq})$ ,  $\text{Cu}(\text{OH})_3^-(\text{aq})$ ,

Table 5.2

Parameters Used for the Modeling of Cu(II) and Pb(II)

Adsorption on  $\alpha$ -Quartz with the

Ion Exchange-Surface Complex Formation Model

---

$$pK_{\text{int}} = -6.8 \quad (\text{Schindler and Kamber (1968)})$$

Density of SiOH groups = 0.0191 moles/kg (Schindler et al.  
(1975))

$$\log^*K_{1, \text{Cu}}^{\text{S}} = -1.8 \quad \log^*\beta_{2, \text{Cu}}^{\text{S}} = -3.8$$

$$\log^*K_{1, \text{Pb}}^{\text{S}} = -1.55 \quad \log^*\beta_{2, \text{Pb}}^{\text{S}} = -4.5$$

$$\log^*K_{1, \text{Na}}^{\text{S}} = -4.15$$

---

$\text{Cu}(\text{OH})_4^{2-}$  (aq), and  $\text{Cu}_2(\text{OH})_2^{2+}$  (aq). Below pH 6.9 most of the copper is in the form of the free metal ion, and above this pH in its hydrolyzed forms. The precipitation of  $\text{Cu}(\text{OH})_2$ (s) does not take place in this pH range. Chloride complexes (Table 4.6) are negligible.

The addition of  $\alpha$ -quartz to this solution causes a new equilibrium to be established. Namely, the equilibrium distribution of a system containing  $10^{-6}$  M  $\text{Cu}_T$  and  $S=50 \text{ m}^2/1$  shows that the adsorption of Cu(II) on  $\alpha$ -quartz is characterized by a sharp increase in adsorption between pH 4 and 6 (Figure 5.5b). The circles represent experimentally obtained data and the lines represent theoretical computations using the James-Healy Model.\* Between pH 4 and 6 the main computed adsorbing species is  $\text{CuOH}^+$ , followed by  $\text{Cu}^{2+}$ . At pH 6.5  $\text{Cu}^{2+}$  becomes less important, but the importance of  $\text{Cu}(\text{OH})_2$ (aq) increases and it becomes dominant above pH 7.5. The other hydroxo species of Cu(II) contribute less than 0.001% to the total amount of Cu(II) adsorbed in all cases.

The supporting electrolyte affects the adsorption of a metal ion in three different ways. First, the ionic strength controls the charge density in the diffuse double layer. The addition of more electrolyte at a constant pH results in the compression of the electrical double

---

\* In the forthcoming analyses of the experimental systems the discussions, if not stated otherwise, correspond to the computations done with the James-Healy Model.

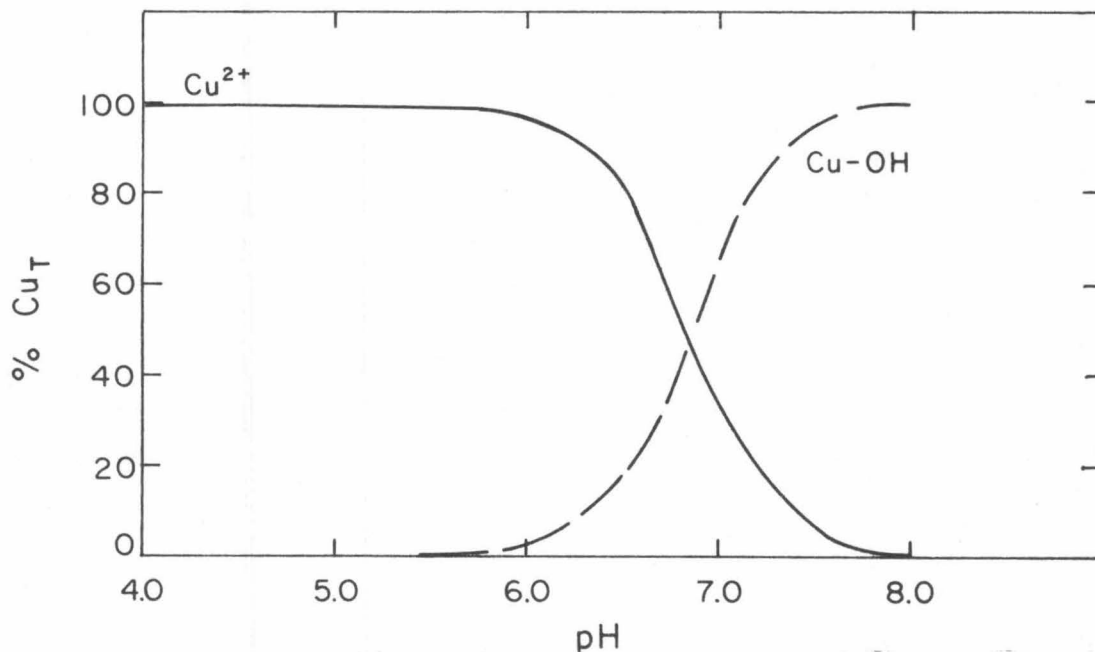


Figure 5.5a Equilibrium speciation of Cu as a function of pH in the solution:  $Cu_T = 10^{-6}$  M,  $I = 10^{-3}$ , carbonate-free.  $\text{Log}^* \beta_2 \text{Cu}(\text{OH})_2(\text{aq}) = -13.7$ .

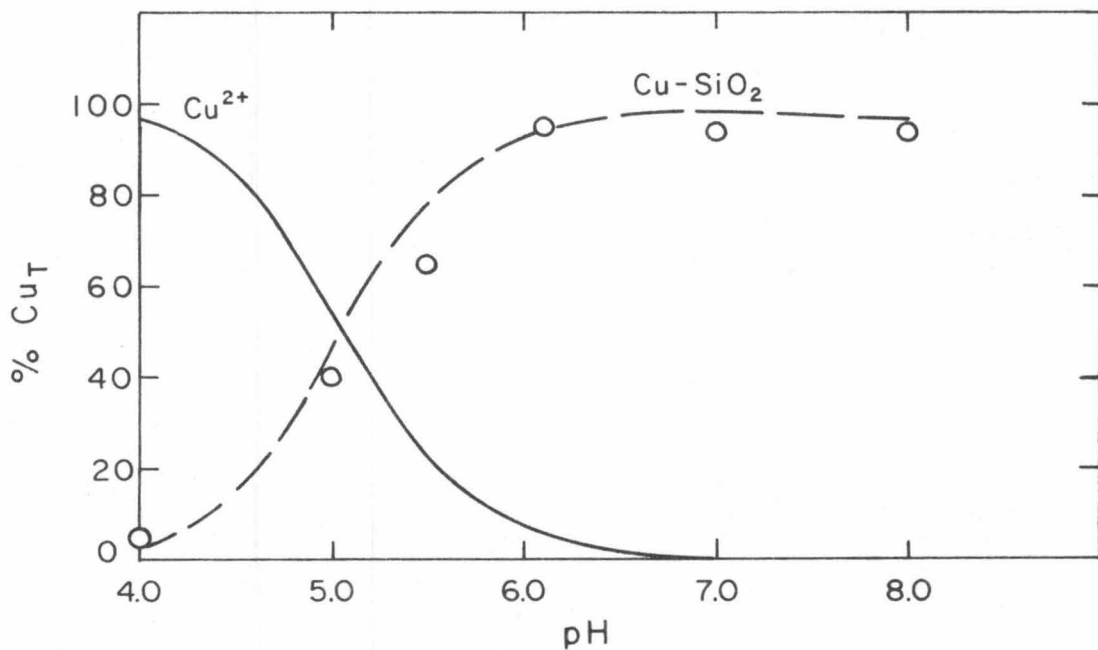


Figure 5.5b Equilibrium distribution of Cu as a function of pH in the system:  $Cu_T = 10^{-6}$  M,  $S = 50 \text{ m}^2 / \text{l Min-U-Sil}$ ,  $I = 10^{-3}$ , carbonate-free. Experimental results modeled with the James-Healy Model.

layer. Consequently, the electric field at a given point is increased and the electrostatic potential at the same point is decreased, resulting in an increased solvation energy and a decrease in coulombic energy. The overall effect of the addition of more electrolyte to the system is a reduced adsorption of a given metal. Second, the ions of the supporting electrolyte can themselves be treated as adsorbates competing for the adsorption sites with a given metal ion. Third, an influence of the supporting electrolyte can occur through complex formation of its anion with the metal ion in question.

At both low and high pH values, changes in the ionic strength do not have any large influence on the adsorption of Cu(II) on SiO<sub>2</sub> (Figure 5.6). However, very pronounced changes do occur in the pH region characterized by the sharp increase in adsorption. An increase in the ionic strength from  $I=10^{-3}$  to  $I=10^{-2}$  results in a shift of the adsorption edge approximately one pH unit higher. At the same time this shift reduces the amount of Cu adsorbed by almost 40% at pH 6. Further increase in the ionic strength ( $I=10^{-2}$  to  $I=10^{-1}$ ) results in a less drastic, but still pronounced change.

### 5.2.3 Adsorption of Pb(II) on $\alpha$ -Quartz as a Function of pH

The hydrolysis of  $5 \times 10^{-7}$  M Pb<sub>T</sub> begins at a slightly lower pH than that of Cu(II) (Figure 5.7a). At about pH 7 concentrations of all hydrolyzed species of Pb(II) are equal to the concentration of free

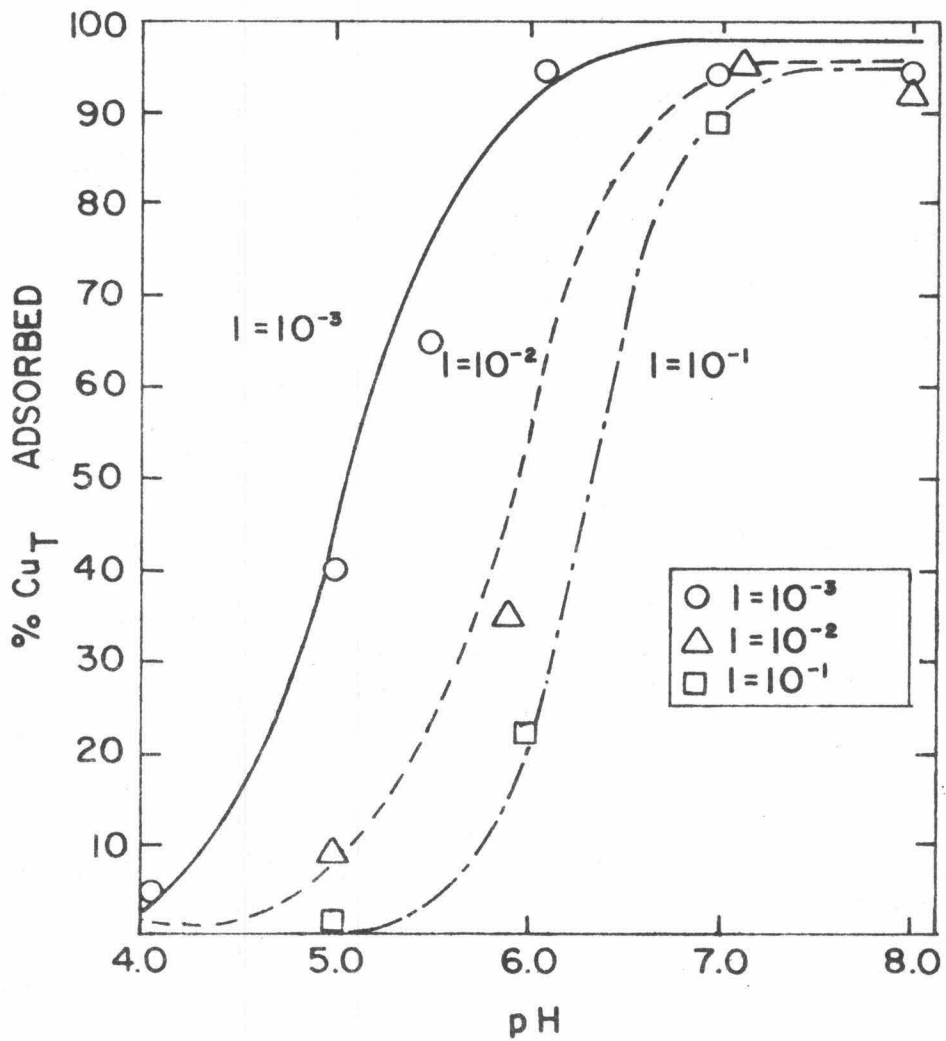


Figure 5.6 Adsorption of Cu(II) from solutions of different ionic strengths.  $Cu_T = 10^{-6}$  M,  $S = 50 \text{ m}^2/\text{l}$  Min-U Sil, carbonate-free.  $\text{Log}^* \beta_2 \text{Cu(OH)}_2(\text{aq}) = -13.7$ . Experimental results modeled with the James-Healy Model.

metal ion,  $\text{Pb}^{2+}$ . Below pH 7 most of the lead is present in the form of  $\text{Pb}^{2+}$ , and above that pH it is hydrolyzed to  $\text{PbOH}^+(\text{aq})$ ,  $\text{Pb}(\text{OH})_2(\text{aq})$ ,  $\text{Pb}(\text{OH})_3^-(\text{aq})$ ,  $\text{Pb}_2(\text{OH})^{3+}(\text{aq})$  (Table 4.2). The given equilibrium is below the precipitation point for  $\text{Pb}(\text{OH})_2(\text{s})$ . Chloride complexes (Table 4.3) amount to less than 3% of  $\text{Pb}_T$ .

The equilibration of this solution with  $\alpha$ -quartz results in a new distribution of Pb which can be computed by using  $\Delta G_{\text{chem, Pb}}^{\circ} = -6.5$  kcal mole<sup>-1</sup> (Figure 5.7c). As in the case of Cu(II), the adsorption of Pb(II) begins at pH 4, increasing on a less steep curve; at pH 6 less than 90%  $\text{Pb}_T$  is bound to the surface.

The solution in equilibrium with  $\alpha$ -quartz has the same normalized equilibrium distribution of species as the original solution prior to being equilibrated with  $\alpha$ -quartz (Figure 5.7b). The lack of a shift in the normalized equilibrium distribution of Pb(II) in solution before and after adsorption reflects the unimportance of the adsorption of polynuclear Pb(II)-hydrolysis products. If polynuclear Pb(II)-hydrolysis products were important, the normalized equilibrium distribution of the Pb(II) species after equilibration with  $\text{SiO}_2(\text{s})$  would be expected to be lower than that prior to equilibration.

#### 5.2.4 Adsorption of both Cu(II) and Pb(II) on $\alpha$ -Quartz from Equimolar Solutions as a Function of pH

In the system containing Cu(II) and Pb(II) at equimolar

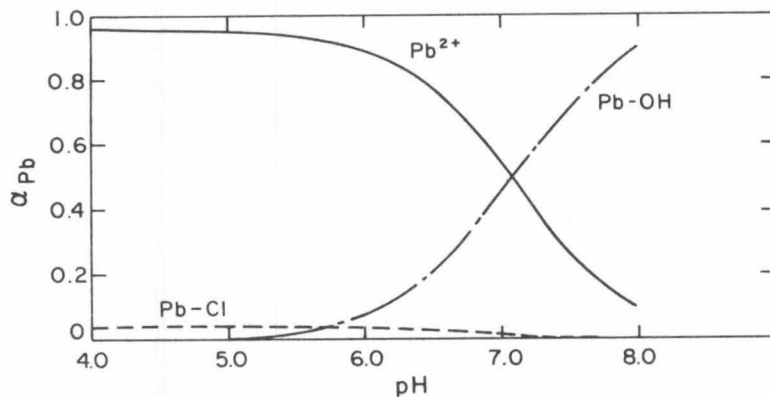


Figure 5.7a Normalized equilibrium speciation of Pb vs. pH in solution:  $Pb_T = 5 \times 10^{-7} M$ ,  $I = 10^{-3}$ , carbonate-free.

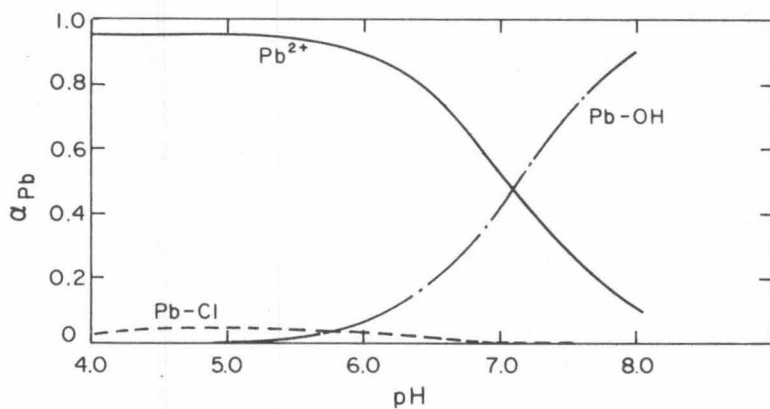


Figure 5.7b Normalized equilibrium speciation of Pb vs. pH in aqueous phase of the system:  $Pb_T(aq) = Pb_T - Pb_{ads}$ ,  $Pb_T = 5 \times 10^{-7} M$ ,  $S = 75 m^2 / \mu$  Min-U-Sil,  $I = 10^{-3}$ , carbonate-free.

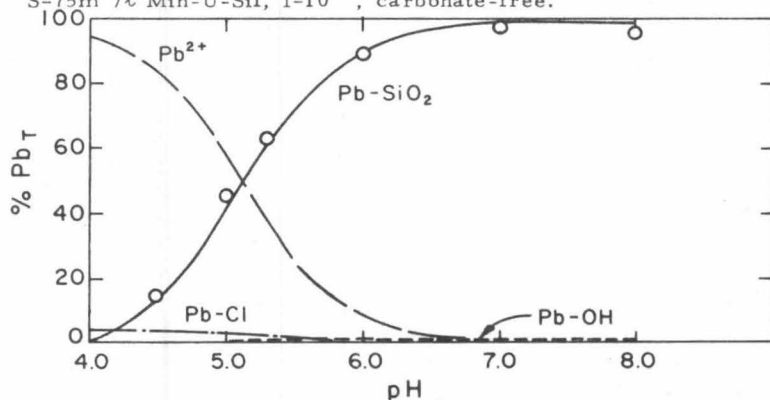


Figure 5.7c Equilibrium distribution of Pb vs. pH in the system:  $Pb_T = 5 \times 10^{-7} M$ ,  $S = 75 m^2 / \mu$  Min-U-Sil,  $I = 10^{-3}$ , carbonate-free. Experimental results modeled with the James-Healy Model.

concentrations (Figure 5.8), an addition of an excess of surface area of  $\text{SiO}_2$  will not cause the competition between these metals for the available sites. As predicted by model computations, the adsorption of Cu(II) is followed very closely by Pb(II) (Figure 5.9). At high pH values close to 100% of both metals is removed from the solution by adsorption on  $\alpha$ -quartz.

#### 5.2.5 Adsorption of Mg(II) and Ca(II) on $\alpha$ -Quartz as a Function of pH

The interactions of Mg(II) and Ca(II) with quartz as a function of pH show that adsorption of both metals occurs at high pH values, where calculations predict the formation of  $\text{MeOH}^+$  (James and Healy (1972a, 1972b)). Clark and Cooke (1968) found that the adsorption of magnesium from a  $2.5 \times 10^{-3}$  M  $\text{Mg}_T$  solution and calcium from a  $2.5 \times 10^{-3}$  M  $\text{Ca}_T$  solution increased sharply at pH 9.5 and 10.5, respectively.

Since  $\text{SiO}_2(\text{s})$  dissolves in the strong alkaline region (e.g., pH 12) forming orthosilicic acid and monomeric and polymeric silicates (Stumm et al. (1967)), Ahmed and Van Cleave (1965) have proposed that apparent increased adsorption of Ca by quartz at pH 12 is due to the formation of calcium silicate from the dissolved colloidal silica.

James and Healy (1972a, 1972b) found that adsorption of Ca on  $\alpha$ -quartz from a  $1.4 \times 10^{-4}$  M  $\text{Ca}_T$  at  $I=10^{-2}$  rises abruptly at pH 9. They modeled their experimentally-obtained adsorption isotherm using

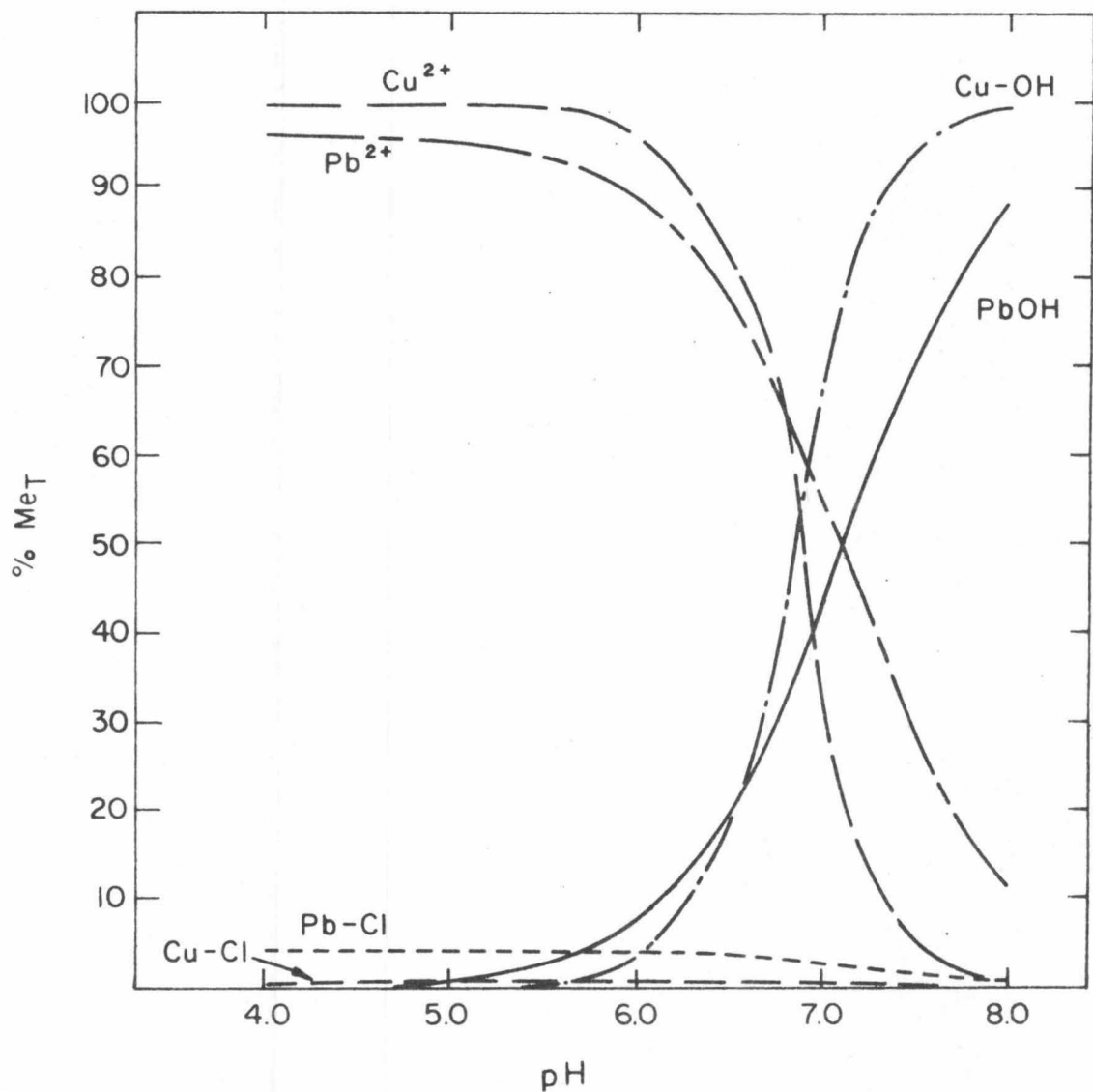


Figure 5.8 Equilibrium speciation of Cu and Pb vs. pH in the solution:  $Cu_T = Pb_T = 5 \times 10^{-7}$  M,  $I = 10^{-3}$ , carbonate-free.

$\text{Log } \beta_2 \text{Cu(OH)}_2(\text{aq}) = -13.7$ .

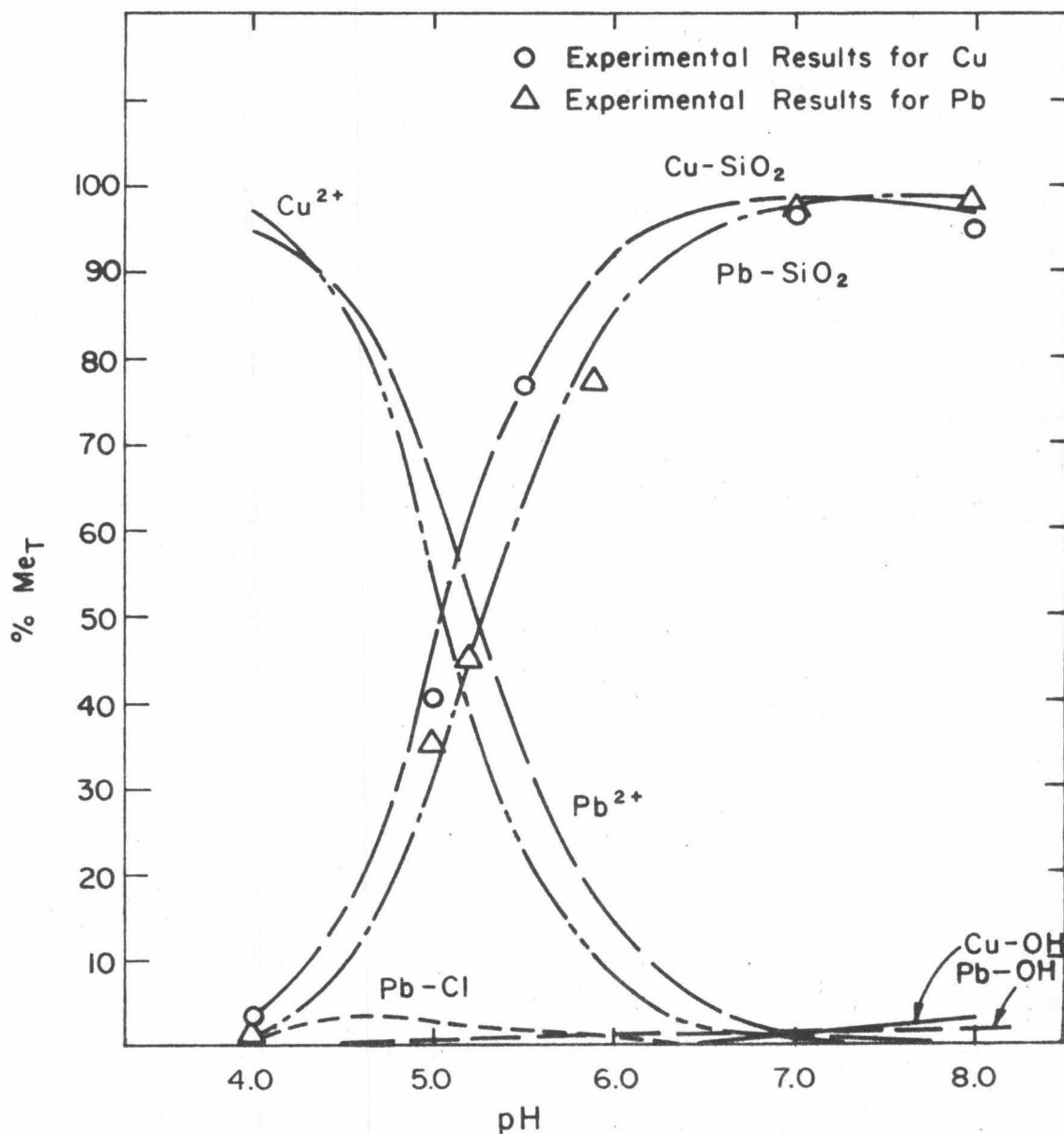


Figure 5.9 Equilibrium distribution of Cu and Pb vs. pH in the system:  $Cu_T = Pb_T = 5 \times 10^{-7} M$ ,  $S = 50 m^2 / l$  Min-U-Sil,  $I = 10^{-3}$ , carbonate-free.  $\log \beta_2 Cu(OH)_2(aq) = -13.7$ . Experimental results modeled with the James-Healy Model.

$\Delta G_{\text{chem, Ca}}^{\circ} = -7.0 \text{ kcal mole}^{-1}$  for both free metal ion and hydroxo species.

In the case of the adsorption of Mg and Ca on  $\text{SiO}_2(\text{s})$  at lower ionic strengths (e. g. ,  $I=10^{-3}$ ) unforeseen problems arise in using the James-Healy Model: the adsorption of  $\text{Me}^{2+}$  on  $\text{SiO}_2$  at lower pH, which was not observed experimentally (Figure 5.10). At high pH the  $\text{SiO}_2$ -surface has a high negative charge (Equation 2.4). A low ionic strength implies a smaller  $\kappa$  (Equation 2.5). Hence, according to Equation 2.3, the electrostatic potential at any distance  $x$ ,  $\Delta\Psi_x$ , is increased, and the resulting electric field  $\frac{d\Psi}{dx}$  (Equation 2.10) is decreased. An increased electrostatic potential and a decreased field strength imply an increased coulombic energy (Equation 2.2) and a decreased desolvation energy (Equation 2.11), and thus an increased adsorption of a given metal. Since the hydrolysis of Mg(II) and Ca(II) is restricted to the higher pH range, the adsorbing species is the free metal ion  $\text{Me}^{2+}$ . Hence, this effect will be more pronounced for Ca(II) than for Mg(II), because the hydrolysis of Ca(II) starts at higher pH. In order to model the experimental results of the adsorption of Mg(II) and Ca(II) on  $\alpha$ -quartz at  $I=10^{-3}$  (Figure 5.11 and 5.12, respectively) it was necessary to promote the adsorption of  $\text{MeOH}^+(\text{aq})$  over  $\text{Me}^{2+}(\text{aq})$  by imposing a different  $\Delta G_{\text{chem, Me}}^{\circ}$  over the pH range of adsorption. The list of the values for  $\Delta G_{\text{chem, Me}}^{\circ}$  used for fitting the experimental

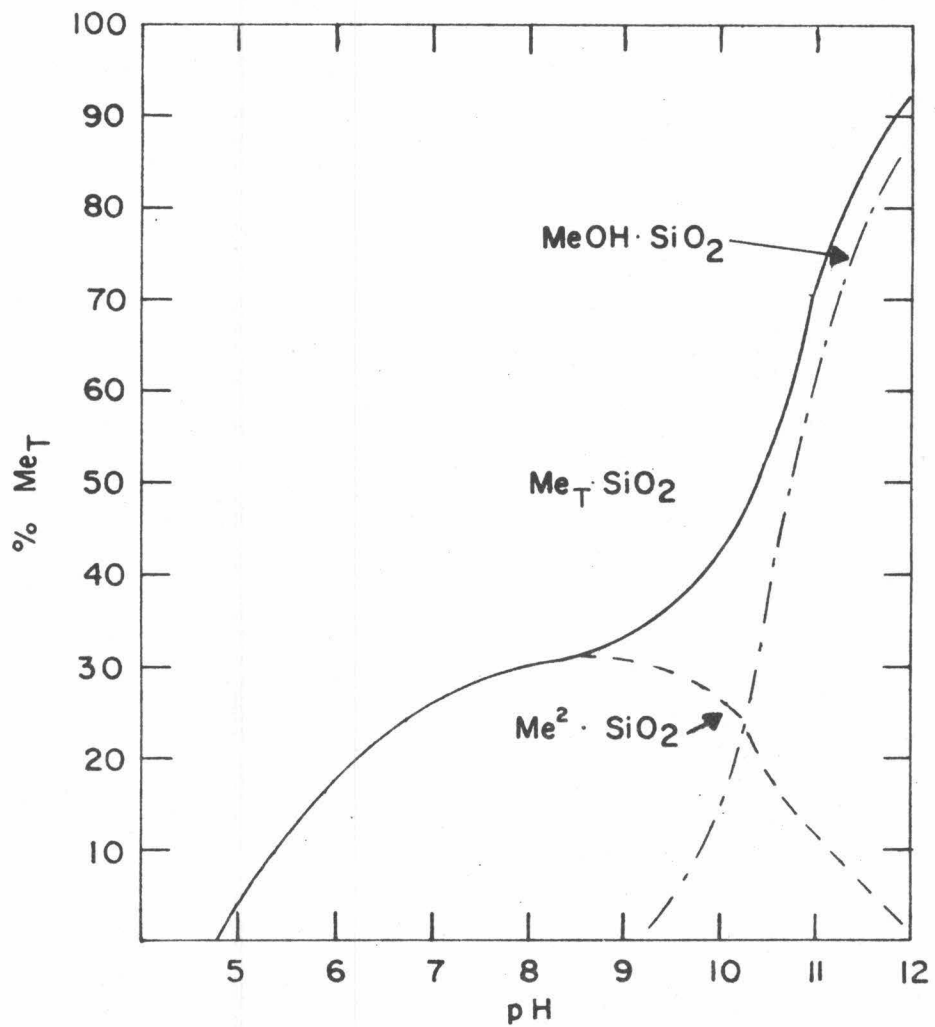


Figure 5.10 Theoretical artifact of the James-Healy Model in modeling the adsorption of Ca(II) and Mg(II) on  $\alpha$ -quartz at low ionic strengths.

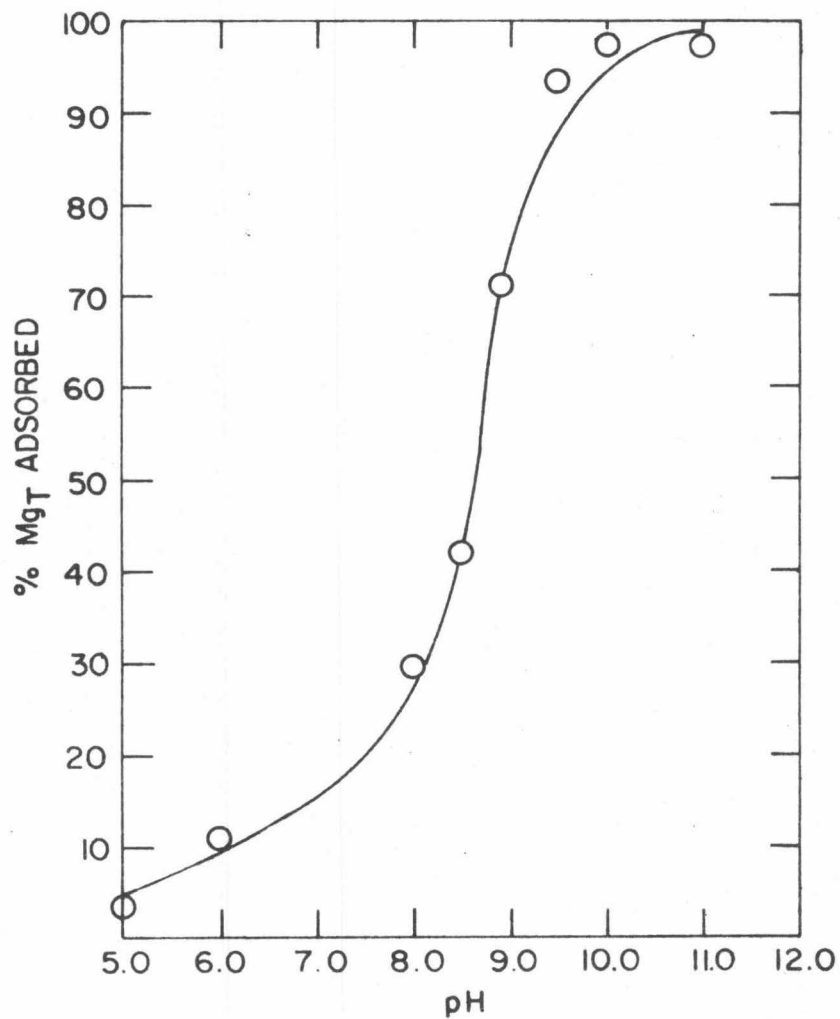


Figure 5.11 Adsorption of Mg as a function of pH;  $Mg_T = 3 \times 10^{-5} M$ ,  $S = 75 m^2/l$ ,  $I = 10^{-3}$ , carbonate-free system. Experimental results modeled with the James-Healy Model.

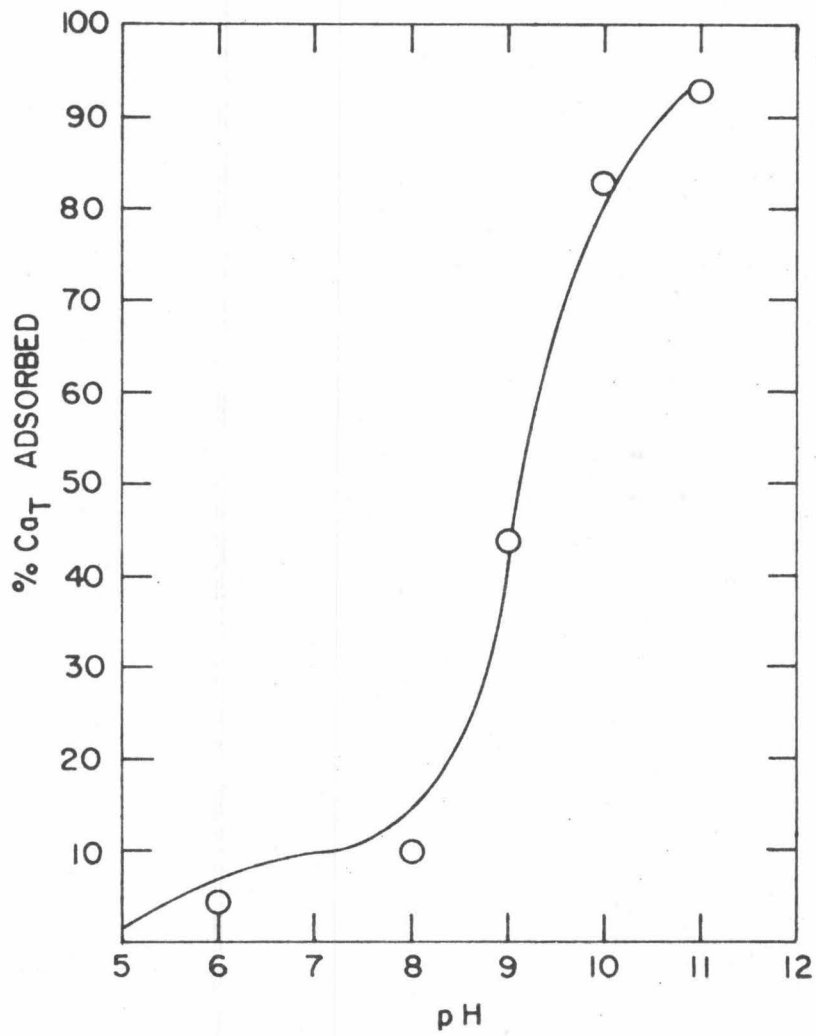


Figure 5.12 Adsorption of Ca on  $\alpha$ -quartz as a function of pH;  $Ca_{T1} = 10^{-4}$  M,  $I = 10^{-3}$ , carbonate-free system. Experimental results modeled with the James-Healy Model.

results of the adsorption of Mg(II) and Ca(II) on  $\text{SiO}_2$  is shown in Table 5.3 and 5.4, respectively.

### 5.3 Influence of Citrate and EDTA on the Adsorption of Cu(II) and Pb(II) on $\alpha$ -Quartz

#### 5.3.1 Modeling Considerations

Since some of the Me-CIT and Me-EDTA complexes are:

a) less charged than, and b) less solvated than  $\text{Me}^{2+}$ , the James-Healy Model would seem to predict an increased adsorption of Me in the presence of these ligands owing to the decrease in the secondary solvation energy. In Chapter 3 it was shown that citrate and protonated citrate themselves do not apparently adsorb on  $\alpha$ -quartz. Therefore, it was necessary to account for the lack of adsorption of metal-citrate complexes in modeling the experimental systems. Following on the development of Chapter 2, metal-ligand complexes can be prevented from adsorbing by making their free energies of adsorption sufficiently positive. Omitting these metal-ligand complexes from the adsorption computations has the same effect. In the present research this second approach was used in modeling Cu(II) and Pb(II) adsorption on  $\text{SiO}_2$  in the presence of citrate and EDTA.

#### 5.3.2 Adsorption of Cu(II) on $\alpha$ -Quartz in the Presence of Citrate

Citrate is a very strong complexing ligand for Cu(II) (see the

Table 5.3

Chemical Free Energies Used for Modeling the  
Adsorption of Mg(II) on SiO<sub>2</sub>(s) with the James-Healy Model

---

$\Delta G_{\text{chem, Mg}}^{\circ}$	= -6.2 kcal mole <sup>-1</sup>	pH 5 to pH 8
$\Delta G_{\text{chem, Mg}}^{\circ}$	= -6.5 kcal mole <sup>-1</sup>	pH 8.5
$\Delta G_{\text{chem, Mg}}^{\circ}$	= -7.1 kcal mole <sup>-1</sup>	pH 9 to pH 11

---

Table 5.4

Chemical Free Energies Used for Modeling the  
Adsorption of Ca(II) on SiO<sub>2</sub>(s) with the James-Healy Model

---

$\Delta G_{\text{chem, Ca}}^{\circ}$	= -5.3 kcal mole <sup>-1</sup>	pH 5 to pH 8
$\Delta G_{\text{chem, Ca}}^{\circ}$	= -6.2 kcal mole <sup>-1</sup>	pH 9
$\Delta G_{\text{chem, Ca}}^{\circ}$	= -7.1 kcal mole <sup>-1</sup>	pH 10 to pH 11

---

equilibrium constants for the Cu(II)-citrate complexes in Table 5.5). Present at concentrations of  $\text{CIT}_T = 0.5 \text{ Cu}_T$ , citrate binds half of the total Cu(II) (Figure 5.13a). Hydrolysis is suppressed and displaced to higher pH. The addition of  $\alpha$ -quartz results in the adsorption of the available  $\text{Cu}^{2+}$  and Cu-OH species, without having any appreciable influence on the Cu-citrate complexes (Figure 5.13b).

The increase in the concentration of citrate so that it is in ten-fold excess over Cu provides enough ligand to complex all Cu in this solution (Figure 5.14a). The Cu(II)-citrate complexes are so strong that they successfully resist the competition of added  $\alpha$ -quartz and, as a result, all the copper remains in the solution (Figure 5.14b).

As discussed in Chapter 4, modeling of the experimentally obtained results for the adsorption of Cu(II) on  $\text{SiO}_2(\text{s})$  will depend on the choice of the second stability constant for the hydrolysis of Cu(II). In order to illustrate this influence, modeling was done with two extreme cases: when  $\text{Cu}(\text{OH})_2(\text{aq})$  was not included in computations (Figure 5.15), and when  $\log^* \beta_2 = -13.7$  (Figure 5.16). Comparison of Figures 5.15 and 5.16 shows that the resulting curves show a slight shift in the adsorption at higher pH;  $\log^* \beta_2 = -13.7$  yields better agreement between experimental and theoretical adsorption isotherms.

In terms of the Ion Exchange-Surface Complex Formation Model, a higher hydrolysis constant implies a shift in the equilibrium

Table 5.5  
Equilibrium Constants for  
Cu(II)-Citrate Complexes

Species	log Equilibrium Constant ( $I=10^{-3}$ )	
Cu CITRATE (aq)	$K_1$	19.6
Cu HCITRATE (aq)	$K_{1H}$	21.8

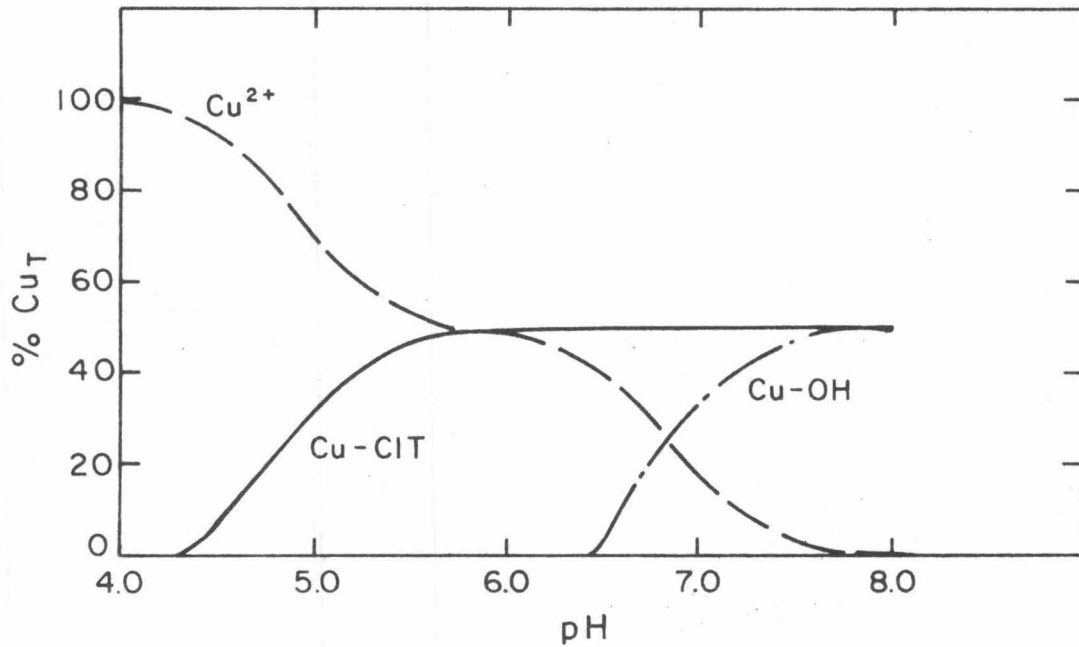


Figure 5.13a Equilibrium speciation of Cu vs. pH in the solution:  
 $\text{Cu}_T = 10^{-6} \text{ M}$ ,  $\text{CIT}_T = 0.5\text{Cu}_T$ ,  $I = 10^{-3}$ , carbonate-free.  
 $\text{Log}^* \beta_2 \text{Cu}(\text{OH})_2(\text{aq}) = -13.7$ .

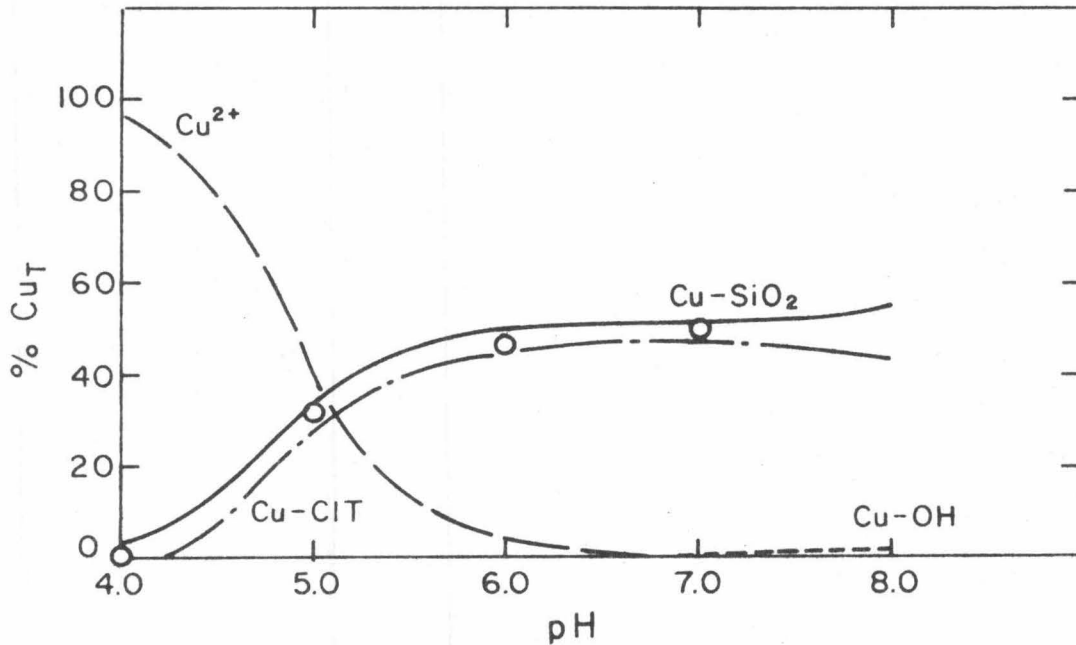


Figure 5.13b Equilibrium distribution of Cu vs. pH in the system:  
 $\text{Cu}_T = 10^{-6} \text{ M}$ ,  $\text{CIT}_T = 0.5\text{Cu}_T$ ,  $S = 50 \text{ m}^2/\text{l}$  Min-U-Sil,  $I = 10^{-3}$ , carbonate-free. Experimental results modeled with the James-Healy Model.

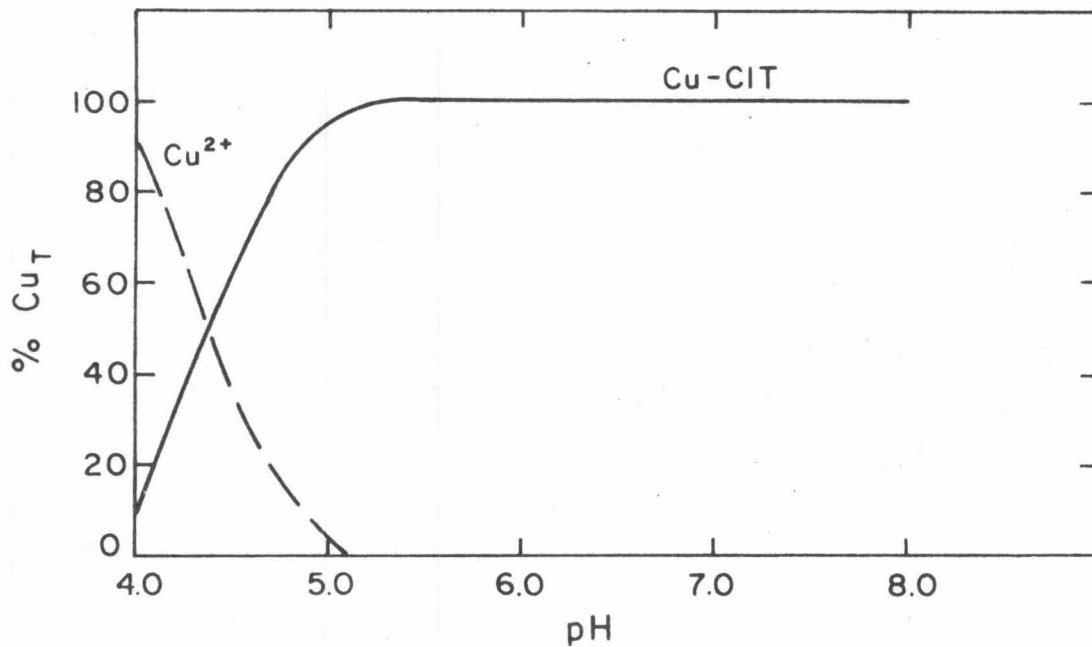


Figure 5.14a Equilibrium speciation of Cu vs. pH in the solution:  $\text{Cu}_T = 10^{-6} \text{ M}$ ,  $\text{CIT}_T = 10\text{Cu}_T$ ,  $I = 10^{-3}$ , carbonate-free.  $\text{Log}^*\beta_2 \text{Cu}(\text{OH})_2(\text{aq}) = -13.7$ .

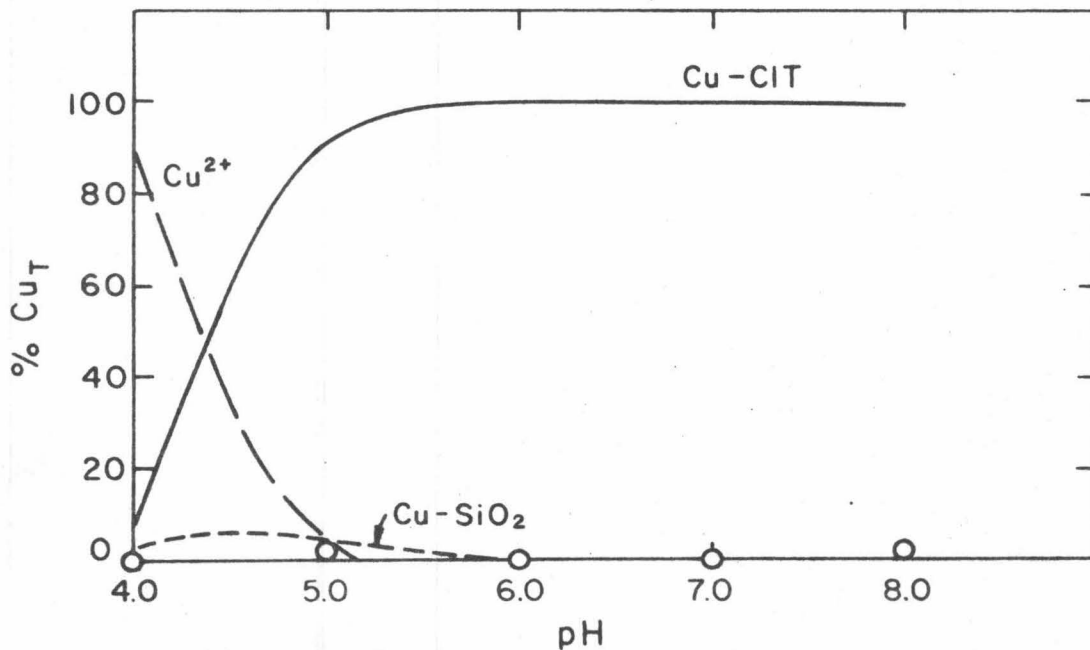


Figure 5.14b Equilibrium distribution of Cu vs. pH in the system:  $\text{Cu}_T = 10^{-6} \text{ M}$ ,  $\text{CIT}_T = 10\text{Cu}_T$ ,  $S = 50 \text{ m}^2 / \text{l Min-U-Sil}$ ,  $I = 10^{-3}$ , carbonate-free. Experimental results modeled with the James-Healy Model.

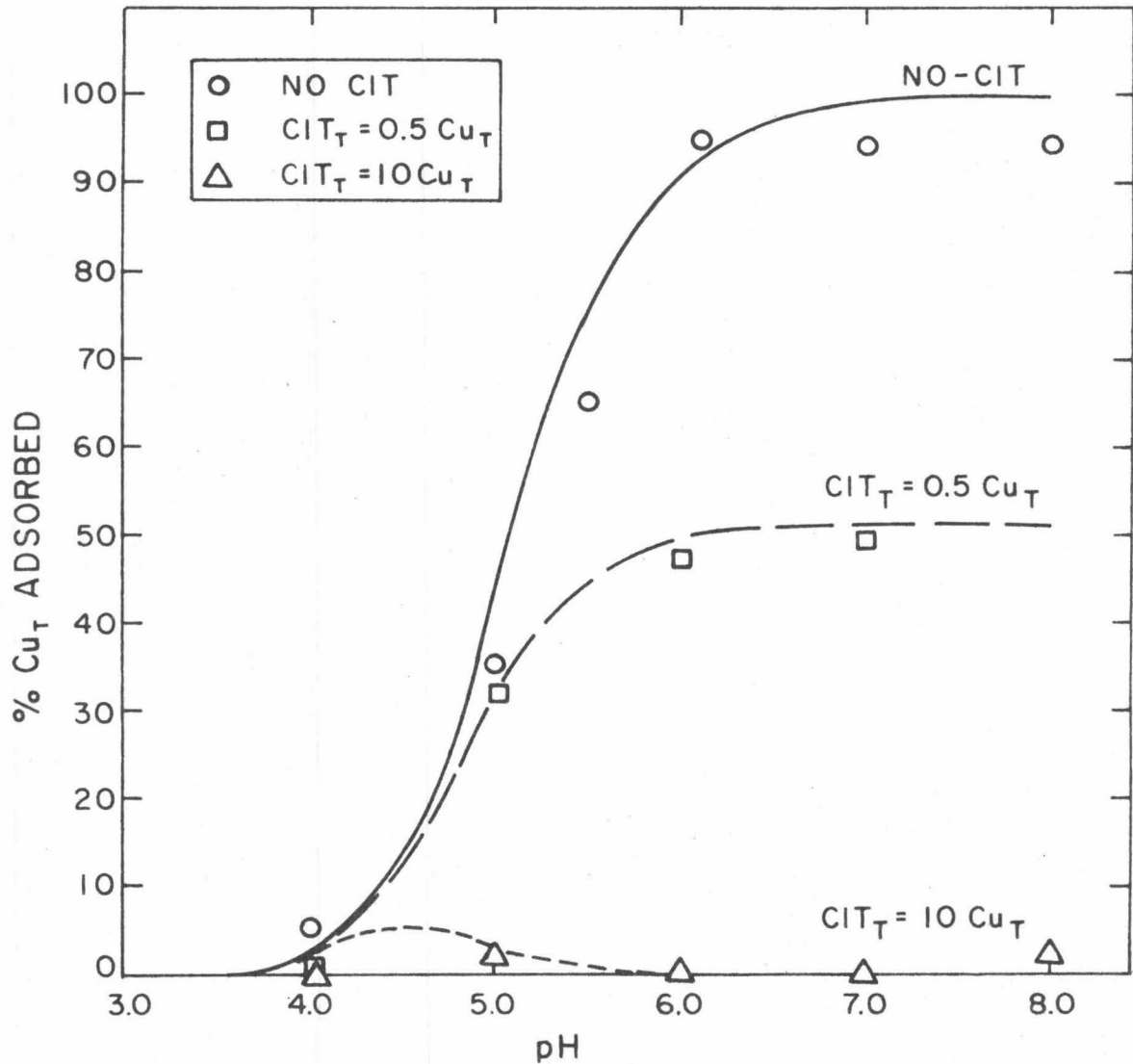


Figure 5.15 Adsorption of Cu vs. pH in the presence and absence of citrate.  $\text{Cu}_T = 10^{-6} \text{ M}$ ,  $S = 50 \text{ m}^2 / \ell$  Min-U-Sil,  $I = 10^{-3}$ , carbonate-free.  $\text{Cu}(\text{OH})_2(\text{aq})$  not included in computations. Experimental results modeled with the James-Healy Model.

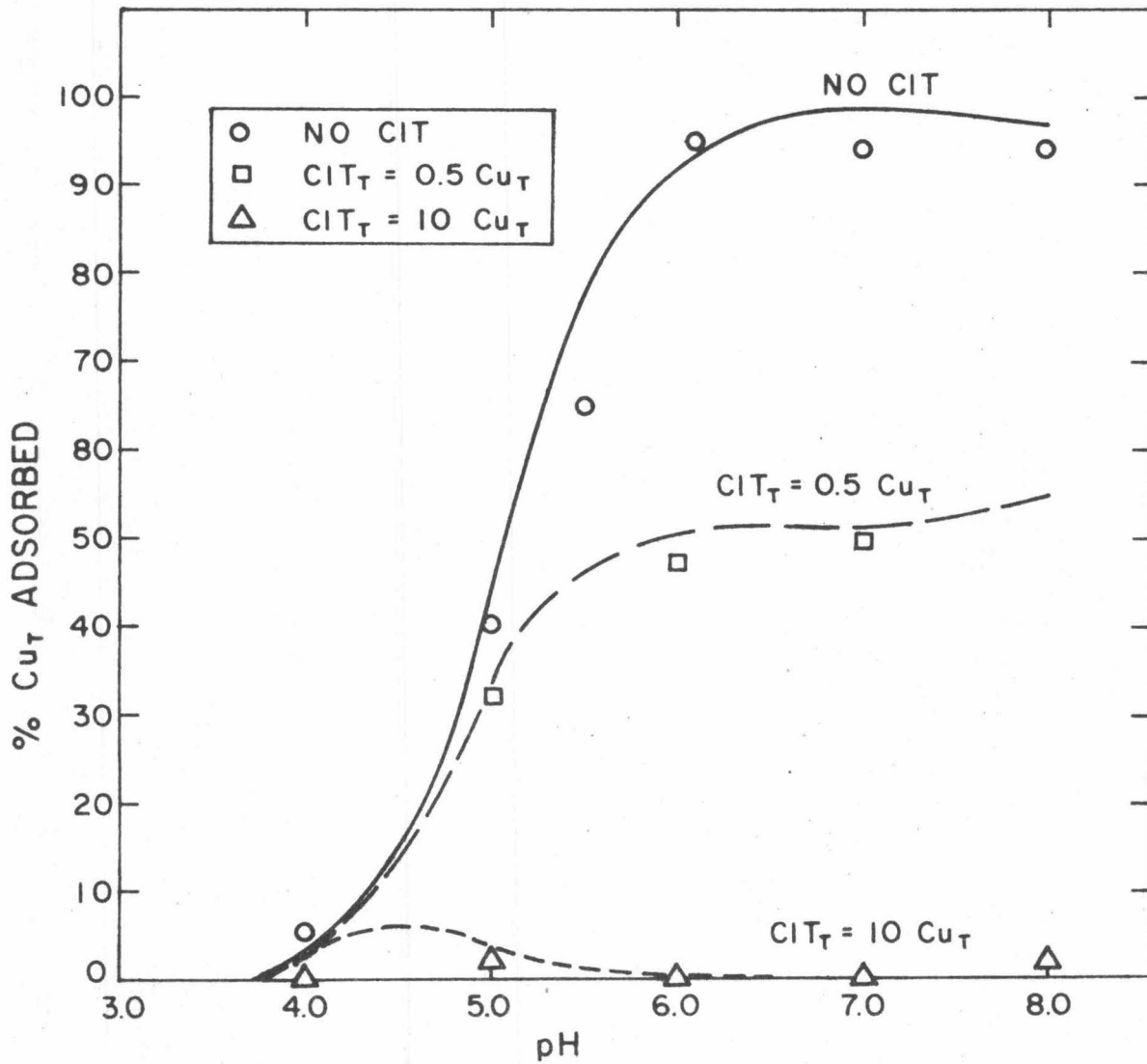


Figure 5.16 Adsorption of Cu vs. pH in the presence and absence of citrate.  $Cu_T = 10^{-6}$  M,  $S = 50 \text{ m}^2/\text{l}$  Min-U-Sil,  $I = 10^{-3}$ , carbonate-free.  $\text{Log}^* \beta_2 \text{Cu}(\text{OH})_2(\text{aq}) = -13.7$ . Experimental results modeled with the James-Healy Model.

away from  $\text{Me}^{2+}$ , and thus a decrease in the adsorption. Computations done with this model indeed show a decrease in adsorption when  $\log^* \beta_2 = -13.7$  (Figure 5.18) compared to those with  $\log^* \beta_2 = -17.3$  (Figure 5.17).

### 5.3.3 Adsorption of Pb(II) on $\alpha$ -Quartz in the Presence of Citrate

Because of quite low stability constants of Pb(II)-citrate complexes (Table 5.6), high concentrations of citrate relative to Pb(II) are needed in order to have Pb(II) complexed to an appreciable amount (Figure 5.19a). If  $\text{CIT}_T = 10 \text{ Pb}_T$ , citrate competes successfully with  $\text{OH}^-$  for the metal ion, resulting in a shift in the "hydrolysis curve" above pH 6. Nevertheless, if the same aqueous system is re-equilibrated with  $\text{SiO}_2(\text{s})$  the affinity of the surface for the metal is much greater than the ability of citrate to complex the metal ion. As predicted theoretically, the Pb-CIT species dominate only at lower pH. In the pH range of normal adsorption of Pb(II) on  $\alpha$ -quartz, Pb(II) remains attached to the surface (Figure 5.19b). Even in the solutions with very high concentrations of citrate relative to Pb(II) (Figure 5.20a) a substantial amount of lead is still adsorbed on  $\text{SiO}_2(\text{s})$  (Figure 5.20b).

The addition of citrate to the inorganic system containing Cu(II) and  $\alpha$ -quartz reduced the total amount of Cu adsorbed over the whole pH range of adsorption; the addition of citrate to the system containing Pb(II) only dislocated the adsorption edge with the shift being toward

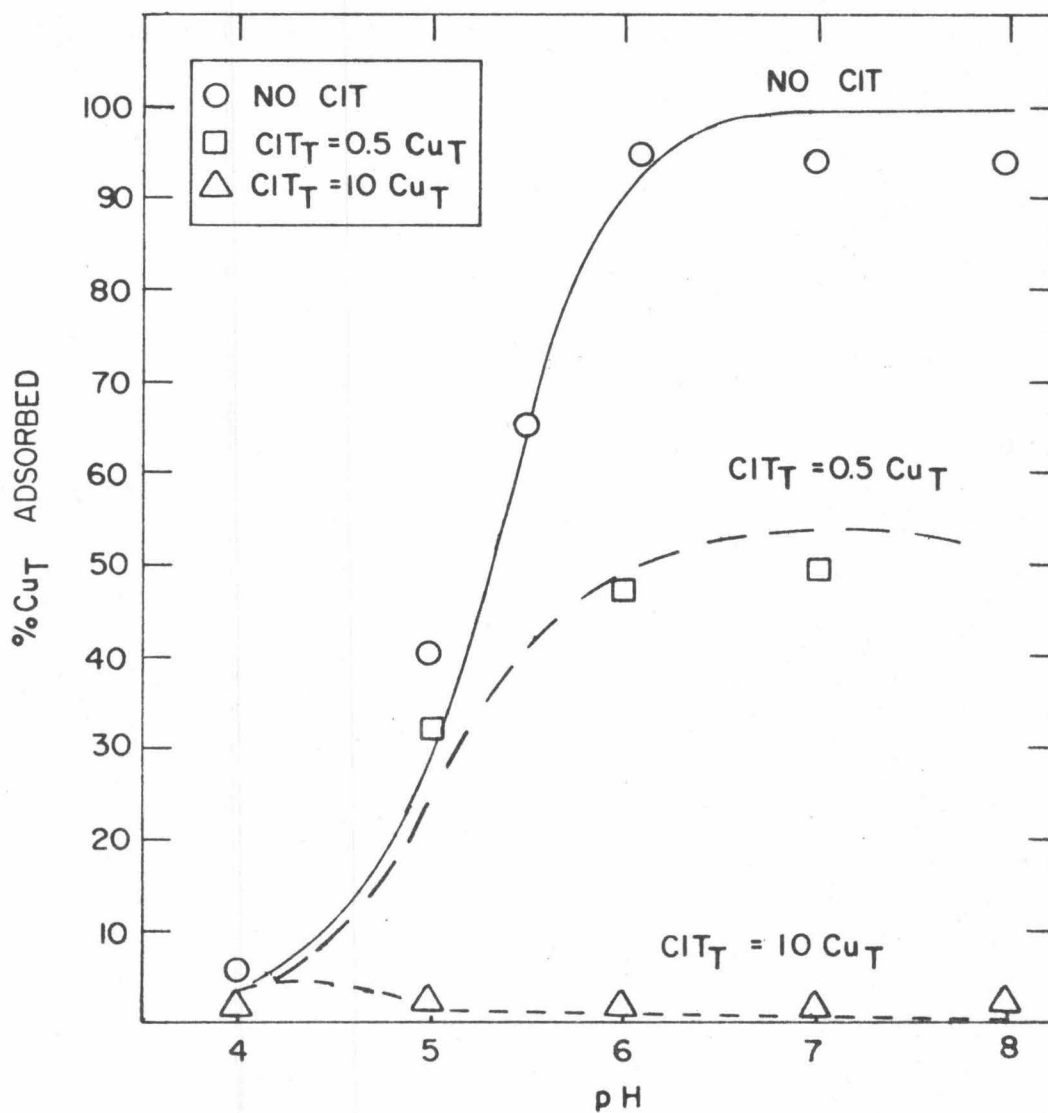


Figure 5.17 Adsorption of Cu vs. pH in the presence and absence of citrate.  $Cu_T = 10^{-6}$  M,  $S = 2.24 \times 10^{-4}$  M,  $I = 10^{-3}$ , carbonate-free.  $\text{Log}^* \beta_2 \text{Cu(OH)}_2(\text{aq}) = -17.3$ . Experimental systems modeled with the Ion Exchange-Surface Complex Formation Model.

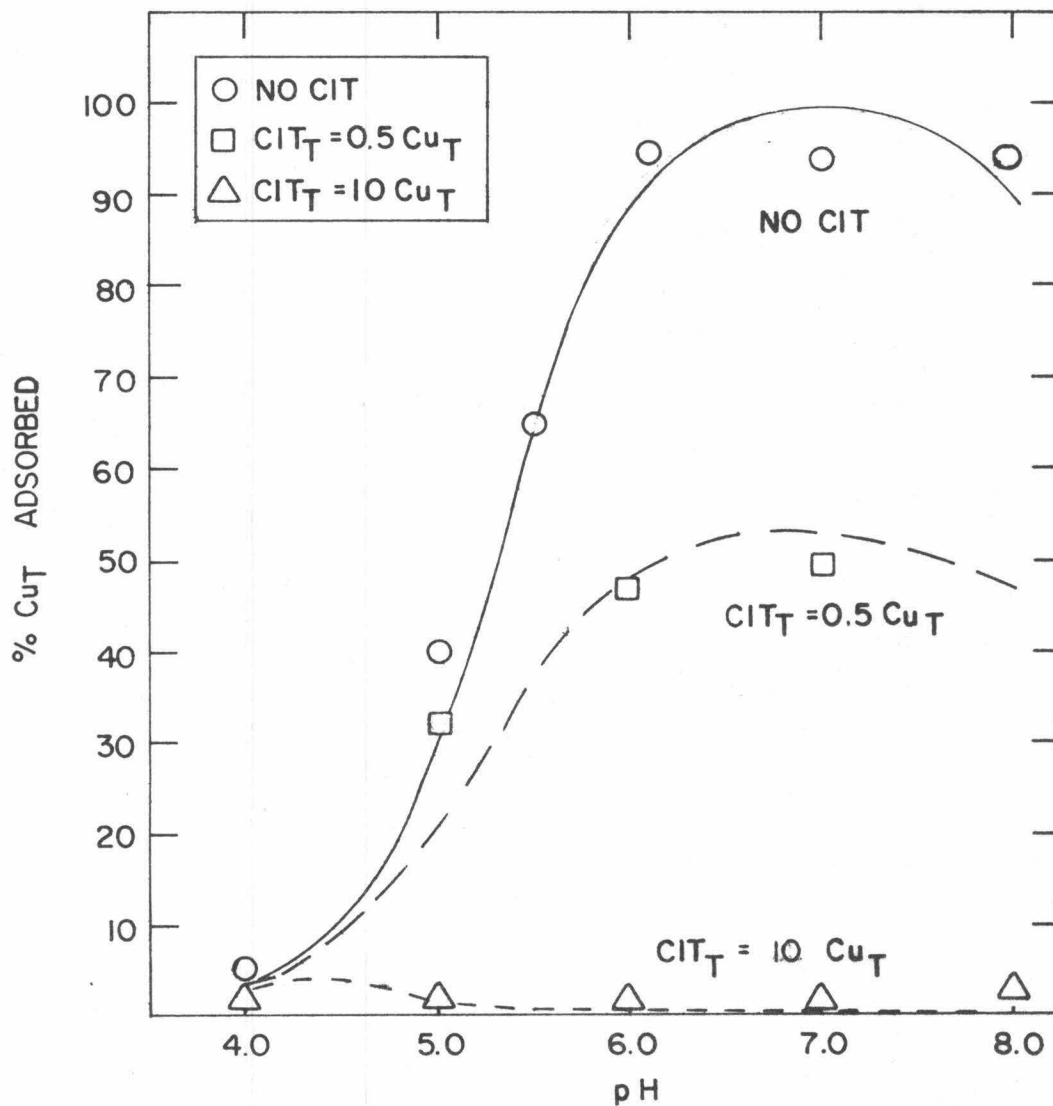


Figure 5.18 Adsorption of Cu vs. pH in the presence and absence of citrate.  $Cu_T = 10^{-6}$  M,  $S = 2.24 \times 10^{-4}$  M,  $I = 10^{-3}$ , carbonate-free.  $\text{Log}^* \beta_2 \text{Cu}(\text{OH})_2(\text{aq}) = -13.7$ . Experimental results modeled with the Ion Exchange-Surface Complex Formation Model.

Table 5.6  
Equilibrium Constants for  
Pb(II)-Citrate Complexes

Species	log Equilibrium Constant (I=10 <sup>-3</sup> )	
Pb CITRATE	K <sub>1</sub>	13.91
Pb HCITRATE	K <sub>1H</sub>	22.99
Pb OHCITRATE	K <sub>1 OH</sub>	28.89

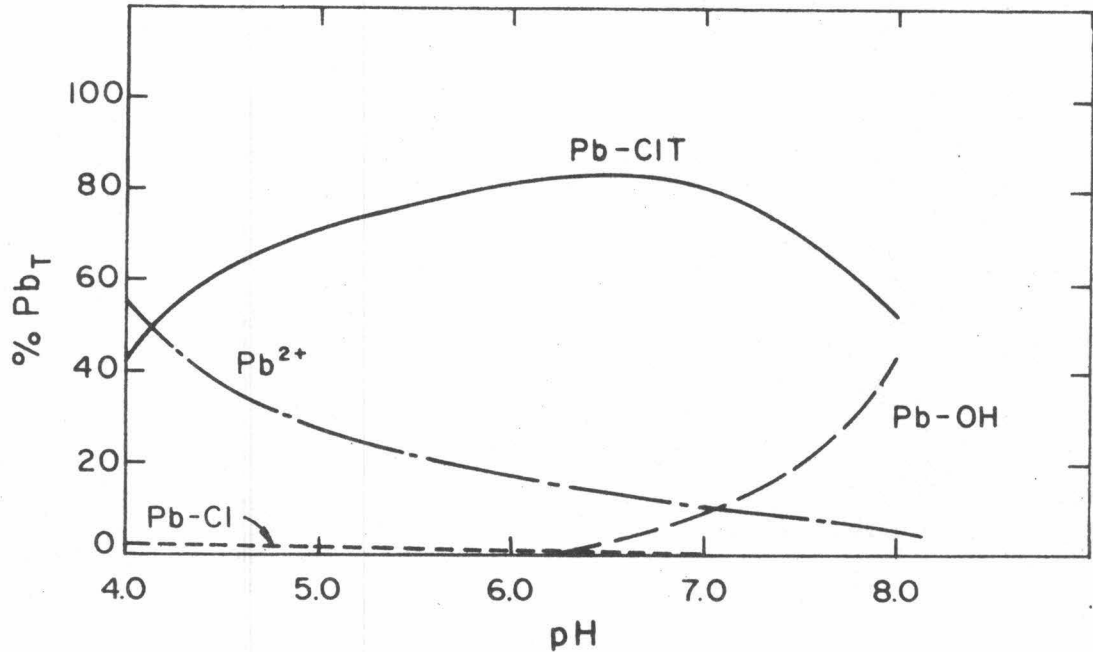


Figure 5.19a Equilibrium speciation of Pb as a function of pH in solution:  $Pb_T = 5 \times 10^{-7} M$ ,  $CIT_T = 10Pb_T$ ,  $I = 10^{-3}$ , carbonate-free.

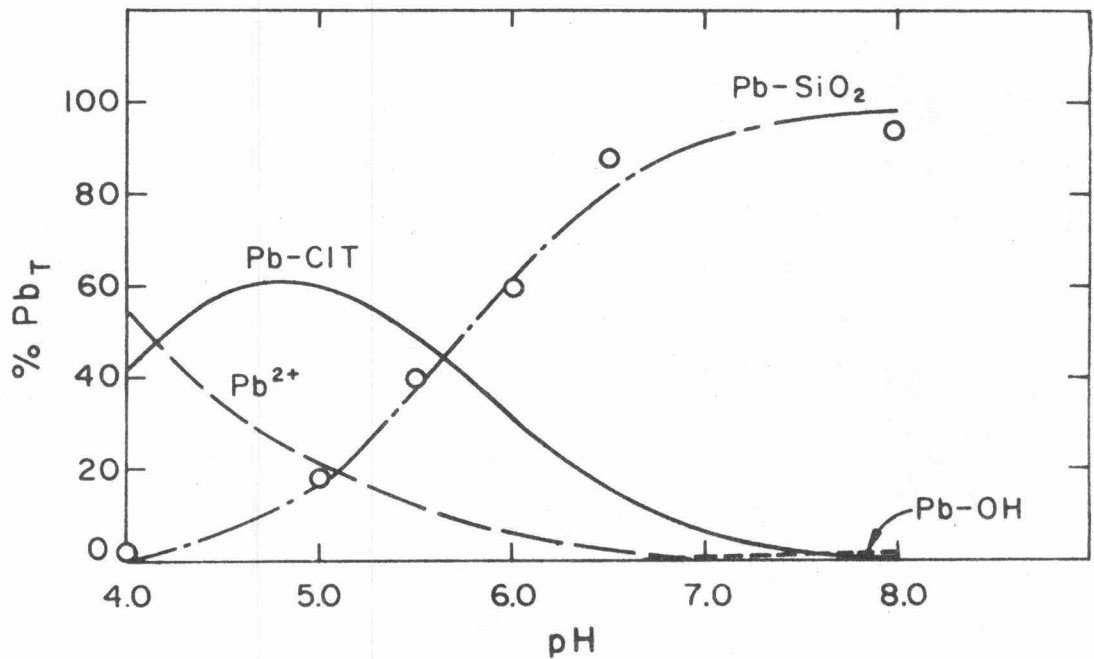


Figure 5.19b Equilibrium distribution of Pb as a function of pH in the system:  $Pb_T = 5 \times 10^{-7} M$ ,  $CIT_T = 10Pb_T$ ,  $S = 75 m^2 / \ell$  Min-U-Sil,  $I = 10^{-3}$ , carbonate-free. Experimental results modeled with the James-Healy Model.

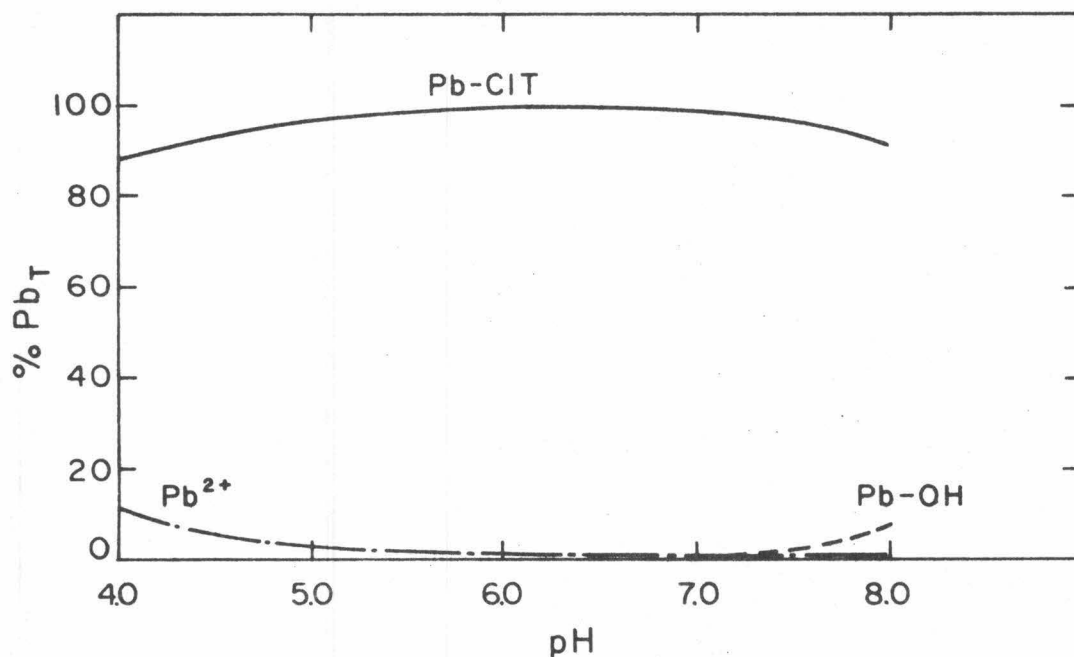


Figure 5.20a Equilibrium speciation of Pb vs. pH in the solution:  $Pb_T = 5 \times 10^{-7} M$ ,  $CIT_T = 100 Pb_T$ ,  $I = 10^{-3}$ , carbonate-free.

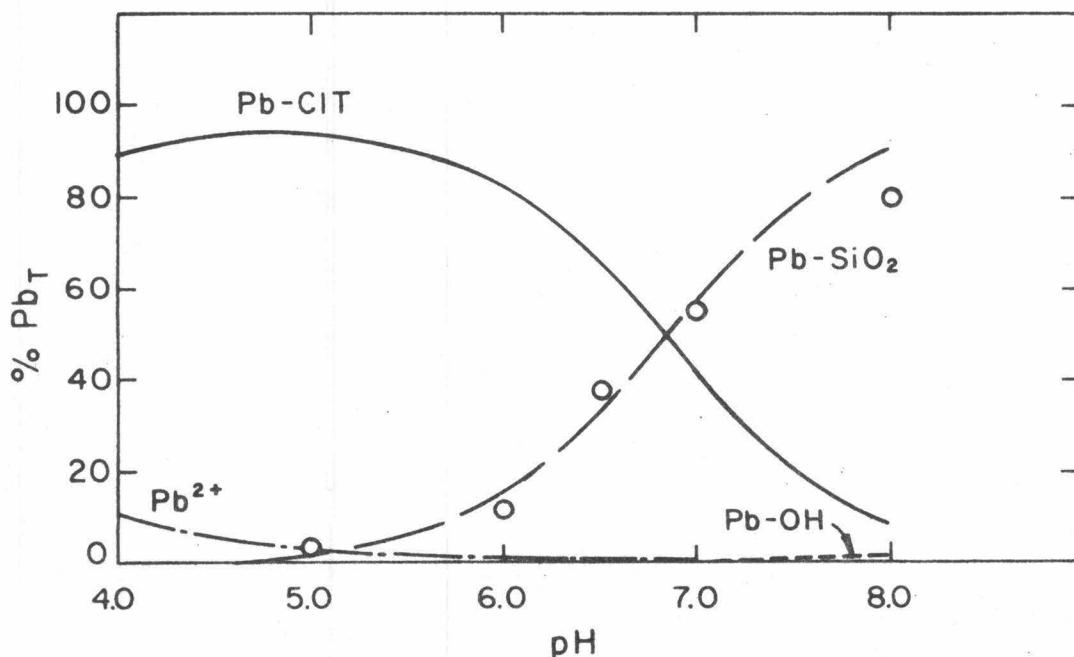


Figure 5.20b Equilibrium speciation of Pb vs. pH in the system:  $Pb_T = 5 \times 10^{-7} M$ ,  $CIT_T = 100 Pb_T$ ,  $S = 75 m^2 / l$  Min-U-Sil,  $I = 10^{-3}$ , carbonate-free. Experimental results modeled with the James-Healy Model.

higher pH (Figure 5.21). As a result, the adsorption at high pH is not subdued to changes to any considerable extent.

Modeling of the adsorption behavior of Pb(II) in the presence of different amounts of citrate with the Ion Exchange-Surface Complex Formation Model is shown in Figure 5.22.

#### 5.3.4 Adsorption of Cu(II) and Pb(II) on $\alpha$ -Quartz in the Presence of EDTA

Addition of a complexing agent to the system containing equimolar concentrations of Cu(II) and Pb(II) results in a slightly more complicated network of the chemical interactions. If the concentrations of metal ions and inorganic ligands are kept constant, the speciation of Cu(II) and Pb(II) will depend only on the amount of the complexing agent added to the system. Figure 5.23 shows that the addition of EDTA (Table 5.7) ( $\text{EDTA}_T = 0.5 \text{ Cu}_T = 0.5 \text{ Pb}_T$ ) mainly affects Cu at pH below 7; the amount of Cu present in the form of the free metal ion,  $\text{Cu}^{2+}$ , is reduced to 60%. Above pH 7 the effect of EDTA on Cu slowly decreases, but at the same time it becomes more effective for Pb(II). Above pH 7.5 the main influence is on Pb(II), decreasing its hydrolysis about 50%. This increased tendency for the complexing of Pb with EDTA at higher pH is also evident in the presence of adsorbent  $\text{SiO}_2(\text{s})$ , causing a decrease in the Pb-adsorption (Figure 5.24). On the other hand, a decrease in the Cu(II)-EDTA complexes results in an increased

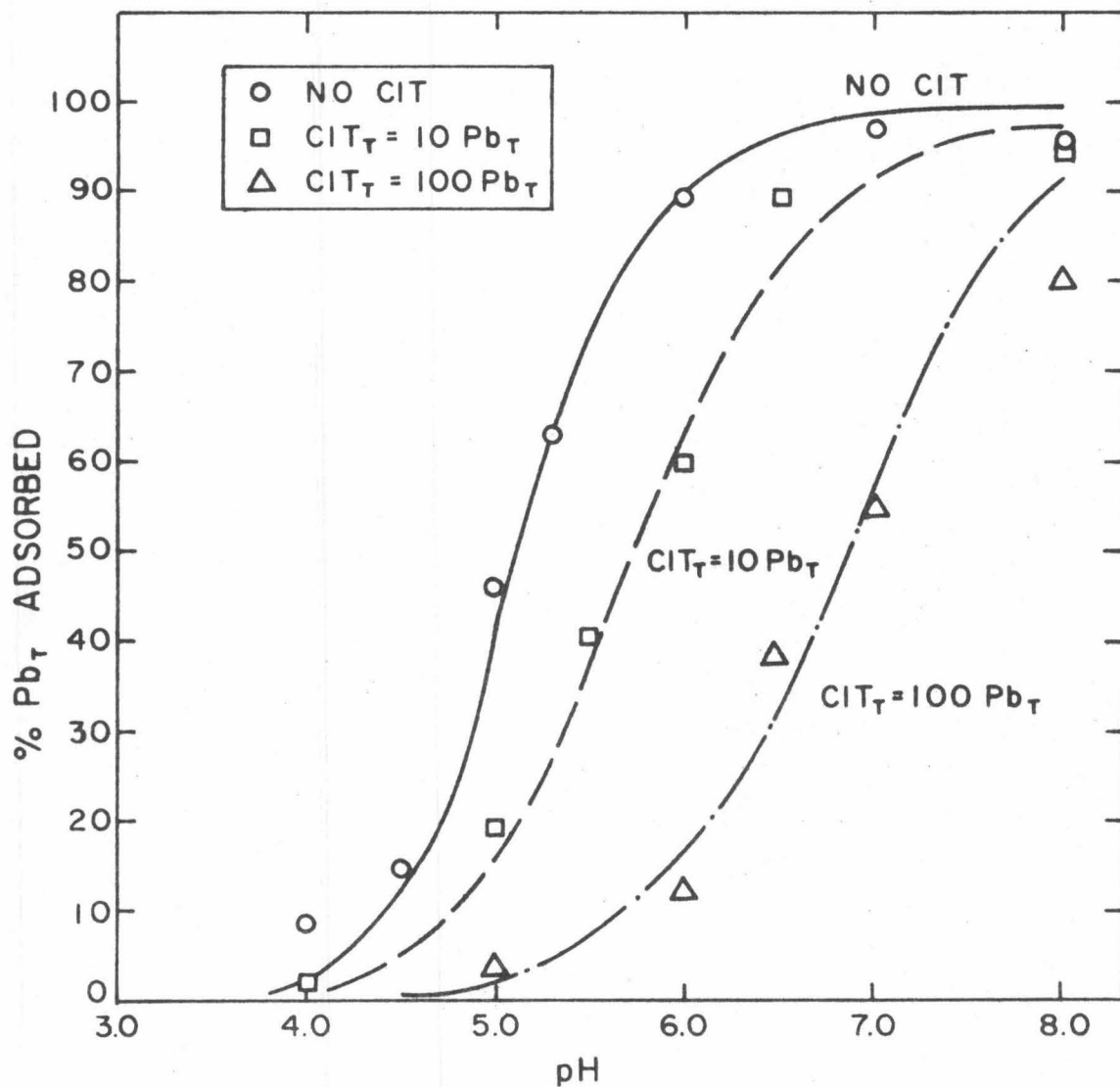


Figure 5.21 Adsorption of Pb on Min-U-Sil vs. pH in the presence and absence of citrate in the system:  $Pb_T = 5 \times 10^{-7}$  M,  $S = 75 \text{ m}^2/\text{l}$ ,  $I = 10^{-3}$ , carbonate-free. Experimental results modeled with the James-Healy Model.

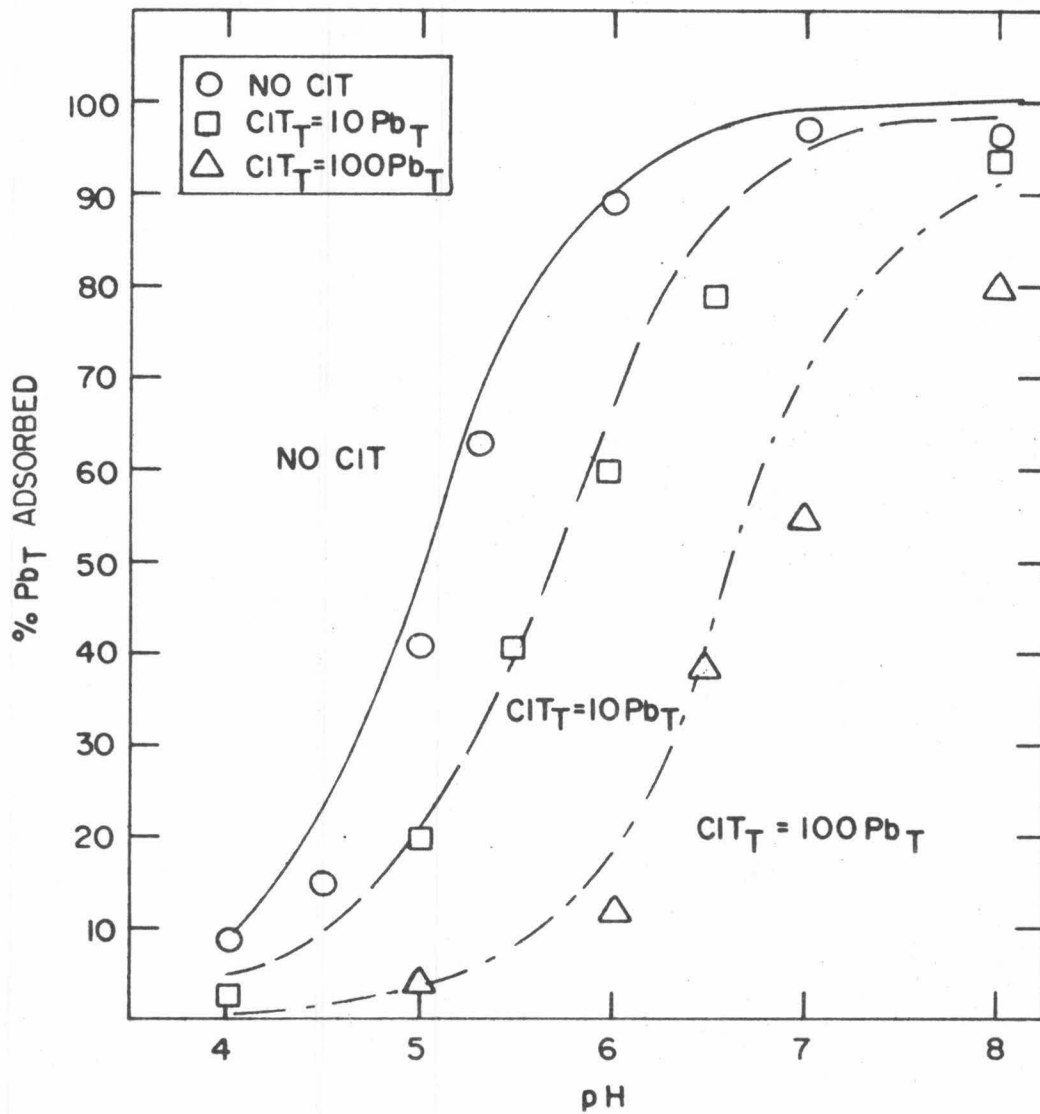


Figure 5.22 Adsorption of Pb on Min-U-Sil vs. pH in the presence and absence of citrate in the system:  $Pb_T = 5 \times 10^{-7} M$ ,  $S = 75 m^2/l$ ,  $I = 10^{-3}$ , carbonate-free. Experimental results modeled with the Ion Exchange-Surface Complex Formation Model.

Table 5.7

Stability Constants for the Cu(II)-EDTA and Pb(II)-EDTA Complexes

Species	log Equilibrium Constant ( $I=10^{-3}$ )	
Cu EDTA(aq)	$K_1$	20.95
Cu HEDTA(aq)	$K_{1H}$	24.49
Cu OHEDTA(aq)	$K_{1 OH}$	8.93
Pb EDTA(aq)	$K_1$	20.25
Pb HEDTA(aq)	$K_{1H}$	23.45

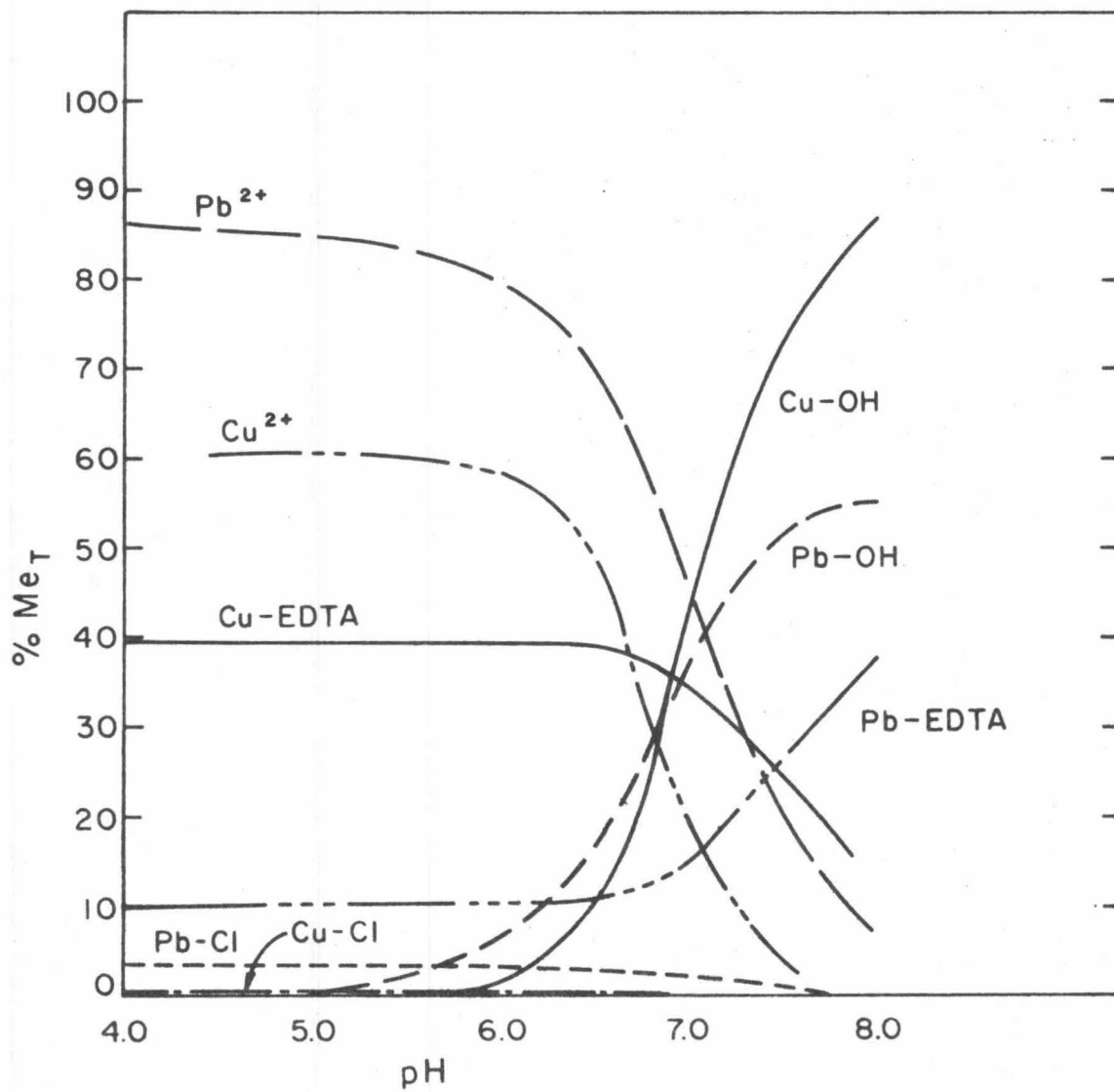


Figure 5.23 Equilibrium speciation of Cu and Pb vs. pH  
 in the solution:  $Cu_T = Pb_T = 5 \times 10^{-7} M$ ,  $EDTA_T = 0.5 Cu_T =$   
 $0.5 Pb_T$ ,  $I = 10^{-3}$ , carbonate-free.  $\log \beta_2 Cu(OH)_2(aq) = -13.7$ .

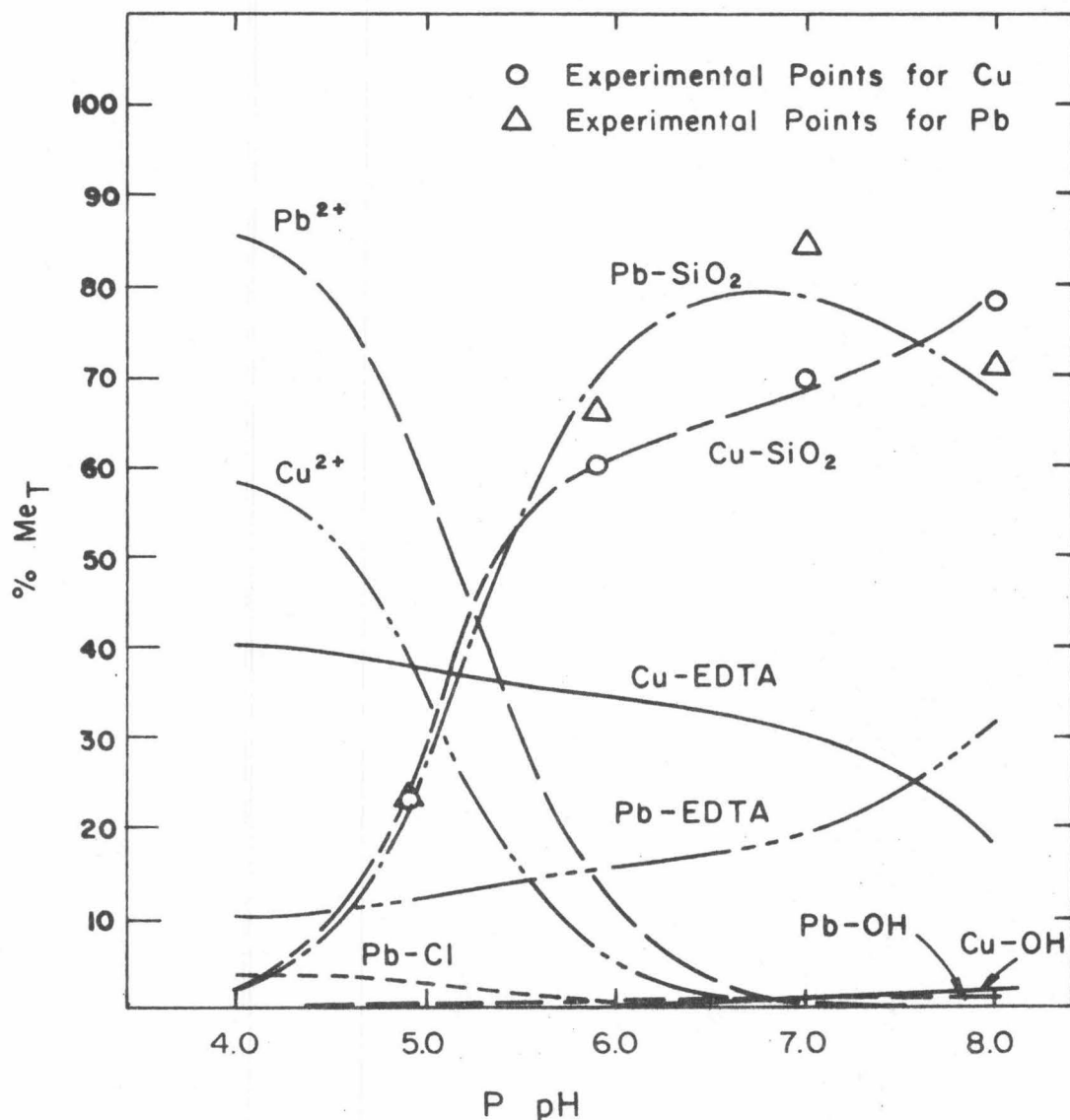


Figure 5.24 Equilibrium distribution of Cu and Pb vs. pH in the system:  $Cu_T = Pb_T = 5 \times 10^{-7} M$ ,  $EDTA_T = 0.5 Cu_T = 0.5 Pb_T$ ,  $S = 50 m^2 / l$  Min-U-Sil,  $I = 10^{-3}$ , carbonate-free.  $\log^* \beta_2 Cu(OH)_2(aq) = -13.7$ . Experimental results modeled with the James-Healy Model.

adsorption of Cu.

The addition of a greater amount of EDTA ( $\text{EDTA}_T = \text{Cu}_T = \text{Pb}_T$ ) alters the speciation of both metals, still having a more profound influence on Cu at lower pH values, and on Pb at higher ones (Figure 5.25). The same effect of EDTA on these two metals exists in the presence of  $\text{SiO}_2(\text{s})$  (Figure 5.26).

It can be concluded that the addition of EDTA has different effects on Pb and Cu. In the case of Pb(II) the effect is manifested more as a restraining of the adsorption (Figure 5.27), while in the case of Cu more as a displacement of the adsorption edge with a slight reduction in the adsorption (Figure 5.28). This effect is the opposite of that obtained by the addition of citrate, but in agreement with the expectations based on the relative stability constants.

#### 5.4 Conclusions

The adsorption of Cu(II) and Pb(II) on  $\alpha$ -quartz is very fast: 90-100% of  $\text{Me}_T$  is adsorbed during the first 5 minutes. For an ionic strength of  $I = 10^{-3}$  the adsorption isotherms of Cu(II) and Pb(II) on  $\alpha$ -quartz are characterized by a sharp increase in adsorption between pH 4 and 6. An increase in the ionic strength results in a shift of the adsorption edge toward higher pH.

Modeling of the experimental systems can be carried out successfully by combining chemical equilibrium and adsorption computations,

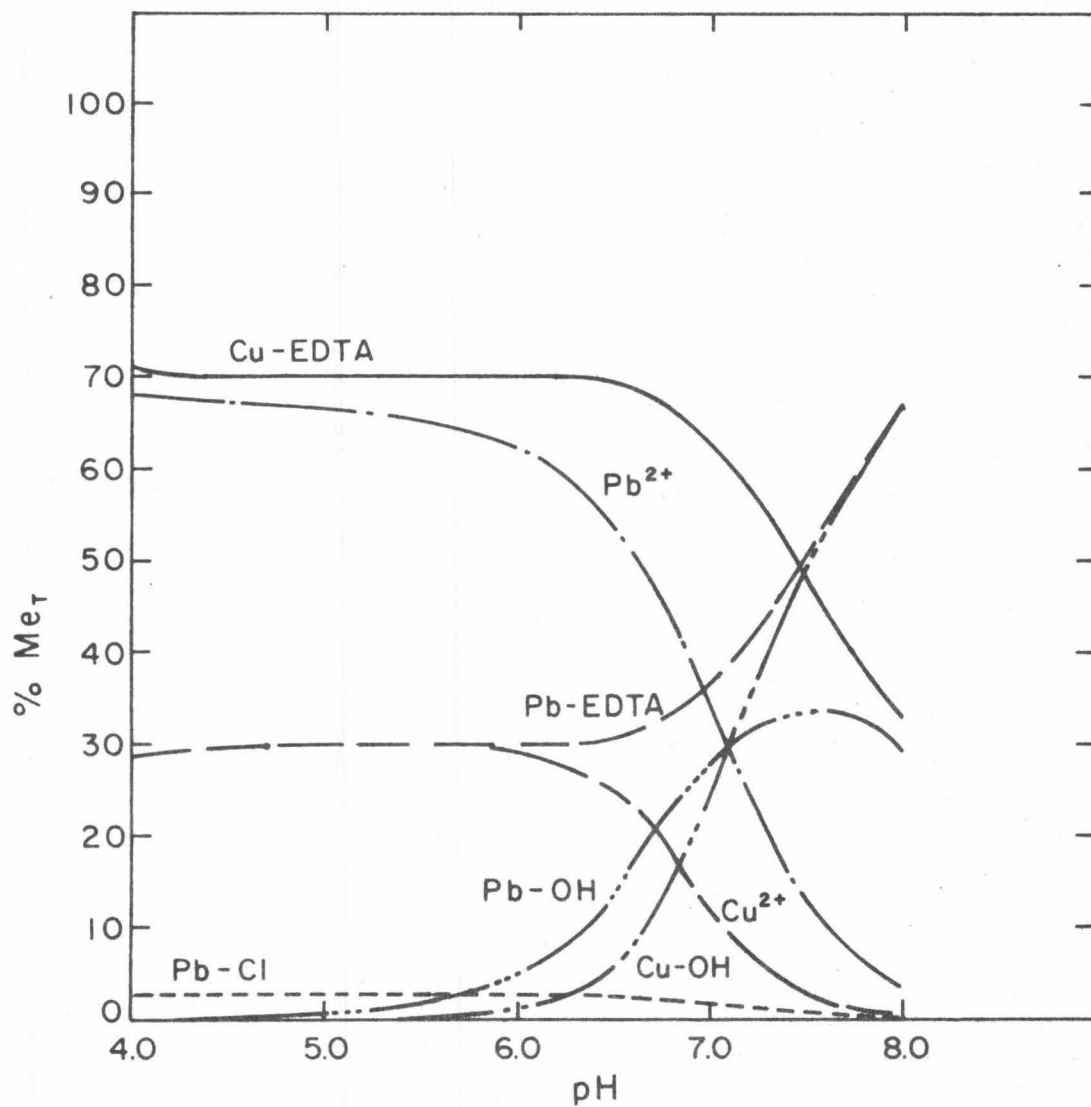


Figure 5.25 Equilibrium speciation of Cu and Pb vs. pH in the solution:  $\text{Cu}_T = \text{Pb}_T = 5 \times 10^{-7} \text{ M}$ ,  $\text{EDTA}_T = \text{Cu}_T = \text{Pb}_T$ ,  $I = 10^{-3}$ , carbonate-free.  $\text{Log } * \beta_2 \text{Cu(OH)}_2(\text{aq}) = -13.7$ .

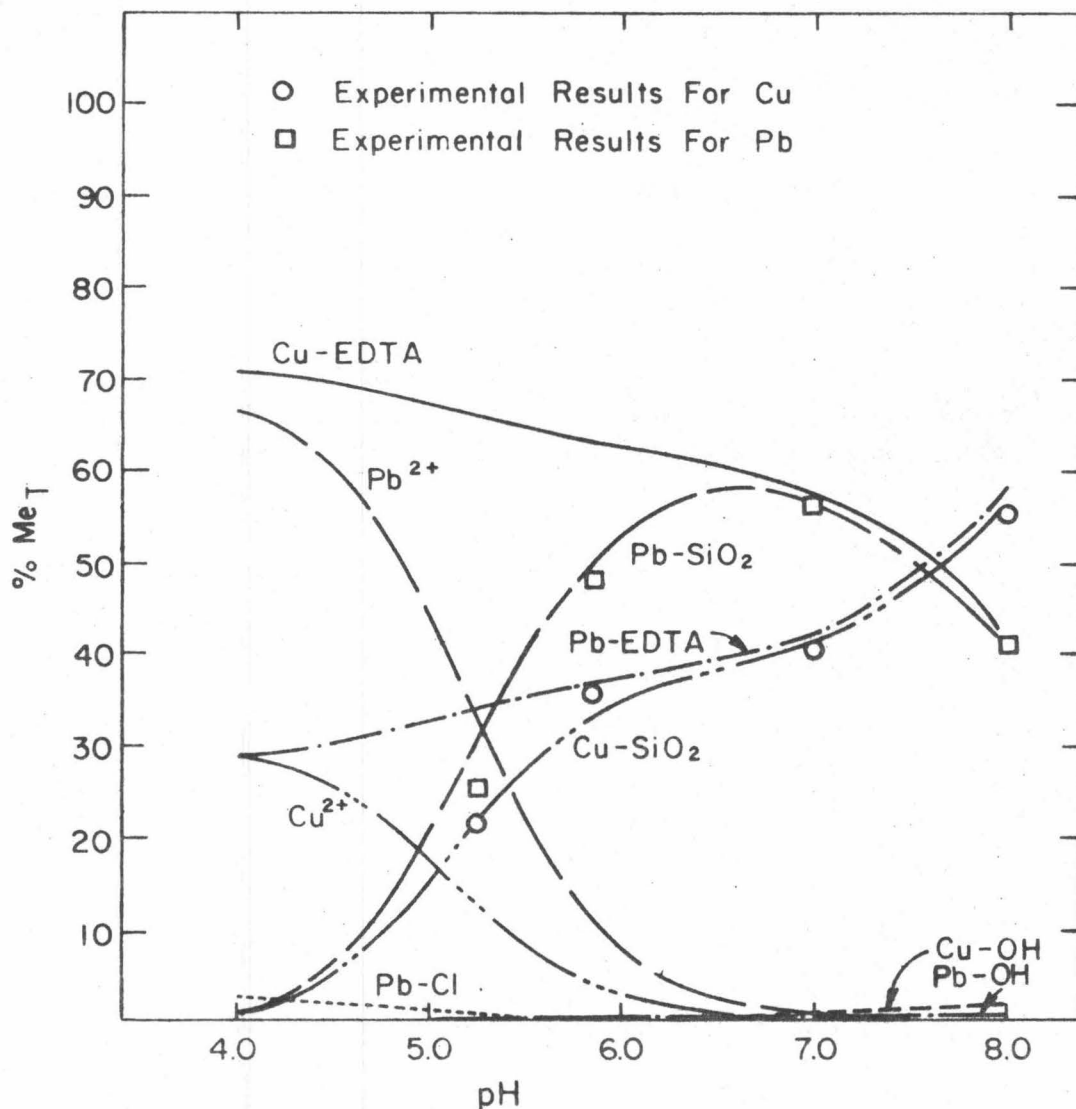


Figure 5.26 Equilibrium distribution of Cu and Pb vs. pH in the system:  $Cu_T = Pb_T = 5 \times 10^{-7} M$ ,  $EDTA_T = Cu_T = Pb_T$ ,  $S = 50 m^2/l$  Min-U-Sil,  $I = 10^{-3}$ , carbonate-free.  $\log \beta_2 Cu(OH)_2(aq) = -13.7$ . Experimental results modeled with the James-Healy Model.

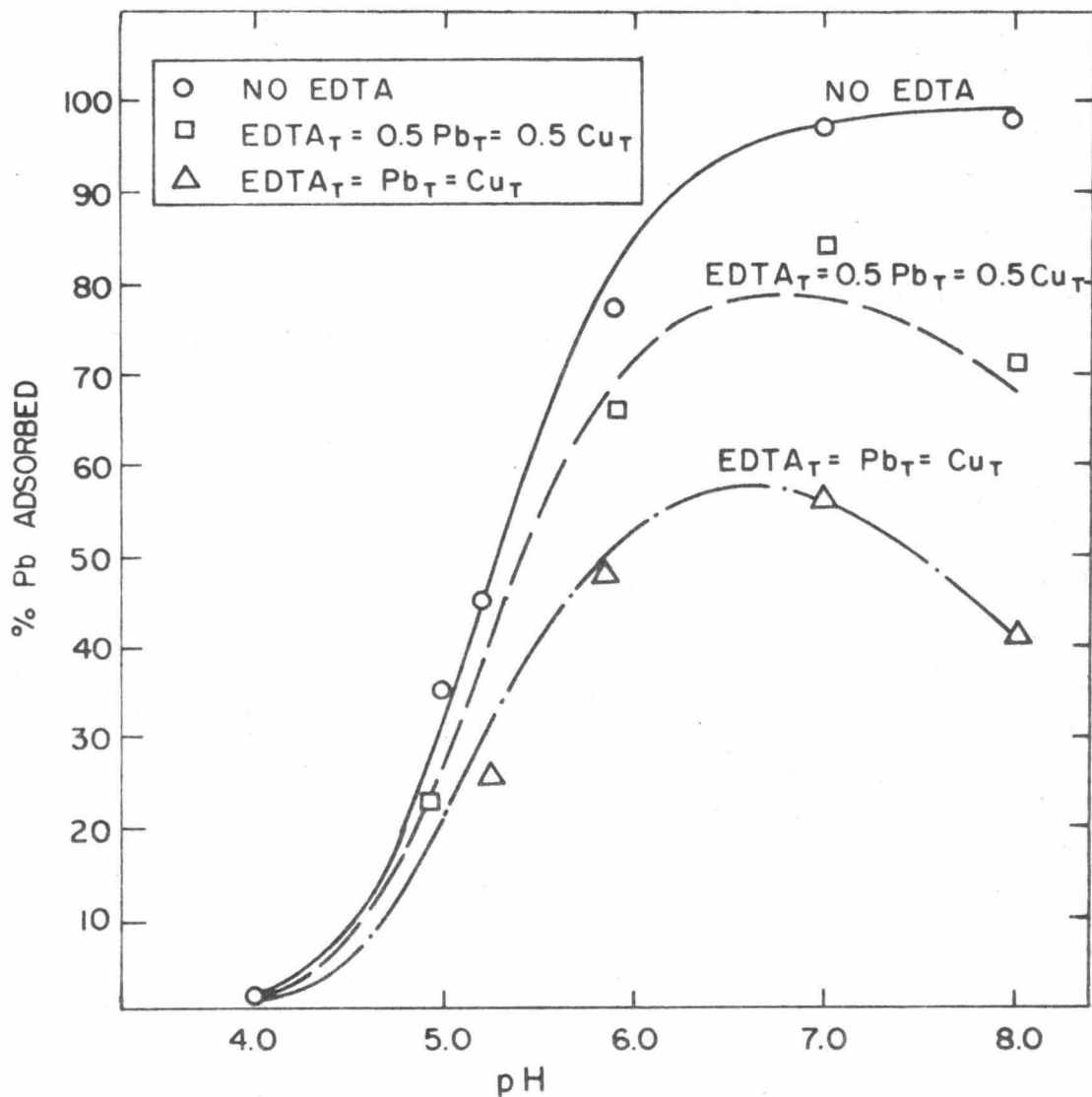


Figure 5.27 Adsorption of Pb on Min-U-Sil vs. pH in the presence and absence of EDTA in the system:  $Pb_T = Cu_T = 5 \times 10^{-7} M$ ,  $S = 50 m^2/l$ ,  $f = 10^{-3}$ , carbonate-free.  $\text{Log} \beta_2 \text{Cu}(\text{OH})_2(\text{aq}) = -13.7$ . Experimental results modeled with the James-Healy Model.

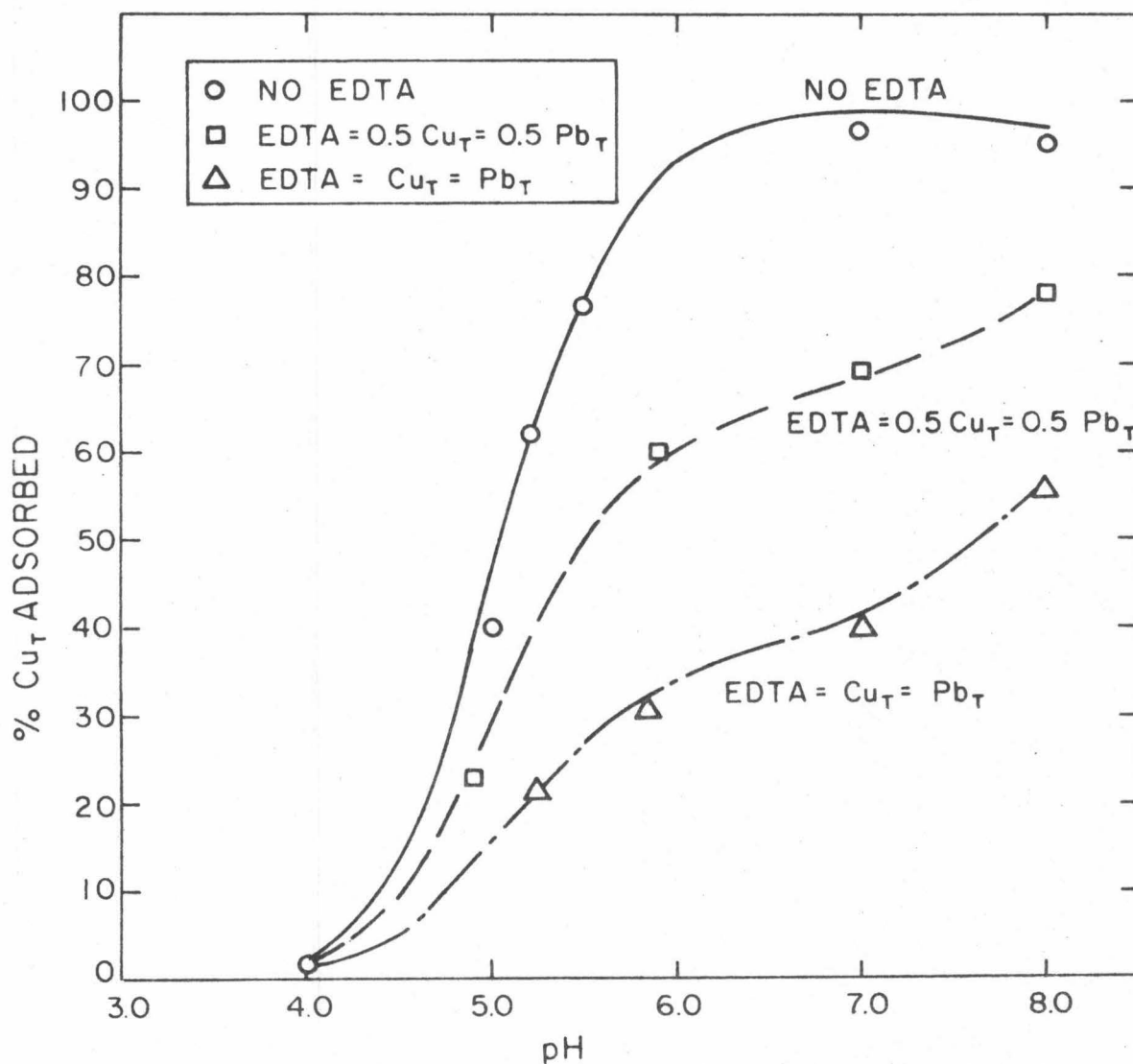


Figure 5.28 Adsorption of Cu on Min-U-Sil vs. pH in the presence and absence of EDTA in the system:  $Cu_T = Pb_T = 5 \times 10^{-7} M$ ,  $S = 50 m^2/l$ ,  $I = 10^{-3}$ , carbonate-free.  $\log^* \beta_2 Cu(OH)_2(aq) = -13.7$ . Experimental results modeled with the James-Healy Model.

using either the Ion Exchange-Surface Complex Formation Model or the James-Healy Model. A sensitivity test of both models shows that for Cu(II) the choice of the hydrolysis constant (e.g.,  $^*\beta_2\text{Cu}(\text{OH})_2(\text{aq})$ ) is an influential factor in modeling the experimental results.

At lower ionic strengths (e.g.,  $I = 10^{-3}$ ) modeling of the adsorption of Ca(II) and Mg(II) on  $\text{SiO}_2$  with the James-Healy Model overestimates the adsorption of  $\text{Me}^{2+}$  at lower pH. This effect can be overcome by imposing different values for the chemical free energy over the pH range of adsorption.

In the presence of citrate and EDTA, the position of the adsorption equilibrium is determined by competition between metal ion complexation in solution and metal adsorption on  $\alpha$ -quartz. Since the computations with the Ion Exchange-Surface Complex Formation Model are based on reactions of the free metal ions with the surface hydroxogroups, any complexation reduces the adsorption. Therefore, no special provisions are necessary to account for decreased adsorption owing to complexation. The resulting computations are in a very close agreement with the experimental results.

The James-Healy Model, on the contrary, does not explicitly account for decreased adsorption owing to complexation. However, by assigning the metal-ligand complexes sufficiently positive chemical free energies, the model can compute a decreased adsorption of

metals in the presence of "non-adsorbing" ligands. The same effect is obtained by omitting the adsorption computations for these metal-ligand complexes, and considering only the adsorption of the free metal ions and the metal-hydroxo species. This approach resulted in a successful modeling of the adsorption of Cu(II) and Pb(II) on SiO<sub>2</sub> in the presence of citrate and EDTA.

## Chapter 6

ADSORPTION OF Pb(II) AND Cu(II) ON  $\alpha$ -QUARTZ  
IN A CARBONATE SYSTEM6.1 Introduction

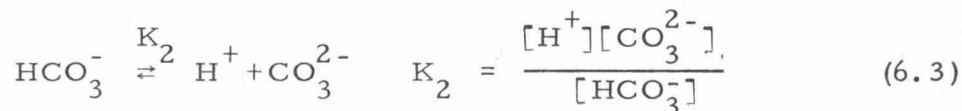
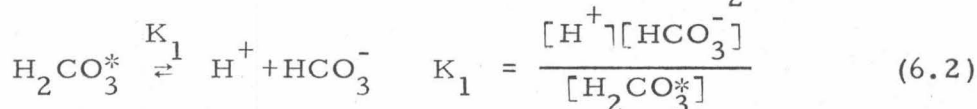
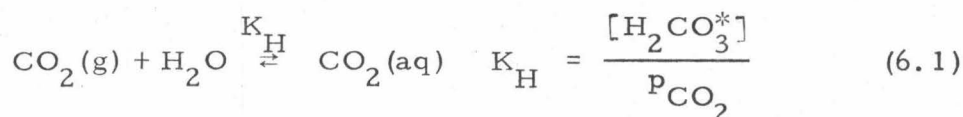
The present investigation on the factors controlling Pb(II) and Cu(II) adsorption on  $\alpha$ -quartz shows that the important environmental parameters are: a) type of the trace metal and its concentrations, b) available surface area, c) pH, d) ionic strength, and e) the identity and quantity of the organic ligand. In order to understand and predict the behavior of Pb(II) and Cu(II) under the conditions encountered in natural aquatic environments, it is necessary to study their chemical behavior with experimental conditions resembling those found in natural waters. Hence, in this chapter the adsorption of Pb(II) and Cu(II) on  $\text{SiO}_2$  is studied in the presence of one of the most abundant ligands in natural waters: carbonate. The order of presentation in this chapter follows closely to that used in the related sections of Chapter 5.

It will be assumed in the following presentation that the reader is acquainted with the equilibrium aspects of carbonate chemistry in aqueous systems. The set of reactions and relationships describing aqueous carbonate chemistry is given in Table 6.1.

Table 6.1

Aqueous Carbonate Solution Opened to the  
Atmosphere with Constant  $p_{\text{CO}_2}$

Aqueous Species:  $\text{CO}_2(\text{aq}), \text{H}_2\text{CO}_3, \text{HCO}_3^-, \text{CO}_3^{2-}, \text{H}^+, \text{OH}^-$   
 $[\text{H}_2\text{CO}_3^*] = [\text{CO}_2(\text{aq})] + [\text{H}_2\text{CO}_3]$   
 $[\text{CO}_2(\text{aq})] \gg [\text{H}_2\text{CO}_3]; [\text{CO}_2(\text{aq})] \approx [\text{H}_2\text{CO}_3^*]$



$$C_T = [\text{H}_2\text{CO}_3^*] + [\text{HCO}_3^-] + [\text{CO}_3^{2-}] \quad (6.4)$$

$$[\text{H}_2\text{CO}_3^*] = C_T \alpha_0 \quad \alpha_0 = \left(1 + \frac{K_1}{[\text{H}^+]} + \frac{K_1 K_2}{[\text{H}^+]^2}\right)^{-1} \quad (6.4)$$

$$[\text{HCO}_3^-] = C_T \alpha_1 \quad \alpha_1 = \left(\frac{[\text{H}^+]}{K_1} + 1 + \frac{K_2}{[\text{H}^+]}\right)^{-1} \quad (6.5)$$

$$[\text{CO}_3^{2-}] = C_T \alpha_2 \quad \alpha_2 = \left(\frac{[\text{H}^+]^2}{K_1 K_2} + \frac{[\text{H}^+]}{K_2} + 1\right)^{-1} \quad (6.6)$$

$$[\text{Alk}] = [\text{HCO}_3^-] + 2[\text{CO}_3^{2-}] + [\text{OH}^-] - [\text{H}^+] \quad (6.7)$$

$$= C_T (\alpha_1 + 2\alpha_2) + [\text{OH}^-] - [\text{H}^+] \quad (6.7a)$$

$$= \frac{K_H p_{\text{CO}_2}}{\alpha_0} (\alpha_1 + 2\alpha_2) + [\text{OH}^-] - [\text{H}^+] \quad (6.7b)$$

## 6.2 Adsorption of Pb(II) on $\alpha$ -Quartz in the Presence and Absence of Citrate

The distribution of Pb(II) species in a carbonate system can be calculated with the constants in Table 6.2.

As explained in Chapter 3, a range of pH values in the carbonate systems was obtained by varying the alkalinity. A pH of 6.2 corresponds to a  $pC_T$  of 4.7, and a pH of 8 to a  $pC_T$  of 3.29. Throughout this chapter, %Me is plotted as a function of pH.

From Figure 6.1a with  $pH > 7$  the complexes of Pb(II) with carbonate ( $Pb-CO_3$ ) are the predominant Pb(II) species. They include two species:  $PbCO_3(aq)$  and  $Pb(CO_3)_2(aq)$  (Table 6.2). For  $pH < 7$ , the predominant species is  $Pb^{2+}$ . At  $pH 7.1$   $[Pb^{2+}] = [Pb-CO_3] = [Pb-OH]$  where Pb-OH stands for all the hydrolysis products of Pb(II) considered in computations. In the presence of  $SiO_2^*$ , 90-100%  $Pb_T$  is adsorbed in the pH range 6.2 - 8 (Figure 6.1b).

In the presence of citrate, the Pb(II) species distribution, including the fraction sorbed, is determined by the amount of citrate added (Figure 6.2a,b and Figure 6.3 a,b). Figure 6.4 shows that relatively high concentration of citrate must be added to the system in order to cause a definite change in the adsorption behavior of Pb(II) in

---

\* Modeling of the adsorption systems with the James-Healy Model considers adsorption of only free metal ions and metal-hydroxo species.

Table 6.2

Equilibrium Constants for the  
 Pb(II)-CO<sub>2</sub>-HCO<sub>3</sub><sup>-</sup>-CO<sub>3</sub><sup>2-</sup> System

Species	log Equilibrium Constant (I=10 <sup>-3</sup> )	
PbCO <sub>3</sub> (aq)	K <sub>1</sub>	7.27
Pb(CO <sub>3</sub> ) <sub>2</sub> <sup>2-</sup> (aq)	β <sub>2</sub>	10.67
PbCO <sub>3</sub> (s)	K <sub>so</sub>	13.07
Pb(OH) <sub>2</sub> (CO <sub>3</sub> ) <sub>2</sub> (s)	*K <sub>so</sub>	19.10

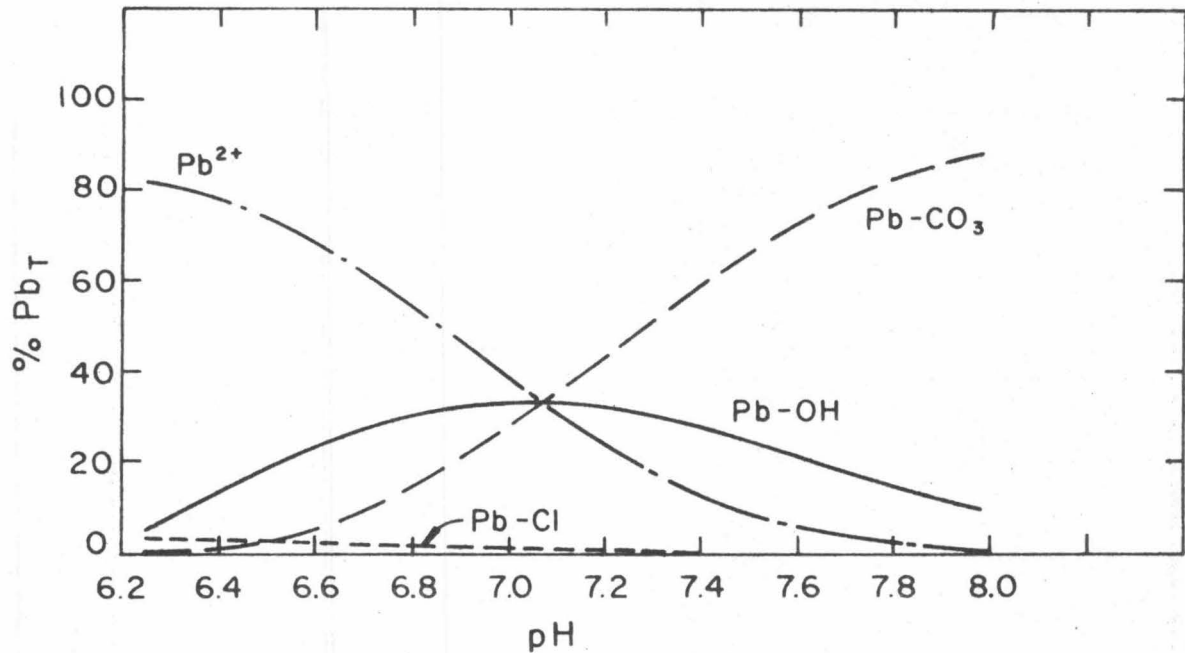


Figure 6.1a Equilibrium speciation of Pb vs. pH in the solution:  
 $Pb_T = 5 \times 10^{-7}$  M,  $I = 10^{-3}$ ,  $pCO_2 = 10^{-3.5}$  atm. pH varied by changing  
 alkalinities ( $pC_T = 3.29$  to  $pC_T = 4.7$ ).

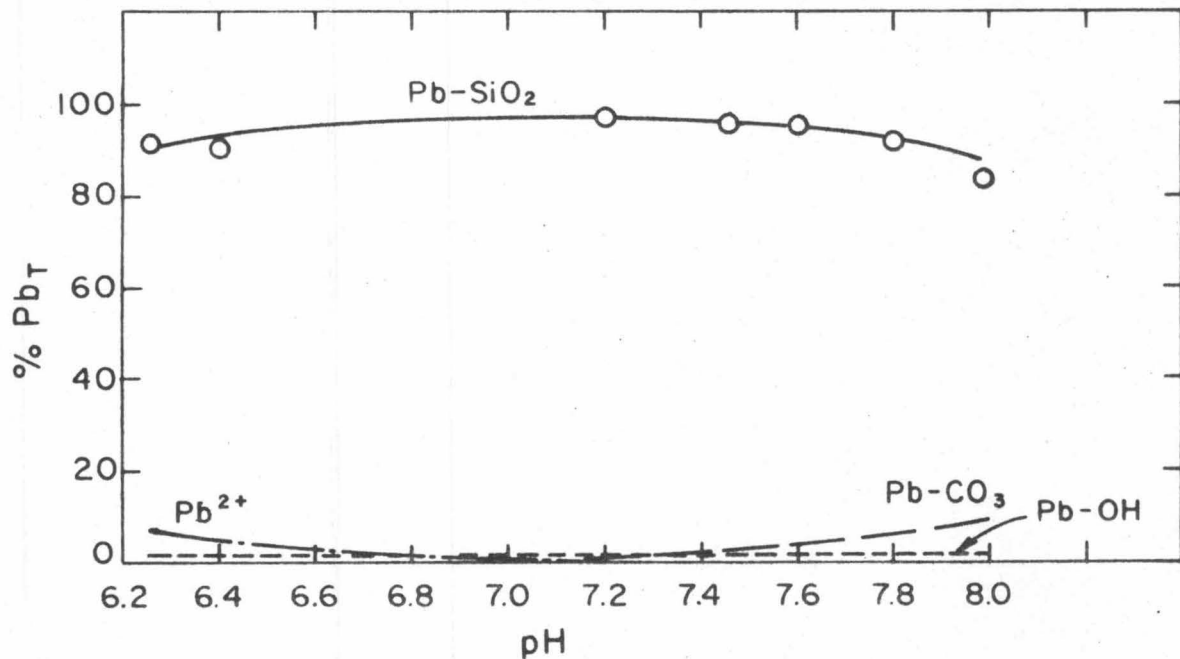


Figure 6.1b Equilibrium distribution of Pb vs. pH in the system:  
 $Pb_T = 5 \times 10^{-7}$  M,  $S = 50 \text{ m}^2/\text{l}$ ,  $I = 10^{-3}$ ,  $pCO_2 = 10^{-3.5}$  atm. Experimental  
 results modeled with the James-Healy Model.

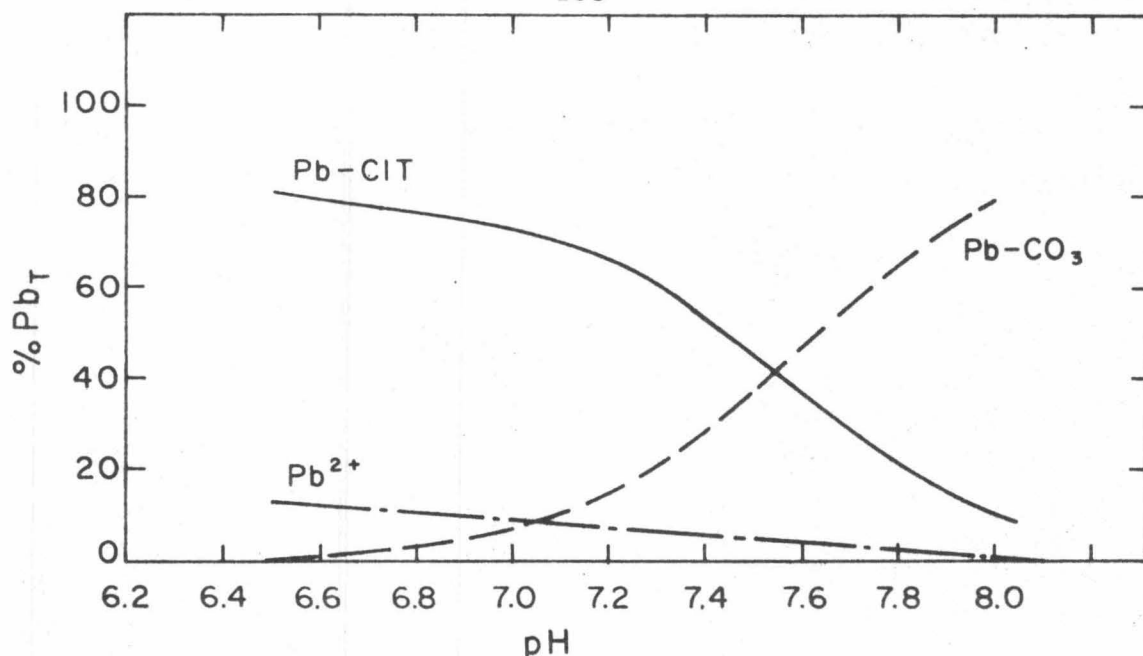


Figure 6.2a Equilibrium speciation of Pb vs. pH in the solution:  $Pb_T = 5 \times 10^{-7}$  M,  $CIT_T = 10Pb_T$ ,  $I = 10^{-3}$ ,  $pCO_2 = 10^{-3.5}$  atm. pH varied by changing alkalinities ( $pC_T = 3.29$  to  $pC_T = 4.7$ ).

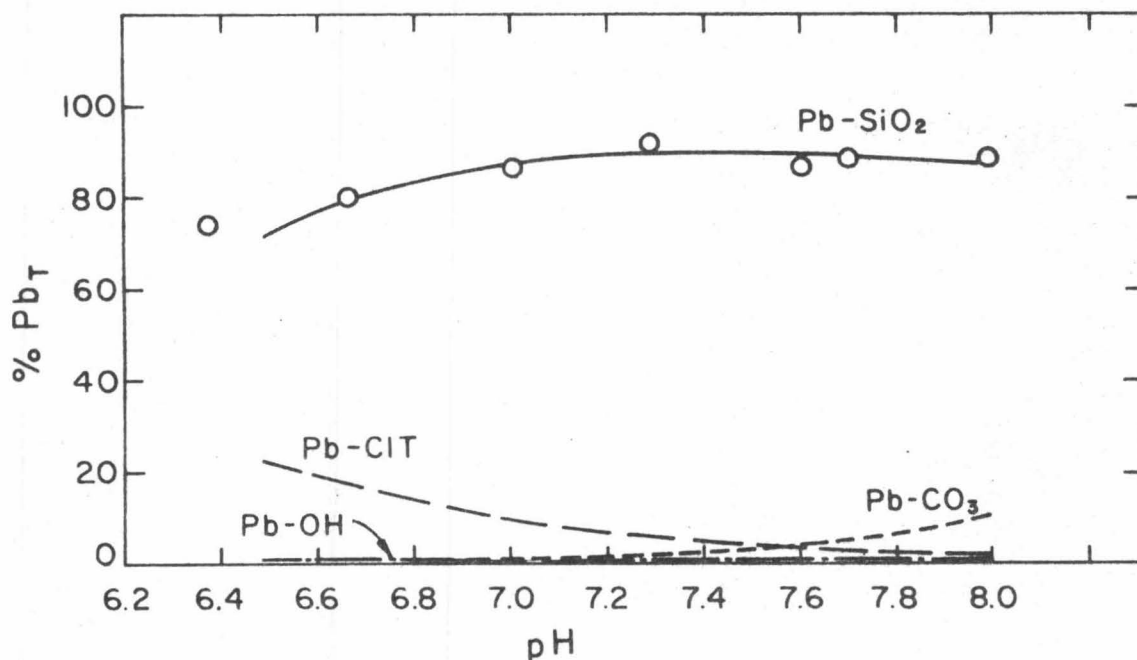


Figure 6.2b Equilibrium distribution of Pb vs. pH in the system:  $Pb_T = 5 \times 10^{-7}$  M,  $CIT_T = 10Pb_T$ ,  $S = 50 \text{ m}^2 / \text{l Min-U-Sil}$ ,  $I = 10^{-3}$ ,  $pCO_2 = 10^{-3.5}$  atm. Experimental results modeled with the James-Healy Model.

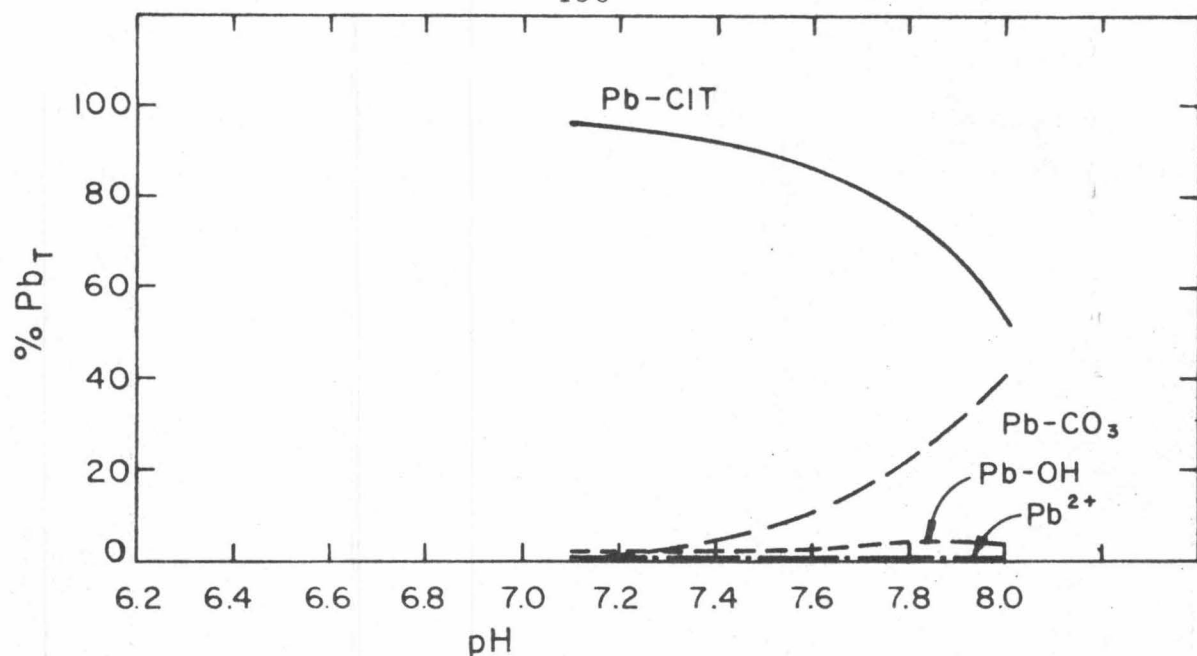


Figure 6.3a Equilibrium speciation of Pb vs. pH in the solution:  $Pb_T = 5 \times 10^{-7}$  M,  $CIT_T = 100 Pb_T$ ,  $I = 10^{-3}$ ,  $pCO_2 = 10^{-3.5}$  atm. pH varied by changing alkalinities ( $pC_T = 3.29$  to  $pC_T = 4.7$ ).

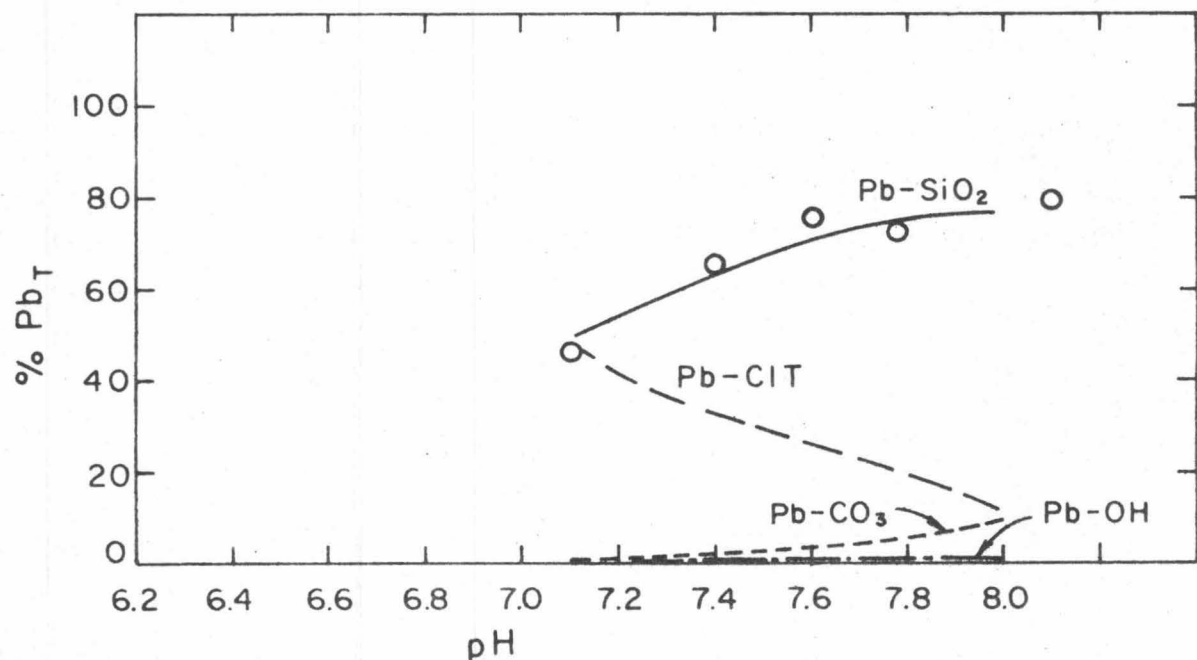


Figure 6.3b Equilibrium distribution of Pb vs. pH in the system:  $Pb_T = 5 \times 10^{-7}$  M,  $CIT_T = 100 Pb_T$ ,  $S = 50 m^2 / l$  Min-U-Sil,  $I = 10^{-3}$ ,  $pCO_2 = 10^{-3.5}$  atm. Experimental results modeled with the James-Healy Model.

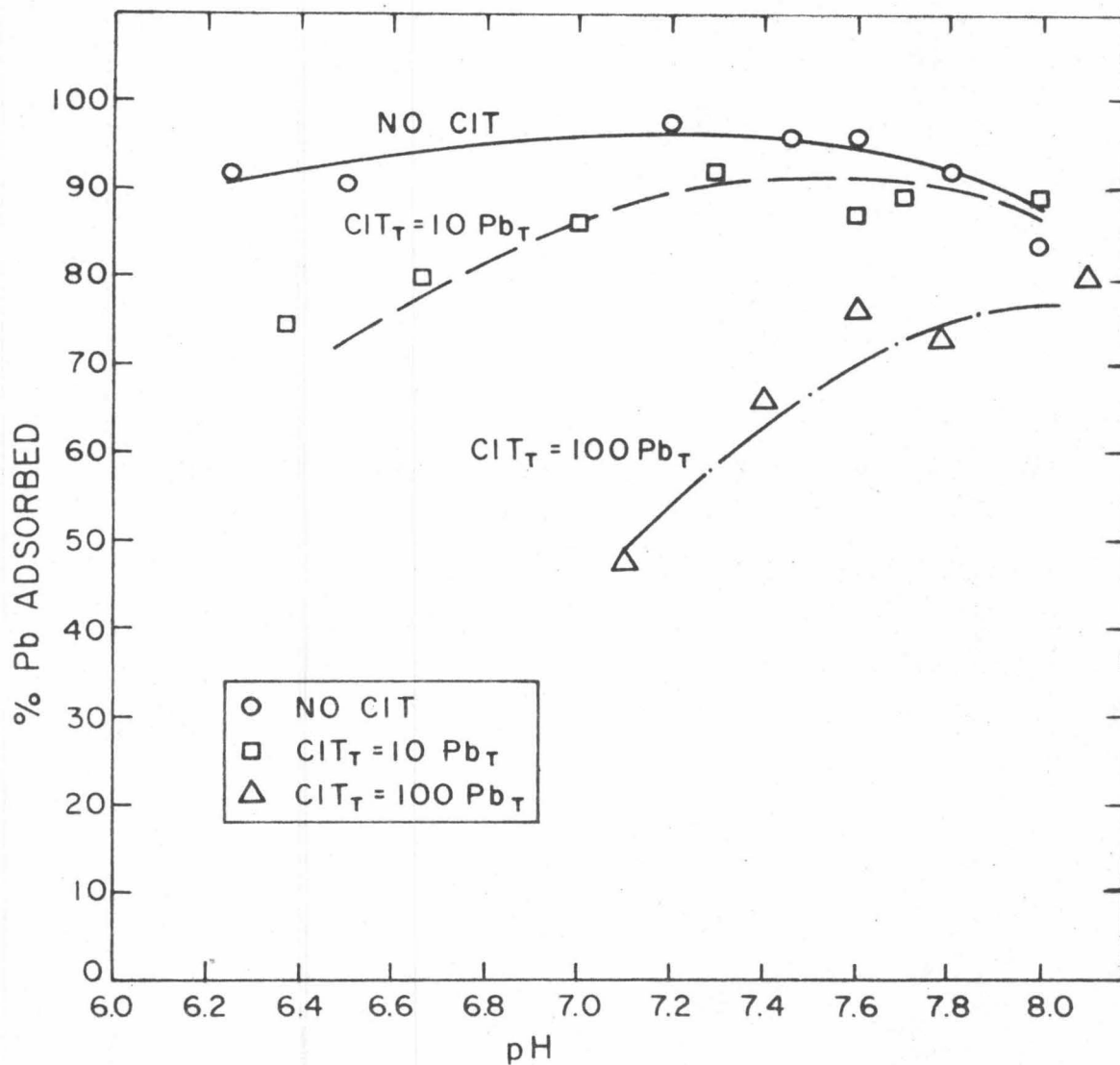


Figure 6.4 Adsorption of Pb on Min-U-Sil vs. pH in the presence and absence of citrate in the system:  $Pb_T = 5 \times 10^{-7} M$ ,  $S = 50 m^2/l$ ,  $I = 10^{-3}$ ,  $pCO_2 = 10^{-3.5}$  atm. pH varied by changing alkalinities. Experimental results modeled with the James-Healy Model.

the pH range 6.2-8.0. High concentrations of citrate shift the suspension pH to slightly higher values. The James-Healy Model (Figure 6.4), as well as the Ion Exchange-Surface Complex Formation Model (Figure 6.5), results in adsorption isotherms which are in close agreement with the experimental results. Hence, both laboratory measurements and the model computations (using either of the adsorption models) indicate no adsorption of  $\text{PbCO}_3(\text{aq})$ . These findings are contrary to those of Stumm and Bilinski (1972).

### 6.3 Adsorption of Cu(II) on $\alpha$ -Quartz in the Presence and and Absence of Citrate

In the presence of carbonate, Cu(II) forms the following species:  $\text{CuCO}_3(\text{aq})$ ,  $\text{Cu}(\text{CO}_3)_2^{2-}(\text{aq})$ , and  $\text{Cu}_2(\text{OH})_2\text{CO}_3(\text{s})$ . The corresponding stability constants are given in Table 6.3. In the system discussed below  $\text{OH}^-$  and  $\text{Cl}^-$  also compete with  $\text{CO}_3^{2-}$  for Cu(II). As a result, the main species below pH 6.8 is  $\text{Cu}^{2+}$  and above pH 6.8, Cu-OH. The species Cu- $\text{CO}_3(\text{aq})$  account for only  $\sim 10\%$  of  $\text{Cu}_T$ , and Cu-Cl species are unimportant (Figure 6.6a). In the presence of  $\alpha$ -quartz, Cu(II) is completely removed from the solution by sorption, as was the case in the carbonate-free system (Figure 6.6b).

The addition of citrate ( $\text{CIT}_T = 0.5 \text{ Cu}_T$  and  $\text{CIT}_T = \text{Cu}_T$ ) reduces the amount of free and hydrolyzed copper species in the absence of  $\alpha$ -quartz to 50% (Figure 6.7a) and to less than 10% (Figure 6.8a),

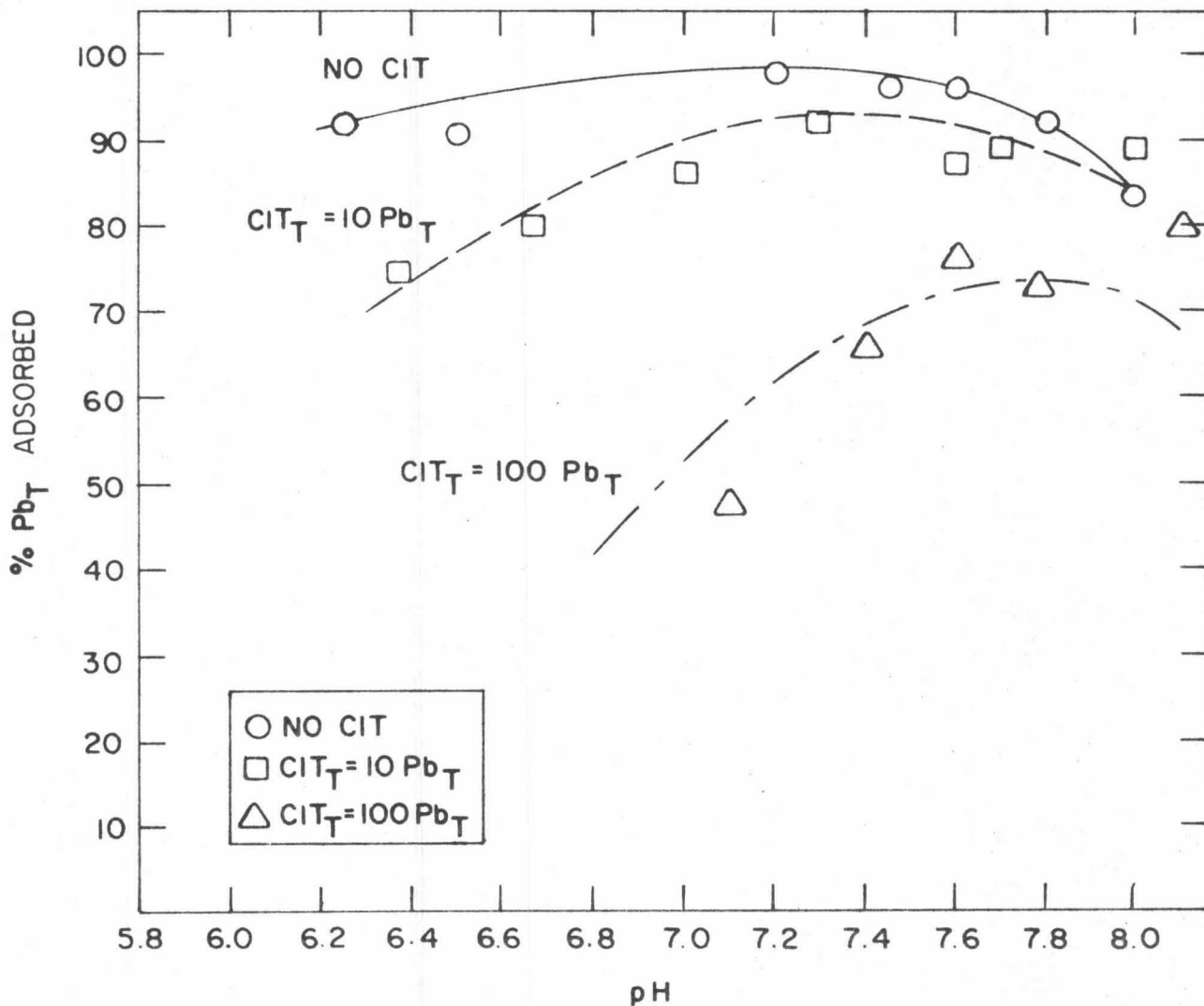


Figure 6.5 Adsorption of Pb on Min-U-Sil vs. pH in the presence and absence of citrate in the system:  $Pb_T = 5 \times 10^{-7} M$ ,  $S = 2.24 \times 10^{-4} M$  ( $50 m^2/l$ ),  $I = 10^{-3}$ ,  $pCO_2 = 10^{-3.5} atm$ . Experimental results modeled with the Ion Exchange-Surface Complex Formation Model.

Table 6.3  
 Equilibrium Constants for the  
 Cu-CO<sub>2</sub>-HCO<sub>3</sub><sup>-</sup>-CO<sub>3</sub><sup>2-</sup> System

Species	log Equilibrium Constant (I=10 <sup>-3</sup> )	
CuCO <sub>3</sub> (aq)	K <sub>1</sub>	6.6
Cu(CO <sub>3</sub> ) <sub>2</sub> <sup>2-</sup> (aq)	β <sub>2</sub>	9.8
Cu <sub>2</sub> (OH) <sub>2</sub> CO <sub>3</sub> (s)	*K <sub>so</sub>	5.82

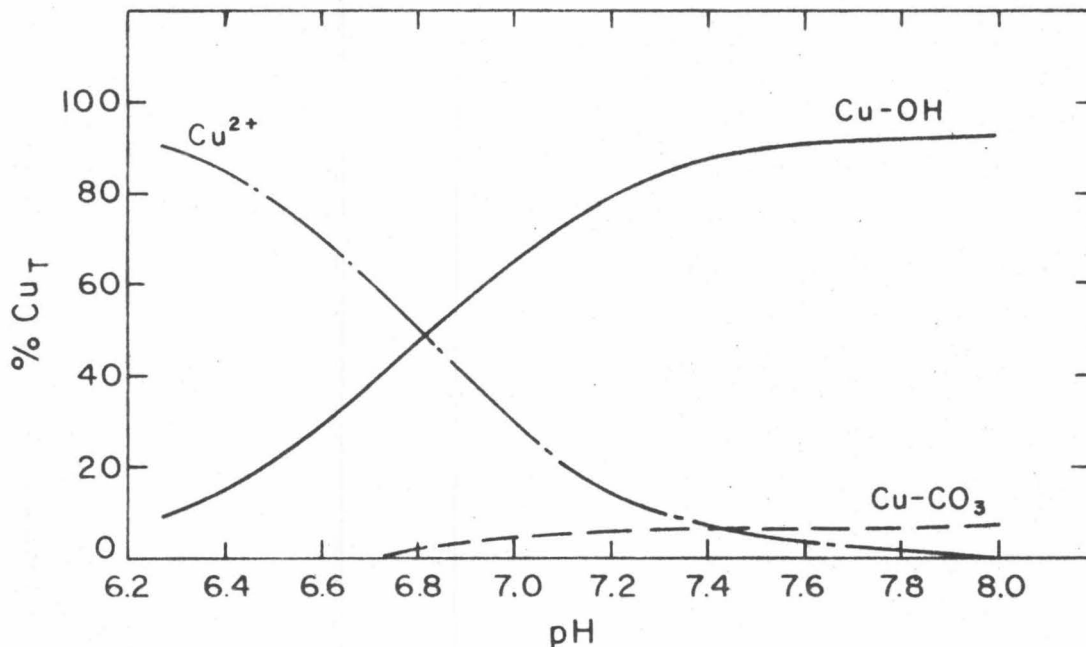


Figure 6.6a Equilibrium speciation of Cu vs. pH in the solution:  $Cu_T = 10^{-7}$  M,  $I = 10^{-3}$ ,  $pCO_2 = 10^{-3.5}$  atm. pH varied by changing alkalinities ( $pC_T = 3.29$  to  $pC_T = 4.7$ ).  $\text{Log}^*\beta_2 \text{Cu}(\text{OH})_2(\text{aq}) = -13.7$ .

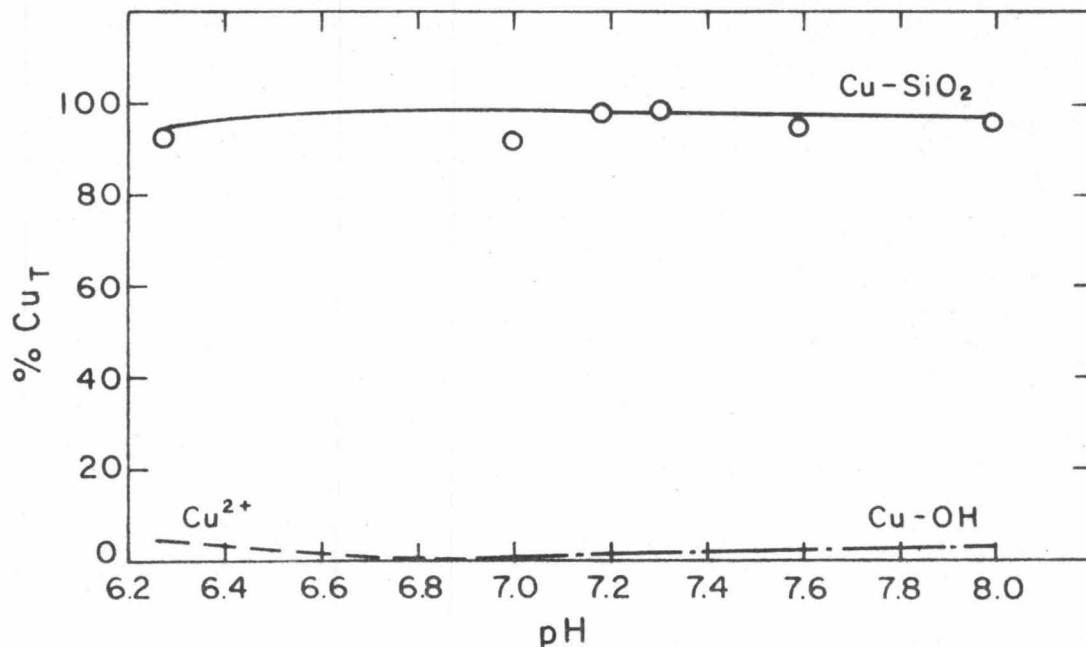


Figure 6.6b Equilibrium distribution of Cu vs. pH in the system:  $Cu_T = 10^{-7}$  M,  $S = 50 \text{ m}^2/\ell$  Min-U-Sil,  $I = 10^{-3}$ ,  $pCO_2 = 10^{-3.5}$  atm. Experimental results modeled with the James-Healy Model.

respectively. Carbonate-containing species are unimportant. In the presence of  $\text{SiO}_2$ , a remarkable degree of adsorption still occurs (Figures 6.7b and 6.8b). If citrate is present in a large excess over  $\text{Cu}_T$  ( $\text{CIT}_T = 10\text{Cu}_T$ ), all the Cu(II) is complexed by citrate, as was the case in the carbonate-free system (Figure 6.9a). Even in the presence of excess of surface area, Cu(II) remains complexed by citrate and, consequently, stays in solution (Figure 6.9b).

Modeling of the experimental systems in the presence and absence of citrate was carried out with both the Ion Exchange-Surface Complex Formation Model and the James-Healy Model. The Ion Exchange-Surface Complex Formation Model with  $\log^*\beta_2 = -17.3$  (Figure 6.10) shows a good agreement with the experimental results for the two extreme cases: with no citrate present, and with ten fold excess of citrate over copper (i. e. ,  $\text{CIT}_T = 10\text{Cu}_T$ ). However, in the intermediate region, that is when  $\text{CIT}_T = 0.5 \text{Cu}_T$  and  $\text{CIT}_T = \text{Cu}_T$ , there are large discrepancies between the theoretical predictions and the experimental results; the theoretically predicted adsorption isotherms curve in a direction opposite to that of the experimental curves. Since the computations with the Ion Exchange-Surface Complex Formation Model are based on competition between ligands and surface for the free metal ion (see Chapter 2), the addition of any ligand reduces the

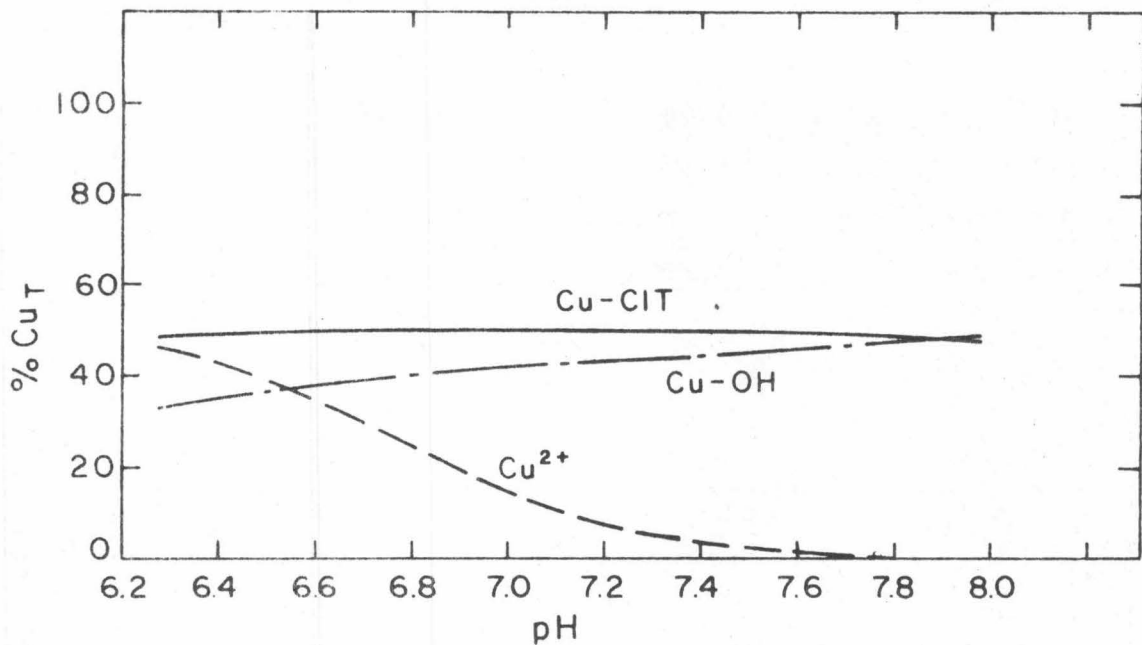


Figure 6.7a Equilibrium speciation of Cu vs. pH in the solution:  $Cu_T = 10^{-7}$  M,  $CIT_T = 0.5Cu_T$ ,  $I = 10^{-3}$ ,  $pCO_2 = 10^{-3.5}$  atm. pH varied by changing alkalinities ( $pC_T = 3.25$  to  $pC_T = 4.7$ ).  $\text{Log}^*\beta_2 Cu(OH)_2(aq) = -13.7$ .

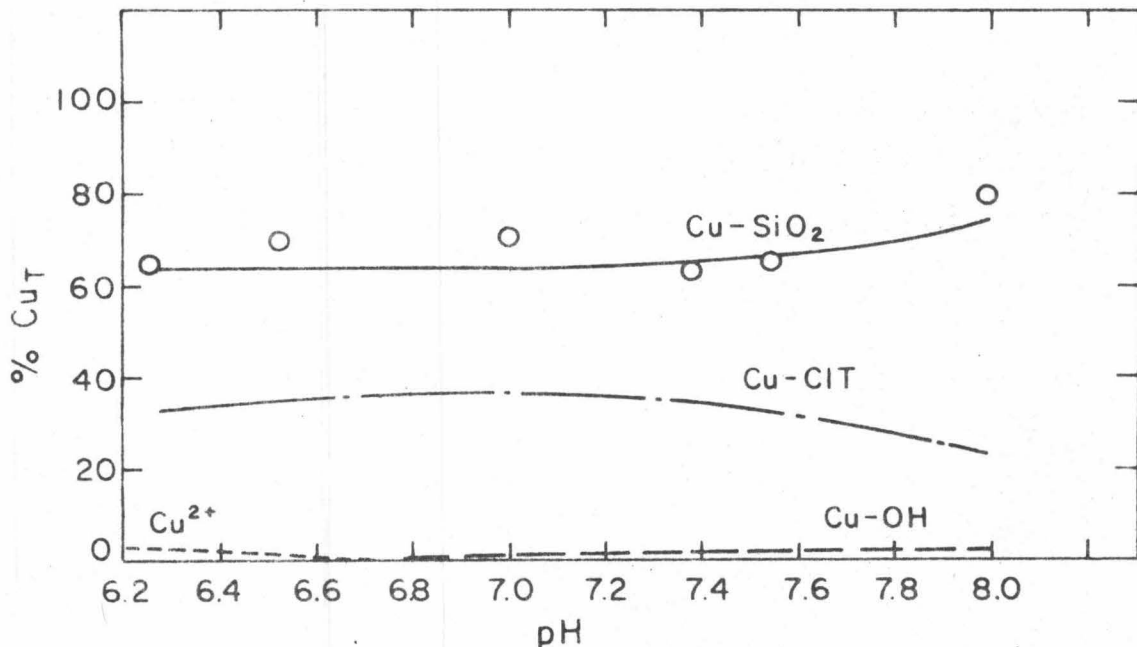


Figure 6.7b Equilibrium distribution of Cu vs. pH in the system:  $Cu_T = 10^{-7}$  M,  $CIT_T = 0.5Cu_T$ ,  $S = 50m^2/l$  Min-U-Sil,  $I = 10^{-3}$ ,  $pCO_2 = 10^{-3.5}$  atm. Experimental results modeled with the James-Healy Model.

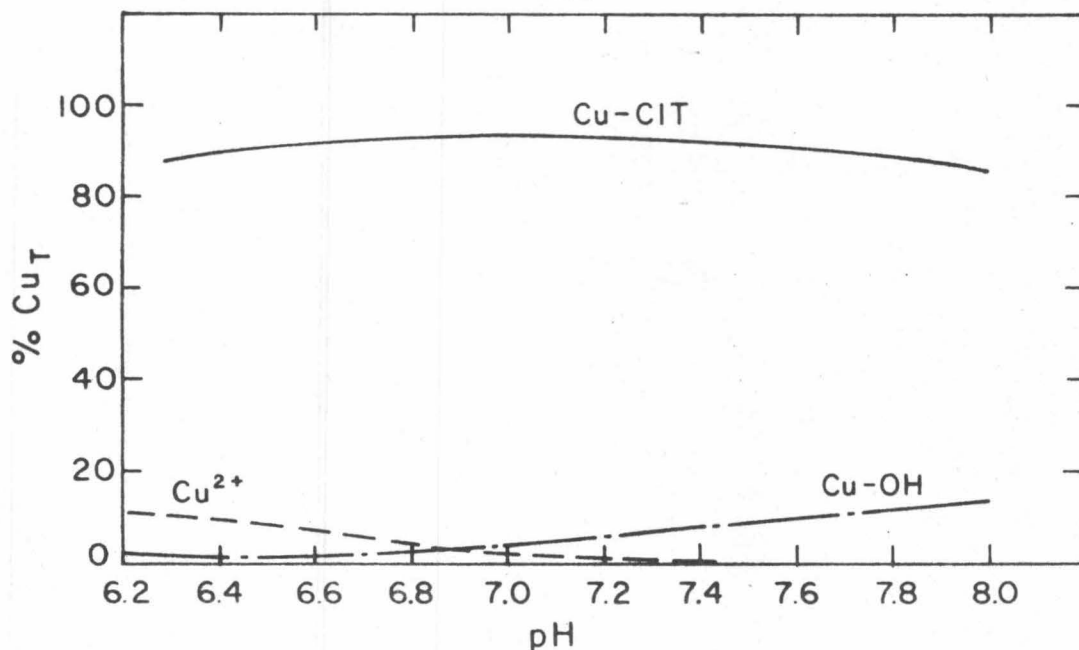


Figure 6.8a Speciation of Cu vs. pH in the solution:  $\text{Cu}_T = 10^{-7} \text{ M}$ ,  $\text{CIT}_T = \text{Cu}_T$ ,  $I = 10^{-3}$ ,  $p\text{CO}_2 = 10^{-3.5} \text{ atm}$ . pH varied by changing alkalinities ( $p\text{C}_T = 3.29$  to  $p\text{C}_T = 4.7$ ).  $\text{Log}^* \beta_2 \text{Cu}(\text{OH})_2(\text{aq}) = -13.7$ .

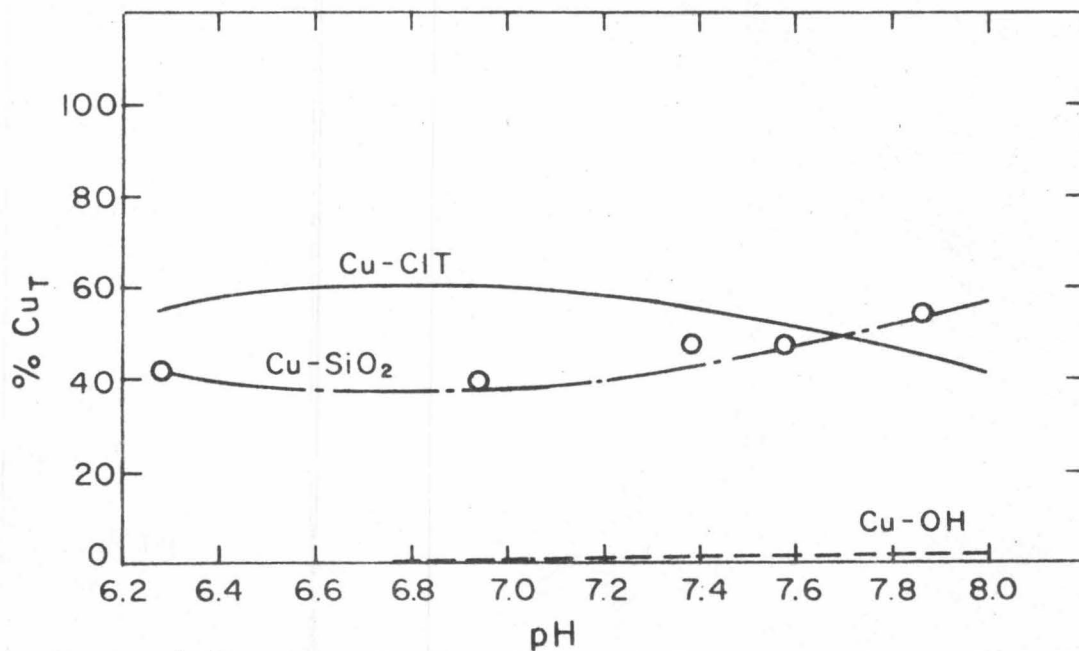


Figure 6.8b Distribution of Cu vs. pH in the system:  $\text{Cu}_T = 10^{-7} \text{ M}$ ,  $\text{CIT}_T = \text{Cu}_T$ ,  $S = 50 \text{ m}^2 / \text{l Min-U-Sil}$ ,  $I = 10^{-3}$ ,  $p\text{CO}_2 = 10^{-3.5} \text{ atm}$ . Experimental results modeled with the James-Healy Model.

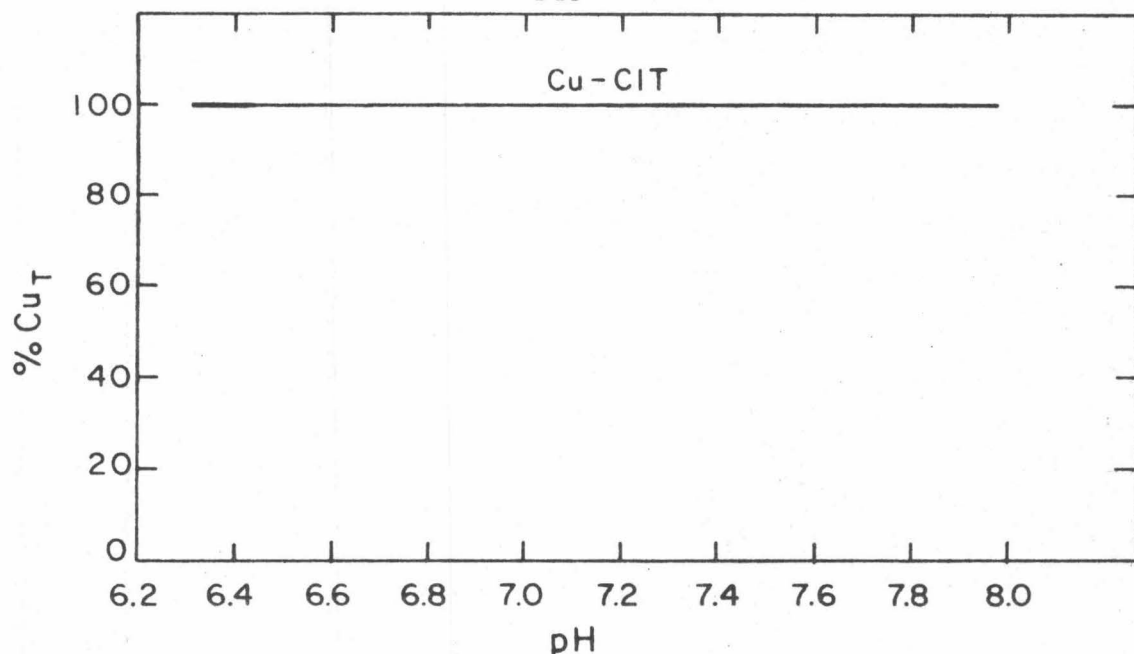


Figure 6.9a Equilibrium speciation of Cu vs. pH in the solution:  $\text{Cu}_T = 10^{-7} \text{ M}$ ,  $\text{CIT}_T = 10\text{Cu}_T$ ,  $I = 10^{-3}$ ,  $p\text{CO}_2 = 10^{-3.5} \text{ atm}$ . pH varied by changing alkalinities ( $p\text{C}_T = 3.29$  to  $p\text{C}_T = 4.7$ ).  $\text{Log}^*\beta_2 \text{Cu}(\text{OH})_2(\text{aq}) = -13.7$ .

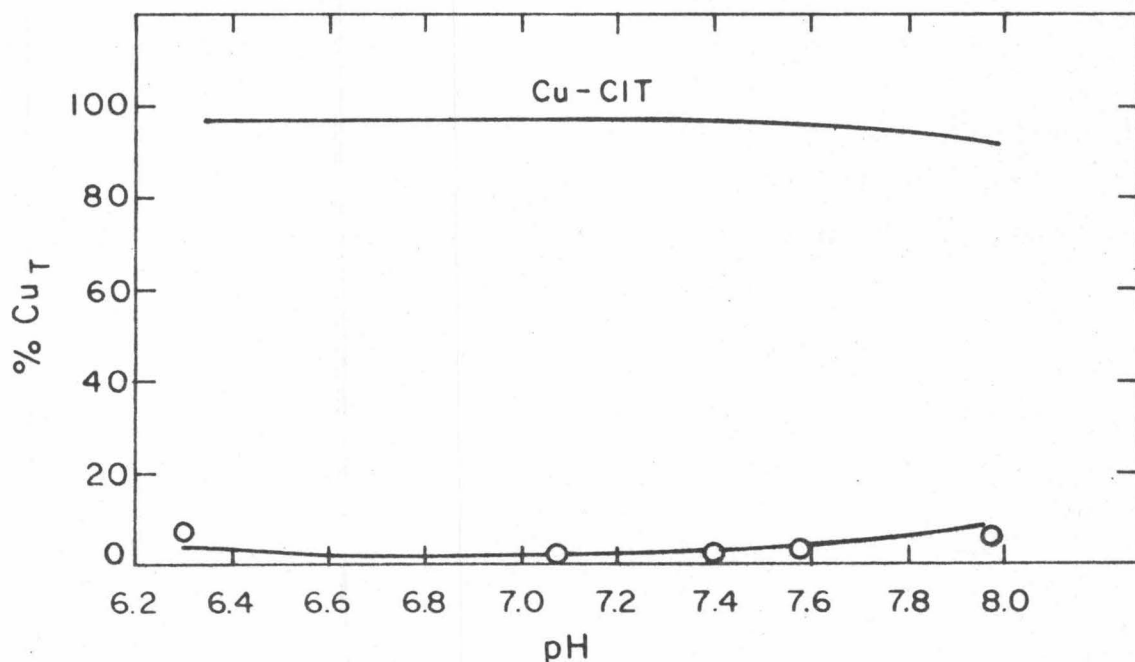


Figure 6.9b Equilibrium distribution of Cu vs. pH in the system:  $\text{Cu}_T = 10^{-7} \text{ M}$ ,  $\text{CIT}_T = 10\text{Cu}_T$ ,  $S = 50 \text{ m}^2 / \text{l Min-U-Sil}$ ,  $I = 10^{-3}$ ,  $p\text{CO}_2 = 10^{-3.5} \text{ atm}$ . Experimental results modeled with the James-Healy Model.

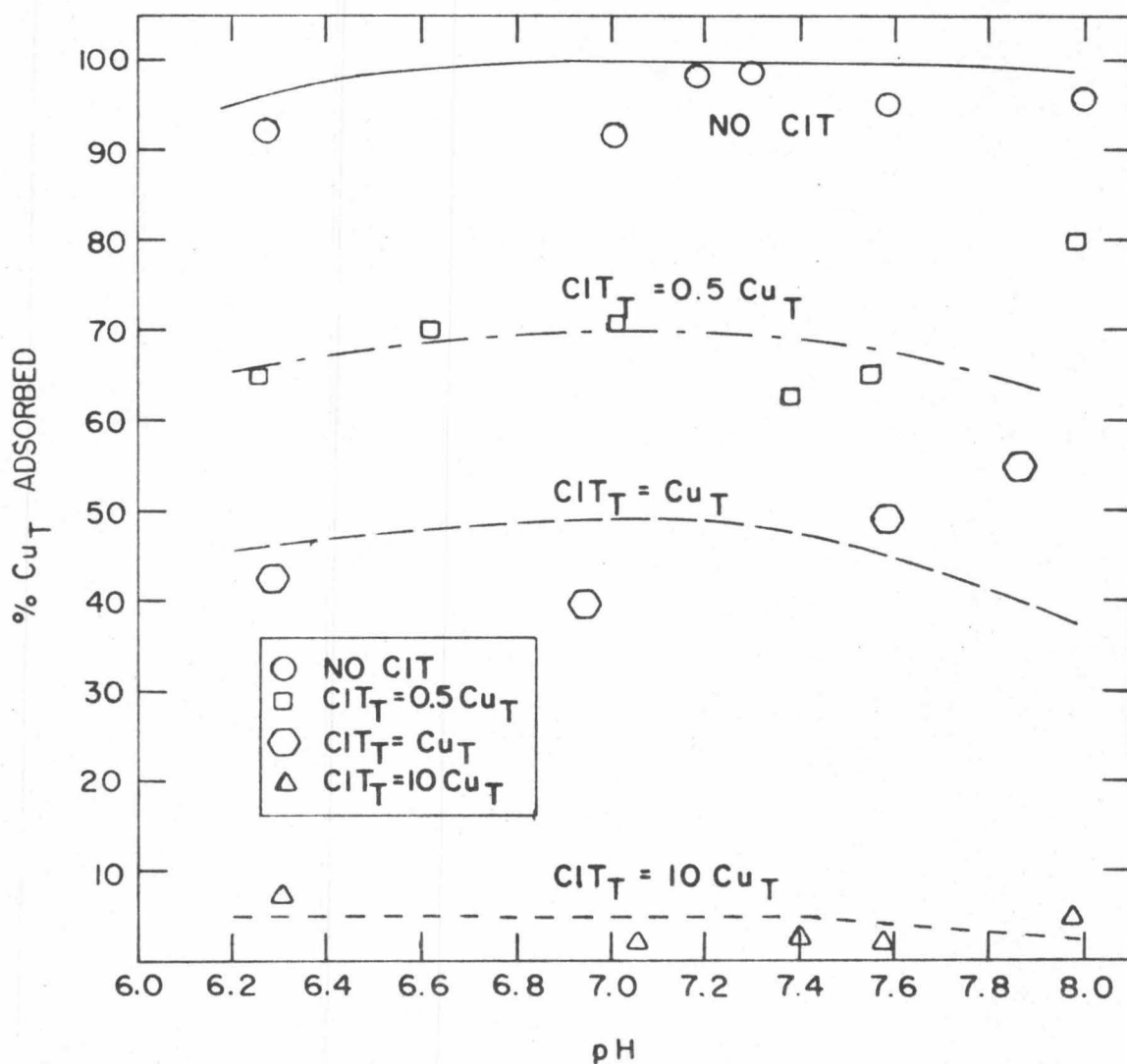
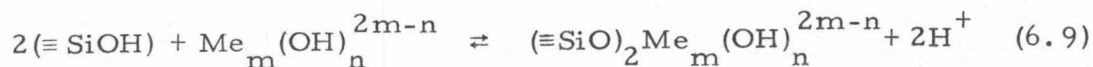
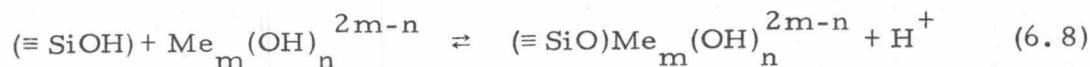


Figure 6.10 Adsorption of Cu on  $\alpha$ -quartz vs. pH in the presence and absence of citrate in the system:  $Cu_T = 10^{-7}$  M,  $S = 2.24 \times 10^{-4}$  M,  $I = 10^{-3}$ ,  $pCO_2 = 10^{-3.5}$  atm. pH varied by changing alkalinities ( $pC_T = 3.29$  to  $pC_T = 4.7$ ).  $\text{Log}^* \beta_2 \text{Cu}(\text{OH})_2(\text{aq}) = -17.3$ . Experimental results modeled with the Ion Exchange-Surface Complex Formation Model.

adsorption by reducing the free metal ion concentration. Since complexation of Cu(II) with both hydroxide and carbonate increases with increasing pH, the expected result is a decrease in the free metal ion with increasing pH and, consequently, a decrease in the adsorption when  $[\text{Me-OH}] + [\text{Me-CO}_3] > [\text{Me}^{2+}]$ . This results in the concave-down nature of the predicted adsorption curves in the pH range 6.2-8.0.

A larger hydrolysis constant implies a shift in the aqueous equilibrium away from  $\text{Cu-CO}_3(\text{aq})$ , toward the production of  $\text{Cu(OH)}_2(\text{aq})$ . This shift would result in a further decrease in the free metal ion. Indeed, Figure 6.11 shows that the larger  $^*\beta_2$  (i. e. ,  $\log^* \beta_2 = -13.7$ ) results in greater disagreement between the experimental results and model predictions. It can be concluded, therefore, that better agreement between the model and the experimental results can be obtained by considering also the reactions between the surface OH groups and the hydrolyzed metal species, i. e. ,



where  $m=1, 2, \dots$  and  $n=0, 1, 2, \dots$  are the stoichiometric coefficients of the (+2) charged metal Me and the OH groups, respectively.

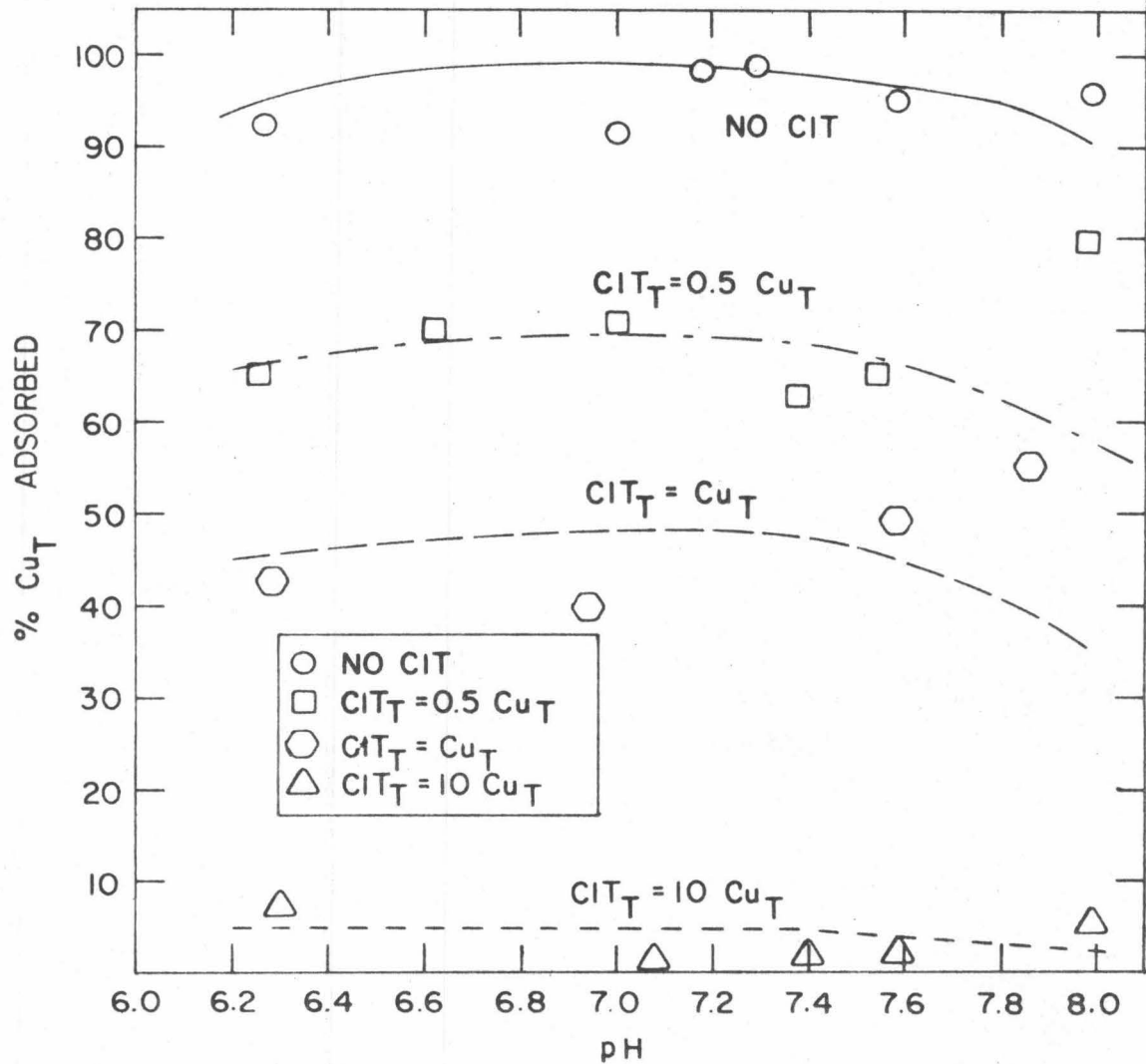


Figure 6.11 Adsorption of Cu vs. pH in the presence and absence of citrate in the system:  $Cu_T = 10^{-7}$  M,  $S = 2.24 \times 10^{-4}$  M,  $I = 10^{-3}$ ,  $pCO_2 = 10^{-3.5}$  atm. pH varied by changing alkalinities ( $pC_T = 3.29$  to  $pC_T = 4.7$ ).  $\log^* \beta_2 Cu(OH)_2(aq) = -13.7$ . Experimental results modeled with the Ion Exchange-Surface Complex Formation Model.

In the James-Healy Model any species with the charge zero can be easily adsorbed if given a  $\Delta G_{\text{chem},i}^{\circ}$  favorable to the adsorption, because its desolvation energy is equal to zero. Hence,  $\text{Cu}(\text{OH})_2(\text{aq})$  will have a significant influence on the over  $\Delta G_{\text{ads}}^{\circ}$ , the tendency being to increase the adsorption (as discussed in Chapters 4 and 5). Modeling with the James-Healy Model was tested for three different cases:

a) when  $\text{Cu}(\text{OH})_2(\text{aq})$  is omitted from computations for the equilibrium system (Figure 6.12), b) when  $\log^* \beta_2 = -17.3$  (Figure 6.13), and c) when  $\log^* \beta_3 = -13.7$  (Figure 6.14). Case a) resulted in a good agreement between experimental and theoretical results only when no citrate is present, or when present in ten-fold excess over copper; for  $\text{CIT}_{\text{T}} = 0.5 \text{ Cu}_{\text{T}}$  and  $\text{CIT}_{\text{T}} = \text{Cu}_{\text{T}}$  there is a large disagreement between computed and experimentally-determined adsorption. Case b) resulted in essentially the same curves, because  $\log^* \beta_2 = -17.3$  is too small a constant to cause any appreciable shift in equilibrium toward production of  $\text{Cu}(\text{OH})_2(\text{aq})$ . A much larger second hydrolysis constant is needed in order to make a significant shift. According to Figure 6.14,  $\log^* \beta = -13.7$  shifted the equilibrium to such an extent that reasonable agreement was obtained for the case when  $\text{CIT}_{\text{T}} = 0.5 \text{ Cu}_{\text{T}}$ , and a very good agreement for  $\text{CIT}_{\text{T}} = \text{Cu}_{\text{T}}$ . Therefore, it can be concluded that the James-Healy Model used with  $\log^* \beta_2 = -13.7$  offers a consistent interpretation of the experimentally obtained results. Actually, the adsorption data can

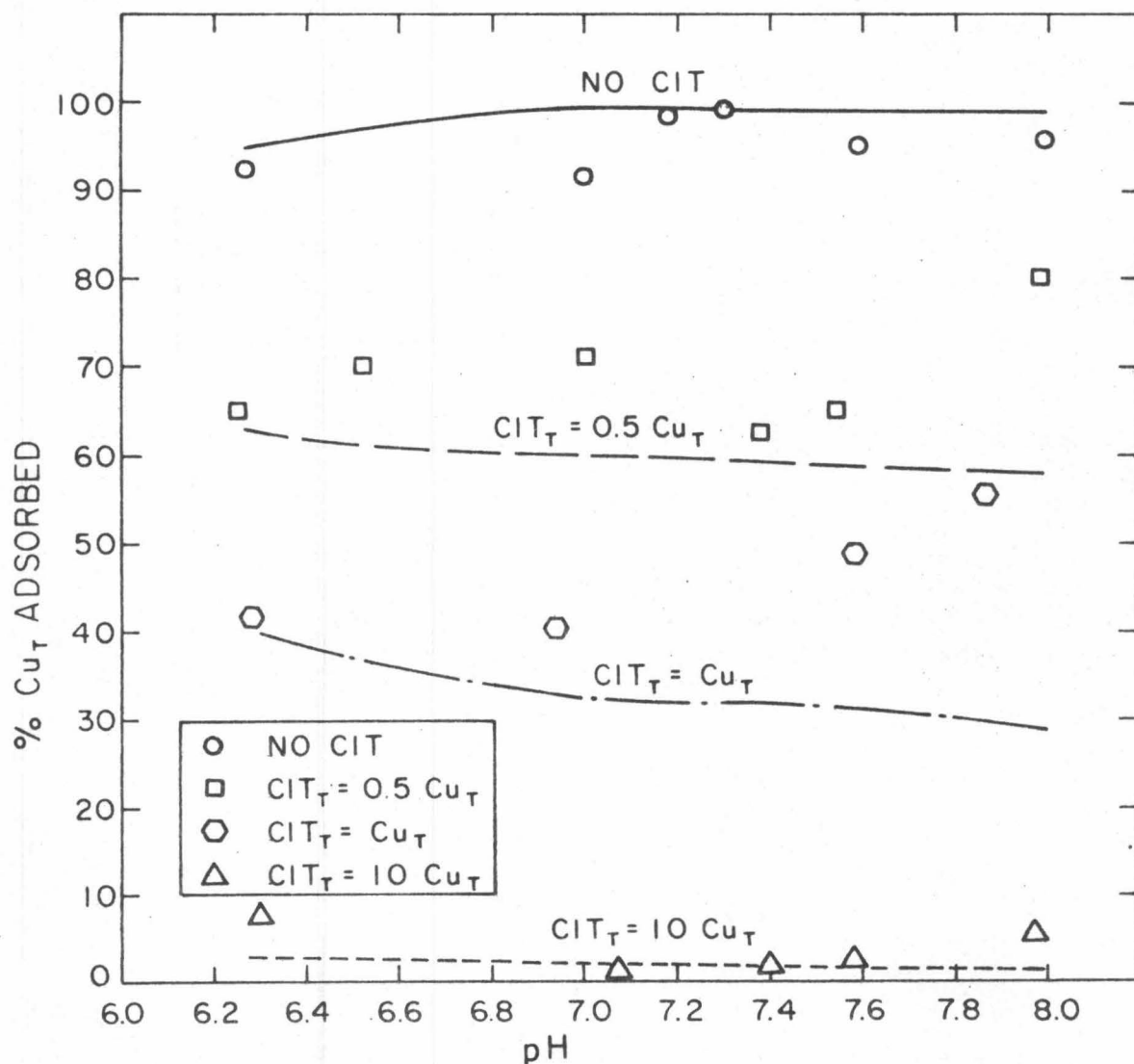


Figure 6.12 Adsorption of Cu on Min-U-Sil vs. pH in the presence and absence of citrate in the system:  $\text{Cu}_T = 10^{-7} \text{M}$ ,  $S = 50 \text{m}^2/\ell$ ,  $I = 10^{-3}$ ,  $\text{pCO}_2 = 10^{-3.5} \text{atm}$ . pH varied by changing alkalinities ( $\text{pC}_T = 3.29$  to  $\text{pC}_T = 4.7$ ).  $\text{Cu}(\text{OH})_2(\text{aq})$  not included in computations. Experimental results modeled with the James-Healy Model.

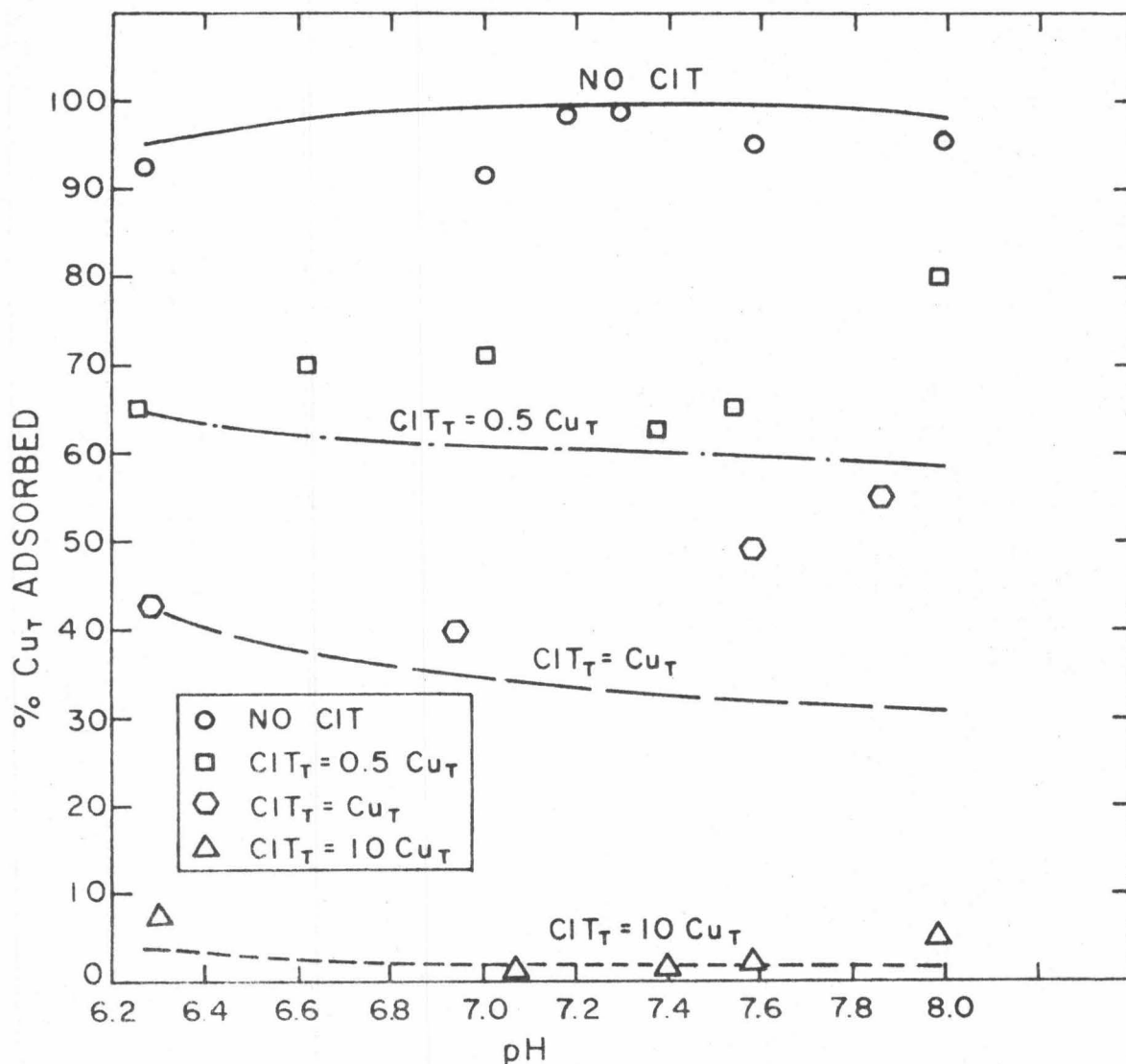


Figure 6.13 Adsorption of Cu on Min-U-Sil vs. pH in the presence and absence of citrate in the system:  $\text{Cu}_T = 10^{-7} \text{M}$ ,  $S = 50 \text{m}^2/\text{l}$ ,  $I = 10^{-3}$ ,  $\text{pCO}_2 = 10^{-3.5} \text{atm}$ . pH varied by changing alkalinities ( $\text{pC}_T = 3.29$  to  $\text{pC}_T = 4.7$ ).  $\text{Log}^* \beta_2 \text{Cu}(\text{OH})_2(\text{aq}) = -17.3$ . Experimental results modeled with the James-Healy Model.

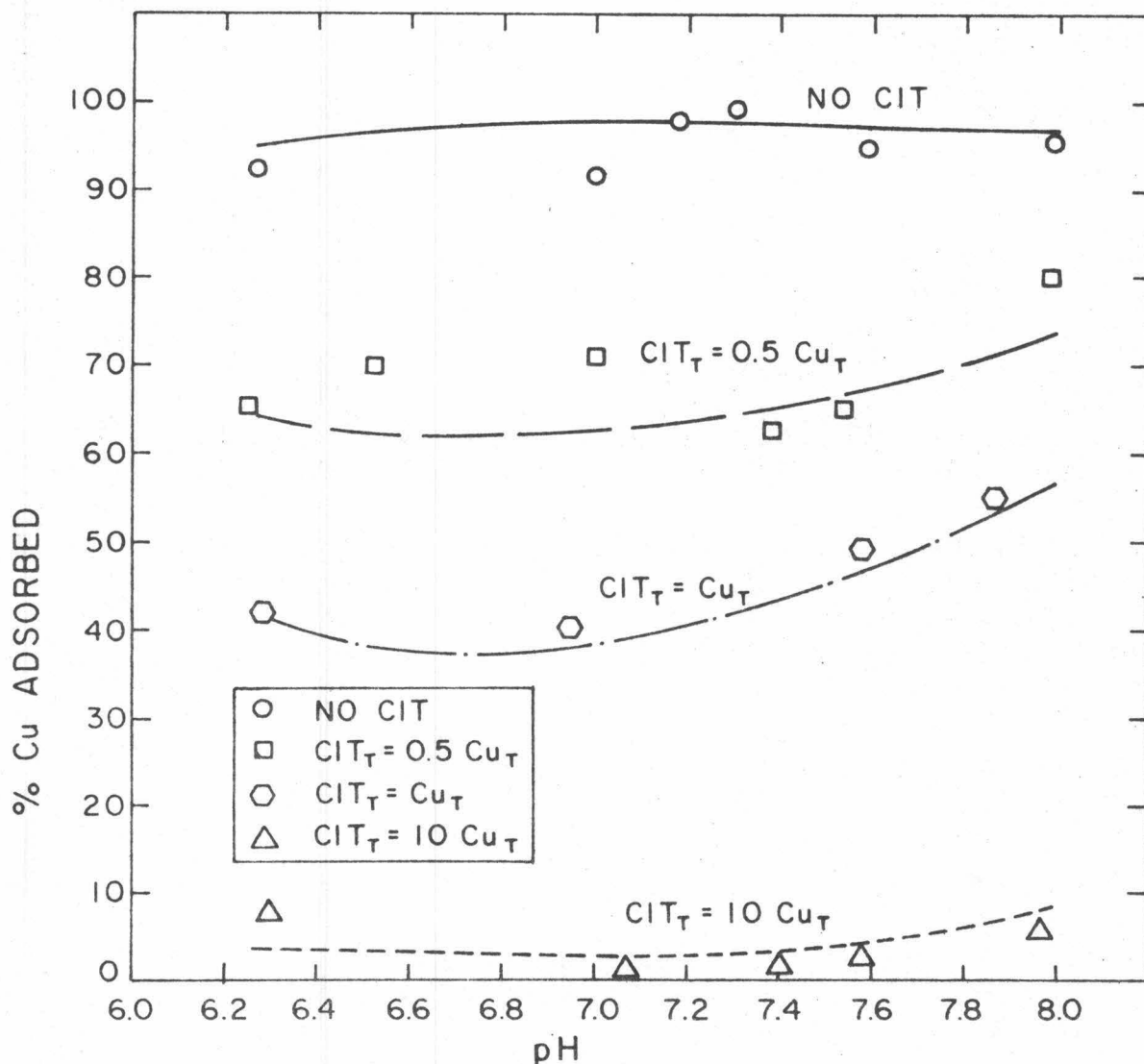


Figure 6.14 Adsorption of Cu on Min-U-Sil vs. pH in the presence and absence of citrate in the system:  $Cu_T = 10^{-7} M$ ,  $S = 50 m^2/l$ ,  $I = 10^{-3}$ ,  $pCO_2 = 10^{-3.5} atm$ . pH varied by changing alkalinities ( $pC_T = 3.29$  to  $pC_T = 4.7$ ).  $\log^* \beta_2 Cu(OH)_2(aq) = -13.7$ . Experimental results modeled with the James-Healy Model.

be viewed as an indirect way of estimating the second hydrolysis constant for Cu(II).

#### 6.4 Conclusions

The discrepancy between the theoretically predicted adsorption and the experimental results for the adsorption of Cu(II) on  $\alpha$ -quartz in the  $\text{CO}_2$ - $\text{HCO}_3^-$ - $\text{CO}_3^{2-}$  system can be attributed to several reasons:

1. adsorption of citrate followed by Cu, or adsorption of Cu-CIT complexes
2. adsorption of  $\text{CuCO}_3(\text{aq})$
3. unreliable hydrolysis constant(s).

As described in Chapter 3, adsorption of citrate was tested with  $\text{C}^{14}$ -CIT. These experiments did not yield any evidence for the adsorption of citrate or copper-citrate complexes.

Experimental results obtained with  $\text{C}^{14}$ - $\text{NaHCO}_3$  seemed to indicate that the adsorption of carbonate species was possible. Nevertheless, the experimental behavior of Pb(II) in the  $\text{CO}_2$ - $\text{HCO}_3^-$ - $\text{CO}_3^{2-}$  systems studied, as well as theoretical predictions based on the available stability constants do not indicate that there is any adsorption of  $\text{PbCO}_3(\text{aq})$ . It is not considered likely that Cu(II) would behave differently than Pb(II). Therefore, the discrepancy between the experimental results and the theoretical predictions in the case of Cu(II) in carbonate systems studied is not caused by the adsorption of  $\text{CuCO}_3(\text{aq})$

on  $\text{SiO}_2(\text{s})$ . Since the adsorption of carbonate followed by the adsorption of the metal ion is indistinguishable from the adsorption of  $\text{Me-CO}_3$  complexes formed in the solution, the implication is that carbonate itself does not adsorb either. The same reasoning can be applied to  $\text{HCO}_3^-$ . That is, the possibility for the adsorption of  $\text{HCO}_3^-$  or  $\text{Pb-HCO}_3$  can be eliminated since a discrepancy between the computations and the experimental points was not observed.

This reasoning brings one to the conclusion that the observed disappearance of  $\text{C}^{14}$  from the solution (in the experiments with  $\text{C}^{14}$ - $\text{NaHCO}_3$  described in Chapter 3) is caused by the adsorption of  $\text{H}_2\text{CO}_3(\text{aq})$  or  $\text{CO}_2(\text{aq})$ . Carbonate, therefore, acts only as a ligand competing for the metal together with citrate and  $\text{SiO}_2(\text{s})$ .

In the carbonate-containing systems, an accurate knowledge of the hydrolysis constant(s) is more important for modeling than in the carbonate-free systems. Predictions with the James-Healy Model depend very much on the choice of the second hydrolysis constant for  $\text{Cu}(\text{II})$ : only  $\log^* \beta_2 = -13.7$  results in theoretical adsorption isotherms which are consistent with the experimental points.

Modeling of the experimental systems with the Ion Exchange-Surface Complex Formation Model did not prove to be satisfactory in the case of  $\text{Cu}(\text{II})$  adsorption on  $\alpha$ -quartz because the model considers only the adsorption of free metal ions. If the model would be expanded

by inclusion of reactions between surface hydroxo groups and metal-hydroxo species, better agreement would be obtained between the model and the experimental results.

## Chapter 7

## SUMMARY OF CHAPTERS 2-6

This research has attempted to interpret the adsorption of hydrolyzable cations in terms of their chemical speciation in aqueous systems. Specifically, experimental studies of the adsorption of Pb(II) and Cu(II) indicated that the extent of the adsorption of these metals on  $\alpha$ -quartz is determined by the composition of the aqueous solution. The addition of a non-adsorbing ligand, such as citrate or EDTA, resulted in a competition between chelation and adsorption. It was shown that the results of such competition could be interpreted and predicted in terms of an equilibrium between those species in the solution and those adsorbed on  $\alpha$ -quartz. The main difficulty with these theoretical predictions was the lack of reliable data for the stability constants of metal-ligand complexes. The fact that  $*\beta_2$  for the hydrolysis of Cu(II) is not accurately known was especially a problem in this research. The choice of this constant was made on the basis of potentiometric titrations of  $\text{Cu}^{2+}$ .

The quantitative analysis of the adsorption systems, obtained with two different adsorption models (the James-Healy Model and the Ion Exchange-Surface Complex Formation Model) revealed that, in some cases, both models gave a reasonable fit for the experimental

results; in other cases, calculations obtained with the James-Healy Model were in much better agreement with the experimental results than those obtained with the Ion Exchange-Surface Complex Formation Model. The discrepancy between the experimental results and the theoretical predictions of the Ion Exchange-Surface Complex Formation Model is believed to be its thesis that only the free metal ions are capable of adsorbing. This model may be improved by including the possibility of reactions between surface OH groups and hydrolyzed metal species.

Figure 7.1, a flow chart summary of the present research, shows that experimental systems of gradually increasing complexity can be successfully modeled if reliable stability constants are available. The types of chemical systems that occur in the natural aqueous environments, may thus be modeled. Unfortunately, it would be an immense task to determine the constants for the adsorption of all metals on the many surfaces found in natural waters, together with the constants for the adsorption of ligands and their metal-ligand complexes. The preceding experimental data and the resulting conclusions about the interaction between adsorption and complexation can be, however, combined with some intelligent estimates and used in models of the chemical behavior of trace metals in more complex aquatic environments. In particular, Chapter 8 will examine the chemical behavior

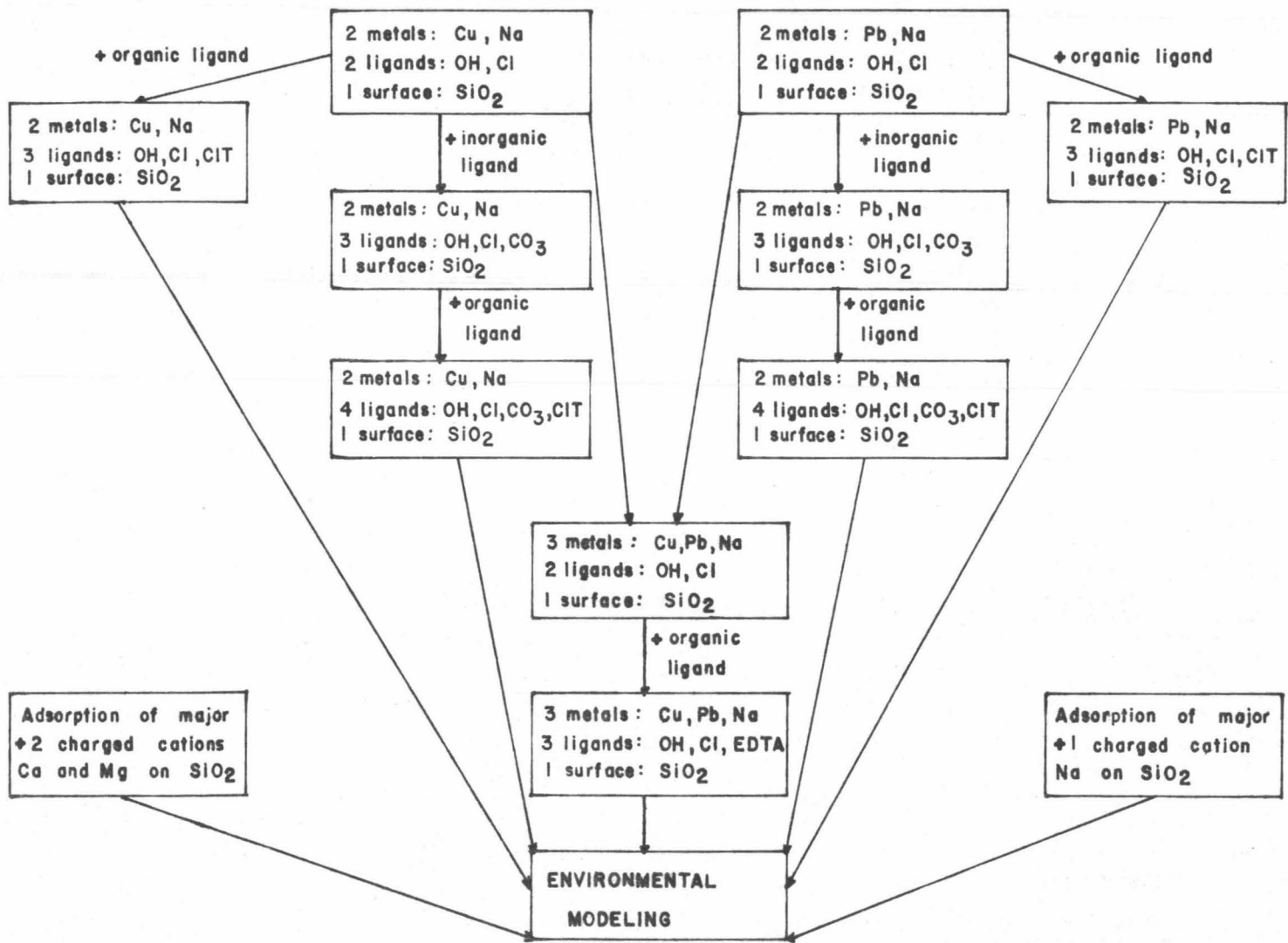


Figure 7.1 Flow chart summary of the present research.

of trace metals in much more complex environments than encountered in the present experimental research, with emphasis on Pb(II) and Cu(II).

## Chapter 8

CHEMICAL MODELS OF FRESH WATERS  
UNDER OXIDIZING CONDITIONS8.1 Introduction

This chapter examines the chemical interactions and the competitions between Pb(II) and Cu(II) and different constituents of natural waters; biological and physical aspects are beyond the scope of this study. The first two sections (8.2 and 8.3) investigate the response of a body of oxic fresh water ( $p_e = 12$ ,  $p_{\text{CO}_2} = 10^{-3.5}$  atm) containing major cations (Ca, Mg, K, Na), 9 trace metals (Pb, Cu, Ni, Zn, Cd, Co, Hg, Mn, Fe), 8 inorganic ligands ( $\text{CO}_3$ ,  $\text{SO}_4$ , Cl, F, Br,  $\text{NH}_3$ ,  $\text{PO}_4$ , OH) and a surface with the adsorption characteristics of  $\text{SiO}_2(\text{s})$ , to changes in pH, types of adsorbing surfaces, surface area, and the presence of organic ligands.

In Section 8.2 inorganic models of oxic fresh waters are presented. Three cases are considered:

- 1) distributions of metals as a function of pH in the presence of constant surface area;
- 2) distributions of metals as a function of different adsorbing surfaces;
- 3) adsorption of metals (at a constant pH) as a function of surface area.

Section 8.3 considers the effect of selected organic ligands (EDTA, citrate, aspartic acid, histidine, cysteine) on the speciation and distribution of metals. These organic models consider:

- 1) distributions of metals as a function of concentration of the above-listed organic ligands at constant pH and constant adsorbing surface area;
- 2) distributions of metals as a function of adsorbing surface area under the conditions of constant pH and equimolar concentrations of the organic ligands;
- 3) adsorption of metals (at a constant pH) as a function of both surface area and organic ligand concentrations.

Section 8.4 summarizes the previous two sections and draws conclusions about the chemical behavior of the above-listed nine trace metals in oxic fresh-water aquatic environments.

## 8.2 Inorganic Models

### 8.2.1 General Considerations

Representative fresh-water concentrations of the above listed metals and inorganic ligands, which are used as the constant inputs for modeling fresh waters, are tabulated in Table 8.1. The compilation does not, however, include chromium, nitrate, and iodine. They were omitted for the following reasons. The speciation and distribution of chromium in river waters is poorly known (Brewer (1975)). It is

Table 8.1

Inputs\* of Metals and Ligands Used for Modeling

Oxic Fresh Waters ( $p\epsilon=12$ ,  $p\text{CO}_2=10^{-3.5}$  atm)

Constituent	-log molar total concentration
Ca	3.4
Mg	3.77
K	4.23
Na	3.56
Fe	5.0
Mn	5.5
Cu	6.0
Cd	6.0
Zn	7.0
Ni	6.5
Hg	9.0
Pb	7.0
Co	7.5
CO <sub>3</sub>	3.0
SO <sub>4</sub>	3.9
Cl	3.65
F	5.5
Br	6.62
NH <sub>3</sub>	5.5
PO <sub>4</sub>	5.0

\* These values are representative of those reported for natural waters by Livingstone (1963) and Bowen (1966).

thought to be critically determined by oxidation-reduction processes in which the equilibrium for the Cr(III)-Cr(VI) redox couple is not attained. Since the model computations predict the equilibrium distribution, chromium would be computed to be present exclusively as Cr(VI) (i. e.,  $\text{CrO}_2^{4-}$ ). Nitrate was not included in model computations because a) it does not form any important aqueous complexes with trace metals, and b) the behavior of nitrate is dominated by its important role in biological cycles. Iodine is present in natural waters both as iodide ( $\text{I}^-$ ) and iodate ( $\text{IO}_3^-$ ). Analytically, it has been determined that iodide forms 20-30% of the total iodine present (Stumm and Brauner (1975)). The biological activity of iodine through photosynthesis, however, often brings about a disequilibrium.

#### 8.2.2 Distributions of Metals as a Function of pH

The pH range investigated in this section is 6.2-8.0 (the same as in the laboratory measurements described in Chapter 6). The surface area of the adsorbent (expressed in  $-\log(\text{hectares}/1)$ ) was estimated to be  $1.55 \text{ m}^2/1$  by assuming 310 mg/1 suspended solids expressed as equivalent  $\text{SiO}_2(\text{s})$ , which has a specific surface area of  $5 \text{ m}^2/\text{g}$ . Adsorption equilibria were computed using the James-Healy Model. The values for the chemical free energies of the adsorption of metals were either determined in the present research, taken from the results of James-Healy (1972c), MacNaughton (1973), or set equal to  $-6.5 \text{ kcal/mole}$ .

According to the model calculations Pb(II) is present mainly as the free metal ion below pH 7.1, and as Pb-CO<sub>3</sub> species above that pH; hydroxo species and adsorption account equally for most of the remaining Pb. The combined total of Pb-OH and Pb-CO<sub>3</sub> never exceeds 15% (Figure 8.1). Complexes with sulfate, chloride, and bromide appear at very small concentrations.

The computed distribution of Cu(II) depends upon the choice of the second hydrolysis constant ( $*\beta_2 \text{Cu(OH)}_2(\text{aq})$ ). A large stability constant ( $\log*\beta_2 = -13.7$ ) results in highly pronounced adsorption throughout most of the examined pH range (Figure 8.2). The hydrolysis products of Cu(II) are present at concentrations Pb-OH  $\approx$  0.25 Pb-ADS. Cu-CO<sub>3</sub> species are present at much lower concentrations, and complexes with halides, sulfate, phosphate, and ammonia are of even smaller significance. A smaller stability constant ( $\log*\beta_2 = -17.3$ ) results in a shift in equilibrium away from the production of hydrolyzed species (Figure 8.3). At the given pH and alkalinity, there will be a tendency towards complexation with carbonate. Precipitation of Cu<sub>2</sub>CO<sub>3</sub>(OH)<sub>2</sub>(s) will occur around pH 7.2, and above pH 7.5 most of the Cu(II) will be removed from solution as Cu<sub>2</sub>CO<sub>3</sub>(OH)<sub>2</sub>(s).

For Co(II), Ni(II), and Zn(II), throughout the pH range 6.2-8.0, the predominant species is the free metal ion (Figures 8.4-8.6, respectively). At a pH less than 7 the second most dominant species

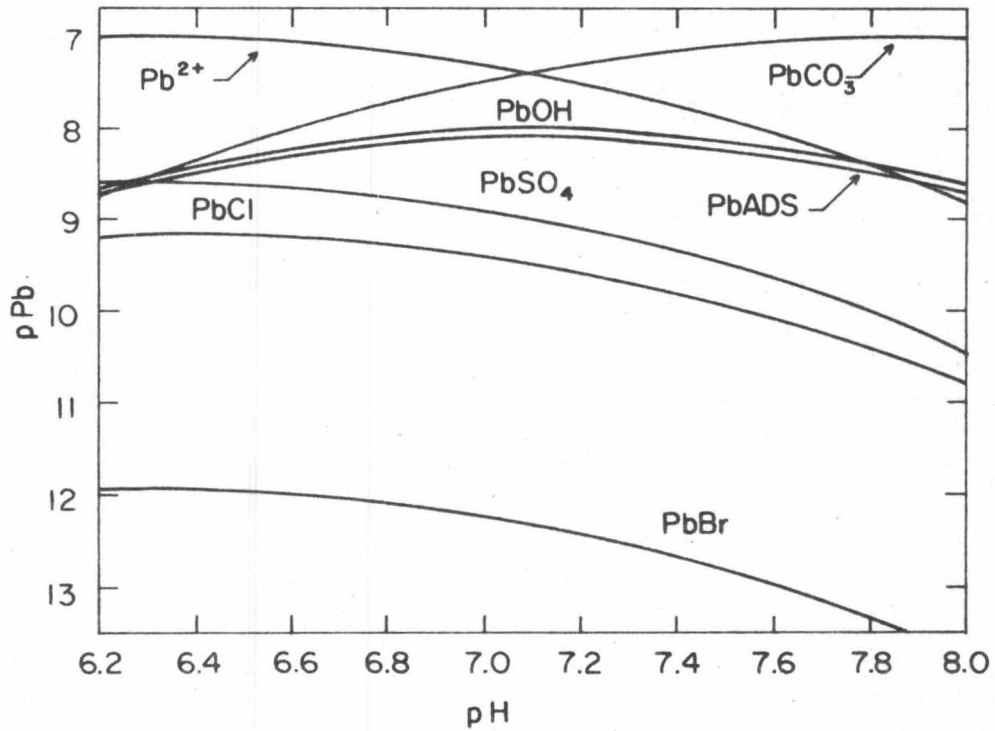


Figure 8.1 Speciation of Pb(II) in natural fresh waters as a function of pH in the presence of 1.55 m<sup>2</sup>/l SiO<sub>2</sub>(s).

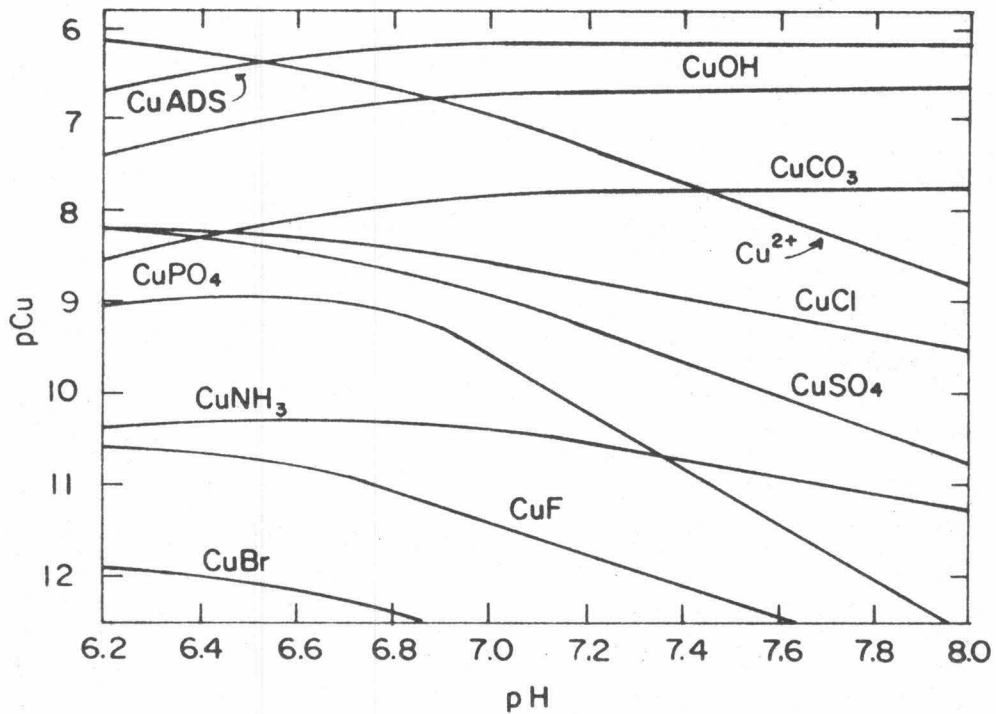


Figure 8.2 Speciation of Cu(II) in natural fresh waters as a function of pH ( $\log^* \beta_2 \text{Cu(OH)}_2(\text{aq}) = -13.7$ ) in the presence of  $1.55 \text{ m}^2/\ell \text{ SiO}_2(\text{s})$ .

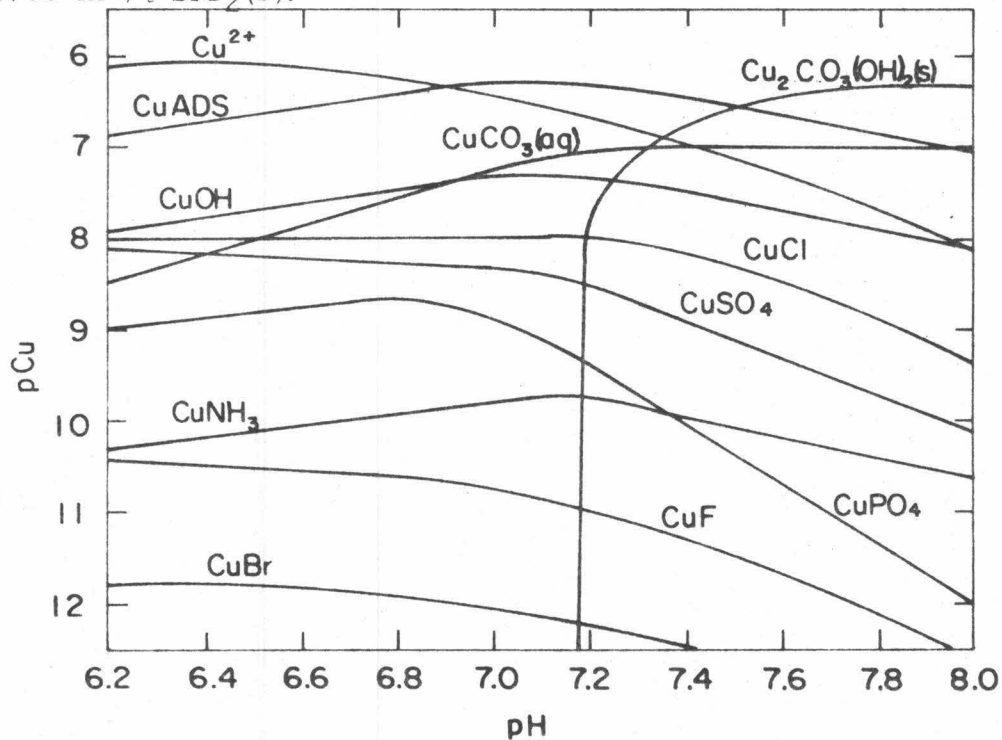


Figure 8.3 Distribution of Cu(II) in natural fresh waters as a function of pH ( $\log^* \beta_2 \text{Cu(OH)}_2(\text{aq}) = -17.3$ ) in the presence of  $1.55 \text{ m}^2/\ell \text{ SiO}_2(\text{s})$ .

for all three metals are their respective metal-sulfate complexes, and at  $\text{pH} > 7$  their carbonate complexes. At  $\text{pH} 8$ , only 2.4%, 6.3%, and 2.6% of Co, Ni, and Zn, respectively, are sorbed on  $\text{SiO}_2(\text{s})$ .

The formation of  $\text{CdCO}_3(\text{s})$  precipitate above  $\text{pH} 6.9$  results in a sudden decrease in the concentration of  $\text{Cd}^{2+}$  (Figure 8.7). Consequently, adsorption and complexation are of much smaller importance.  $\text{Hg}(\text{II})$ , under the model environmental conditions, is present mainly either in chloro complexes (below  $\text{pH} 7.1$ ), or in hydroxo complexes (above  $\text{pH} 7.1$ ); at  $\text{pH} 8.1$  less than 15% of  $\text{Hg}(\text{II})$  is adsorbed on  $\text{SiO}_2(\text{s})$  (Figure 8.8).

### 8.2.3 Distributions of Metals at a Constant pH as a Function of Different Adsorbing Surfaces

The equilibrium distributions of trace metals in oxic fresh waters at  $\text{pH} 7$  in the presence of  $1.55 \text{ m}^2 / \text{l} \text{ SiO}_2(\text{s})$  are shown in Table 8.2. The numbers are the negative logarithms of the molar concentrations, and dashed lines indicate that the species were not considered in the computations. The following results are of particular interest. The free metal ion is the predominant species for the following nine metals:  $\text{Ca}(\text{II})$ ,  $\text{Mg}(\text{II})$ ,  $\text{K}(\text{I})$ ,  $\text{Na}(\text{I})$ ,  $\text{Cd}(\text{II})$ ,  $\text{Zn}(\text{II})$ ,  $\text{Ni}(\text{II})$ ,  $\text{Pb}(\text{II})$ , and  $\text{Co}(\text{II})$ .  $\text{Cu}(\text{II})$  is primarily adsorbed on  $\text{SiO}_2(\text{s})$ , while  $\text{Hg}(\text{II})$  is mainly hydrolyzed. The inorganic ligands are associated mainly with  $\text{Ca}(\text{II})$ ,  $\text{Mg}(\text{II})$ ,  $\text{K}(\text{I})$ , and  $\text{Na}(\text{I})$ . The complexes

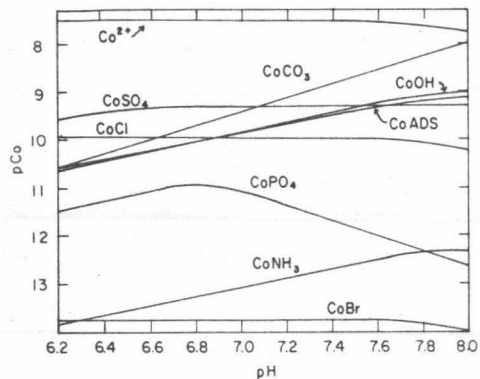


Figure 8.4 Speciation of Co(II) in natural fresh waters as a function of pH in the presence of  $1.55 \text{ m}^2/\text{t SiO}_2(\text{s})$ .

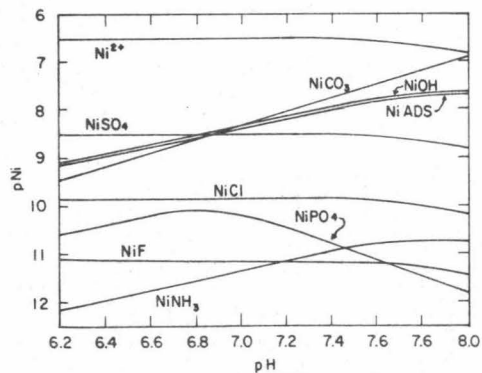


Figure 8.5 Speciation of Ni(II) in natural fresh waters as a function of pH in the presence of  $1.55 \text{ m}^2/\text{t SiO}_2(\text{s})$ .

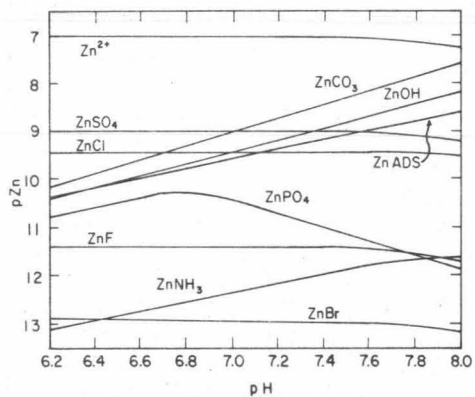


Figure 8.6 Speciation of Zn(II) in natural fresh waters as a function of pH in the presence of  $1.55 \text{ m}^2/\text{t SiO}_2(\text{s})$ .

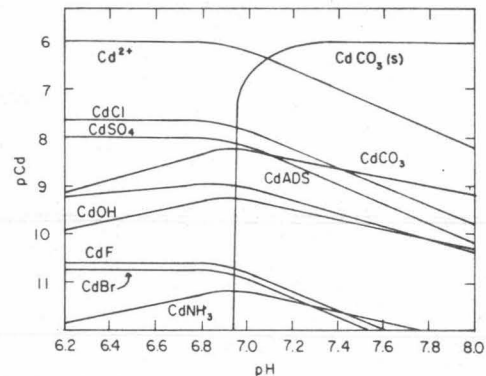


Figure 8.7 Distribution of Cd(II) in natural fresh waters as a function of pH in the presence of  $1.55 \text{ m}^2/\text{t SiO}_2(\text{s})$ .

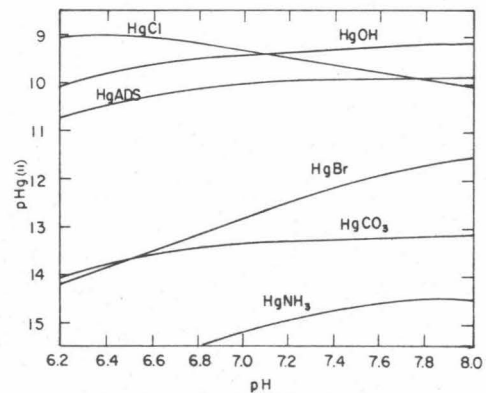


Figure 8.8 Speciation of Hg(II) in natural fresh waters as a function of pH in the presence of  $1.55 \text{ m}^2/\text{t SiO}_2(\text{s})$ .

Table 8.2

Equilibrium Speciation\*\* in an Oxidic River Water of pH 7 in the Presence of  $1.55 \text{ m}^2/\ell \text{ SiO}_2(\text{s})$

	Total conc. ↓	Free conc. →	CO <sub>3</sub>	SO <sub>4</sub>	Cl	F	Br	NH <sub>3</sub>	PO <sub>4</sub>	SiO <sub>2</sub> (s)	OH
			3.0	3.9	3.65	5.5	6.62	5.50	5.0	3.8	-
			7.27	3.92	3.65	5.50	6.62	7.52	10.97	4.01	6.93
Ca†	3.4	3.41	6.41	5.41	-	8.01	-	11.04	7.41	6.05	8.72
Mg	3.77	3.78	6.77	5.67	-	7.67	-	11.20	7.27	6.85	8.09
K	4.23	4.23	-	7.24	-	-	-	-	-	6.90	-
Na	3.56	3.56	9.82	6.97	-	-	-	-	-	6.24	-
Fe(III) <sup>#</sup>	5.0	17.77	-	18.14	20.30	17.92	23.76	-	15.84	8.91	10.28
Fe(II)	-	17.00	-	18.99	19.94	-	-	23.22	13.99	-	18.71
Mn*	5.5	9.91	12.42	11.90	12.65	-	15.82	16.73	12.90	11.84	13.12
Cu	6.0	6.93	7.84	8.92	8.55	11.32	12.64	10.36	9.51	6.17	6.73
Cd‡	6.0	6.16	8.17	8.15	7.79	10.75	10.87	11.18	13.78	9.00	9.27
Zn	7.0	7.01	9.08	9.00	9.44	11.41	12.92	12.34	10.40	9.58	9.48
Ni	6.5	6.52	8.40	8.51	9.86	11.12	12.73	11.35	10.21	8.39	8.33
Hg	9.0	17.06	13.39	18.95	9.30	21.15	12.47	14.59	-	10.06	9.39
Pb	7.0	7.29	7.50	8.88	9.41	-	12.20	-	-	8.14	8.10
Co	7.5	7.52	9.49	9.31	9.96	-	13.73	13.04	11.11	9.87	9.82
H	-	7.00	4.16	8.88	-	9.57	-	5.50	5.29	-	-

\*  $\text{pMnO}_2(\text{s})=5.5$  #  $\text{pFe}(\text{OH})_3(\text{s})=5.0$  †  $\text{pCa}_5(\text{PO}_4)_3\text{OH}(\text{s})=5.8$  ‡  $\text{pCdCO}_3(\text{s})=6.56$

\*\*Concentrations are expressed as negative logarithms.

with other metals are less significant. Approximately 61.6% of the  $\text{SiO}_2(\text{s})$  surface remains free; the rest is associated with  $\text{Ca}(\text{II})$  (14.5%),  $\text{Cu}(\text{II})$  (9.8%),  $\text{Na}(\text{I})$  (9.4%),  $\text{K}(\text{I})$  (2.5%), and  $\text{Mg}(\text{II})$  (2.0%). Four solid phases are formed:  $\text{MnO}_2(\text{s})$ ,  $\text{Fe}(\text{OH})_3(\text{s})$ ,  $\text{Ca}_5(\text{PO}_4)_3\text{OH}(\text{s})$ , and  $\text{CdCO}_3(\text{s})$ . It has been proposed by Jenne (1968) that hydrous oxides of Mn and Fe provide the principal control on the fixation of metals in soils and fresh-water sediments. In order to include iron hydroxide and manganese dioxide as adsorbing surfaces in modeling of oxic fresh waters, one can use Table 8.2 to generate a more realistic result by converting the units of the precipitated  $\text{Fe}(\text{OH})_3(\text{s})$  and  $\text{MnO}_2(\text{s})$  (moles/l) into surface area/l. The respective specific surface areas were found to be very high, ranging from 230 to  $320 \text{ m}^2/\text{g}$  for  $\text{Fe}(\text{OH})_3(\text{s})$  (Jenne (1968); MacNaughton (1973)), and from 260 to  $300 \text{ m}^2/\text{g}$  for  $\text{MnO}_2(\text{s})$  (Morgan and Stumm (1964); Murray (1973)). The conversion of moles/l of the precipitated  $\text{Fe}(\text{OH})_3(\text{s})$  and  $\text{MnO}_2(\text{s})$  into surface area/l results in  $S_{\text{Fe}(\text{OH})_3(\text{s})} = 0.3 \text{ m}^2/\text{l}$  (assuming an average of  $275 \text{ m}^2/\text{g}$ ) and  $S_{\text{MnO}_2(\text{s})} = 0.08 \text{ m}^2/\text{l}$  (assuming an average of  $280 \text{ m}^2/\text{g}$ ). The values for the chemical free energies for adsorption of metal ions on  $\text{MnO}_2(\text{s})$  are:  $\Delta G_{\text{chem, Cu}}^{\circ} = -5.17 \text{ kcal/mole}$ ,  $\Delta G_{\text{chem, Co}}^{\circ} = -5.5 \text{ kcal/mole}$ ,  $\Delta G_{\text{chem, Mn}}^{\circ} = -5.48 \text{ kcal/mole}$ ,  $\Delta G_{\text{chem, Ni}}^{\circ} = -4.25 \text{ kcal/mole}$ , and  $\Delta G_{\text{chem, Zn}}^{\circ} = -4.85 \text{ kcal/mole}$  (Murray (1973)). The chemical free energies for the other metals were selected to be

-4.85 kcal/mole. Since it was shown in Chapter 2 that the  $\text{Fe}(\text{OH})_3(\text{s})$ -adsorption characteristics should resemble those of  $\text{SiO}_2(\text{s})$ , the adsorption free energies of all the trace metals on  $\text{Fe}(\text{OH})_3(\text{s})$  were assumed to be -6.5 kcal/mole. The resulting computations are shown in Table 8.3.

Comparison between Tables 8.2 and 8.3 shows that the addition of  $\text{MnO}_2(\text{s})$  and  $\text{Fe}(\text{OH})_3(\text{s})$  did not cause any changes in the amounts of metals either sorbed on  $\text{SiO}_2(\text{s})$  or complexed and precipitated with the inorganic ligands, since both  $\text{MnO}_2(\text{s})$  and  $\text{Fe}(\text{OH})_3(\text{s})$  are present in small quantities in the model calculations. Thus, in order to make some conclusions about adsorbability of metals on  $\text{SiO}_2(\text{s})$ ,  $\text{Fe}(\text{OH})_3(\text{s})$ , and  $\text{MnO}_2(\text{s})$ , it is necessary to compare these surfaces on the basis of moles of metals adsorbed per unit surface area. Table 8.4, which was derived from Tables 8.2 and 8.3, shows that both  $\text{Fe}(\text{OH})_3(\text{s})$  and  $\text{MnO}_2(\text{s})$  adsorbed significant amounts of trace metals as compared to  $\text{SiO}_2(\text{s})$ . For some metals,  $\text{MnO}_2(\text{s})$  is a more powerful adsorbent than  $\text{SiO}_2(\text{s})$  (e.g., Co, Ni, Zn, Cd, Mn); similarly Hg adsorbs more strongly on  $\text{Fe}(\text{OH})_3(\text{s})$  than on  $\text{SiO}_2(\text{s})$ . Percentage-wise, the fraction of the total metal adsorbed by  $\text{Fe}(\text{OH})_3(\text{s})$  and  $\text{MnO}_2(\text{s})$  is not great since, under the conditions assumed for these calculations, both of these surfaces are present in small quantities compared to  $\text{SiO}_2(\text{s})$  (see the column under " $\% \text{Me}_T$  adsorbed" in Table 8.4). (In some

\*\*  
Table 8.3  
Equilibrium Speciation of Metals in an Oxidizing Fresh Water in the Presence  
of  $1.55\text{m}^2/\text{l}$   $\text{SiO}_2(\text{s})$ ,  $0.3\text{m}^2/\text{l}$ ,  $\text{Fe}(\text{OH})_3(\text{s})$ , and  $0.08\text{m}^2/\text{l}$   $\text{MnO}_2(\text{s})$

	Total conc. ↓	Free conc. →	$\text{CO}_3$	$\text{SO}_4$	Cl	F	Br	$\text{NH}_3$	$\text{PO}_4$	$\text{SiO}_2(\text{s})$	$\text{Fe}(\text{OH})_3(\text{s})$	$\text{MnO}_2(\text{s})$	OH
			3.0	3.90	3.65	5.50	6.62	5.50	5.0	3.80	4.52	5.1	-
			7.27	3.92	3.65	5.50	6.62	7.52	10.97	4.01	4.67	8.56	6.93
Ca <sup>+</sup>	3.4	3.41	6.41	5.41	-	8.01	-	11.04	7.41	6.05	9.09	6.70	8.72
Mg	3.77	3.78	6.77	5.67	-	7.67	-	11.20	7.27	6.85	9.59	6.92	8.09
K	4.23	4.23	-	7.24	-	-	-	-	-	6.90	7.28	11.70	-
Na	3.56	3.56	9.82	6.97	-	-	-	-	-	6.24	6.59	10.90	-
Fe(III) <sup>#</sup>	5.0	17.77	-	18.14	20.30	17.92	23.76	-	15.84	8.91	13.13	13.94	10.28
Fe(II)	-	17.00	-	18.99	19.94	-	-	23.22	13.99	-	-	-	18.71
Mn*	5.5	9.91	12.42	11.90	12.65	-	15.82	16.73	12.90	11.84	15.55	11.73	13.12
Cu	6.0	6.93	7.84	8.92	8.56	11.32	12.64	10.36	9.51	6.18	8.00	8.94	6.73
Cd <sup>†</sup>	6.0	6.16	8.18	8.15	7.79	10.75	10.87	11.18	13.78	9.00	11.71	8.49	9.27
Zn	7.0	7.01	9.09	9.01	9.44	11.41	12.92	12.34	10.41	9.58	11.25	9.24	9.48
Ni	6.5	6.52	8.40	8.52	9.86	11.12	12.73	11.35	10.22	8.39	11.29	9.15	8.33
Hg	9.0	17.07	13.40	18.96	9.31	21.16	12.48	14.60	-	10.07	10.72	15.83	9.40
Pb	7.0	7.29	7.50	8.88	9.41	-	12.20	-	-	8.14	11.05	9.59	8.10
Co	7.5	7.52	9.50	9.32	9.96	-	13.73	13.05	11.12	9.88	12.60	9.31	9.83
H	-	7.00	4.16	8.88	-	9.57	-	5.50	5.28	-	-	-	-

\* $\text{pMnO}_2(\text{s})=5.5$  #  $\text{pFe}(\text{OH})_3(\text{s})=5.0$  †  $\text{pCa}_5(\text{PO}_4)_3\text{OH}(\text{s})=5.8$  ‡  $\text{pCdCO}_3(\text{s})=6.56$

\*\*Concentrations are expressed as negative logarithms.

Table 8.4

Compilation from Tables 8.2 and 8.3

Me	Adsorption in the presence of three surfaces								Adsorption in the presence of only SiO <sub>2</sub>	
	SiO <sub>2</sub>		Fe(OH) <sub>3</sub>		MnO <sub>2</sub>		∪ surfaces		moles/m <sup>2</sup>	%Me <sub>T</sub>
	moles/m <sup>2</sup>	%Me <sub>T</sub>	moles/m <sup>2</sup>	%Me <sub>T</sub>	moles/m <sup>2</sup>	%Me <sub>T</sub>	moles/m <sup>2</sup>	%Me <sub>T</sub>	moles/m <sup>2</sup>	%Me <sub>T</sub>
Fe(III)	7x10 <sup>-10</sup>	0.01	2.47x10 <sup>-13</sup>	<<0.001	1.4x10 <sup>-13</sup>	<<0.001	3.63x10 <sup>-10</sup>	0.01	7x10 <sup>-10</sup>	0.01
Mn	9.32x10 <sup>-13</sup>	<<0.001	9.4x10 <sup>-16</sup>	<<0.001	2.32x10 <sup>-8</sup>	<<0.001	1.25x10 <sup>-11</sup>	<<0.001	9.32x10 <sup>-13</sup>	<<0.001
Cu	4.26x10 <sup>-7</sup>	66.1	3.33x10 <sup>-8</sup>	1.0	1.43x10 <sup>-8</sup>	0.11	1.58x10 <sup>-7</sup>	67.21	4.36x10 <sup>-7</sup>	67.6
Cd	6x10 <sup>-10</sup>	0.1	6.5x10 <sup>-12</sup>	<<0.001	4x10 <sup>-8</sup>	0.32	2.1x10 <sup>-8</sup>	0.42	6x10 <sup>-7</sup>	0.1
Zn	1x10 <sup>-10</sup>	0.26	1.87x10 <sup>-11</sup>	<<0.001	7.1x10 <sup>-9</sup>	0.58	3.74x10 <sup>-9</sup>	0.84	1x10 <sup>-10</sup>	0.26
Ni	2.6x10 <sup>-9</sup>	1.3	1.71x10 <sup>-11</sup>	<<0.001	8.8x10 <sup>-9</sup>	0.22	5.9x10 <sup>-9</sup>	1.52	2.6x10 <sup>-9</sup>	1.3
Hg	5.49x10 <sup>-11</sup>	8.51	6.35x10 <sup>-11</sup>	1.9	1.48x10 <sup>-16</sup>	<<0.001	6.1x10 <sup>-11</sup>	9.41	5.6x10 <sup>-11</sup>	8.7
Pb	4.6x10 <sup>-9</sup>	7.24	2.97x10 <sup>-11</sup>	<<0.001	3.2x10 <sup>-9</sup>	0.26	4.05x10 <sup>-9</sup>	7.5	4.6x10 <sup>-9</sup>	7.2
Co	8.5x10 <sup>-11</sup>	0.42	8.37x10 <sup>-13</sup>	<<0.001	4x10 <sup>-10</sup>	1.55	2.51x10 <sup>-10</sup>	1.97	8.7x10 <sup>-11</sup>	0.4

natural waters however,  $\text{Fe}(\text{OH})_3(\text{s})$  and  $\text{MnO}_2(\text{s})$  are present at levels comparable to and higher than that of  $\text{SiO}_2(\text{s})$ . In such cases, it is clear that their presence cannot be neglected). Consequently, for the present calculations the amounts of trace metals adsorbed by all three surfaces can be approximated by the presence of  $\text{SiO}_2(\text{s})$  only (see the first and third column from the right, Table 8.4). Therefore, further computations will be performed with  $\text{SiO}_2(\text{s})$  as the only adsorbing surface.

At the present time, the REDEQL2 program cannot handle the adsorption of metals on surfaces with constant surface charge such as clays. Therefore, the adsorption of metals on clays is not considered in these models of fresh waters. Nevertheless, examining the behavior of different systems under conditions of increasing adsorbing surface area will, in a way, compensate for the absence of clays and other adsorbing surfaces.

#### 8.2.4 Adsorption of Metals as a Function of Surface Area

The distribution of trace metals between suspended particles and solution depends upon the availability of surface area. Figure 8.9 shows that an increase in surface area results in increased adsorption of all the metals. The most easily adsorbed metal is  $\text{Cu}(\text{II})$ , followed by  $\text{Pb}(\text{II})$  and  $\text{Hg}(\text{II})$ . At the very low surface areas of  $\text{pS}=4.1$ , approximately 50% of the total  $\text{Cu}(\text{II})$  is adsorbed. In order to have the

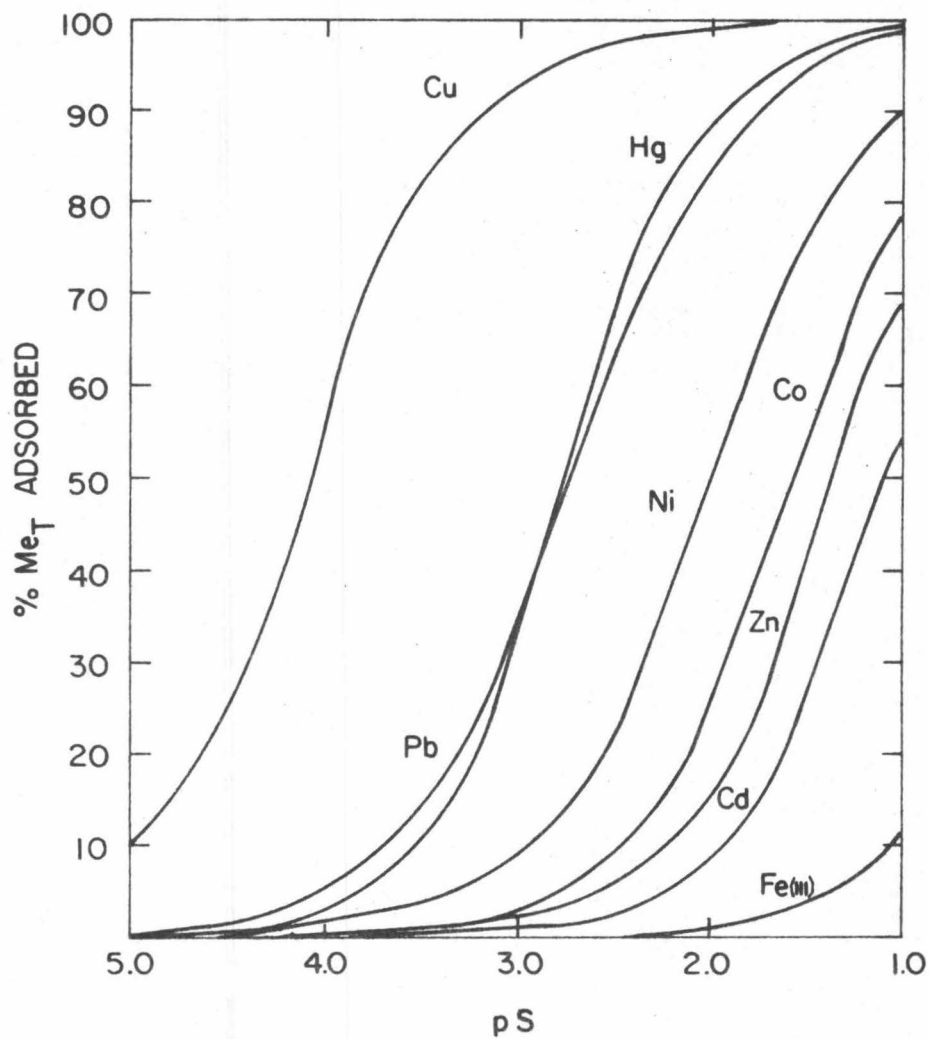


Figure 8.9 Adsorption of trace metals in oxidizing fresh waters ( $\text{pH}=7$ ,  $\text{p}\epsilon=12$ ,  $\text{pCO}_2=10^{-3.5}$  atm) as a function of surface area of  $\text{SiO}_2(\text{s})$  in  $\text{ha}/\ell$ .

same amount of  $Pb_T$  adsorbed, it is necessary to have 20 times as much surface area present (i. e.,  $pS=2.75$ ). Fifty percent of the total Ni(II) Co(II), Zn(II), and Cd(II) are sorbed at the even higher surface areas of  $pS=2.0$ ,  $pS=1.5$ ,  $pS=1.4$ , and  $pS=1.1$ , respectively. With the very high surface areas of  $1000 \text{ m}^2/\text{l}$ , 10% of the precipitated iron hydroxide dissolves and the released Fe(III) is adsorbed by  $SiO_2(s)$ .

### 8.3 Organic Models

#### 8.3.1 General Considerations

Organic matter in natural waters is a very influential factor, affecting the speciation and distribution of trace metals and thus also the underlying sediments and suspended particles. The importance of organic compounds in natural waters will be demonstrated by choosing a few representative organic ligands and examining the composition of the system when these organics are present at a variety of concentrations. The organic matter in the model calculations is represented either as a strong complexing agent (e. g., EDTA), or as an agent of weaker complexing capability (e. g., citrate), or as amino acids (histidine (HIS), aspartic acid (ASP), and cysteine (CYST)\*). The

---

\* Under oxic conditions, as a free ligand, cysteine is not stable with respect to oxidation to cystine. For the purposes of these computations however, cysteine has been assumed to be present as a metastable constituent.

range of concentration of each kind of organic used in these calculations is  $10^{-9}$  to  $10^{-5}$  moles/l.

### 8.3.2 EDTA

The presence of a very strong complexing agent, such as EDTA, will markedly alter the speciation of most of the trace metals at low concentrations of this ligand (Figure 8.10). For example, the speciation of Cu(II) is affected when  $\text{EDTA}_T > 0.01 \text{ Cu}_T$ . The presence of EDTA causes a decrease in the percentage of free copper ion, Cu-ADS, Cu-CO<sub>3</sub>, and Cu-OH species. When  $\text{EDTA}_T = 3\text{Cu}_T$ , Cu(II) is completely complexed by EDTA. Below  $\text{EDTA}_T = \text{Pb}_T$ , Pb(II) is present mainly as  $\text{Pb}^{2+}$ , Pb-CO<sub>3</sub>, Pb-OH, and Pb-ADS. Above  $\text{EDTA}_T = 5\text{Pb}_T$ , the Pb-EDTA complexes are the predominant Pb(II) species. Complete complexation of Pb(II) by EDTA takes place when  $\text{EDTA}_T = 30\text{Pb}_T$ . The presence of EDTA will begin to alter the speciation of other metals at the following concentrations of this ligand:  $\text{EDTA}_T > 0.01 \text{ Ni}_T$ ,  $\text{EDTA}_T > 0.1 \text{ Fe}_T$ ,  $\text{EDTA}_T > \text{Cd}_T$ ,  $\text{EDTA}_T > 3\text{Zn}_T$ ,  $\text{EDTA}_T > 20\text{Co}_T$ . Hg(II) is only partially complexed by EDTA at very high EDTA concentrations ( $\text{EDTA}_T > 1000 \text{ Hg}_T$ ). Mn remains precipitated as  $\text{MnO}_2(\text{s})$ .

### 8.3.3 Citrate

According to this model citrate mostly affects the speciation of Cu(II), and the effect becomes most evident at  $\text{CIT}_T > 0.01 \text{ Cu}_T$

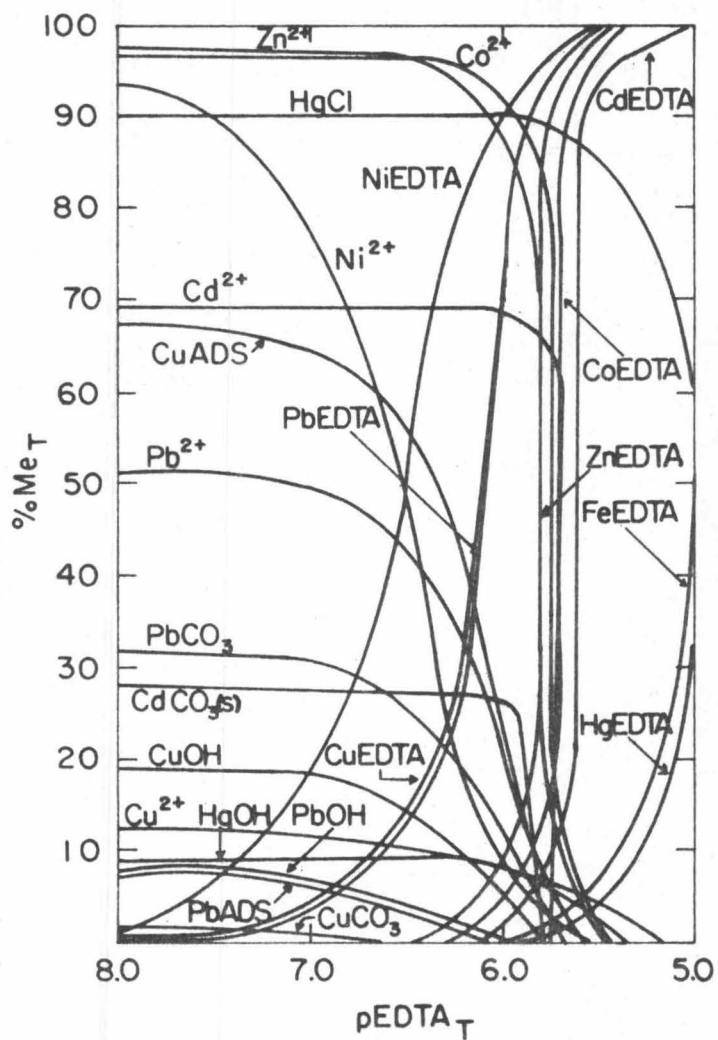


Figure 8.10 Distribution of metals in natural waters at pH 7 as a function of EDTA.  $S=1.55 \text{ m}^2/\ell \text{ SiO}_2(\text{s})$ .

(Figure 8.11). Under these conditions there is a competition between adsorption and complexation. At  $CIT_T \approx 0.4Cu_T$ , Cu-ADS is 75% of that when  $CIT_T = 0$ . When  $CIT_T = 3Cu_T$ , adsorption is completely suppressed and all the Cu(II) remains in solution as citrate complexes. Appreciable complexation of Pb(II) by citrate appears at higher concentrations of citrate, i. e.,  $CIT_T > 10Pb_T$ . This complexation results in a decrease in the concentration of Pb-CO<sub>3</sub> and Pb-OH species. At  $CIT_T = 100Pb_T$  only 30% Pb<sub>T</sub> is in the form of Pb-CIT complexes. The speciation of Fe(III), Ni(II), and Cd(II) is affected by the presence of citrate at concentrations of  $CIT_T > 0.1Fe_T$ ,  $CIT_T > Ni_T$ , and  $CIT_T > 10Cd_T$ , respectively. Co-CIT species are unimportant; the stability constants for Hg-CIT complexes have not been determined.

#### 8.3.4 Histidine

The presence of histidine affects Cu(II) at concentrations of  $HIS_T > 0.01Cu_T$  (Figure 8.12). At  $HIS_T \approx 3Cu_T$ , adsorption of Cu(II) on SiO<sub>2</sub> is reduced by approximately 30%. The speciation of Pb(II) is affected by histidine only at concentrations of  $HIS_T > 10Pb_T$ , the major effect being a decrease in the concentrations of Pb<sup>2+</sup> and Pb-CO<sub>3</sub> species. The amount of Pb(II) adsorbed on SiO<sub>2</sub>(s) essentially remains the same. The effect of histidine on the speciation of Ni(II), Cd(II), Co(II), and Zn(II) becomes evident at concentrations of  $HIS_T > 0.1Ni_T$ ,

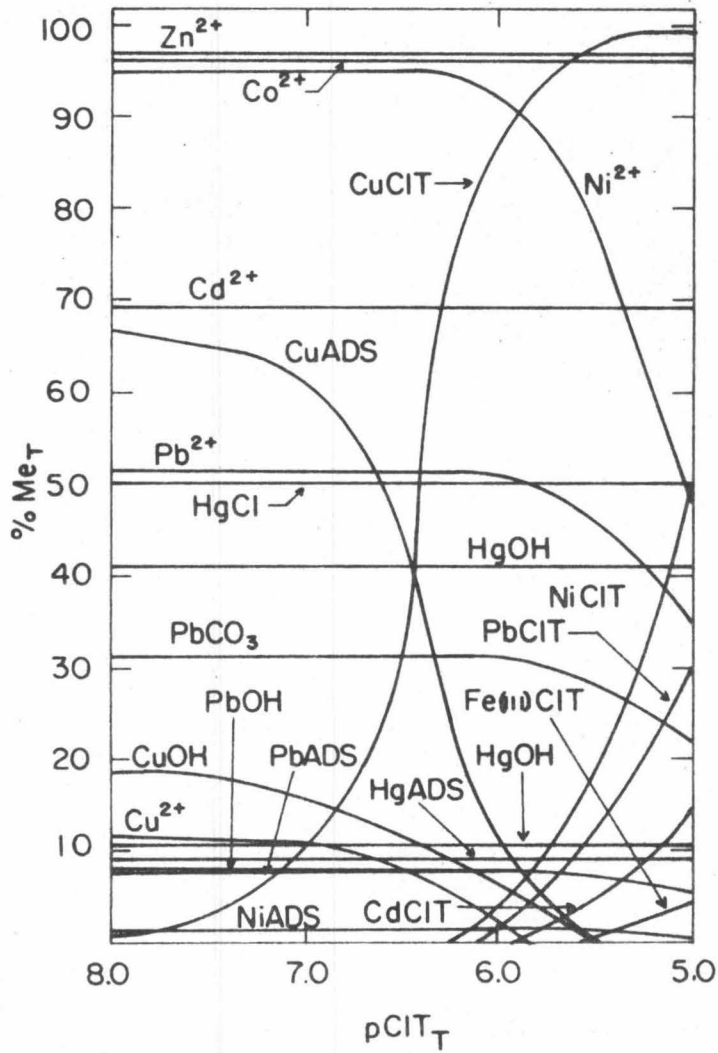


Figure 8.11 Distribution of metals in natural fresh waters at pH 7 as a function of  $pCIT$ .  $S=1.55 \text{ m}^2/\text{l SiO}_2(\text{s})$ .

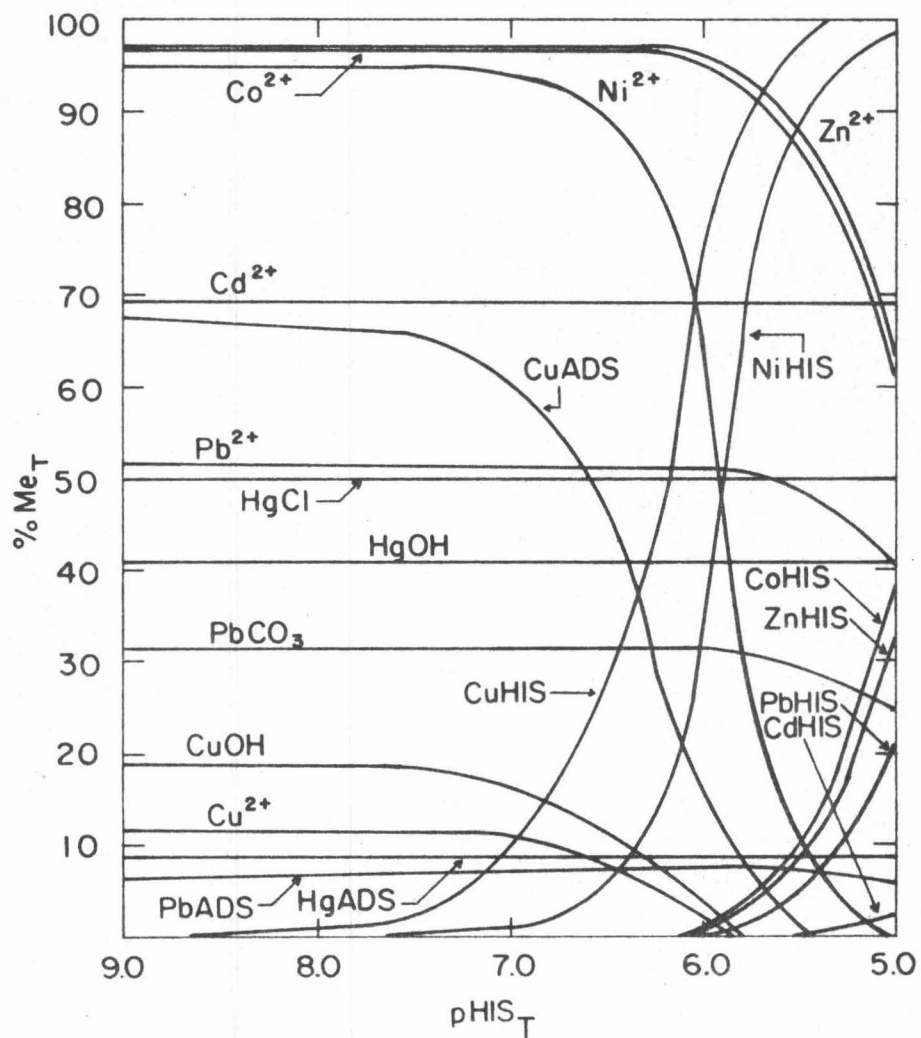


Figure 8.12 Distribution of metals in natural fresh waters in the presence of different amounts of histidine.  $pH = 7$ ,  $S = 1.55 \text{ m}^2/\text{l SiO}_2(\text{s})$ .

$\text{HIS}_T > \text{Cd}_T$ ,  $\text{HIS}_T > 30\text{Co}_T$ , and  $\text{HIS}_T > 30\text{Zn}_T$ , respectively. Hg(II) speciation is unaffected.

### 8.3.5 Aspartic Acid

The presence of aspartate (Figure 8.13) alters the speciation of Cu(II) and Ni(II) above  $\text{pASP}_T = 7.0$  (i. e.,  $\text{ASP}_T > 10\text{Cu}_T$ ;  $\text{ASP}_T > 30\text{Ni}_T$ , respectively), the main effect being reduction in the extent of the adsorption of Cu(II) on  $\text{SiO}_2(\text{s})$ , and a decrease in the free Ni(II) ion concentrations. The effect of aspartate on Zn(II) and Co(II) speciation is very small; at very high concentrations of this ligand (i. e.,  $\text{ASP}_T = 100\text{Zn}_T = 300\text{Co}_T$ ) only 2-3% of Zn(II) and Co(II) is complexed. For other metals, either the Me-ASP complexes are insignificant relative to the concentrations of other species, as in the case for Fe, Mn, and Cd, or the stability constants for Me-ASP complexes have not been determined (Pb, Hg).

### 8.3.6 Cysteine

Cysteine has an extremely large affinity for Hg(II); if mercury(II) is present in the total concentration of  $10^{-9}$  moles/l, cysteine present at a concentration of  $\text{CYST}_T = 3\text{Hg}_T$  complexes all the mercury(II) (Fig. 8.14). Complexation with Pb(II) affects the speciation of Pb(II) at  $\text{CYST}_T > 0.03\text{Pb}_T$  by reducing the concentration of the four species  $\text{Pb}^{2+}$ ,  $\text{Pb-CO}_3$ ,  $\text{Pb-OH}$ , and  $\text{Pb-ADS}$ . At  $\text{CYST}_T > 30\text{Pb}_T$  all the lead(II) will

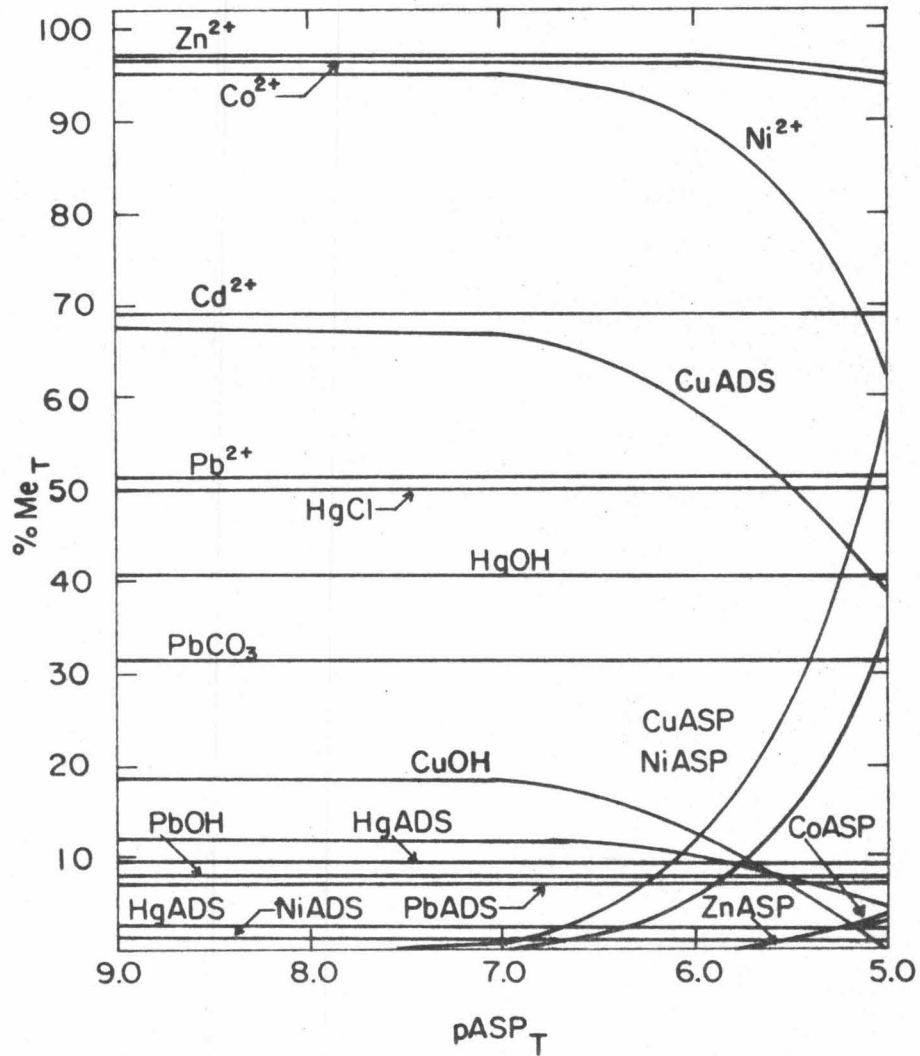


Figure 8.13 Distribution of metals in natural fresh waters in the presence of different amounts of aspartic acid.  $\text{pH} = 7$ ,  $S = 1.55 \text{ m}^2/\text{l SiO}_2(\text{s})$ .

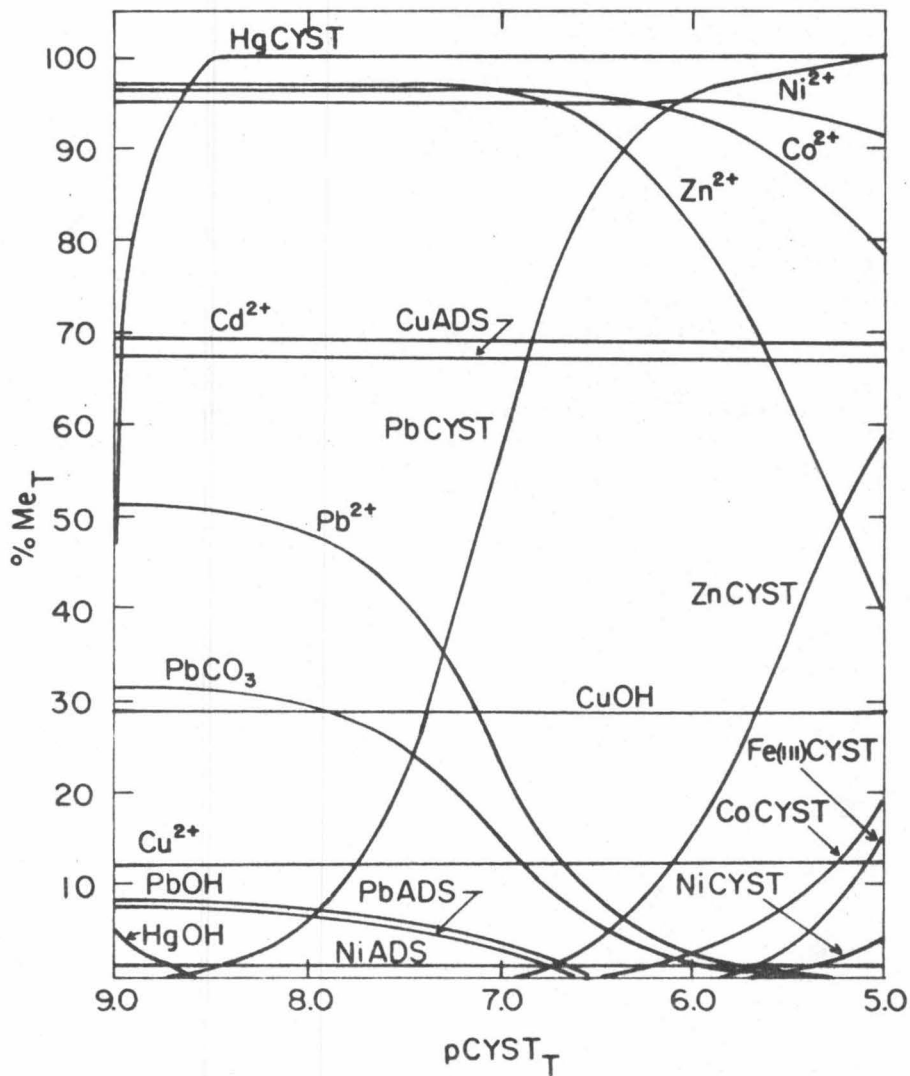


Figure 8.14 Distribution of metals in fresh waters in the presence of different amounts of cysteine.  
 $pH = 7$ ,  $S = 1.55 \text{ m}^2 / \text{l SiO}_2(\text{s})$ .

be in the form of Pb-CYST complexes. Constants for the complexation of Cu(II) with cysteine are not available and, hence, the computed speciation of Cu(II) in the presence of cysteine remains unchanged. Complexation of cysteine with Fe(III), Zn(II), Co(II), and Ni(II) is important at the following concentrations of cysteine:  $CYST_T > 0.1Fe_T$ ,  $CYST_T > Zn_T$ ,  $CYST_T > 10Co_T$ , and  $CYST_T > Ni_T$ , respectively.

### 8.3.7 Distribution of Metals in the Presence of Organic Ligands as a Function of Surface Area

The next step in the modeling of the natural waters is to examine the speciation of trace metals as a function of surface area in the presence of fixed amounts of organic ligands. All of the previously mentioned organic ligands will be considered to be present at equimolar concentrations, e. g. ,  $pEDTA_T = pCIT_T = pHIS_T = pASP_T = pCYST_T = 6.0$ . The computations show that Hg(II) and Ni(II) are complexed by CYST and EDTA, respectively (Figure 8.15). For the other trace metals there are two distinct zones: the region of low surface area extending to the left of the pS-3-line, and the region of higher surface area to the right of pS=3. At low surface areas concentration changes in the surface area do not cause any large changes in the speciation of trace metals. Cu(II) is present mainly in the form of histidine, EDTA, and citrate complexes. The predominant species of Pb(II) in this region is Pb-EDTA, followed by Pb-CYST. Cd(II) and Co(II) are

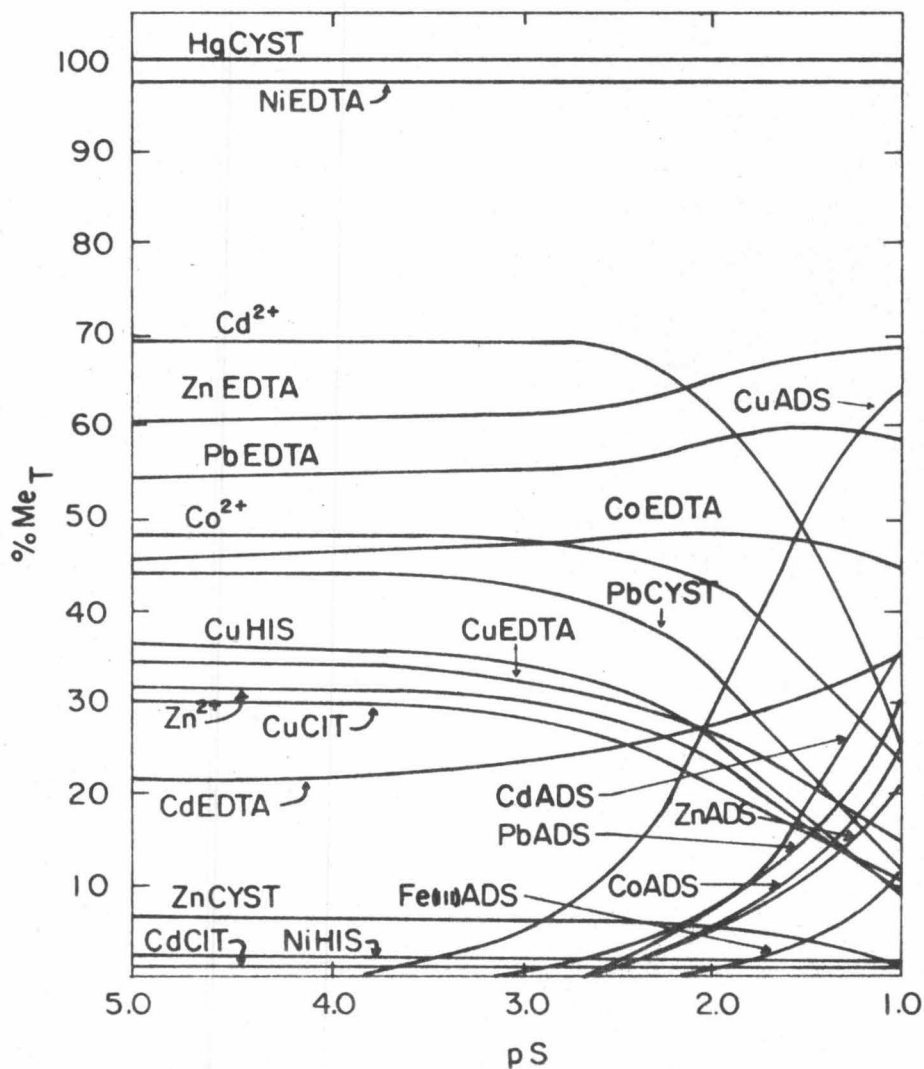


Figure 8.15 Speciation of trace metals in natural fresh waters in the presence of organic ligands ( $pCIT=pEDTA=pCYST=pHIS=pASP=6.0$ ) as a function of surface area of  $SiO_2(s)$  in  $ha/l$ .

present predominantly in the form of the free aquo metal ions and Me-EDTA complexes. Zn(II) occurs as EDTA and cysteine complexes, and as a free metal ion. Above pS=3-line there is a marked increase in the adsorption of Cu(II), with similar increases in the adsorption of Cd(II), Pb(II), Co(II), Zn(II), and Fe(III), occurring at higher surface areas.

#### 8.3.8 Adsorption of Metals at Constant pH as a Function of Surface Area and Citrate Concentrations

In the preceding analyses of different models, it was shown that the distribution of metal ions is affected markedly by both surface area and organic ligand concentrations. In order to examine the changes that occur in the distribution of trace metals when changing both the surface area and the organic ligand concentration, some additional calculations were made: the equilibrium distributions of metals in the presence of different surface area concentrations were computed as a function of concentration of citrate. The results for each metal are graphed separately. Moving from upper left to lower right on any of the forthcoming figures represents the simultaneous increase of both surface area and citrate concentration.

Cu(II) speciation is a strong function of citrate concentration (Figure 8.16). At a pS=4 ( $S=10^{-2} \text{ m}^2/\text{l}$ ) and  $\text{CIT}_T=10\text{Cu}_T$ , there is no Cu(II) adsorption. Increasing the surface area (with constant  $\text{CIT}_T$ )

past this point causes the onset of adsorption. With surface area concentrations of  $100 \text{ m}^2/\text{l}$  and  $1000 \text{ m}^2/\text{l}$ , 10% and 40%  $\text{Cu}_T$ , respectively, are adsorbed.

In the case of Pb(II) (Figure 8.17), when pS is in the range 4-1 the presence of citrate at concentrations of  $\text{CIT}_T = 100\text{Pb}_T$  results in a decrease in the adsorption of Pb(II) on  $\text{SiO}_2(\text{s})$ . This decrease never exceeds 10%.

At  $\text{CIT}_T = 30\text{Ni}_T$ , the adsorption of Ni(II) on  $\text{SiO}_2(\text{s})$  is lowered by ca. 2% at pS=4, and by ca. 13% at pS=1.0 (Figure 8.18). For Cd(II) (Figure 8.19) and Fe(III) (Figure 8.20) both adsorption and complexation influence the precipitation of  $\text{CdCO}_3(\text{s})$  and  $\text{Fe}(\text{OH})_3(\text{s})$ , respectively. Citrate present at the level of  $\text{CIT}_T = 10\text{Cd}_T$  reduces the precipitation of  $\text{CdCO}_3(\text{s})$  by up to 13% in the range of surface area concentration pS=5.0 to pS=1.5. The presence of high surface area concentrations ( $S > 30 \text{ m}^2/\text{l}$ ) results in a complete dissolution of the  $\text{CdCO}_3(\text{s})$ , with the released Cd(II) then being adsorbed. If citrate is also present ( $\text{CIT}_T = 10\text{Cd}_T$ ) at  $S > 100 \text{ m}^2/\text{l}$ , the extent of adsorption and the concentration of the free metal ion  $\text{Cd}^{2+}$  are both slightly reduced. When citrate is present at concentration equal to that of  $\text{Fe}_T$ , there is no effect on the adsorption of Fe(III) if the available surface area is high. At low surface area the presence of the same amount of citrate reduces the extent of precipitation of  $\text{Fe}(\text{OH})_3(\text{s})$  by 3.5%.

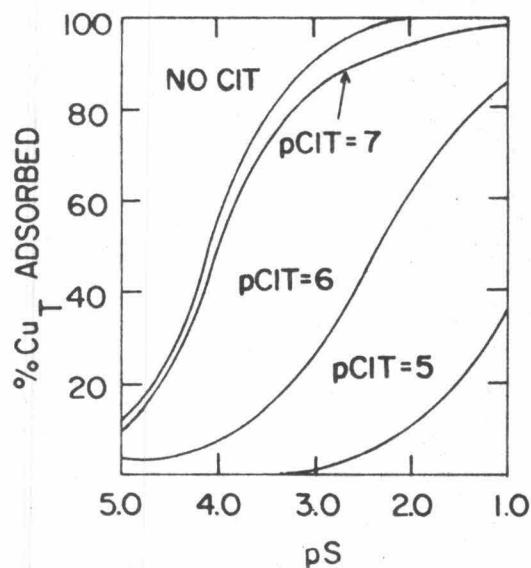


Fig. 8.16 Adsorption of Cu on  $\text{SiO}_2(\text{s})$  in oxidizing fresh waters of pH 7 as a function of surface area ( $\text{ha}/\ell$ ) and concentration of citrate.

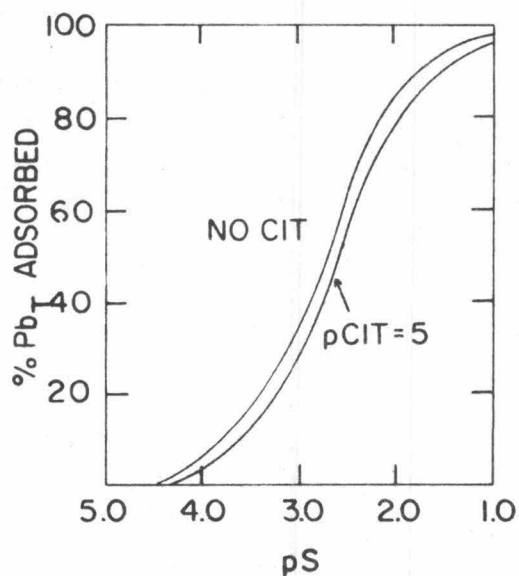


Fig. 8.17 Adsorption of Pb on  $\text{SiO}_2(\text{s})$  in oxidizing fresh waters of pH 7 as a function of surface area ( $\text{ha}/\ell$ ) in the presence and absence of citrate.

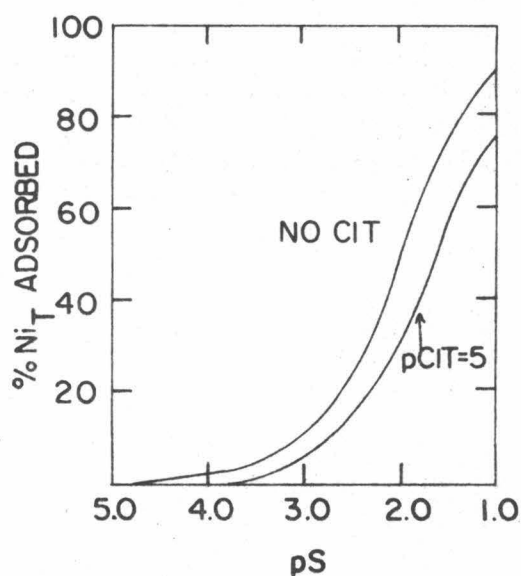


Fig. 8.18 Adsorption of Ni on  $\text{SiO}_2(\text{s})$  in oxidizing fresh waters of pH 7 as a function of surface area ( $\text{ha}/\ell$ ) in the presence and absence of citrate.

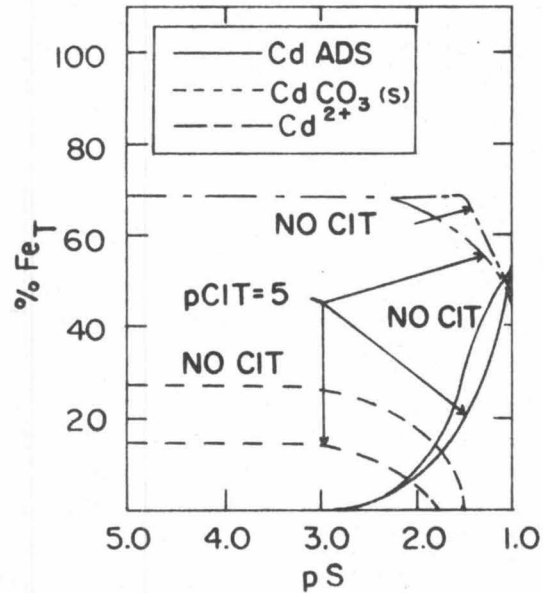


Figure 8.19 Speciation of Cd in oxidizing fresh waters of pH 7 as a function of surface area ( $ha/l$ ) in the absence and presence of citrate.

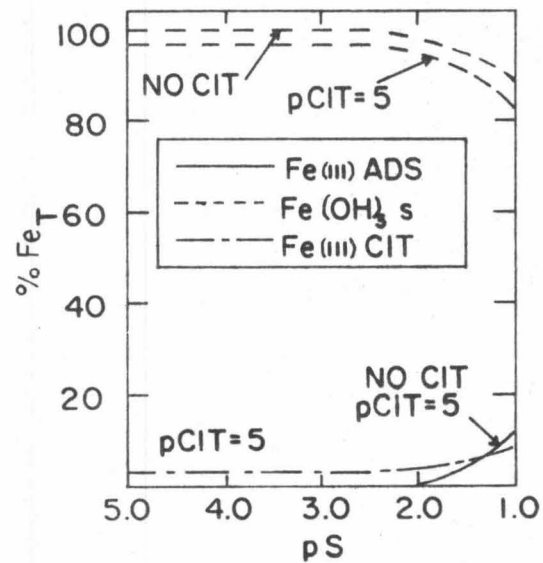


Figure 8.20 Speciation of Fe in oxidizing fresh waters of pH 7 as a function of surface area ( $ha/l$ ) in the absence and presence of citrate.

#### 8.4 Conclusions

The modeling of the equilibrium distribution of trace metals is affected not only by the choice of metals, inorganic and organic ligands, and surfaces, but also by the availability and choice of their respective stability constants. The concentrations, identities of organic constituents, and the stability constants for many metal-ligand and metal-surface interactions are poorly known. It is possible, however, to augment our present knowledge with educated chemical estimates and thereby gain some insight into the complicated, interdependent chemical equilibria of many metals in natural aquatic systems. Specific conclusions from the equilibrium computations are summarized below.

The extent of adsorption of dissolved Cu(II) species on colloidal  $\text{SiO}_2(\text{s})$  depends strongly upon availability of organic ligands and surfaces. When complexing agents are absent (or present in extremely low concentrations) Cu(II) is expected to be substantially removed from solution by adsorption. The main aqueous species would be either  $\text{Cu-OH}$  or  $\text{Cu-CO}_3$ , depending on the specific environmental conditions. Higher concentrations of complexing agents would result in the partial or total release of the adsorbed copper, depending on the surface/organic ligand ratio. The main aqueous species would be complexes with organic ligands.

The distribution of Pb(II) between aqueous and adsorbed species will depend mainly on the availability of surface area. When little or no organic ligand is present, the predominant aqueous species are expected to be  $\text{Pb}^{2+}$ ,  $\text{Pb-CO}_3$ , and  $\text{Pb-OH}$ . Appreciable changes in such a distribution will occur only if the organic ligand has a high affinity for Pb(II).

Ni(II), Zn(II), and Co(II) are expected to be present in solution as  $\text{Ni}^{2+}$ ,  $\text{Zn}^{2+}$ , and  $\text{Co}^{2+}$ , respectively. An increase in surface area and organic ligand concentrations will result in some adsorption and complexation.

Computations show that most of the Cd(II) present will be the free metal ion  $\text{Cd}^{2+}$ . At the proper alkalinity and pH, Cd(II) will partially precipitate as  $\text{CdCO}_3(\text{s})$ . In the presence of large amounts of complexing agents, or large surface areas, the percentage of precipitated  $\text{CdCO}_3(\text{s})$  is expected to decrease.

In an oxidizing environment Fe and Mn are oxidized to Fe(III) and Mn(IV) and precipitated as  $\text{Fe(OH)}_3(\text{s})$  and  $\text{MnO}_2(\text{s})$ , respectively. The presence of adsorbing surfaces or complexing agents will only slightly decrease the degree of precipitation of  $\text{Fe(OH)}_3(\text{s})$ . Under normal conditions, the abundance of surfaces and complexing agents will never be large enough to prevent substantial or even complete precipitation of  $\text{Fe(OH)}_3(\text{s})$ . According to these computations,

manganese will always remain as  $\text{MnO}_2(\text{s})$ . On the basis of moles of trace metals adsorbed per unit surface area, both precipitates adsorb significant amounts of trace metals.

## Appendix 1

## TABLE OF NOTATIONS

A	= Dielectric constant of the oriented water molecules
B	= $1.2 \times 10^{-17} \text{ m}^2 \text{ V}^{-2}$
D	= Dielectric displacement
e	= Elementary charge
F	= Faraday's constant
$G^{\circ}$	= Standard free energy
$\Delta G^{\circ}$	= Change in the standard free energy
$\Delta G_{\text{chem}}^{\circ}$	= Change in the standard chemical free energy
$\Delta G_{\text{coul}}^{\circ}$	= Change in the standard coulombic free energy
$\Delta G_{\text{solv}}^{\circ}$	= Change in the standard secondary solvation free energy
I	= Ionic strength
j	= Charge of a ligand
k	= Constant
K, *K	= Stability constants for aqueous complexes
*K <sup>s</sup>	= Stability constant for surface complexes
$K_a$	= Acidity constant of the surface silanol groups in the presence of an electric field
$K_{\text{ads}}$	= Stability constant for the adsorption
$K_{\text{so}}, *K_{\text{so}}$	= Solubility products

$l$	=	Stoichiometric coefficient of ligand
$L$	=	Ligand
$m$	=	Stoichiometric coefficient of metal ion
$Me$	=	Metal ion
$n$	=	Stoichiometric coefficient of silanol groups and OH groups
$N$	=	Avogadro's number
$o$	=	Unoccupied surface in moles/l
$pH_{PZC}$	=	pH of the point of zero charge
$r_{ion}$	=	Radius of ion
$r_w$	=	Radius of water
$R$	=	Gas constant
$S$	=	Total number of silanol sites in moles/l
$(-SO^-), (-SOH)$	=	Surface hydroxyl groups
$(\equiv SiO^-), (\equiv SiOH)$	=	Surface silanol groups
$T$	=	Absolute temperature
$u$	=	Unoccupied surface in moles/l
$v$	=	Volume
$x$	=	Distance of the closest approach
$X$	=	Mole fraction
$\bar{X}$	=	Electric field vector
$z, z_i$	=	Charge of the metal ion, and charge of the adsorbing species

## Greek Notation

$\alpha_0$	=	Degree of formation of protonated silanol groups
$\beta, *R$	=	Stability constants for aqueous complexes
$*R^s$	=	Stability constant for surface complexes
$\gamma$	=	Area in $\text{cm}^2$ covered by each mole of adsorbed metal species
$\Gamma_{\text{max}}, \Gamma_{\text{Me}}^{\text{max}}$	=	Maximum coverage assuming a monolayer of adsorbed species
$\Gamma_{\text{Me}}$	=	Adsorption density of Me-species in moles/ $\text{cm}^2$
$\epsilon$	=	Dielectric constant
$\epsilon_{\text{bulk}}$	=	Dielectric constant of water in bulk solution
$\epsilon_{\text{int}}$	=	Dielectric constant of interfacial water
$\epsilon_0$	=	Dielectric constant of vacuum
$\epsilon_{\text{solid}}$	=	Dielectric constant of solid
$\zeta$	=	Polar coordinate
$\eta$	=	Fraction of the unprotonated silanol sites
$\theta$	=	Fraction of the protonated silanol sites for the case of one metal reacting with two surface silanol groups (i. e. , 1:2 stoichiometry)
$\kappa$	=	Double-layer parameter
$\xi$	=	Fraction of the silanol sites bound to the metal

- $\rho$  = Polar coordinate  
 $\Phi$  = Polar coordinate  
 $\psi_0$  = Potential of the surface  
 $\Delta\psi_x$  = Change in the potential across the distance  $x$  away from the surface  
 $\left(\frac{d\psi}{dx}\right)_x$  = Electric field strength at distance  $x$   
 $\phi$  = Fraction of the protonated silanol groups for the case of one metal ion reacting with two silanol groups

## Other Notations

- $\rightarrow 0$  = Extrapolated to  $I = 0$   
 $[ \ ]$  = Concentration in moles/l  
 $\{ \}$  = Chemical activity in moles/l

## REFERENCES

- Ahmed, S. M. and Van Cleave, A. B. (1965), "Adsorption and Flotation Studies with Quartz; Part 1: Adsorption of Calcium, Hydrogen, and Hydroxyl Ions on Quartz", *Can. J. Chem. Eng* 43: 23.
- Ahrland, H. E., Grenthe, I., and Norén, B. (1960), "The Ion Exchange Properties of Silica Gel", *Acta Chim. Scand.* 14: 1059.
- Allen, H. E., Matson, W. R., and Mancy, K. H. (1970), "Trace Metal Characterization in Aquatic Environments by Anodic Stripping Voltammetry", *J. WPCF* 42: 573.
- Andersen, T. N. and Bockris, J. O. (1964), "Forces Involved in the Specific Adsorption of Ions on Metals from Aqueous Solution", *Electrochim. Acta*, 9: 347.
- Barsdate, R. J. and Matson, W. R. (1967), "Trace Metals in Arctic and Sub-Arctic Lakes with Reference to the Organic Complexes of Metals" in Radioecological Concentration Processes, B. Aberg and F. P. Hungate, eds., *Proc. Intern. Symp.*, Stockholm, 1966, Pergamon Press.
- Berecki-Biedermann, C. (1955), "Studies on the Hydrolysis of Metal Ions; Part 13. The Hydrolysis of the Copper (II) Ion,  $Cu^{2+}$ ", *Arkiv för Kemi* 9: 175.
- Blaedel, W. J. and Dinwiddie, D. E. (1974), "Study of Behavior of Copper Ion-Selective Electrodes at Submicromolar Concentration Levels" *Anal. Chem.* 46: 873.
- Block, L. and DeBruyn, P. L. (1970a), "The Ionic Double Layer at the ZnO Solution Interface-I. The Experimental Point of Zero Charge", *J. Colloid Interface Sci.* 32: 518.
- Block, L. and DeBruyn, P. L. (1970b), "The Ionic Double Layer at the ZnO Solution Interface-II. Composition Model of the Surface", *J. Colloid Interface Sci.* 32: 527.
- Bockris, J. O., Devanathan, M. A. V., and Müller, K. (1963), "On the Structure of Charged Interface", *Proc. Roy. Soc. A* 274: 55.
- Bowen, H. J. M. (1966), Trace Elements in Biochemistry, Academic Press.

- Brewer, P. G. (1975), "Minor Elements in Sea Water" in Chemical Oceanography, 2nd edition, J. P. Riley and G. Skirrow, eds, Academic Press.
- Carell, B. and Olin, A. (1960), "Studies on the Hydrolysis of Metal Ions; 31. The Complex Formation Between  $Pb^{2+}$  and  $OH^-$  in  $Na^+$  ( $OH^-$ ,  $ClO_4^-$ ) Medium", *Acta Chem. Scand.* 14: 1999.
- Clark, S. W. and Cooke, S. R. B. (1968), "Adsorption of Calcium, Magnesium and Sodium by Quartz", *Trans. AIME* 241: 334.
- Dugger, D. L., Stanton, J. H., Irby, B. N., McConnell, B. L., Cummings, W. W. and Maatman, R. W. (1964), "The Exchange of Twenty Metal Ions with the Weakly Acidic Silanol Groups of Silica Gel", *J. Phys. Chem.* 68: 757.
- Duursma, E. K. (1970), "Organic Chelation of  $^{60}Co$  and  $^{65}Zn$  by Leucine in Relation to Sorption by Sediments" in Organic Matter in Natural Waters, Symposium on Organic Matter in Natural Waters held at the University of Alaska Sept. 2-4, 1968, D. W. Hood, ed., Institute of Marine Science Occasional Publication No. 1.
- Ediger, R. D., Peterson, G. E., and Kerber, J. D. (1974), "Application of the Graphite Furnace to Saline Water Analysis", *Atomic Absorption Newsletter* 13: 61.
- Faucherre, J. (1954), "Sur la Constitution des Ions Basique MétaIliques. II. La Plomb", *J. Bull. Soc. Chim, France* p. 128.
- Gadde, R. R. and Laitinen, H. A. (1974), "Studies of Heavy Metal Adsorption by Hydrous Iron and Manganese Oxide", *Anal. Chem.* 46: 2022.
- Gibbs, R. J. (1973), "Mechanism of Trace Metal Transport in Rivers", *Science* 180: 71.
- Greenberg, S. A. (1956), "A Chemisorption of Calcium Hydroxide by Silica", *J. Phys. Chem.* 60: 325.
- Hahn, H. and Stumm, W. (1968), "Coagulation by Al(III); The Role of Adsorption of Hydrolyzed Aluminum in the Kinetics of Coagulation", *Adv. Chem. Ser. No.* 79: 91.

- Healy, T. W. and Jellet, V. R. (1967), "Adsorption-Coagulation Reactions of Zn(II) Hydrolyzed Species at the Zinc Oxide-Water Interface", *J. Colloid Interface Sci.* 24: 41.
- Healy, T. W., James, R.O. and Copper, R. (1968), "The Adsorption of Aqueous Co(II) at the Silica-Water Interface", *Adv. Chem. Ser.* No. 79: 62.
- Hill-Cottingham, D.G. and Lloyd-Jones, C.P. (1957), "Behavior of Iron Chelates in Calcareous Soils. I. Laboratory Experiments with Fe-EDTA and Fe-HEEDTA", *Plant Soil* 8: 263.
- Hill-Cottingham, D.G. and Lloyd-Jones, C.P. (1958a), "Behavior of Iron Chelates in Calcareous Soils. II. Laboratory Experiments with some Further Chelating Agents", *Plant Soil* 9: 189.
- Hill-Cottingham, D.G. and Lloyd-Jones, C.P. (1958b), "Behavior of Iron Chelates in Calcareous Soil. III. Laboratory Experiments with a Further Range of Chelating Agents", *Plant Soil* 10: 194.
- Hodgson, J. F. (1960), "Cobalt Reactions with Montmorillonite", *Soil Sci. Soc. Amer. Proc.* 24: 165.
- Hodgson, J. F., Lindsay, W.L. and Trierweiler, J.F. (1966), "Micro-nutrient Cation Complexing in Soil Solution: II. Complexing of Zinc and Copper in Displaced Solution from Calcareous Soils", *Soil. Sci. Soc. Amer. Proc.* 30: 723.
- Hohl, H. and Stumm, W. (1975), "Interactions of  $Pb^{2+}$  with Hydrous  $\gamma-Al_2O_3$ ", 49th Nat. Colloid Symposium, Clarkson College, Potsdam, New York.
- Hugel, R. (1964), "Étude de l'Hydrolyse de l'Ion  $Pb^{2+}$  dans les Solutions de Perchlorate de Sodium", *Bull. Soc. Chim. France* p. 1462.
- Hugel, R. (1965), "Étude de l'Hydrolyse de l'Ion  $Pb^{2+}$  dans les Solutions de Nitrate de Sodium", *Bull. Soc. Chim. France* p. 968.
- Ion Selective Electrodes (1969), Proceedings of a Symposium held at National Bureau of Standards, R. A. Durst, ed., NBS.
- James, R.O. and Healy, T.W. (1972a), "Adsorption of Hydrolyzable Metal Ions at the Oxide-Water Interface-I. Co(II) Adsorption on  $SiO_2$  and  $TiO_2$  as Model System", *J. Colloid Interface Sci.* 40: 42.

- James, R. O. and Healy, T. W. (1972b), "Adsorption of Hydrolyzable Metal Ions at the Oxide-Water Interface-II. Charge Reversal of  $\text{SiO}_2$  and  $\text{TiO}_2$  Colloids by Adsorbed  $\text{Co(II)}$ ,  $\text{La(III)}$ , and  $\text{Th(IV)}$  as Model Systems", *J. Colloid Interface Sci.* 40: 53.
- James, R. O. and Healy, T. W. (1972c), "Adsorption of Hydrolyzable Metal Ions at the Oxide-Water Interface-III. A Thermodynamic Model of Adsorption", *J. Colloid Interface Sci.* 40: 65.
- Jasinski, R., Trachtenberg, I. and Andrychuk, D. (1974), "Potentiometric Measurements of Copper in Seawater with Ion Selective Electrode", *Anal. Chem.* 46: 364.
- Jenne, E. A. (1968), "Controls of Mn, Fe, Co, Ni, Cu and Zn Concentrations in Soil and Water: the Significant Role of Hydrous Mn and Fe Oxides", *Adv. Chem. Ser. No.* 73: 337.
- Johansson, G. and Edström, K. (1972), "Studies of Copper (II) Sulphide-Ion-Selective Electrodes", *Talanta* 19: 1623.
- Kopp, J. F. and Kroner, R. C. (1968), "A Comparison of Trace Elements in Natural Waters, Dissolved Versus Suspended" in Developments in Applied Spectroscopy, W. K. Baer, ed., v. 6, Plenum Press.
- Kozawa, A. (1961), "Ion-Exchange Adsorption of Zn and Cu Ions on Silica", *J. Inorg. Nucl. Chem.* 21: 315.
- Kurbatov, M. H. and Wood, G. B. (1952), "Rate of Adsorption of Cobalt Ions on Hydrous Ferric Oxide", *J. Phys. Chem.* 56: 698.
- Lindsay, W. L., Hodgson, J. F. and Norvell, W. A. (1966), "The Physico-Chemical Equilibrium of Chelates in Soils and their Influence on the Availability of Micronutrient Cations", *Int. Soc. Soil Sci., Trans Comm.* II, IV, Aberdeen, Scotland, p. 305.
- Lindsay, W. L. and Norvell, W. A. (1969), "Equilibrium Relationship of  $\text{Zn}^{2+}$ ,  $\text{Fe}^{3+}$ ,  $\text{Ca}^{2+}$ , and  $\text{H}^+$  with EDTA and DTPA in Soils", *Soil Sci. Soc. Amer. Proc.* 33: 62.
- Livingstone, D. A. (1963), "Chemical Composition of Rivers and Lakes", *U.S. Geol. Survey Profess. Paper* 400G.

- Loganathan, P. (1971), "Sorptions of Heavy Metals on a Hydrous Manganese Oxide", Ph.D. Thesis, University of California, Davis.
- Lohmann, F. (1972), "Ionenadsorption an den Grenzfläche Oxide/Electrolyt", Kolloid-Z. u. Z. Polymere 250: 248.
- MacNaughton, M. G. (1973), "Adsorption of Mercury (II) at the Solid-Water Interface", Ph.D. Thesis, Stanford University.
- MacNaughton, M. G. and James, R. O. (1974), "Adsorption of Aqueous Mercury (II) Complexes on the Oxide/Water Interface", J. Colloid Interface Sci. 47: 431.
- Matijević, E., Abramson, M. B., Schultz, K. F. and Kerker, M. (1960), "Detection of Metal Ion Hydrolysis by Coagulation: II. Thorium", J. Phys. Chem. 64: 1157.
- Matijević, E., Mathai, K. G., Ottewill, R. H. and Kerker, M. (1961), "Detection of Metal Ion Hydrolysis by Coagulation. III. Aluminum", J. Phys. Chem. 65: 826.
- Matijević, E. (1967), "Charge Reversal of Lyophobic Colloids" in Principles and Applications of Water Chemistry, S. D. Faust and J. V. Hunter, eds., Wiley and Sons.
- McDowell, L. A. and Johnston, H. L. (1936), "The Solubility of Cupric Oxide in Alkali and the Second Dissociation Constant of Cupric Acid. The Analysis of Very Small Amounts of Copper", J. Amer. Chem. Soc. 58: 2009.
- McDuff, R. E. and Morel, F. M. (1973), "Technical Report EQ-73-02: Description and Use of the Chemical Equilibrium Program REDEQL2", W. M. Keck Laboratory of Environmental Engineering Science, California Institute of Technology, Pasadena (Updated July 1975).
- McKenzie, J. M. W. and O'Brien, R. T. (1969), "Zeta Potential of Quartz in the Presence of Nickel (II) and Cobalt (II)", Trans. AIME 244: 168.

- Mesmer, R. E. and Baes, C. F. Jr., (1974), The Hydrolysis of Cations; A Critical Review of Hydrolytic Species and Their Stability Constants in Aqueous Solution, Oak Ridge National Laboratory, ORNL-NSF-EATC-3, Part III.
- Morgan, J. J. and Stumm, W. (1964), "Colloid-Chemical Properties of Manganese Dioxide", J. Colloid Interface Sci. 19: 347.
- Morrison, G. H. and Freiser, H. (1957), Solvent Extraction in Analytical Chemistry, J. Wiley and Sons.
- Murray, D. J., Healy, T. W. and Furstenu, D. W. (1968), "The Adsorption of Aqueous Metal on Colloidal Hydrated Manganese Oxide", Adv. Chem. Ser. No. 79: 74.
- Murray, D. J. (1973), "The Interaction of Metal Ions at the Hydrated Manganese Dioxide-Solution Interface", Ph.D. Thesis, Massachusetts Institute of Technology, Woods Hole Oceanographic Institution.
- New England Nuclear (1974), Aquasol Universal LSC Cocktail.
- Norvell, W. A. and Lindsay, W. L. (1969), "Reactions of EDTA Complexes of Fe, Zn, Mn, and Cu with Soils", Soil Sci. Soc. Amer. Proc. 33: 86.
- Norvell, W. A. and Lindsay, W. L. (1970), "Lack of Evidence for  $ZnSiO_3$  in Soils", Soil. Sci. Soc. Amer. Proc. 34: 360.
- Norvell, W. A. (1972), "Equilibria of Metal Chelates in Soil Solution" in Micronutrients in Agriculture, Soil. Sci. Soc. Amer., Inc. Wisconsin.
- Olin, A. (1960a), "Studies on the Hydrolysis of Metal Ions; 25. The Hydrolysis of Lead (II) in Perchlorate Medium", Acta Chem. Scand. 14: 126.
- Olin, A. (1960b), "Studies on the Hydrolysis of Metal Ions; 28. Applications of the Self-Medium Method to the Hydrolysis of Lead (II) Perchlorate Solution", Acta Chem. Scand. 14: 814.
- Olson, L. L. and O'Melia, C. R., (1973), "The Interactions of Fe(III) with  $Si(OH)_4$ ", J. Inorg. Nucl. Chem. 35: 1977.

- Onoda, G. Y. and DeBruyn, P. L. (1966), "Proton Adsorption at the Ferric Oxide/Aqueous Solution Interface", *Surface Sci.* 4: 48.
- Orion Research Inc. (1968), Instruction Manual, Cupric Ion Selective Electrode Model 94-29.
- Orion Research Inc. (1972), Instruction Manual, Lead Ion Electrode Model 94-82A.
- Pajdowski, L. and Olin, A. (1962), "Studies on the Hydrolysis of Metal Ions; 39. The Hydrolysis of  $Pb^{2+}$  in  $Mg(ClO_4)_2$  and  $Ba(ClO_4)_2$  Medium", *Acta Chem. Scand.* 16: 983.
- Pedersen, K. J. (1943), "The Acid Dissociation of the Hydrated Cupric Ion; The Formation of Dimeric Cupric Compounds", *Kgl. Danske Vidensk. Mat.-Fys. Medd.* 20: No. 7.
- Pedersen, K. J. (1945), "The Acid Dissociation of the Hydrated Lead Ion and the Formation of Polynuclear Ions", *Kgl. Danske Vidensk. Selsk., Mat.-Fys. Medd.* 22: No. 10.
- Pennsylvania Glass Sand Corp., Min-U-Sil Data Sheet No. 1001-31167 MH, Pittsburgh.
- Perhac, R. M. (1972), "Distribution of Cd, Co, Cu, Fe, Mn, Ni, Pb and Zn in Dissolved and Particulate Solids from Two Streams in Tennessee", *J. Hydrology* 15: 177.
- Perrin, D. D. (1960), "The Hydrolysis of Copper (II) Ion", *J. Chem. Soc.* 3189.
- Posselt, H. S., Anderson, F. J. and Weber, W. J. (1968), "Cation Sorption on Colloidal Hydrated Manganese Dioxide", *Environ. Sci. Tech.* 2: 1087.
- Quintin, M. (1937), "Sur l'Hydrolyse du Benzene Sulfonate de Cuivre", *Compt. Rend.* 204: 968.
- Sandell, E. B. (1959), Colorimetric Determination of Traces of Metals, Interscience.
- Schindler, P. and Kamber, H. R. (1968), "Die Acidität von Silanolgruppen", *Helv. Chim. Acta* 51: 1781.

- Schindler, P. W. and Gamsjäger, H. (1972), "Acid-Base Reactions of the  $\text{TiO}_2$  (Anatase)-Water Interface and the Point of Zero Charge of  $\text{TiO}_2$  Suspensions", *Kolloid-Z. u. Z. Polymers* 25: 759.
- Schindler, P. W., Fürst, B., Dick, R. and Wolf, P. (1975), "Ligand Properties of Surface Silanol Groups - I. Surface Complex Formation with  $\text{Fe}^{3+}$ ,  $\text{Cu}^{2+}$ ,  $\text{Cd}^{2+}$ , and  $\text{Pb}^{2+}$ ", 49th Nat. Colloid Symposium, Clarkson College, Potsdam, New York.
- Schnitzer, M. (1969), "Reactions between Fulvic Acid, a Soil Humic Compound and Inorganic Soil Constituents", *Soil Sci. Soc. Amer. Proc.* 33: 75.
- Schorsch, G. and Ingri, N. (1967), "Determination of Hydroxide Ion Concentration by Measurements with Lead Amalgam Electrode. Plumbate and Borate Complexes in Alkaline 3.0 M NaCl-Medium: Absence of Monoborate (-2) and (-3) Ions", *Acta Chem. Scand.* 21: 2727.
- Siegel, A. (1966), "Equilibrium Binding Studies of Zinc-Glycine Complexes to Ion-Exchange Resins and Clays", *Geochim. Cosmochim. Acta* 30: 757.
- Sillén, L. G. and Martell, A. E. (1971), Stability Constants of Metal Ion Complexes, Supplement No. 1, Chem. Soc. London.
- Spivakovskii, V. B. and Makovskaya, G. V. (1968), "Copper (II) Hydroxide Chlorides, Hydroxide and Hydroxo-Complexes. A New Version of the Method of Three Variables", *Russ. J. Inorg. Chem.* 13: 815.
- Starik, I.E. and Kositsyn, A. V. (1957a), "The State of Small Amounts of Radioactive Elements in Solutions. I. State of Tri- and Tetravalent Ruthenium in Hydrochloric Acid Solutions", *Zhur. Neorg. Khim.* 2: No. 2, 444; Engl. trans. p. 332.
- Starik, I. E. and Kositsyn, A. V. (1957b), "The State of Small Amounts of Radioactive Elements in Solutions. II. The State of Thallium in Sulfuric Acid Solutions", *Zhur. Neorg. Khim.* 2: No. 5, 1171; Engl. trans. p. 286.
- Stiff, M. J. (1971), "The Chemical States of Copper in Polluted Fresh Water and a Scheme of Analysis to Differentiate Them", *Water Research* 5: 587.

- Stumm, W. (1967), "Metal Ions in Aqueous Solutions" in Principles and Applications of Water Chemistry, S. D. Faust and J. V. Hunter, eds., Wiley and Sons.
- Stumm, W., Hürper, H. and Champlin, R. L. (1967), "Formation of Polysilicates as Determined by Coagulation Effects", *Envir. Sci. Tech.* 1: 221.
- Stumm, W. and O'Melia, C. R. (1968), "Stoichiometry of Coagulation", *JAWWA* 60: 514.
- Stumm, W., Huang, C. P. and Jenkins, S. R. (1970), "Specific Chemical Interaction Affecting the Stability of Dispersed Systems", *Croat. Chim. Acta* 42: 223.
- Stumm, W. and Bilinski, H. (1972), "Trace Metals in Natural Waters: Difficulties of Interpretation Arising from our Ignorance of their Speciation" in Advances in Water Pollution Research, Proceedings of the Sixth International Conference held in Jerusalem June 18-23, 1972, S. H. Jenkins, ed., Pergamon Press.
- Stumm, W. and Brauner, Ph. A. (1975), "Chemical Speciation" in Chemical Oceanography, 2nd edition, J. P. Riley and G. Skirrow, eds., Academic Press.
- Wallace, A., Mueller, R. T., Lunt, O. R., Aschcroft, R. T. and Shannon, L. M. (1955), "Comparison of Five Chelating Agents in Soils, in Nutrient Solutions, and in Plant Responses", *Soil Sci.* 80: 101.
- Wallace, A. and Lunt, O. R. (1956), "Reactions of some Iron, Zinc and Manganese Chelates in Various Soils", *Soil Sci. Amer. Proc.* 20: 479.
- Weber, W. J. and Stumm, W. (1964), "Formation of Silicato-Iron (III) Complexes in Dilute Aqueous Solution", *J. Inorg. Nucl. Chem.* 27: 237.